PolyPublie
Polytechnique Montréal

POLYTECHNIQUE MONTRÉAL
UNIVERSITÉ D'INGÉNIERIE

Titre: Title:	Design, Experimentation, and Modeling of a Novel Continuous Biodrying Process
Auteur: Author:	Shahram Navaee-Ardeh
Date:	2009
Type:	Mémoire ou thèse / Dissertation or Thesis
Référence: Citation:	Navaee-Ardeh, S. (2009). Design, Experimentation, and Modeling of a Novel Continuous Biodrying Process [Thèse de doctorat, École Polytechnique de Montréal]. PolyPublie. https://publications.polymtl.ca/168/

Document en libre accès dans PolyPublie
Open Access document in PolyPublie

URL de PolyPublie: PolyPublie URL:	https://publications.polymtl.ca/168/
Directeurs de recherche: Advisors:	François Bertrand, & Paul R. Stuart
Programme: Program:	Génie chimique

Ce fichier a été téléchargé à partir de PolyPublie, le dépôt institutionnel de Polytechnique Montréal
This file has been downloaded from PolyPublie, the institutional repository of Polytechnique Montréal

https://publications.polymtl.ca

UNIVERSITÉ DE MONTRÉAL

DESIGN, EXPERIMENTATION, AND MODELING OF A NOVEL CONTINUOUS BIODRYING PROCESS

SHAHRAM NAVAEE-ARDEH

DÉPARTEMENT DE GÉNIE CHIMIQUE

ÉCOLE POLYTECHNIQUE DE MONTRÉAL

THÈSE PRÉSENTÉE EN VUE DE L'OBTENTION

DU DIPLÔME DE PHILOSOPHIAE DOCTOR (Ph.D.)

(GÉNIE CHIMIQUE)

NOVEMBRE 2009

© Shahram Navaee-Ardeh, 2009.

UNIVERSITÉ DE MONTRÉAL

ÉCOLE POLYTECHNIQUE DE MONTRÉAL

Cette thèse intitulée:

DESIGN, EXPERIMENTATION, AND MODELING OF A NOVEL CONTINUOUS BIODRYING PROCESS

présentée par: NAVAEE-ARDEH Shahram

en vue de l'obtention du diplôme de: Philosophiae Doctor

a été dûment acceptée par le jury d'examen constitué de:

M. PERRIER Michel, Ph.D., président

M. STUART Paul, Ph.D., membre et directeur de recherche

M. BERTRAND François, Ph.D., membre et codirecteur de recherche

M. FRADETTE Louis, Ph.D., membre

M. KUDRA Tadeusz, Ph.D., membre

ACKNOWLEDGMENTS

First of all, all praise and thanks to almighty Allah who enabled me to finish this research work.

I would like to express my utmost and sincere appreciation to my director *Professor Paul Stuart* and my co-director *Professor François Bertrand* at École Polytechnique de Montréal for their supervision, extended supports, helpful advises, and fruitful discussions during all these years from the beginning to the end.

Special gratitude and thanks to my jury members for their time dedication on reading my thesis.

I'm very grateful to our industrial partner Kruger Inc.; specially *Dr. Balázs Tolnai*, who without his help this project would not have come to this end, and his fellows at Corner Brook, Bromtonville, and Wayagamack Pulp and Paper mills are gratefully appreciated.

Special thanks to *Carl Tchoryk*, not only for his dedication efforts in the experimental phase but also his help on the techno-economic assessment and other frequent discussion during this research work. The experimental part of this work would not have been completed without the assistance of *Kheng Huynh*, *Omar Ben Ndiaye* and *Antonin Paquet*.

I would also like to acknowledge fruitful discussions with *Dr. Christophe Devals*, *Prof. Mario Jolicoeur*, and *Prof. Jamal Chaouki* from the Department of Chemical Engineering at École Polytechnique Montreal, and *Prof. Tom Richard* from the Department of Agricultural and Biological Engineering at Pennsylvania State University and *Prof. Stephen Whitaker* from the Department of Chemical Engineering at the University of California.

Financial support of FQRNT and NSERC are gratefully acknowledged.

There are many individuals that I'm indebted to them: our past and present students in the *Environmental Design Chair*, specially *Dr. Matty Janssen*, *Jean-Martin Brault*, *Dr. Ilich Lama*, *Lucy Cotter*, and *Agnès Dévarieux* and *Rosanne Cole*, and my friends in the Chemical Engineering Department at Ecole Polytechnique Montreal, *Dr. Babak Esmaeili Pour Farsangi, Ali Shekari*, *Jean-Philippe Laviolette*, and *Rouzbeh Jafari*.

A special thank goes to *Robert Delisle, Daniel Dumas*, *and Gino Robin* for their technical supports in the experimental phase.

Finally I would like to gratefully and sincerely thank my wife and my son for their supports, dedications, and patience all the time.

RÉSUMÉ

La production massive de boue provenant de l'industrie des pâtes et papiers rend la gestion efficace de cette boue un problème grandissant et critique pour l'industrie des pâtes et papiers. Ceci est dû aux hauts coûts d'enfouissement et de transport, ainsi que des cadres de normalisation complexes pour les options d'épandage et de compostage. Les défis concernant le séchage mécanique des boues se sont aggravés dans plusieurs usines dus à la progression de la récupération interne de fibre complémentée par une augmentation de la production de boue secondaires, ce qui résulte en une boue mixte avec une haute proportion de matière biologique, qui est difficilement asséchée mécaniquement.

Dans cette thèse, un réacteur de bio-séchage en continu novateur a été conçu et développé pour sécher la boue mixte d'usine de pâtes et papiers à un niveau de solide permettant la combustion sécuritaire et économique pour la récupération d'énergie dans une chaudière à combustion de biomasse. En plus de l'aération forcée, le procédé de séchage est amplifié par la génération de chaleur biologique provenant de l'activité microbienne des bactéries mésophiles et thermophiles naturellement présentes dans la boue. Ceci rend le procédé de bio-séchage plus attrayant comparativement à des technologies de séchages conventionnelles, puisque le réacteur est un procédé auto-chauffant. Le réacteur est divisé en quatre compartiments nominaux, sur le vertical, et la boue bouge de haut vers le bas du réacteur. Les temps de résidence étudiés ont été de 4-8 jours, ce qui est 2-3 fois plus court que les temps de résidence avec le réacteur de bio-séchage en mode batch et ce pour des siccités finales de la boue semblables.

Une analyse des variables du procédé a été performée pour déterminer les variables clés du procédé de bio-séchage en continu. Les paramètres ayant été étudiés sont : la biomasse en terme du pH et du ratio C/N, le temps de résidence, le recyclage de la boue bio-séchée et le profile de l'humidité relative à la sortie. Deux de ces paramètres ont été reconnus comme ayant le plus d'impact sur le bio-séchage en continu : le type de biomasse en terme de nutriments (ratio C/N), une variable incontrôlable, et le profile d'humidité relative à la sortie, une variable contrôlable. Le type de biomasse est fixé par choix, donc l'influence du profil d'humidité relative à la sortie a été étudiée sur la performance générale et celle en deux dimensions du réacteur de bio-séchage en continu. La meilleure efficacité, avec le bio-séchage, a été obtenue avec un profil d'humidité relative à la sortie qui contrôle l'évaporation d'eau interstitielle et libre à la température de bulbe

humide pour le 1er et 2e compartiments du réacteur et l'évaporation d'eau liée et de surface à la température de bulbe sèche dans le 3e et 4e compartiments.

À l'aide d'une approche systématique de modélisation, un modèle distribué en 2-D a été développé, qui décrit les phénomènes d'échanges dans le réacteur de bio-séchage en continu. Les résultats du modèle en 2-D étaient proches des données expérimentales. Il a été trouvé que le transfert de chaleur par convection est responsable d'environ 30% de l'évaporation d'eau totale (majoritairement l'eau libre et interstitielle dans le haut du réacteur). Pour ce qui est de la chaleur biologique, elle est responsable du reste de l'évaporation sous le mécanisme de diffusion (évaporation de l'eau de surface et liée dans le bas du réacteur).

Une analyse adimensionnelle a été faite sur le modèle en 2-D et a établi les critères préliminaires pour la mise à l'échelle du procédé de bio-séchage en continu.

Finalement, une étude technico-économique du procédé de bio-séchage en continu a démontré le grand potentiel de ce procédé dans les usines de pâtes et papiers. Les résultats de l'étude technico-économique ont été comparés avec d'autres technologies de séchage.

Il a été démontré que le procédé de bio-séchage développé est une solution potentielle pour régler les problèmes industriels associés à la gestion de la boue, et résulte en une réduction substantielle d'émission de GES.

ABSTRACT

Massive production of sludge in the pulp and paper industry has made the effective sludge management increasingly a critical issue for the industry due to high landfill and transportation costs, and complex regulatory frameworks for options such as sludge landspreading and composting. Sludge dewatering challenges are exacerbated at many mills due to improved in-plant fiber recovery coupled with increased production of secondary sludge, leading to a mixed sludge with a high proportion of biological matter which is difficult to dewater.

In this thesis, a novel continuous biodrying reactor was designed and developed for drying pulp and paper mixed sludge to economic dry solids level so that the dried sludge can be economically and safely combusted in a biomass boiler for energy recovery. In all experimental runs the economic dry solids level was achieved, proving the process successful. In the biodrying process, in addition to the forced aeration, the drying rates are enhanced by biological heat generated through the microbial activity of mesophilic and thermophilic microorganisms naturally present in the porous matrix of mixed sludge. This makes the biodrying process more attractive compared to the conventional drying techniques because the reactor is a self-heating process. The reactor is divided into four nominal compartments and the mixed sludge dries as it moves downward in the reactor. The residence times were 4-8 days, which are 2-3 times shorter than the residence times achieved in a batch biodrying reactor previously studied by our research group for mixed sludge drying.

A process variable analysis was performed to determine the key variable(s) in the continuous biodrying reactor. Several variables were investigated, namely: type of biomass feed, pH of biomass, nutrition level (C/N ratio), residence times, recycle ratio of biodried sludge, and outlet relative humidity profile along the reactor height. The key variables that were identified in the continuous biodrying reactor were the type of biomass feed and the outlet relative humidity profiles. The biomass feed is mill specific and since one mill was studied for this study, the nutrition level of the biomass feed was found adequate for the microbial activity, and hence the type of biomass is a fixed parameter. The influence of outlet relative humidity profile was investigated on the overall performance and the complexity index of the continuous biodrying reactor. The best biodrying efficiency was achieved at an outlet relative humidity profile which controls the removal of unbound water at the wet-bulb temperature in the 1^{st} and 2^{nd}

compartments of the reactor, and the removal of bound water at the dry-bulb temperature in the 3rd and 4th compartments.

Through a systematic modeling approach, a 2-D model was developed to describe the transport phenomena in the continuous biodrying reactor. The results of the 2-D model were in satisfactory agreement with the experimental data. It was found that about 30% w/w of the total water removal (drying rate) takes place in the 1st and 2nd compartments mainly under a convection dominated mechanism, whereas about 70% w/w of the total water removal takes place in the 3rd and 4th compartments where a bioheat-diffusion dominated mechanism controls the transport phenomena.

The 2-D model was found to be an appropriate tool for the estimation of the total water removal rate (drying rate) in the continuous biodrying reactor when compared to the 1-D model. A dimensionless analysis was performed on the 2-D model and established the preliminary criteria for the scale-up of the continuous biodrying process.

Finally, a techno-economic assessment of the continuous biodrying process revealed that there is great potential for the implementation of the biodrying process in Canadian pulp and paper mills. The techno-economic results were compared to the other competitive existing drying technologies. It was proven that the continuous biodrying process results in significant economic benefits and has great potential to address the current industrial problems associated with sludge management.

CONDENSÉ EN FRANÇAIS

La production massive de boue provenant de l'industrie des pâtes et papiers rend la gestion efficace de cette boue de plus en plus difficile et critique pour l'industrie des pâtes et papiers. Ceci est dû aux hauts coûts d'enfouissement et de transport, ainsi que des cadres de normalisation complexes pour les options d'épandage et de compostage. Les défis concernant le séchage mécanique des boues se sont aggravés dans plusieurs usines dû à la progression de la récupération interne de fibre complémentée par une augmentation de la production de boues secondaires, ce qui résulte en une boue mixte avec une haute proportion de matière biologique, qui est difficilement asséchée mécaniquement. Différentes technologies de séchage ont surgi pour s'attaquer au problème de la gestion de la boue, ayant comme but d'augmenter le taux de solides de la boue mixte à un niveau permettant la combustion efficace et économique dans une chaudière générant de la vapeur et de l'énergie. Une étude complète de ces technologies a été effectuée et a révélé que la majorité de ces technologies étaient incertaines et questionnables économiquement.

Un procédé de bioséchage, amplifié par la génération de chaleur biologique sous une aération forcée, a permis d'obtenir des succès significatifs en augmentant le niveau de siccité de la boue mixte, qui permet sa valorisation par une combustion économiquement viable dans les usines de pâtes et papiers. Malgré les résultats intéressants obtenus avec le bioséchage en procédé batch développé antérieurement dans notre chaire de recherche, quelques points faibles ont été identifiés, souvent associés à la configuration 'batch' : inflexibilité des opérations, temps de résidence long (jusqu'à 16 jours), grande superficie, limite du facteur d'agrandissement liée à la configuration 'batch', possible court-circuitage dû à des conditions non-uniformes et la possibilité de zones anaérobiques (points chauds). Dans le but de surmonter ces limitations, une nouvelle configuration de réacteur à bioséchage était nécessaire.

Un plan pilote novateur du réacteur de bioséchage en continu a été conçu et installé dans notre laboratoire à l'École Polytechnique de Montréal. L'accent a été mis sur trois objectifs majeurs : a) surmonter les faiblesses du bioséchoir en batch, b) identifier les variables clés, ainsi que leurs impacts sur la performance du bioséchoir en continu, c) comprendre les phénomènes d'échanges

qui se produisent dans le bioséchoir en continu en utilisant une approche systématique de modélisation. Plusieurs points faibles de la conception initiale ont été modifiés pour avoir un temps de résidence uniforme, une masse constante de solides dans le réacteur et une lecture de l'humidité relative fiable.

Dans la phase suivante, des expériences préliminaires ont été conduites dans le but de réduire la liste de paramètres importants. Plusieurs paramètres doivent être considérés dans le réacteur en continu et faire des modifications sur plus d'un paramètre à la fois rendrait difficile l'observation de leurs effets respectifs. Les paramètres ayant été retenus sont : la biomasse en terme du pH et du ratio C/N, le temps de résidence, le recyclage de la boue bioséchée et le profil de l'humidité relative à la sortie. Deux de ces paramètres ont été reconnus comme ayant le plus d'impact sur le bioséchage en continu : l'alimentation de la biomasse en termes de nutriments (ratio C/N) et de pH et le profil d'humidité relative à la sortie. Le type d'alimentation en biomasse à l'entrée est une variable incontrôlable et a été fixée. La boue traitée lors des expériences provient d'une seule usine de pâtes et papiers PTM, dans laquelle le pH et le ratio C/N varient dans un intervalle qui ne supprime pas l'activité microbienne des bactéries mésophiles et thermophiles. La seconde variable clé, le profil de l'humidité relative à la sortie, a été étudié selon deux profils d'humidité relative; a) un niveau faible (85%) et b) un niveau élevé (96%). Le niveau faible du profil d'humidité relative contrôle le procédé de bioséchage à la température de bulbe humide, et est donc efficace dans la période de séchage constante, qui correspond à l'évaporation de l'eau interstitielle et libre. Le niveau élevé du profil d'humidité relative contrôle le procédé de bioséchage à la température de bulbe sèche, et permet l'activation de la biodégradation microbienne (Berg et al. 2002), et est efficace dans la période de séchage décroissante (Nissan et al. 1959), ce qui correspond à l'évaporation de l'eau liée et de surface. Les meilleures performances ont été obtenues pour les profils d'humidité relative à la sortie suivants :

- Contrôler le bioséchoir à la température de bulbe humide (Humidité relative à la sortie de 85%) dans le haut du réacteur (1er et 2^{e} compartiments) où il y a plus d'eau interstitielle et libre;
- Contrôler le bioséchoir à la température de bulbe sèche (Humidité relative à la sortie de 96%) dans le bas du réacteur (3^{e} et 4^{e} compartiments) où il y a plus d'eau liée ou de surface.

L'efficacité du bioséchage du cas précédent est de 94%, une amélioration importante par rapport à l'efficacité de 86% du meilleur cas avec le bioséchage en batch.

La troisième phase de cette étude a été faite pour établir une approche de modélisation systématique qui permet de comprendre les phénomènes d'échanges prédominant dans le réacteur de bioséchage en continu. La stratégie principale est de commencer avec un modèle simple et d'augmenter graduellement la complexité à mesure que la compréhension des procédés de transport est appréhendée. Donc, dans la première étape de modélisation, une approche de modélisation globale par bloc a été développée pour estimer la masse solide et/ou la quantité d'humidité de la boue mixte dans le réacteur de bioséchage en continu. Il a été trouvé que le modèle par bloc était trop simpliste pour bien prédire les procédés de transport du bioséchage, vu que les prédictions de siccité étaient plus élevées que les données expérimentales. Ceci est dû à l'inflexibilité inhérente à la modélisation par bloc, qui est incapable de bien refléter le mécanisme de transfert des différents types d'eau de la boue mixte, ainsi le modèle présumait le même mécanisme de transfert pour l'eau liée et libre.

Par la suite, un modèle distribué des phénomènes d'échanges unidimensionnel a été développé dans un effort d'améliorer la compréhension phénoménologique du procédé de bioséchage en continu. Puisque ce modèle n'est qu'en une seule dimension, la prédiction de la température à été faite selon l'écoulement des solides, en utilisant la moyenne dans la direction de l'écoulement du gaz. Ceci correspond à une faiblesse majeure du modèle unidimensionnel, puisque les phénomènes d'échanges dans l'écoulement du gaz n'étaient pas utilisés ou investigués. Une autre faiblesse majeure du modèle distribué unidimensionnel est la simplification excessive des paramètres physiques qui sont dépendants de la masse et de la température. Ceci a mené à une simplification significative des procédés de transport qui surviennent dans la direction du gaz. Également, ceci a mené à une tendance du profil de la température de la matrice qui, à un certain point, était trompeur puisqu'il ignorait plusieurs facteurs essentiels comme la génération de chaleur biologique non-uniforme dans chaque compartiment et les transferts de masse et de température dans la direction du gaz. Donc, d'un côté, les faiblesses du modèle unidimensionnel et de l'autre, les données expérimentales qui supportent des phénomènes d'échanges sur deux dimensions dans le réacteur de bioséchage en continu nous ont permis de déduire qu'un modèle bidimensionnel (à 2D) était nécessaire.

Le modèle à 2-D a donc été développé en élargissant le modèle distribué unidimensionnel en y ajoutant des mécanismes supplémentaires. Ces dispositifs additionnels sont les termes relatifs au procédé de transport dans la direction du gaz, ainsi que les paramètres physiques sous une forme qui tient compte de leur dépendance à la masse et à la température. Deux profils de vitesse ont été utilisés pour décrire l'écoulement dans la matrice poreuse de la boue mixte : profil de vitesse plat et un profil d'écoulement semi-parabolique. Un accord satisfaisant a été atteint entre les résultats du modèle et les données expérimentales. En général, les données expérimentales démontraient un profil de vitesse plat à l'exception de l'entrée d'air aux 1er, 2^{e}, et 3^{e} compartiments, qui étaient plus en accord avec le profil semi-parabolique. En fournissant un profil de température pour les directions de l'écoulement des solides et l'écoulement des gaz, le modèle à 2-D est un outil flexible pour décrire les processus de transport complexes dans la matrice poreuse du réacteur de bioséchage en continu. Les résultats démontrent que l'approche de modélisation développée est un outil versatile pour estimer le profil de température et le taux d'évaporation totale. Il permet aussi d'analyser les implications de différentes variables du procédé, leurs impacts sur l'efficacité globale du réacteur de bioséchage en continu, ce qui permet d'identifier des conditions d'opération favorables, rendant plus attrayant économiquement l'implantation du procédé de bioséchage en continu dans l'industrie des pâtes et papiers. Les données expérimentales et celles du modèle pour le taux d'évaporation d'eau étaient concordaient relativement bien. De plus, seulement 25-35% w/w du taux d'évaporation totale (principalement de l'eau interstitielle et libre) proviennent des premier et second compartiments, où la chaleur de convection et d'évaporation domine face à la chaleur biologique. À l'inverse, 65-75% w/w du taux d'évaporation totale (principalement de l'eau interstitielle et liée) provient des 3^{e} et 4^{e} compartiments, où la chaleur biologique domine face à la chaleur de convection et d'évaporation. Un tel phénomène est principalement dû à la haute température de la matrice résultant de la grande génération de chaleur biologique des bactéries dans les 3^{e} et 4^{e} compartiments, ce qui augmente drastiquement la capacité de l'air à stocker de l'humidité. Ceci permet une meilleure diffusion de l'eau, de la matrice solide vers la phase gazeuse.

Une analyse adimensionnelle a aussi été faite sur le modèle à 2-D et a permis d'établir les critères préliminaires pour la mise à l'échelle du procédé de bioséchage en continu.

Finalement, l'étude techno-économique du procédé de bioséchage en continu a révélé le grand potentiel d'implantation de cette technologie dans les usines de pâtes et papiers. Les résultats techno-économiques ont été comparés avec des technologies de séchage en compétition. Le taux de siccité obtenu avec le bioséchage en continu est suffisant pour stabiliser la chaudière de combustion et pour l'auto-combustion et ce avec un temps de résidence inférieur à 5 jours et avec un temps de recouvrement du projet de moins de 2 ans (et dans certaines cas 1 an). Un bilan massique a permis de démontrer une réduction importante des émissions de GES si le bioséchage est intégré à l'usine.

Il a été conclu que le réacteur de bioséchage en continu permet une meilleure flexibilité et un meilleure contrôle du procédé, une meilleure performance, des coûts d'investissement et d'opération moindre dû majoritairement à un temps de résidence plus court, et un meilleur potentiel d'intégration dans une usine de pâtes et papiers entassée. Plus particulièrement :

- Cette étude confirme que la boue mixte des pâtes et papiers peut être séchée à un niveau économique de siccité avec un temps de résidence de moins de 5 jours;
- Le profil d'humidité relative à travers la sortie, du haut jusqu'en bas, a un grand impact sur la performance générale du procédé et a été identifié comme un critère de conception pour un procédé de bioséchage à grande échelle;
- Les phénomènes d'échanges complexes dans le réacteur de bioséchage en continu ont été étudiés par une approche de modélisation systématique. La recherche a démontré qu'un modèle 2-D est un outil versatile pour prédire les procédés de transport complexes dans un réacteur de bioséchage en continu. Cette approche de modélisation permet une amélioration du contrôle, une meilleure optimisation et une mise à l'échelle du procédé de bioséchage plus facile.

Les travaux futurs incluent:

- ❖ Tester une vaste gamme de types de biomasse provenant de différentes usines de pâtes et papiers pour identifier les possibles inflexibilités et limites du présent procédé de bioséchage;
- ❖ Puisque la chaleur biologique joue un rôle critique dans la performance du procédé et les mécanismes du séchage, il serait nécessaire d'effectuer une étude complète au niveau microbiologique. Celle-ci devrait se concentrer sur les cinétiques de biodégradation

microbiennes de différentes biomasses sous différentes conditions d'opération et environnementales, dans le but d'explorer les conditions optimales pour réacteur de bioséchage;

- Des expériences sur le bioséchage dans des conditions réelles n'ont pu être effectuées puisque les conditions du laboratoire sont contrôlées par l'université. Il serait utile d'étudier les effets de conditions ambiantes réelles, particulièrement l'air glacial de l'hiver et celui humide et chaud de l'été, sur les performances du réacteur de bioséchage en continu;
- L'optimisation de la présente conception du procédé n'a pas été faite; il serait utile que celle-ci soit effectuée pour éventuellement améliorer la géométrie du réacteur;
- La simplification du modèle 2-D en un modèle unidimensionnel modifié fournirait un outil de conception.

TABLE OF CONTENTS

LIST OF TABLES

LIST OF FIGURES

LIST OF APPENDICES

LIST OF SYMBOLES AND ABBREVIATIONS

a	Constant coefficient of the microbial growth reaction
A_i	Dimensionless number in the 1-D model for compartment i
$a_{w,i}$	Correction factor for evaporation heat in compartment i
BOD	Biological oxygen demand
b	Constant coefficient of the microbial growth reaction
B_i	Dimensionless number in the 1-D model for compartment i
c	Constant coefficient of the microbial growth reaction
CFU	Colony forming unit (microbial population)
CI	Complexity index
$Comp\ i$	Compartment i, i=1,2,3,4
Cp	Arbitrary specific heat capacity (=1 J/kg ^oC)
$Cp_{g,i}$	Specific heat capacity of gas phase in compartment i(J/kg ^oC)
$Cp^*_{g,i} = \frac{Cp_g}{Cp_{g,in}}$	Gas phase dimensionless specific heat capacity
Cp_{H_2O}	Specific thermal heat capacity of water (J/(kg ^oC))
Cp_{mix}	Overall curve-fitted specific heat capacity of solid phase used in COMSOL programming (J/kg ^oC)
$Cp_{mix,i}$	Specific heat capacity of solid phase in compartment i (J/kg ^oC)
$Cp^*_{mix,i} = \frac{Cp_{mix}}{Cp_{s,in}}$	Solid phase dimensionless specific heat capacity
$Cp_{ms,i}$	Specific thermal heat capacity of dried solids in compartment i (J/(kg ^oC))
d	Constant coefficient
D	Height of each compartment (m)
$Da = \frac{Reaction\ rate}{Convective\ mass\ transfer\ rate}$	Damkohler number
$d.b.$	Dry basis
$d\dot{m}_{g,i}$	Mass flowrate of inlet air through control volume in compartment i (kg/s)
$d\dot{m}_s$	Mass flowrate of solid phase in control volume i (kg/s)
d_p	Average particle size (mm)
$dV = LWdz$	Control volume (m^3)
e	Constant coefficient
$E_{1,i}$	The ratio of evaporative heat to conductive heat
$E_{2,i}$	The ratio of bioheat to evaporative heat
f	Constant coefficient
GHG	Greenhouse gas emission

H	Effective height of the reactor (=1.6 m)
HHV	Higher heating value (kJ/g d.b.)
k	Matrix of thermal conductivity in COMSOL Multiphysics (W/(m^{o}C))
k_s	Thermal conductivity of solid phase (W/(m^{o}C))
L	Width of the biodrying reactor (0.4 m) (gas flow direction)
M	Moisture content (=1-w_{ms})
$\dot{m}_{g,j} = Q_{g,j}\rho_g$	Mass flowrate of the gas phase in compartment j (kg/s), j=1,2,3,4
$\dot{m}_{total}$	Total mass flowrate of solid phase (kg/s)
Pe_i	Gas Peclet number in the 1-D model in compartment i
Pe_g	Gas phase Peclet number in the 2-D model
Pe_s	Solid phase Peclet number in the 2-D model
$PMHE$	Porous media heat exchangers
Pr	Prandtl number
$\dot{Q}_{bio,j}$	Bioheat generated in compartment j through metabolic activities (W/m^3) , j=1,2,3,4
$\dot{Q}_{bio,i}$	Bioheat generated in compartment i through metabolic activities (W/m^3)
$Q_{bio\text{-}standard}$	Standard biological heat production in aerobic systems (J/ kg O_2)
$Q_{g,i}$	Gas flowrate in compartment i (m^3/h)
$Q_{g,j}$	Gas flowrate in compartment j (m^3/h), j=1,2,3,4
RAS	Return activated sludge
RDF	Refuse-derived fuel
Re_j	Reynolds number in compartment j, j=1,2,3,4
RH_i	Relative humidity of gas phase in compartment i (%)
RH_{in}	Relative humidity of gas phase at the inlet (x=0) (%)
$RH_{out,j}$	Relative humidity of the outlet gas in compartment j (%)
ROI	Return on investment
RR	Recycle ratio of biodried mixed sludge (% w/w)
RT	Residence time (days)
$St = \frac{h}{\rho u_g Cp}$	Stanton number
T_{bot}	Temperature of matrix at the bottom of the biodrying reactor (z=1.6m) (^{o}C)
T_i	Temperature of the matrix in compartment i (^{o}C)
$T_i^* = \frac{T_i - T_{in}}{T_{bot} - T_{in}}$	Dimensionless temperature in compartment or compartment i
T_{in}	Temperature of gas phase at the inlet (x=0) (^{o}C) and initial temperature of feed mixed sludge (z=0) (^{o}C)
$T_{out,i}$	Temperature of the outlet gas in compartment i(^{o}C)
TCL	Total carbon loss (biodegradation rate) (kg/day)
TMP	Thermomechanical pulp
T_r	Reference temperature (^{o}C)
TWL	Total water loss (total drying rate) = $\sum WRR_i$ (kg/day)
$\vec{u}$	Vector of velocity (m/s)
$u_{g,i}$	Gas phase velocity in compartment i (m/s)

$u_g^* = \frac{u_g}{u_{g,in}}$	Gas phase dimensionless velocity
$u_s^* = \frac{u_s}{u_{s,in}}$	Solid phase dimensionless velocity
$UHMW$	Ultra high molecular weight
$(V_{O_2}/V_{Air})_{in,j}$	Volume percentage (absolute value) of oxygen at the inlet gas flow in compartment j
$(V_{O_2}/V_{Air})_{out,j}$	Volume percentage (absolute value) of oxygen at the outlet gas flow in compartment j
W	Depth of the biodrying reactor (1 m)
WAS	Waste activated sludge
$w_{ms,i}$	Mixed sludge dry solids content in compartment i
$w.b.$	Wet basis
WRR_j	Water removal rate (drying rate) in compartment j (kg/day)
x	The axial distance from the gas inlet in each compartment (m)
$x^* = \frac{x}{L}$	Dimensionless width
X_i	Absolute moisture content of gas phase in compartment i(kg H_2O/kg Air)
X_{in}	Absolute moisture content of gas phase at the inlet (x=0) (kg H_2O/kg Air)
$X_{out,i}$	Absolute moisture content of gas phase at the outlet of compartment i (x=0.4 m) (kg H_2O/kg Air)
y	Reactor depth direction
z_i	The vertical distance from the reactor top (m)
$z_{0,j}$	The vertical distance between the reactor top and the middle of compartment j (m)
$z^* = \frac{z}{D}$	Dimensionless height

Greek letters

β_i	Constant coefficient of the analytical solution of temperature in the 1-D model
γ_i	Constant coefficient of the analytical solution of temperature in the 1-D model
δ_1	Constant coefficient of bioheat equation (W/m^3)
δ_2	Constant coefficient of bioheat equation (m^{-1})
δ_i	Constant coefficient of the analytical solution of temperature in the 1-D model
ΔH_r	Exothermic heat of biological reaction (J/kg-biomass)
$\Delta H_{eva,i}$	Evaporation heat of water in compartment i(J/kg-H_2O)
$\Delta H_{eav,i}^* = \frac{\Delta H_{eav,i}}{\Delta H_{eav,in}}$	Gas phase dimensionless evaporation heat
ΔP	Pressure drop (Pa)
$\vec{\nabla}$	Gradient operator (m^{-1})
ε_i	Porosity of the matrix in compartment i (dimensionless)

μ	Viscosity of the gas phase (Pa.s)
η	Biodrying reactor efficiency index
ρ	Reference density (=1 kg/m^3)
ρ_{CO_2}	Density of carbon dioxide (1.9 kg/m^3) (Perry and Green (1997))
$\rho_{g,i}$	Density of the gas phase in compartment i (=1.16 kg/m^3)
$\rho_{ms,i}$	Density of mixed sludge in compartment i(kg/m^3)
ρ_{O_2}	Density of oxygen (1.35 kg/m^3) (Perry and Green (1997))
Π_1	Ratio of latent heat to conductive heat
Π_2	Ratio of bioheat to conductive heat

CHAPTER 1: INTRODUCTION

1.1. Problem Statement

In recent years, a movement towards minimizing pulp and paper mill discharges into receiving environments has led to an incremental increase in biosolids or mixed sludge production from wastewater treatment processes. Current disposal alternatives include landfilling, landspreading and boiler incineration. Both landfilling and landspreading have encountered increasingly high costs and mounting environmental pressures. A survey of the Canadian pulp and paper industry sector in 1995 and 2002 indicated that landfilling of pulp and paper mixed sludge and solid residues in 2002 decreased by 50% compared to 1995 values mainly due mainly to higher costs, tightened environmental regulations, and increased public awareness (Elliott and Mahmood, 2005).Mixed sludge can reduce fossil fuel requirements and GHG emissions if combusted to produce steam and/or power. The trend towards developing new technologies that could enhance the adaptation of "sludge to energy technologies", primarily in Europe and very recently in North America, has resulted in Canadian pulp mill operators to recognize sludge combustion as an attractive alternative. Furthermore, with the emergence of GHG trading markets, it is expected that there will be additional economic driving forces for efficient sludge combustion at pulp and paper mills. For these reasons, many mills are currently seeking to dispose of their sludge by combustion, and some mills are already employing this alternative technology to improve their operating efficiencies.

However, the main challenge with the combustion of the mixed sludge is its low and variable dry solids content from the sludge dewatering processes at many mills, which not only introduces variability into the boiler operation but also can be economically undesirable when supplemental fossil fuels are needed to stabilize the boiler operation. It is critical for many mills, therefore, to develop an efficient way to increase the dry solids content of mixed sludge from pulp and paper mills to a level that guarantees safe and economic combustion. Several drying

technologies have been adapted to sludge drying, but many of them have technical uncertainty and/or questionable economics (CANMET, 2005).

Biological drying ("biodrying") represents an important opportunity for the treatment of mixed sludge to consistently raise the dry solids content so that the sludge can be economically disposed of in boilers for the generation of steam and/or power.

Although previous batch biodrying technology developed by this research group at Ecole Polytechnique (Frei et al., 2004; and Roy et al., 2006) demonstrated the potential for drying of the pulp and paper mixed sludge while preserving its calorific value, there are several drawbacks associated with the application of the batch configuration such as non-uniformity, process inefficiencies, and labor intensity.

1.2. General Objective

The title of this thesis is "Design, Experimentation and Modeling of a Novel Continuous Biodrying Process". The main hypothesis of this work is:

> *It is possible to determine the operating conditions under which a novel continuous biodrying reactor can be economically applied for the treatment of pulp and paper mixed sludge through a sound understanding of the implicated transport phenomena.*

The main hypothesis is divided into three sub-hypotheses:

- *Design level:*

A continuous biodrying process can be developed for drying mixed sludge from pulp and paper processes such that the sludge can be dried to an economic dry solids level in less than 5 days.

- *Process analysis level:*

For the continuous biodrying process under development, the key operating parameter is the outlet air relative humidity profile down the reactor height.

- *Modeling level:*

A two-dimensional (2-D) distributed model can be developed, which provides the basis for a useful design tool that considers: a) 2-D transport phenomena, and b) the full-scale continuous biodrying reactor.

The problem statement and the hypotheses require that a methodology be developed in order to address the following project objectives:

- To develop a pilot-scale biodrying reactor that is capable of solving an industrial problem related to pulp and paper mixed sludge drying
- To identify key parameters that greatly impact the process performance and transport phenomena in the continuous biodrying reactor
- To develop a model that: a) provides insight into the transport phenomena prevailing in the continuous biodrying reactor, and b) can be used to estimate the full-scale biodrying process design.

1.3. Thesis Organization

This thesis is organized as follows: first, the literature relevant to the hypotheses is reviewed and the gaps in the body of knowledge and specific objectives are identified. Next, the overall methodology in this work is presented. This is followed by a synthesis of the experimental results that were obtained in order to demonstrate the use of the developed biodrying process. Furthermore, the modeling aspects of this methodology are presented and evaluated against the experimental data. Then, the general aspects of the methodology are discussed, and finally, the contributions to the body of knowledge are enumerated and direction for future work is given.

CHAPTER 2: LITERATURE REVIEW

2.1. Pulp and Paper Mill Mixed Sludge

On a yearly basis, the production of the pulp and paper mixed sludge in Canada is estimated to be about 2.6 million tonnes (Elliott, and Mahmood, 2005). Environmental legislation passed in 1995, requires all pulp and paper mills to have secondary (biological) treatment installed in an attempt to remove the organic load (dissolved and colloidal) from wastewater streams. The activated sludge process is one of the most common methods used for this purpose (Metcalf and Eddy, 1991). Nowadays, the wastewater treatment plants include primary and secondary clarifiers (Figure 2.1). First, primary solids are removed through flotation or settling in a clarifying step. This produces what is termed "primary solids", which are generally composed of fibers and other cellulosic materials along with any other settling solid particles from the process (fillers, grit, etc.). This sludge is relatively easy to dewater. The term mixed sludge refers to the mixture of sludges from the primary (1^o) and secondary (2^o)lines.

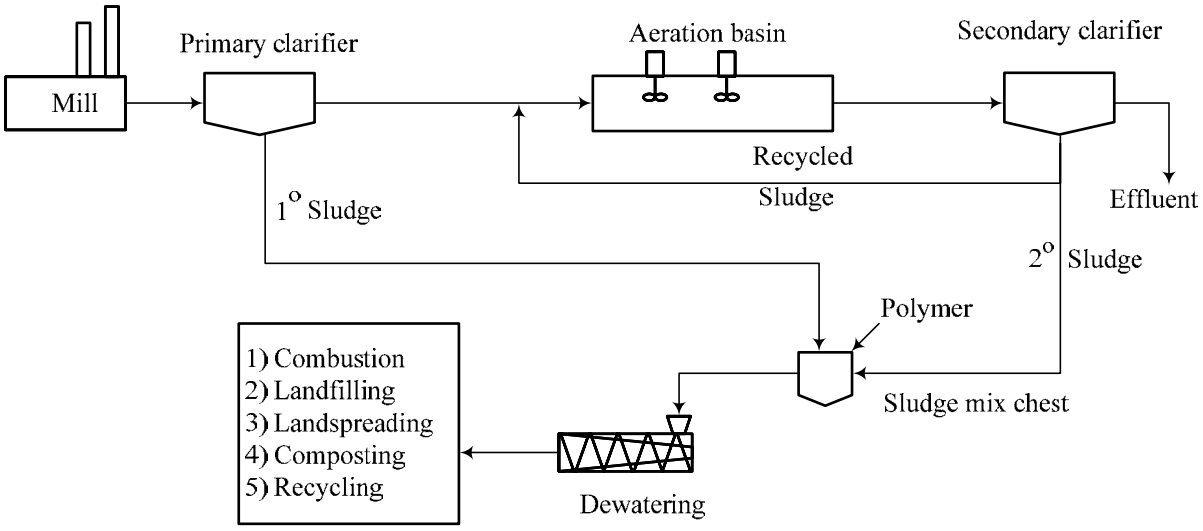

Figure 2.1: Schematic of wastewater treatment and sludge treatment

The clarified water is then fed to an aerated basin where biological treatment takes place. Here, a resident microbiological community acts to consume the organic components of the wastewater as a nutrient source in terms of biological oxygen demand (BOD), eliminating a

large portion (typically > 90%) of the BOD load. The microorganisms produce CO_2 and H_2O as they degrade the waste, but more importantly, they go through their normal life cycle, eventually being extracted as a solid waste stream from the secondary clarifier. A large portion of this cellular mass stream is recycled (return activated sludge (RAS)) to the inlet of the treatment process to maintain microbial population, but a certain amount is purged from the secondary clarifier in the form of waste activated sludge (WAS) or secondary sludge. The amount of secondary sludge produced depends on the design and operation of the AST, and typically is purged from the treatment system in ranges from 40 to 85 kg sludge per tonne of BOD removed (PAPTAC, 1999). This type of sludge is very difficult to dewater.

2.1.1. Mixed Sludge Generation and Dewatering

The Canadian pulp and paper industry has evolved into a paper recycling oriented industry, which has led to an increased generation of secondary sludge. Sludge dewatering challenges are exacerbated at many mills due to improved in-plant fiber recovery coupled with increased production of secondary sludge, leading to a mixed sludge with a high proportion of biological matter which is difficult to dewater.

As shown in Figure 2.1, the primary and secondary sludges are mixed in the blend tank, and polymers are added to the mixture to help the coagulation and flocculation of the solid particles in the dilute (1-3% w/w solids) stream. The mixed sludge consists of a complex mixture of microorganisms, fibrous materials, lignin, mineral components (limestone and phosphorus), and clay (Chen et al., 2002; Hippinen, and Ahtila, 2004; Hynninen and Laine, 1998). This complex mixture contains 2 types of water: unbound and bound water (Vaxelaire and Cezac, 2004; Tsang and Vesilind, 1990). The majority of pulp and paper sludges, such as biological (secondary) sludge, contain a large fraction of molecular or cellular bound water that is difficult to dewater. As a matter of fact, an increased emphasis is being placed on finding solutions or alternatives for sludge drying.

Due to inefficient sludge pre-conditioning, non-optimized sludge dewatering operations, high proportion of secondary sludge (high biosolids content), and the presence of different types of water in the mixed sludge, screw presses often achieve less than 40% w/w solids in practice and

often under 30% w/w (PAPTAC, 1999). In most cases, the dewatered sludges are very wet and not high enough in dry solids content for auto-thermal and economic combustion in a boiler.

2.1.2. Mixed Sludge Characteristics

The heating value of mixed sludge on a dry basis is 12-19 MJ/kg, which the upper range is relatively close to the values of wood or peat (Vanhatalo and Ahtila, 2001). Table 2.1 summarizes elemental analyses and calorific values of mixed sludge for different operations.

Table 2.1 Elemental analysis and calorific value of mixed sludge and other paper rejects

Process	Solids% w/w	Ash % w/w	C% w/w	H% w/w	S% w/w	O% w/w	N% w/w	HHV (MJ/kg) (d.b.)
Pulp	42.0	4.9	51.6	5.7	0.9	29.3	0.9	19.2
Kraft	37.6	7.1	55.2	6.4	1.0	26.0	4.4	18.5
De-inking	42.0	20.2	28.8	3.5	0.2	18.8	0.5	12.0
Recycle	45.0	3.0	48.4	6.6	0.2	41.3	0.5	14.8
Bark	50.0	0.4	50.3	6.2	0	43.1	0	20.8
Wood chip	79.5	0.2	49.2	6.7	0.2	43.6	0.1	19.4

It has been reported that the density of the mixed sludge ranges from 400 to about 700 kg/m^3 (Kraft and Orender, 1993). However, these numbers are related to mixed sludges that contain a higher proportion of primary sludge, resulting in a higher dry solids level was achieved after the dewatering. These dry solids contents can not be achieved for the mixed sludge currently produced in pulp and paper mills because it contains a high proportion of secondary sludge. For instance, the highest dry solids content that can be achieved for current kraft mixed sludge is about 27% w/w or less, far less than the value in Table 2.1.

2.2. Mixed Sludge Disposal Alternatives

There are various sludge disposal options available to pulp and paper mills in Canada, the United States, Europe and other countries, and the selection of one or more of these options will be site specific. It is interesting to note that the distribution of mills using each of the main

disposal options varies from province to province and country to country based on local barriers to each option relative to environmental, economic, legislative and public perception factors. Below are the three most popular practical alternatives:

2.2.1. Landfilling

Historically landfilling has been the practical method of choice for biomass disposal, and remains the primary disposal technique for many mills (Scott et al., 1995; NCASI, 1999; Hackett et al., 1999; Reid, 1998). In recent years, landfilling of mixed sludge has dramatically decreased because of rapidly shrinking landfill space, public opposition to opening new landfill sites (Rouleau and Sasseville, 1996), leachate-related issues and, above all, poor economics to afford high associated costs such as transportation. In many cases the costs of opening a new landfill site are prohibitive due simply to legal restrictions (Lagace´ et al., 1998 and 2000; Mahmood and Elliott, 2006). A survey of the Canadian pulp and paper industry sector in 1995 and 2002 indicated that landfilling of pulp and paper mixed sludge and solid residues in 2002 had decreased by 50% compared to 1995 values (Elliott and Mahmood, 2005). This decrease can be greatly related to the fact that no economic benefit can be derived from the waste if it is lanfilled. In addition, there is the cost of transporting the sludge as well as the increasing environmental restrictions placed on disposal sites. Landfills must now be constructed with leachate collection systems and a plan for closing out the site and monitoring it in the future. Current trends show that mills are moving away from this disposal technique and are looking to increase combustion and other beneficial options.

2.2.2. Composting and Landspreading

Composting of sludge is another alternative. However several inconveniences such as odor and non-maturity of the compost made from the pulp and paper sludge are prohibitive factors aside from the long residence times required to compost the mixed sludge. It has been reported that the residence time for pulp and paper sludge is about 30-50 days due mainly to poor and hard biodegradation of sludge components (Haug, 1993). Therefore, this alternative is not unfeasible,

given the large quantities of sludge produced in pulp and paper mills. It has been reported that the costs of composting are higher than for simple landfilling. Furthermore, advanced systems require infrastructure such as enclosed buildings, aeration equipment, material handling, and control systems. Besides all mentioned above, the market size and how far the compost products can be sent, are main barriers for this option.

The GHG emissions from landspreading have compounded the problems with existing sludge management practices. Landspreading of sludge, which was widely practiced in Quebec in the past, is increasingly regulated in the current situation. Landspreading of pulp and paper residues only accounts for disposal of less than 5% of the total residues generated (Reid, 1998). Public opposition to this disposition method has limited the widespread use of this method as well. It is apparent that the conventional sludge management methods, which might have been acceptable in the past, can no longer be considered optimal to meet present and future requirements. The majority of mill operators in North America are gradually moving towards burning a portion of the sludge in existing bark boilers to recover the intrinsic heat value. In conclusion, both composting and landspreading are not feasible, and mill operators are considering "waste solids to energy" alternatives (CANMET, 2005).

2.2.3. Combustion

For many waste products, combustion is an attractive and/or necessary element of waste management. Occasionally, it is called disposal of waste in boilers. Combustion provides several potential advantages including:

- Substantial volume reduction: This is an important element while dealing with bulky materials such as mixed sludge and/or materials with high moisture content.
- Detoxification: This is specifically important for pathologically contaminated materials, toxic organic compounds, or biologically active materials such as mixed sludge.
- Environmental impact mitigation: Organic materials such as mixed sludge can produce leachate when landfilled. Furthermore, the impact of the CO_2 (GHG) generated in incinerating solid wastes is less than that of the methane (CH_4) and CO_2 generated in

landfilling operations. Also, the CO_2 generation per kilowatt of power produced due to incineration of solid wastes is significantly less than that generated by the coal and oil-burning utility plants whose electricity would be replaced by waste-to-energy facilities.

- Energy recovery: This is an important element when large quantities of solid wastes are available such as those from pulp and paper mills, and a reliable market and need for by-product steam and electricity are nearby.

These and several other advantages have encouraged the development of a variety of incineration systems of widely different complexity and functionality to meet the needs of research institutions, industry, and commercial firms. Contrary to these advantages are the disadvantages such as high capital costs of the combustion facilities, public sector concerns, technical risks, and staffing and operating problems (Niessen, 2002).

Sludge has been described as "difficult to burn" (Kraft and Orender, 1993) due mainly to its high moisture content and occasionally high ash content. As mentioned earlier, sludge dewatering typically can only bring the sludge up to a solids content of 30 to 40% w/w (NCASI, 1992), with the upper range being more and more difficult to achieve with increasing concentrations of secondary sludge (Frei et al., 2004). As a result of low dry solids content, boiler efficiency drops significantly when the materials with higher moisture content (>65% w/w) are combusted (Kraft and Orender, 1993).

Table 2.2 summarizes the main alternatives for pulp and paper mixed sludge disposal.

Table 2.2: Pulp and paper industry sludge disposal techniques

Disposal Technique	Advantages	Disadvantages
Landfilling	-Established -Simple disposal -No complex treatment	-Greenhouse gas emissions -Transport offsite -Increasing environmental restrictions -Increasing high cost -Odor problem -Needs suitable sites
Landspreading	-Improves soil characteristics -Returns some nutrients & carbon to environment	-Potential liabilities (metals, pathogens and non-elemental particles) -Odor problem -Transportation & spreading equipment -Regulatory complexity and requirements

Composting	-Produces saleable product -Destroys pathogens -Low energy consumption -Well-established at the full scale	-Capital costs associated with facilities -Reliable market for product -Long residence time required for treatment -Mostly batch operation (except VCU technology) -Transportation of the product
Recycling to the process	-Reclaims value in new products -Reduces burden on other sludge disposal techniques	-Reduces product quality (mostly paper quality) -Limited to specific board and paper products -Sludge pretreatment process sometimes required
Combustion	-Energy recovery -Significant volume reduction of wastes -Displaces fossil fuels (at appropriate dryness level) -Reduces GHG emissions	-High capital costs (if the boiler does not already exist in the mill) - Operating risk (if moisture content is too high) - High maintenance cost -Ash management required -Equipment corrosion
Thermal processes	-Energy is derived from waste heat sources -Potential for profitable operation - Sludge kept onsite	-Complex technology (due to process integration) - Not yet proven commercially -High capital cost

2.2.3.1. Effect of Dry Solids Content on Combustion

One of the main criteria for a successful combustion operation is the dry solids content of the biomass feed into the incinerator. Previous research reported that in order to guarantee stable conditions in the boiler, the critical level of dry solids content of combustible materials should be about 45% w/w (Kudra et al., 2002; Kraft et al., 1996; Roy et al., 2006). The moisture content of mixed sludge has a significant negative impact on the overall efficiency of thermal oxidation. Boiler efficiency can drop considerably at a high moisture level. Figure 2.2 describes the inverse relationship between the efficiency of the boiler and the moisture content of the biomass being burned (Liang et al., 2003).

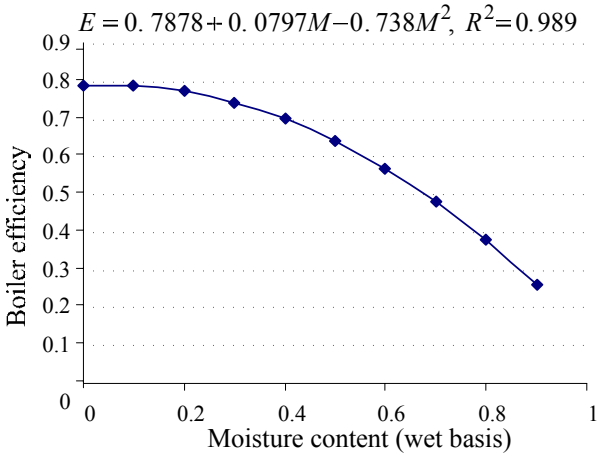

Figure 2.2: Boiler efficiency vs. moisture content of biomass (Adapted from Liang et al., 2003)

Boilers are required to deal with the excess moisture found in wet biomass, which leads to larger volumes of flue gas being produced. This results in more elaborate air handling systems downstream of the boiler (Kraft and Orender, 1993). Therefore, with these issues being stated, mixed sludges require drying prior to being feed to the boiler for combustion.

2.3. Principle of Porous Media Drying

Drying technology generally reduces the moisture content of a matrix by the application of heat, causing water to evaporate into the air phase (vapor) resulting in drier outputs (solids) of desired characteristics (Dufour, 2006). Drying phenomena have been widely researched. However, the micro-scale mechanisms of porous media drying are highly complex and not fully understood (Konovalov, 2005). Drying technology has been developed within the scope of the food, agricultural, pharmaceutical, pulp and paper, and many other industries (Mujumdar, 2004 and 2007). For environmental engineering applications, dryers using external sources of heat have been used for refuse-derived fuel (RDF) drying (e.g., rotary cascade and thermo-pneumatic) (Manser and Keeling, 1996) and sludge dewatering (Chen et al., 2002).

Whilst no relevant research particular to biodrying is available, relevant science has been summarized elsewhere for the cases of drying of foods (Basu et al., 2006), grains (Mujumdar and Beke, 2003), and wood (Krupinska et al., 2007).

The vapor-carrying capacity of air is limited at each temperature by the saturation point, after which condensation occurs. At a given level of relative humidity of air, the mass of water vapor that the air can hold increases with the temperature. Relative humidity has been used in near ambient drying modeling to estimate the distance from saturation point of inlet air, i.e., it can be perceived as a surrogate measure of its drying potential (Mujumdar, 2007).

2.3.1. Drying of Pulp and Paper Mixed Sludge

For the various reasons cited above, the pulp and paper industry is seeking to develop efficient techniques to dry mixed sludge that can guarantee the economic viability of sludge combustion. However, the main question is "what would be a cost effective drying technique pertinent for sludge drying?", given the relatively low calorific value of sludge and technical difficulties such as stickiness, shrinking, and deformable characteristics that demand substantial maintenance. An interesting observation with sludge energy content at different moisture content shows that the energy content of the pulp and paper mixed sludge is doubled when the dry solids content is increased from 20% w/w to about 50% w/w. As can be observed in Figure 2.3, further drying (>50% w/w dry solids content) brings little additional value to the energy content of the mixed sludge. Therefore, if drying of sludge from an initial value of 30 % w/w to about 50% w/w dry solids content can be accomplished in an efficient and economically viable way without facing major technical complexities, it can result in a significant economic benefit to the boiler operations (Hippinen and Ahtila, 2002). Roy et al. (2006) found that a 45% w/w dry solids content is an economically feasible level for most of the pulp and paper mills considered.

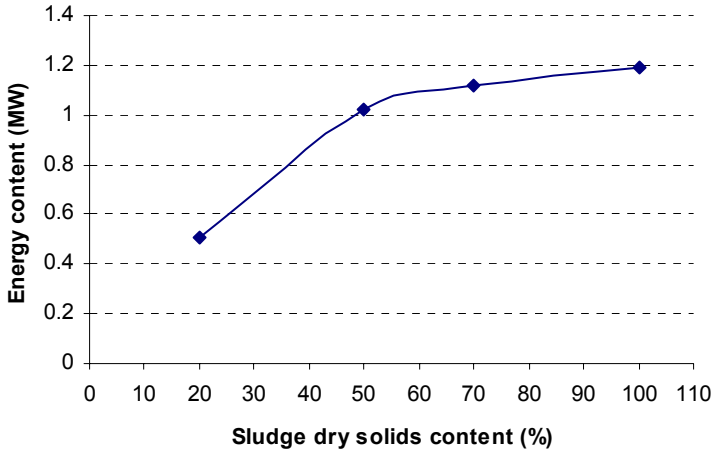

Figure 2.3: Energy content of mixed sludge vs. dry solids content
(Adapted from Hippinen and Ahtila, 2002)

In recent years, a number of sludge drying innovations have entered the market with the objective to provide economic solutions that address the problem of low and variable solids content of dewatered mixed sludge in the pulp and paper industry.

Chen et al. (2002) provided an overview of pulp and paper sludge dewatering and possible drying alternatives. Direct, indirect, and combined drying alternatives were reviewed for the drying of activated sludge from the pulp and paper industry. However, based on the preliminary assessment, it was concluded that it is necessary to develop a new drying process that can be economically feasible and thermally efficient.

Banerjee et al. (1998) and Beckley and Banerjee (1999) developed an impulse drying method to dry mixed sludge from pulp and paper mills. The mixed sludge is briefly exposed under pressure to a hot surface. This technique enhanced drying compared to a purely thermal drying approach, but implies high temperatures and a complex technology. Vaxelaire et al. (2000) studied the convective drying of activated sludge with ambient air at temperatures of 41-60^{o}C. The results showed that the activated sludge was very difficult to dry because of the crust formation. Kudra et al. (2002) studied the hydrodynamics and drying kinetics of pulp and paper sludge via a lab scale batch pulsed fluid bed dryer, where high dry solids contents (88% w/w) of the disintegrated mixed sludge were achieved. The hydrodynamics considered included the development of pressure drop, minimum pulsed-fluidization velocity, dynamic bed height, and mass flowrate coefficient equations. However, there is no information available at full scale.

Hippinen and Ahtila (2004) reported an experimental small-scale approach for the drying of activated sludge under partial vacuum by means of waste energy streams. Waste heat sources are widely available in pulp and paper mills, particularly since recent environmental legislation and restrictions have prompted mills to minimize water consumption which leads to an increase of the water temperature in the system. The warm water needs to be cooled in order to be reused in the process, and one possibility would be to use this energy to dry activated sludge. It was concluded that partial vacuum drying of mixed pulp and paper sludge can provide a competitive solution to this challenge. However, this conclusion was made based on small-scale laboratory experimentation. Léonard et al. (2006) found that the controlling mechanism in the early stage of activated sludge lab-scale convective air drying was the external heat transfer. However, all of the above-mentioned conclusions of various studies were made either in lab-scale or without economic consideration.

2.3.2. Pilot-Scale Drying Technologies for Mixed Sludge Drying

Dry-Rex is a commercially proven technology that uses waste heat to dry mixed sludges and relies solely on the moisture concentration gradient as the primary driving force for drying. The Dry-Rex system uses unsaturated ambient air drawn through a moving bed of wet particulate material or palletized paste. Drying is carried out in two stages (Figure 2.4): in the first stage, large-size material (such as sugarcane or bark) is chopped to enhance the heat and mass transfer area as well as to reduce resistance to moisture diffusion. Pasty or semisolid feeds may be mechanically pressed to form a granular product of required dimensions. In the second stage, drying occurs as ambient air passes through the stationary bed placed on a multi-desk perforated belt conveyor. The competitive aspect of this type of dryer is the low temperature required for drying. These advantages are partially offset by the need for high capacity fans to provide air velocity high enough to compensate for the lower heat transfer rates due to the use of lower air temperature. Also, the ambient air should be sufficiently dry for this method to work efficiently. An alternative model of the Dry-Rex system includes a heat exchanger to preheat ambient air utilizing low-grade heat such as waste process water, steam, or exhaust air from other thermal processes. The ambient air dryer as shown in Figure 2.4 has been tested by a manufacturer for a

variety of materials including solids (bark, wood chips, and sugarcane residues), pastes (wood pulp, pulp and paper mill sludge), and powders (ash and fly ash). Table 2.3 presents representative data on ambient air drying of various wastes from paper mills.

However, the capital cost of this type of dryer is quite high, and except for a few cases, the economics of the process are unattractive for the Canadian pulp and paper mills. Nevertheless, this technology has proven that low temperatures near ambient conditions have the potential to dry the mixed sludge under forced convection and vacuum conditions.

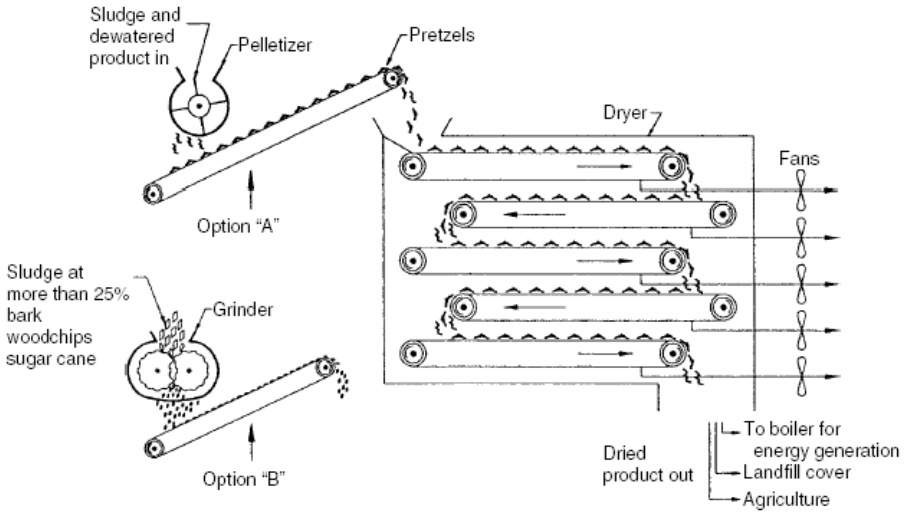

Figure 2.4: Dry-Rex schematic

Table 2.3: Dry-Rex typical operating conditions (Barré and Bilodeau, 2001)

Primary/secondary sludge ratio	Air temperature (^{o}C)	Air relative humidity (%)	Initial dry solids content (%w/w)	Final dry solids content (%w/w)
10/90	17	60	12.6	69
66/33	17	60	14.6	68
64/36	5.5	30	29.8	73
35/65	18	62	15.6	78
30/70	15	40	24	83
60/40	17	62	19	78
Deinking sludge (50 % w/w clay)	16	92	38	92
Frozen bark	20	62	40	70
50/50 % w/w Bark /sludge	20	29	40	79

A comprehensive review of available drying technologies was conducted for the CANMET Energy Technology Centre in Canada including fluidized bed, rotary, paddle, superheated steam pneumatic (GEA exergy steam dryer), belt dryer, integrated sludge dewatering and drying systems (J-VAP and DryVac), integrated sludge drying and combustion systems, the TLG sludge drying process, the Dry-Rex dryer, solar dryers, and cyclonic dryers (CANMET, 2005). The main advantages and disadvantages of each are summarized in Table 2.4.

Table 2.4: Advantages and disadvantages of conventional drying technologies

Disposal Technique	Advantages	Disadvantages
Fluidized bed dryers	-direct drying -gentle, fast and uniform drying at low temperature -low space requirements -high degree of product dryness	- high initial capital costs - requires off-gas handling and cleaning equipment - high degree of auxiliary equipment required
Rotary dryers	-provides for drying and granulation in one step - allows for reclamation of waste heat - versatile in configuration - well-suited for heavy products	- large floor space requirement -high capital and maintenance costs - back mixing to avoid sludge agglomeration required
Paddle dryers	-high ratio of heat transfer surface area to overall dryer volume - self-cleaning of the intermeshing paddles - low space requirement - low capital and installation costs - well-proven, commercially available technology	- relatively high complexity of equipment - high maintenance costs - sensitivity to large agglomerates, grit, or rocks in the sludge - jamming or premature wear of the paddles
Superheated steam pneumatic dryer	- compact design - short product residence time - low floor space requirements - 80-90 % energy recovery from the drying process possible - closed-loop steam cycle	- back mixing of dried product with wet feed - relatively high specific energy consumption - turbulent drying conditions and high capital cost
Belt dryers	- ability for low-grade energy usage - low air temperatures required (30^{o}C - 90^{o}C) - no back-mixing of dried product with wet feed required	- large floor space requirement - relatively high degree of auxiliary equipment - high complexity of equipment - high maintenance, and long residence time
Integrated sludge dewatering and drying systems	- indirect sludge drying	- new technology - no installation for pulp and paper mixed sludge
Integrated sludge drying and combustion systems	-surplus heat generation -cyclone furnace is used for incineration	- treatment of boiler flue gas required - high degree of auxiliary equipment - large floor space requirement
TLG dryer	- low-temperature drying - no loss of energy - surplus heat generation	- relatively high floor space requirements - manufactured in only two sizes

	- low degree of auxiliary equipment required	(1.6 and 20 tonnes per day)
Dry-Rex dryer	- low-temperature air (30^{o}C - 70^{o}C) - accelerated drying process	- huge volume of air is required - powerful vacuum system required for large air volumes - many moving parts - investment cost very high
Carver-Greenfield	- efficient heat transfer rates - dries difficult (very wet) substrates	- very high capital cost - complex system - not generally applied in the P&P industry
Solar dryers	- natural energy from sun	- large space requirement - odor problem - regional and seasonal
Cyclonic dryers	- Direct drying - Better contact - Short residence time	- not proven commercially - wet sludge feeding problem
VCU	- Less footprint and low maintenance - Fully biodegrade food type wastes - Provides uniform and better end product quality	- not proven for pulp and paper mixed sludge - It does not work based on forced convection - relatively long residence times (14-20 days)

The majority of these technologies suffers from technical uncertainty and has questionable economic benefits. Therefore, new efficient drying technologies for mixed sludge continue to be explored so that the dry solids content of mixed sludge may be raised to values above critical levels for safe and economic combustion. One such solution is the biodrying technology, which can provide both economic and environmental benefits.

A recent review conducted by Velis et al. (2009) revealed that the biodrying process is a new concept, and published literature in this field is very limited. The biodrying process depends on several factors which are discussed below.

2.4. Biodrying Process

To the knowledge of the author, the term biodrying was coined by Jewell et al. (1984) whilst reporting on the operational parameters relevant for drying cattle manure. Here, the term biodrying denotes: a) the bioconversion reactor within which waste is processed, b) the physiobiochemical process, which takes place within the reactor.

In biodrying, in addition to the forced convection, the drying rates are enhanced by the biological heat generated from the metabolic activity of mesophilic and thermophilic microorganisms within the matrix. The matrix dries by means of two main steps: a) water molecules evaporate (i.e., change phase from liquid to gaseous) from the surface of waste fragments into the surrounding air, and b) the evaporated water is transported through the matrix by airflow and removed with the exhaust gases.

On the biochemical side, aerobic biodegradation of readily decomposable organic matter occurs. On the physical side, convective moisture removal is achieved through controlled forced aeration. Whilst the general reactor configuration and physio-biochemical phenomenon is similar to composting, the way in which it is operated is significantly different. During multiple cycles of biodegradation, a widely diverse population of micro-organisms catabolizes substrates through complex biochemical reactions to satisfy metabolic and growth needs (Richard et al., 2004).

In biodrying, air convection and molecular diffusion are the main transport mechanisms responsible for moisture flow through the matrix (Frei et al., 2004). Air convection, induced by engineered airflow through the matrix, is almost exclusively responsible for the water losses that are readily removable. Air carries the water evaporated from the surface of matrix particles (free moisture) with which it is in contact. Removal of water content from the waste matrix (desorption) by convective evaporation is governed by the thermodynamic equilibrium between the wet waste matrix (solid phase) and the air flowing through the matrix (gas phase).

Klaus (1992a, and 1992b) studied the effect of operating variables on the biodrying process for municipal sludge, i.e. the ratio of sewage sludge to flocculating agent, the throughput of the sludge, the temperature of the inlet air, as well as the residence time on the controllability of the biodrying process. By controlling these variables, it was possible to optimize the biodrying operation. Additives were added as conditioning agents to the sludge. Nellist et al. (1993, 1997) reported that fast biodrying determines low biological stability and vice versa. A similar result was confirmed by Adani et al. (2002). Adani et al. (2002) reported that the biological stability provided by the biodrying process could minimize odors and biogas production of municipal waste sludge. Choi et al. (2001) concluded that high moisture removal can be achieved in a full-scale, well insulated biodrying reactor. Hansjoerg et al. (2004) developed a method for the continuous biological drying of garbage residues and sewage sludge. The technique involved

continuous measurement of carbon dioxide in the exhaust air along a closed transport track in order to control the air supply, so that the carbon dioxide in the exhaust air was kept within a range of 0.05 to 0.4 % by volume. Sugni et al. (2005) reported that biodrying could be a good solution for municipal solid waste management, allowing for the production of fuel with attractive energy content. Lhadi et al. (2005) studied the evolution of organic matter and the humidification process during the co-composting of the organic fraction of municipal solid waste and poultry manure with two different particle sizes (0.2 and 1 cm). The results suggested that hemicelluloses were readily degradable compared to cellulose and lipids. It was also pointed out that the degradation phenomena were more marked for mixtures with lower particle sizes. The techno-economic analysis of Laflamme-Mayer et al. (2004) illustrated that biodrying could be an attractive alternative for those pulp and paper mills that are seeking to eventually achieve zero-effluent operations when compared with other alternatives such as low sludge production and retrofit of hollow fiber membranes into the aeration basin.

2.4.1. Microbiological Aspect of the Biodrying Process

Within the biodrying reactors, waste is dried by air convection, and the necessary heat is provided by exothermic decomposition of the readily decomposable waste fraction. Therefore, the knowledge of the microbial aspect of biodrying is essential for better process understanding and control. As described earlier, the biodrying technology refers to the method of achieving mesophilic and thermophilic aerobic biological activity in the biodrying reactor and aims largely at preserving the higher heating value of the biomass under treatment in the biodryer. Sludge may be mixed with a bulking agent to absorb moisture and assist aeration by providing sufficient pneumatic aerobic conditions. As soon as the bacteria decompose the organic matter, the biodrying reactor heats up. The main parameters to consider in an aerobic degradation process are the microbiology, oxygen, nutrient, and moisture requirements. Aerobic decomposition is an exothermic process, and for pilot-scale reactors the limited surface to volume ratio limits heat loss and causes temperatures to rise (Haug, 1993; Finstein et al., 1985). The higher temperatures result in an accelerated biodegradation process, reflecting in microbial growth rates, new cell production, rapid microbial multiplications and more CO_2 and H_2O production. However, there is an optimum temperature where the microbial growth is at peak

value, and further rise in temperature suppresses the microbial growth cycle. Depending on the type of biomass, the optimum temperature could vary, but several studies have confirmed that the optimum range of microbial growth for thermophilic microorganisms is 50-65^{o}C. This suppression results from a number of factors, both on a molecular scale as enzymes required to catalyze biodegradation reaction are denatured, and at an ecological scale as individual microorganisms and hence entire species experience thermal death (Richard, 1997). Chemical and physical conditions also have an influence. The physical, biological, and chemical decomposition processes are so complex that it becomes difficult to ascertain exactly how these processes are interrelated because they are in a continuous state of change.

2.4.1.1. Microbial Reaction in Biodrying Process

The following aerobic exothermic microbial reaction takes place in the matrix of mixed sludge:

$$Substrate + aO_2 \rightarrow bCO_2 + cH_2O + New\ cell,\ \Delta H_r < 0 \quad (2.1)$$

The biodrying reactor is self-heating, relying on microbial heat production to obtain the required process temperatures. This provides an advantage over conventional drying systems that require an external heat source (Mason and Milke, 2005a and 2005b). In reaction Eq. (2.1), the substrate represents readily biodegradable components in the mixed sludge. Table 2.5 covers the majority of these components and their degradability. As can be seen, the most readily biodegradable components are kraft cellulose and hemicellulose, whereas the least biodegradable component is lignin.

Table 2.5: Degradability of mixed sludge and its composition (Adapted from Haug, 1993)

Component		%w/w (d.b.)	Degradability (%)
Cellulose	Mechanical pulping	15	50
	Kraft pulping	40	90
Hemicellulose		10	70
Lignin		10	0
Lipids		8	50
Protein		4	50
Other sugars		10	70

2.4.1.2. Microorganisms Classification

Metabolic distinctions between organisms provide a useful tool to understand both the effect of an organism on its surroundings and the environment necessary for proper growth of the microorganism. A wide range of microorganisms (bacteria, actinomycetes and fungi) metabolize organic compounds in waste; however, not all the decomposition of organic material in composting is biological in nature. The microbiological strains found in a composting environment are highly varied. The effectiveness of bacteria and fungi in decomposing the organic material is based on the operational conditions of the process involved. This encompasses a range of different groups of organisms that can be categorized based on their temperature tolerances. Bacterial species responsible for biological activity can be classified into four groups based on temperature preferences (Figure 2.5): psychrophiles (active at 0-20^{o}C), mesophiles (active at 8-48^{o}C), thermophiles (active at 42-68^{o}C) and hyperthermophile (active at 70-110^{o}C) (Madigan and Martinko, 2006). Only mesophilic and thermophilic bacteria are considered in the biodrying process because they are active within the usual temperature range of the reactor. As reported by Frei et al. (2004) and Roy et al. (2006), the typical temperature range for microbial degradation in the batch biodrying reactor was 15-55^{o}C, although high temperatures of up to 65^{o}C have also been observed. The bacteria are very sensitive to the temperature of the matrix in which they grow. As shown in Figure 2.5, higher temperatures kill mesophilic bacteria while favoring growth of thermophiles. Nevertheless, thermophilic bacteria also suffer from extremely high temperatures.

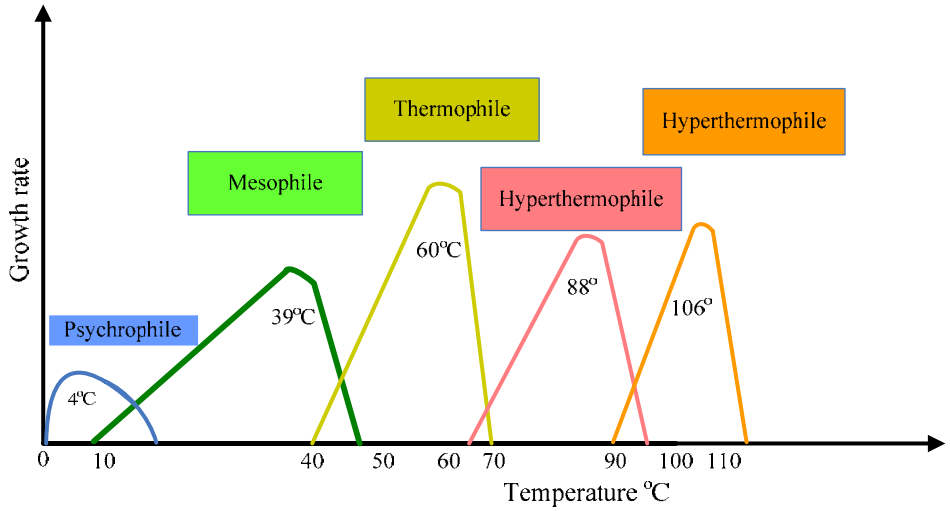

Figure 2.5: Effect of temperature on microbial growth rate of different microbes (Adapted from Madigan and Martinko (2006))

2.4.1.3. Oxygen Requirements

Oxygen availability remains one of the critical factors in all biodegradation processes. The presence or absence of oxygen even provides the basic terminology for classifying the bioprocesses as aerobic and anaerobic. Nevertheless, a pure aerobic bioprocess is always difficult to achieve. This difficulty is compounded by transport limitations both in microscopic and macroscopic scales. Aerobic biodegradation requires uniform and sufficient oxygen transfer to ensure that microorganisms are able to respire at optimum levels. For instance, in aerated composting, a compost pile should be adjusted to keep oxygen percentages between 5-15 % v/v as compared to 21% v/v in air (Campbell et al., 1991). This translates to about 1 to 4 grams of oxygen per gram of biodegradable material (or ~ 4 to 17 grams of air per gram of material) (Haug, 1993). However, these values represent only the oxygen required for metabolism. When drying of the material is considered (as with the biodrying application of this work), the aeration rates are far in excess (10 to 30 times) of those required for biological oxidation (Haug, 1993). Air must be properly diffused and be able to reach all pockets of material to minimize anaerobic zones. If the air does not penetrate into clumps of material, local anaerobic conditions develop.

As for the mechanisms of the oxygen transfer, the air is first supplied to the porous space of the mixed sludge, and then oxygen is transferred to the gas/liquid interface. It then diffuses across

the interface and reaches the microbes through the liquid phase (Figure 2.6) in which the microbial reaction takes place. Microbial degradation will cause a concentration gradient and drive the diffusion of oxygen from air to the liquid phase. Conversely, the products of the biological reaction, i.e. CO_2, H_2O and NH_3 (to some extent) will transport towards the gas phase (airflow). The transfer of O_2 is a slow phenomenon and is mainly controlled by diffusion. Therefore, the superimposition of forced aeration in the biodrying process can enhance the mass transfer.

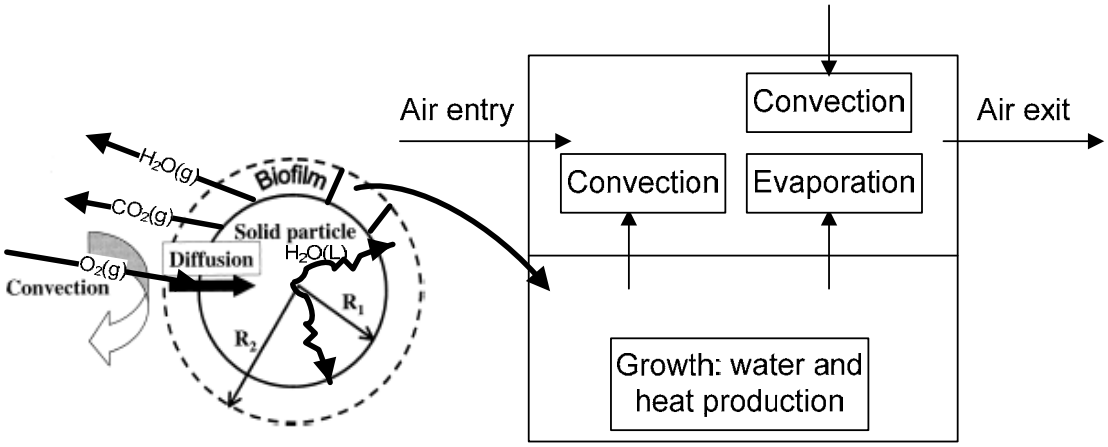

Figure 2.6: Schematic representation of mass transfer mechanisms

In the biodrying process, like aerobic composting, oxygen and carbon dioxide profiles are mirror images of each other (Kulcu et al., 2008).

2.4.1.4. Nutrition Level

Sufficient concentrations of key nutrients (nitrogen, phosphorus, sulfur, and other trace nutrients) are required by organisms for proper cell growth. The carbon to nitrogen ratio is the most often cited nutrient parameter. The ideal range for active microbial biodegradation is a 20:1 to 40:1 C/N ratio (Campbell et al., 1991; Naylor, 1996). In the pulp and paper industry, nutrient carryover from the wastewater treatment facilities typically meets this range. Table 2.6 shows some data for C/N ratio in a variety of materials.

Table 2.6: C/N ratios for various biomass materials

Biomass category	Biomass material	C/N ratio	Reference
Pulp and paper	Primary sludge	23-930:1	Thaker (1985)
	Secondary sludge	9-81:1	Shimek et al. (1988)
	Mixed sludge	6-115:1	Scott et al. (1995)
	Wood chips	492-535:1	McBurney (1993) ; Durai-Swamy et al. (1991)
	Bark	160-534:1	James and Kane (1991) McBurney (1993)
	Recycle paper sludge	487:1	Kara (1994)
Municipal	Synthetic food waste	8.4:1	Richard (1997)
	Sewage sludge	7.2	

Different mixtures of biomass substrates (sludge, bark, etc.) will result in unique C/N ratio. While secondary sludge has a very low C/N ratio, materials such as bark and fiber possess little nitrogen and therefore very high ratios. Larsen and McCartney (2000) found a negative linear correlation between heat generation and the C/N ratio for paper mill sludge, with high levels of heat generation occurring in the range of C/N=15-30. As the amount of bulking agent (bark) increases, the C/N ratio will also increase, so the amount of heat generation must be balanced against the increased porosity that the bulking agent provides.

2.4.1.5. Moisture Content

Moisture is vital to the proper functioning of the microorganisms. The cell membranes must remain permeable to a steady flow of soluble nutrients by osmosis (Naylor, 1996). The metabolic reaction can theoretically take place at high moisture levels, but such levels decrease the availability of oxygen needed to sustain aerobic decomposition. This is due to the slow diffusion of oxygen into the thick liquid biofilm that separates it from the microorganisms. Nakasaki et al. (1994) reported that the optimum moisture content for the microbial activity is 45-65% w/w. This has been confirmed elsewhere (Liang et al., 2003; Campbell et al., 1991; Naylor, 1996; Haug, 1993). If the moisture content is too high, oxygen will have difficulty

traveling through the system, and if it is too low, the microorganisms exhibit reduced performance. Due to variations in pore size distribution, surface tension, and internal porosity, the moisture content might vary from one point to another even though the residence times are nearly the same (Richard, 1997). Operating the biodrying process under optimum conditions will preserve the higher heating value of the sludge and thus lead to higher energy recovery when the sludge is combusted in the boiler.

2.4.2. Critical Review of the Batch Biodrying Process

The batch biodrying reactor was developed by Frei et al. (2004) for the drying of pulp and paper mixed sludge. The reactor was a 1-m^3 lab scale reactor equipped with two sets of conduits for the air inlet and outlet. Temperature and pressure were measured within the porous matrix of the mixed sludge, and relative humidity and air flowrates were measured in the inlet and outlet air flows.

Mixed sludges were dried using a combination of injected and extracted air streams that were heated by thermophilic microorganisms within the mixed sludge that generate heat through their metabolic activity. The mixed sludges combined with wood waste were deposited into the batch biodrying reactor. The locations of temperature and pressure probes inside the batch biodrying reactor are illustrated in Figure 2.7.

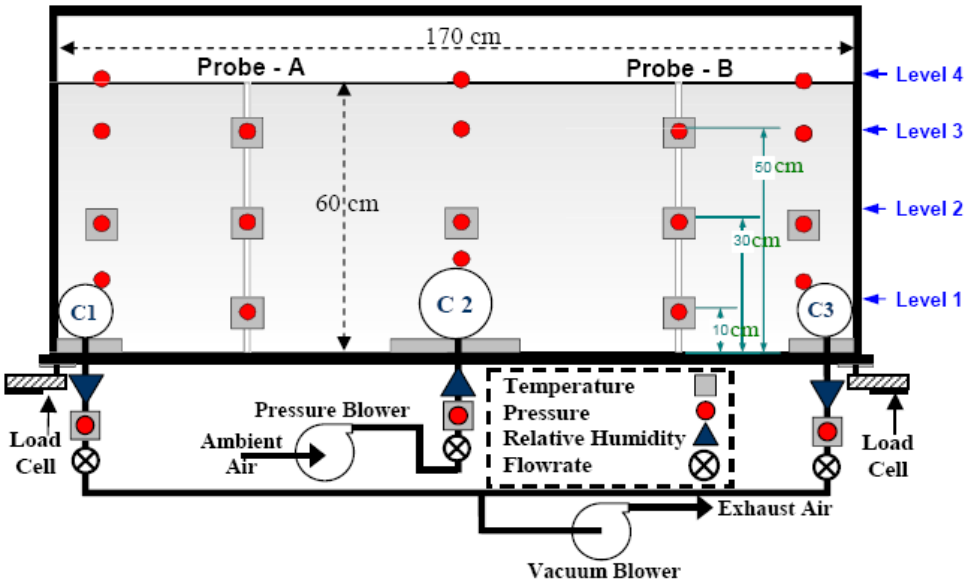

Figure 2.7: Schematic of the batch biodrying reactor

This study found that a sludge to wood waste ratio of 2:1 (dry mass basis) provided acceptable pneumatic conditions. The internal heat generation (bioheat) raised temperatures to peak values of approximately 65°C, and carbon losses from biological activity ranged from 5% w/w to 18% w/w. The results highlighted a clear correlation between the peak temperature of the matrix and the rate of water removal. The study also included a techno-economic analysis that demonstrated the economic viability of implementing the technology in the Canadian pulp and paper industry (Frei et al., 2006).

In summary, the followings were achieved:

- Moist air rewets dried sludge when air flow is reversed, resulting in renewed biological activity and increased matrix temperatures for a period of 10-20 hours
- The rewetting period and increased biological activity increased outlet air temperature, permitting saturated air to carry more moisture on a mass basis, thus increasing the drying rate
- The matrix rewetting is most significant in the earlier periods of the batch experiments when the overall matrix is still quite wet
- There are indications that air flow preferentially passes via the shortest route between the inlet and outlet air ports, preferentially drying the lower matrix
- As the matrix dries, the permeability of the matrix increases dramatically, lowering the pressure loss across the matrix and reducing the extent of preferential flow in the lower reactor
- It was found that there was more air passage in the lower portions of the batch reactor configuration than near the top (especially in the early stages of the batch treatment).

In the second study, Roy et al. (2006) conducted extended batch biodrying experiments to technically investigate the reliability of the batch biodrying reactor and to optimize the process with a 1 m^3 modified batch biodrying reactor as shown in Figure 2.8. The reactor contained online instruments capable of measuring temperature, pressure, and relative humidity.

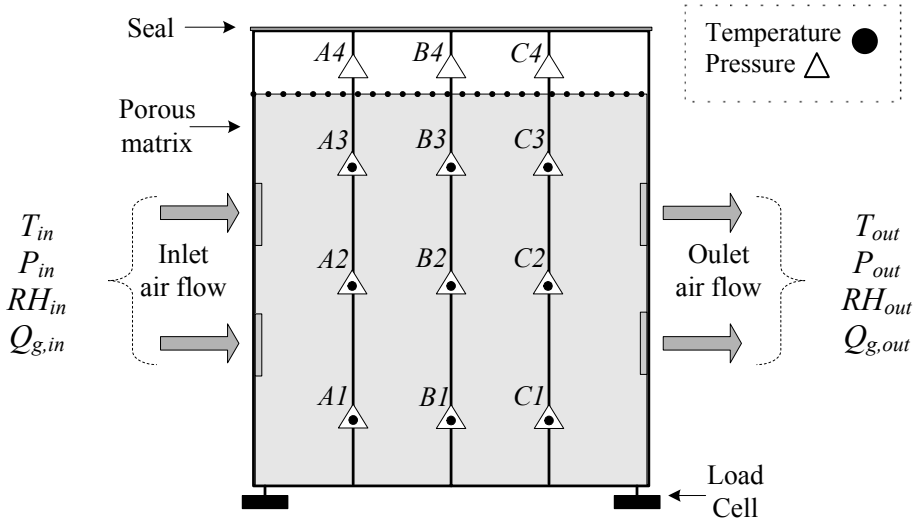

Figure 2.8: Schematic diagram of the batch biodrying reactor

Several experimental runs were conducted on biodrying of mixed sludge from the pulp and paper industry over a 15-day residence time period. It was found that:

- After 15 days of treatment, the average cumulative mass loss was 223 kg +/- 23 kg for average initial water content of 474 kg, representing a 47% decrease
- For each experiment, maximum spatial temperature gradients (≈ 50°C) occurred at the beginning of the experiment
- The temperature gradient declined exponentially throughout the experiments to approximately 20°C in the final days of treatment
- The most influential parameters were: C/N ratio and matrix outlet temperature
- The least influential parameters were: initial sludge and bark dry solids content , and storage time of material prior to treatment
- Cell counts on samples taken before and after the exponential growth rate period confirmed that cell concentrations increased from approximately 10^6 CFU/g to 10^8 CFU/g
- Energy balances resulted in average biological energy production rates of 23 - 39 W/kg-dry basis
- Due to the precipitation of moisture on mixed sludge, air flow inversion favored biodegradation rather than biodrying

- It was concluded that based on the experimental results, the biodrying process appears to be a promising energy efficient drying technology, providing a potential solution to the problems inherent in the combustion of wet sludge.

A techno-economic assessment of a case study based on the results of the batch biodrying reactor performance yielded maximum return on investment at a dry solids level of 45% w/w (Figure 2.9).

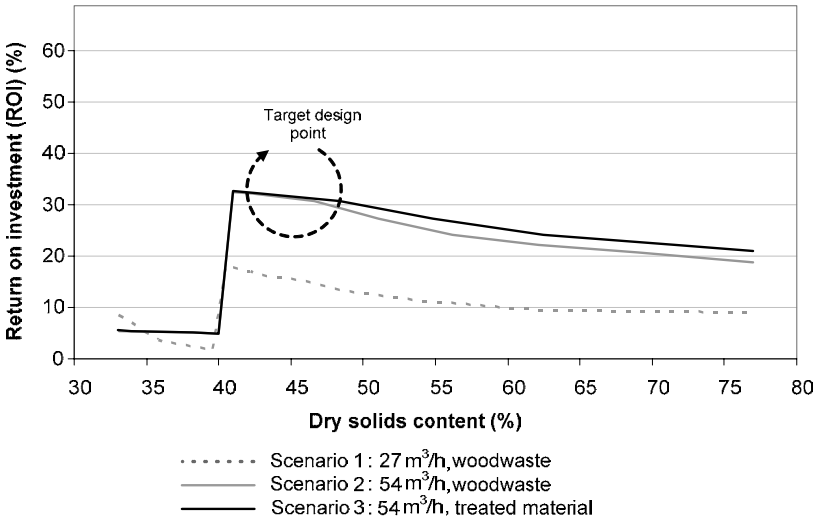

Figure 2.9: Impact of dry solids content on return on investment
(Adapted from Roy et al. (2006))

In conclusion, the techno-economic assessment of this study revealed that the biodrying technology could be very attractive if the sludge dry solids content of more than 45% w/w can be achieved in less than 5 days. These two studies found that the biodrying process has significant potential to be a suitable solution for drying pulp and paper mixed sludges with minimum energy requirements and side impacts. However, the following major drawbacks associated with the batch configuration were identified:

A) Non-uniformity in matrix dry solids content :

Non-uniformity in the dry solids content is the result of several problems such as:

- Anaerobic conditions in dead space which create hot spots in the batch reactor
- Can not optimize drying conditions for bound and unbound moisture

- Changes in air flow direction (for good pneumatic matrix conditions) result in moisture precipitation on dried mixed sludge.

B) Process inefficiencies that result in a relatively long residence time, and therefore a large reactor size:

- Increased capital costs
- Difficult to fit into the crowded mill sites.

C) Labor intensive batch system, especially for sludge management operations to charge and discharge the reactor

2.4.3. Conceptualization of a Continuous Biodrying Process

So far it is only VCU (Vertical Composting Unit), a New Zealand based company that has developed a continuous composting reactor that works based on a "plug flow" principle, as shown in Figure 2.10. Shredded mixed municipal sludge flows from the top to the bottom of the reactor by means of gravity.

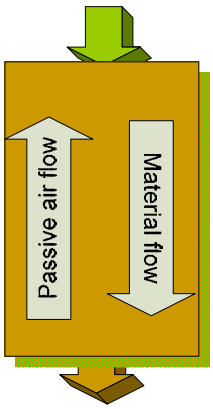

Figure 2.10: VCU principle

The compost is removed daily from the bottom. The residence time is about 14-21 days. This residence time is much shorter than in convectional composting reactors, which is always above 30 days. The biological heat generated can raise the reactor temperature to 40-70^{o}C, which destroys pathogens present in the municipal sludge waste. It is claimed that this system is an energy-efficient process and does not require agitation, bio-filtration, external heating, or air

injection. With minimal moving components, maintenance, and operating costs, the continuous vertical reactor appears to function well according to both economic and operational aspects (VCU Technology Ltd., 2005). However, the physiochemical characteristics of pulp and paper mixed sludges significantly differ from that of the municipal sludge and no application of VCU has been reported in the pulp and paper industry. This technology has demonstrated that a vertical biological system can be developed and operated.

2.5. Key Process Variables for Mixed Sludge Drying

The form in which the water is present within the solid fragments of the matrix has a decisive influence on the drying phenomenon. Air convection may eventually dry the surface of the particle, reaching the hygroscopic limit, i.e., leaving no surface areas saturated with water, resulting in less water to evaporate. For further drying, additional moisture has to migrate from the particle interior (bound water) to its surface, a process governed by diffusion mechanisms (Roy et al., 2006); e.g., during the drying of hygroscopic porous media, such as wood (Stanish et al., 1986). This requires a higher temperature to boost the diffusion mechanism of water migration from the particle interior to its exterior.

At most mills, the mechanical dewatering process (alone) is neither feasible nor economically viable for the target dry solids levels sought for efficient sludge disposal by combustion. In the context of drying technology terminology, two types of water are present in mixed sludge: unbound water and bound water. Unbound water constitutes free, interstitial, and part of the surface water that is physically adhered to the surface of the particles, whereas bound water stands for those that are chemically embedded into the particles' structure. Each of these types of water requires different physical mechanisms for the removal, as described elsewhere (Basu et al., 2006; Brazier, 1996; Mujumdar and Beke, 2003; Vaxelaire and Cezac, 2004; Tsang and Vesilind, 1990; Smith and Vesilind 1995). Figure 2.11 qualitatively describes different types of water available in mixed sludge. The constant drying rate (free water removal) is followed by first (interstitial water removal), second (surface water removal), and third (bound water removal) falling rates. The constant drying rate period takes place nearly at wet-bulb temperature under a convection dominated mechanism, and it is the external mass transfer that

controls the drying mechanism, which depends on temperature, relative humidity, and air velocity.

In the falling rate periods, however, an intensive drying process is required to remove the moisture arriving at the surface of the mixed sludge particle. The drying is mainly conducted at dry-bulb temperature, since the internal diffusion is the limiting factor (Mujumdar, 2007; Vaxelaire and Cezac, 2004). Large amount of the free and interstitial water can be mechanically removed by an efficient dewatering process, but the surface and intercellular (bound) water require thermal treatment techniques.

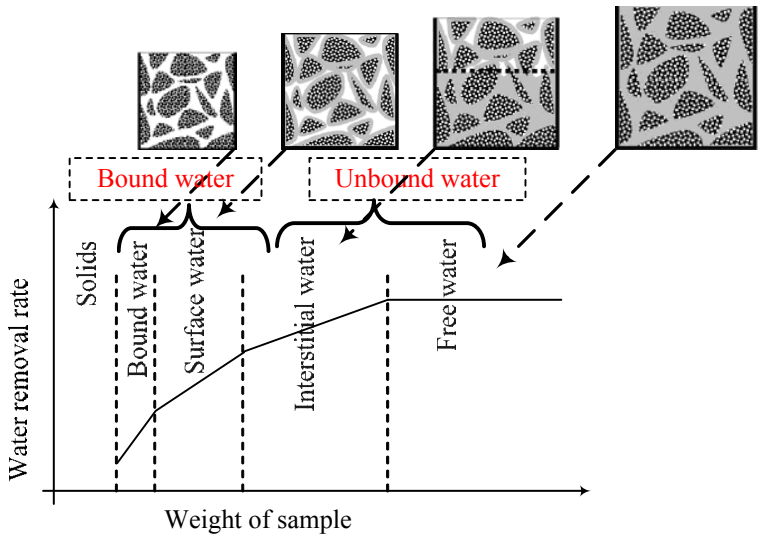

Figure 2.11: Typical drying curve for sludge drying (Adapted from Vaxelaire & Cezac, 2004; and Tsang &Vesilind, 1990)

Morales et al. (2003) studied the effect of inlet air relative humidity (RH_{in}) on the drying rate of a biofilter and found that the drying rate reduced to half at RH_{in}=90% compared with RH_{in}=50%. Roy et al. (2006) found that the outlet air temperature and the exit air relative humidity are critical parameters for the batch biodrying process. Several researchers have studied inlet air RH as an influential parameter for drying food materials, but the literature is lacking in controlling the drying mechanism using outlet relative humidity. Mujumdar (2007) stated that the relative humidity could be one of the controlling parameters in drying processes, but no further detail was provided.

Therefore, despite an enormous amount of research done on air convective drying, little information is available to answer what will happen to the transport phenomena if the outlet relative humidity is controlled.

2.6. Transport Phenomena in Drying of Porous Matrix of Biosolids

Porous media are undoubtedly among the most complex structures found in nature. The major complexity arises from the large local variation in terms of pore size, particle size and connectivity, which brings into play a wide range of length scales and fluid velocity.
As described in Figure 2.11, the presence of different types of unbound and bound water makes the process even more complicated as their removal mechanism is very complex.
Laboratory tests conducted by Adani et al. (2002) emphasized the inverse correlation between biodrying and biodegradation: fast biodrying results in low biological stability, whereas high biodegradation results in high biological stability. For biodrying, a combination of two parameters must be taken into account: air flow rate (which directly affects the ability of the system to eliminate water) and outlet air temperature (which directly affects the ability of the air to contain water). Therefore, the understanding of the temperature profile is very important for the success and control of the biodrying process, and for this reason, the modeling of the biodrying process is an important step.

2.6.1. Modeling Aspects of Transport Processes in Heterogeneous Biodrying and Porous Media of Biosolids

Modeling can provide dynamic coupling between mass and heat transfer mechanisms, which can not be clearly identified through extensive experimentation. Considering the operational obstacles and extremely high costs associated with performing extensive experiments at different scales, there is an additional incentive to simulate the biodrying process mathematically. Through modeling, one can seek the compromise between the extent of biological reaction in order to achieve the target dry solids content, while at the same time preserving the calorific value of the mixed sludge for maximum energy recovery in the power boiler.

In order to understand the science and engineering of biodrying processes adequately, it is necessary to resort to an appropriate modeling approach. The hydrophilic nature of the mixed sludge biosolids makes the mass transfer mechanism very complex because the materials can hold a significant amount of bound water. Most often several assumptions and modifications to the originally developed model are required in order to solve the problems.

Ilic and Turner (1986) investigated the drying of wet porous media using an external drying medium to evaporate and remove the moisture content from the wet porous medium. The modeling involved simultaneous mass and heat transfer with four nonlinear partial differential equations describing the physical process which were solved using the finite difference method. To simplify the model, neither the heat source term nor bound water removal were considered in the drying process.

Kulasiri and Samarasinghe (1996) studied the heat and mass transfer modeling of the drying of biological materials. Luikov's theory of mass and heat transfer for capillary-porous materials was applied, and in particular the results for wood and peanut pod showed a good agreement between the predicted values of temperature and moisture contents and the experimental data. However, no biological reaction term was included in the model.

Richard et al. (2004) studied the relationship between air-filled porosity and permeability during in-vessel composting for a residence time of two weeks. An experimental and theoretical approach for the composting of straw-manure mixture under aerobic conditions was conducted for developing an analytical framework for engineering design purposes. The air-filled porosity of composting materials was predicted by simple measurements of bulk density, moisture content, and organic matter content. The permeability of the matrix was found to be in the range of 10^{-10} to 10^{-7} m^2. No heat transfer modeling was investigated in this work.

The applications for chemically reacting fluid problems can be found in many works in the literature. Gatica et al. (1987a& 1987b) carried out a numerical solution and stability analysis on free convection in a confined porous medium with zero-order exothermic reactions. Vafai et al. (1993) have investigated the heat transfer process in a chemically reacting packed bed. Huang et al. (2003) used an iterative regularization method in order to determine variable heat and mass source terms simultaneously in a chemically reacting fluid, while Huang and Kim (2005) used the method to evaluate a time-dependent reaction coefficient in an autocatalytic reaction pathway.

Characterization of the biodrying process using a strictly experimental approach is challenging due to the number of variables involved, including air velocity, inlet air temperature and humidity, feed dry solids content, ratio of bulking agent (in this study, the recycle ratio of biodried sludge), and residence time. Modeling is then an interesting option since it can lead to a reduction of the number of experiments required to tune and optimize the process by helping gain insight into the transport processes in the biodrying reactor.

Numerous studies have been conducted at laboratory, pilot, and full scales in the field of modeling of composting operations (Mason and Milke, 2005a &2005b, and Mason, 2006). Heat balance analyses were presented by Bach et al. (1987), Harper et al. (1992), Koenig and Tao (1996), and Bari et al. (2000). Mass balance evaluations were provided by Robinzon et al. (2000), Batista et al. (1995), and Straatsma et al. (2000). All of these studies were performed on composting processes where, in contrast to the biodrying process, the goal is to fully biodegrade and stabilize the biomass. Mathematical models incorporating heat and mass transfers have also been developed for solid state fermentation and composting (Von Meien and Mitchell, 2002; Rajagopalan and Modak, 1994a & 1994b).

Roy at al. (2006) applied thermodynamic analysis in a lumped modeling approach to quantify the biological heat in a batch biodrying reactor. However, this study did not address the transport phenomena in the biodrying process. The bioheat values were found to be 3900-6500 W/m^3.

In a recent effort to model the heat and mass transfer in a porous matrix containing biological materials, Prud'homme and Jasmin (2006) used an inverse solution approach to describe the biochemical heat source. Surprisingly, changes in temperature did not correspond to amounts of released heat. This observation was attributed to the slow diffusion of released heat. This study only investigated a free convection system, and the results were not verified experimentally. However, compared to the biodrying technology, two major deficiencies were identified: only free convection heat transfer was considered, and no experimental validation was made.

Despite enormous modeling work on conventional drying, composting, and transport phenomena in porous media, a systematic modeling effort has not yet been established for the biodrying process so that it can address the prevailing process dynamics and evaluate the relative role and contribution of the bio-conversion vs. the physical mechanism of aeration.

2.6.2. The Role of Dimensionless Analysis in Porous Media

The dimensionless (non-dimensional) numbers (criteria, groups, products, quantities, ratios, and terms) possess the following features. They are algebraic expressions, namely fractions, where in both the numerator and denominator are powers of physical quantities with the total physical dimension equal to unity. The dimensionless numbers are useful for several reasons. They reduce the number of variables needed for description of the problem. They can thus be used for reducing the amount of experimental data and making correlations. They simplify the governing equations, both by making them dimensionless and by neglecting 'small' terms with respect to 'large' terms. They produce valuable scale estimates, whence order-of-magnitude estimates, of important physical quantities. When properly formed, they have clear physical interpretation and thus contribute to physical understanding of the phenomenon under study (Ruzicka, 2008).

Convective heat transfer in porous media with heat generation within channels was investigated numerically by Du and Wang (2001). The results indicated that, only when the solid conductivity is smaller than that of the fluid and the fluid velocity within the pores of porous media is low, the temperature difference between the solid and the fluid must be considered. The thermal equilibrium assumption does not mean ignorance of the heat transfer between the two phases, but this assumption can simplify the analysis of heat transfer in porous media by introducing an effective thermal conductivity and a unique heat transfer equation. The study revealed that a local thermal equilibrium assumption is valid if $Re>10$, mainly because of the accelerated heat transfer coefficient that minimizes the temperature difference between two phases. It also revealed that the transport phenomena can be governed by Reynolds number (*Re*), Prandtl number (*Pr*), H/d_P. But this study did not use these dimensionless numbers to extrapolate for a large scale reactor.

Nakayam et al. (2007) used a lumped model approach for a large scale static aerobic composting pile. The normalization and dimensionless analysis on the model revealed key dimensionless groups: Damkohler number (*Da*), which is the ratio of biodegradation rate to convection rate, and Stanton number (*St*), which is the ratio of heat loss to environment to convection heat. Although the study revealed these two dimensionless groups in the equation of heat transfer, the discussion was at a given *Da* for three *St* numbers (4, 6, 7). The study did not further extrapolate

the result for a large scale compost pile because it is in the early stage of design tool development for aerobic composting.

Nield and Kuznetsov (2008) studied forced convection in a porous medium with internal heat generation. The heat and mass transfer equation revealed that *Re* and *Pe* had a strong effect on the temperature profile. The authors speculated that the general trends illustrated by the model will carry over to specific biological situations. However, this system was related to a nuclear facility and the results were not verified experimentally.

As a conclusion, the specific geometry, non-homogeneous porous matrix, and complexity of the biological and transport processes occurring in the continuous biodrying process have not yet been addressed.

2.7. Gaps in the Body of Knowledge

Based on the literature review, the following holes in the body of knowledge have been recognized:

- A continuous biodrying reactor that could dry mixed sludge from the pulp and paper industry to economic dry solids levels has not been developed,
- The effect of key variables on the overall performance of a biodrying process for drying pulp and paper mixed sludge is not well understood,
- There is no mathematical model that has been developed to address the transport phenomena in a continuous biodrying reactor that would provide a basis for a useful design tool development.

2.8. Specific Objectives

The problem statements and hypotheses require that a methodology be developed in order to address the following objectives:

- To develop a pilot-scale continuous biodrying reactor that is capable of solving an industrial problem related to the management of pulp and paper mixed sludge drying
- To identify key variable(s) that greatly impact the performance and the complexity of the transport phenomena in the continuous biodrying reactor
- To develop an appropriate model that: a) enhances better understanding of the transport phenomena prevailing in the continuous biodrying reactor, and b) is able to reflect a full-scale biodrying process.

CHAPTER 3: OVERALL METHODOLOGY

The overall methodology consists of a systematic approach illustrated in Figure 3.1.

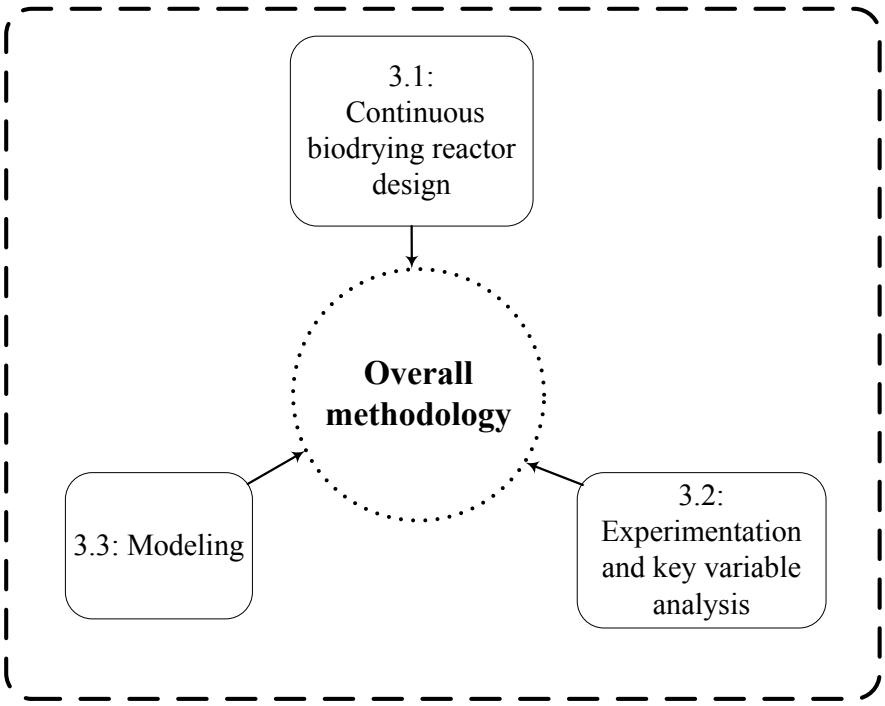

Figure 3.1: Overall methodology of the research

3.1. Continuous Biodrying Reactor Design

The principle of the continuous biodrying reactor is the same as the batch biodrying reactor and relies on the aerobic exothermic biological heat generated through microbial metabolic activity that can enhance the drying of mixed sludge under forced aeration. Like the batch biodrying reactor, the continuous reactor also uses a combination of engineered physical and biochemical processes. However, unlike the batch biodrying reactor, the continuous biodrying reactor is flexible enough to accept a different aeration control strategy from the top to the bottom, allowing more flexibility for removing unbound water at the top, and bound water at its bottom.

By the insights gained through the batch biodrying reactor and the limitations identified in the batch reactor, the following issues were included in the design of the continuous biodrying reactor:

Mixed Sludge Stickiness

Pulp and paper mixed sludge has a complex and sticky structure. This has been a real obstacle for several technologies that attempt to dry mixed sludge. In addition to the fibrous components (cellulose, hemicelluloses, lignin and other types of carbohydrates), there are also mineral materials, either from the papermaking process (clay, fillers) or wastewater treatment system (mainly phosphorous, limestone and nitrogen), microorganisms (tiny biological flocs), and heterogeneous bark or wood waste residues. All of these components make a mixture that is very sticky and deformable. In the design of the biodrying reactor, two important aspects were considered to minimize this issue: a) vertical configuration for the continuous biodrying reactor to result in a gravity-driven movement, and b) use of a special material, UHMW (Ultra High Molecular Weight) polyethylene, to facilitate the movement of the sludge in the vertical direction.

Matrix Non-Uniformity

The mixed sludge is a very complex porous matrix, due mainly to a wide range of materials involved in water treatment processes as well as agglomeration of the particles during preconditioning, polymerization, and mechanical dewatering. Another source of non-uniformity is the use of bark as a bulking agent that was used in the batch biodrying reactor. Such a non-uniform matrix demands a reactor that involves minimum process and technical problems. Recycling of the biodried sludge is a practice that minimizes this non-uniformity. A portion of the biodried sludge is recycled and used to provide adequate pneumatic conditions and minimize non-uniformity of the mixed sludge in the feed. Therefore, the utilization of bark as a bulking agent is avoided in the continuous biodrying reactor.

Low Labor Intensity, Minimum Mixing Requirement, and Less Area Footprint

As stated earlier, the batch biodrying reactor could be very labor intensive. In the continuous biodrying process, the vertical configuration of the biodrying reactor provides not only virtual mixing and movement of the sludge particles but also avoids extra labor on airflow adjustment and materials handling. Besides, a gravity-driven movement reduces the technical problems and minimizes maintenance time on the biodrying reactor. The vertical configuration also results in a reduced area footprint, which is critical for already crowded pulp and paper mill sites.

Uniform Gas Distribution

It is essential for the entire matrix to receive a minimum amount of air in order to prevent anaerobic conditions and to minimize non-homogeneity in the drying process and the dry solids content of the final product. Therefore, in both sides of each compartment, a series of perforated plates uniformly meshed were installed for the air inlet and outlet.

Multiple Solid and Gas Sampling Ports

Multiple solid and gas sampling ports are essential for several reasons; namely a) to verify online experimental data being logged automatically, b) to extract gas and solid samples for further analyses which are not done online, c) to be able to continue the experimentation and data collection even if the online system fails, d) to correctly position the temperature and pressure probes inside the reactor for online data logging, and e) to extract necessary space-dependent experimental data for the modeling assessment.

Biodryer Automatic Materials Discharge System

It is essential that the materials are uniformly pulled out from the bottom of the continuous biodrying reactor so that the discharge materials spend the same residence times receiving the treatment in the reactor. Therefore, the screws were designed to uniformly discharge the biodried mixed sludge from the bottom of the continuous biodrying reactor. When the screws turn, the materials flow downward by means of gravity. A non-uniform discharging system could cause bridging problems, and non-uniformity in the dry solids content of the discharge materials. Therefore, the screws were designed to minimize this problem and were modified (see section 3.2.3.2) to meet these requirements.

With the above-mentioned considerations and consultation with experts in the field of drying processes and reactor design, the continuous biodrying reactor was designed, fabricated, and installed in our laboratory at Ecole Polytechnique Montreal. The reactor is divided into four nominal compartments. The experimental set-up includes two pilot-scale vertical stainless-steel reactors, each of which is 200 cm high, 100 cm deep, and 40 cm wide (Figures 3.2 &3.3). One of the reactors is fully instrumented and controlled online, whereas the second reactor has limited instrumentation and was used primarily to generate data for repeatability purposes. The reactor is insulated with UHMW (ultra high molecular weight) polyurethane on the inside and Styrofoam on the outer surface, with a thickness of 2.5 and 1.5 cm, respectively. The instrumented biodrying reactor is shown in Figure 3.3. The set-up permits online monitoring of internal temperature and pressure, changes in the CO_2 level, relative humidity, and the temperature of the inlet and outlet airstreams in each compartment. An online O_2 measurement set-up was also designed and connected to an Oxymat 61 apparatus (Siemens Inc., USA) to verify the rate of biological reaction. Temperature, relative humidity, pressure and CO_2 level were measured using six RH&T probes (one for inlet, 4 for outlet and one for manual reading) (HMW60U/Y, Vaisala, Helsinki, Finland), 12 pressure probes (Dwyer Instrument Inc., USA), and a CO_2 analyzer (MSA Instrument Division, Ultima gas monitor, USA), respectively. All of these process variables, including incoming gas temperature and relative humidity, were logged at 8 min intervals using LabView (LabView 8.0.1, National Instrument Inc., USA) (Figure 3.3).

The reactor was insulated on the inside by UHMW (Ultra High Molecular Weight) polyethylene and on the outside by regular insulation materials. The wet mixed sludge is fed at the top of the reactor (1st compartment) and flows downward by means of gravity. This mixed sludge consists of fresh sludge (received from the pulp and paper mill) and recycled sludge (obtained from the discharge of the biodryer) which are mixed in a 40 liter container prior to manually feeding into the top of the reactor. The dried sludge is extracted by two parallel screws installed at the bottom of the reactor.

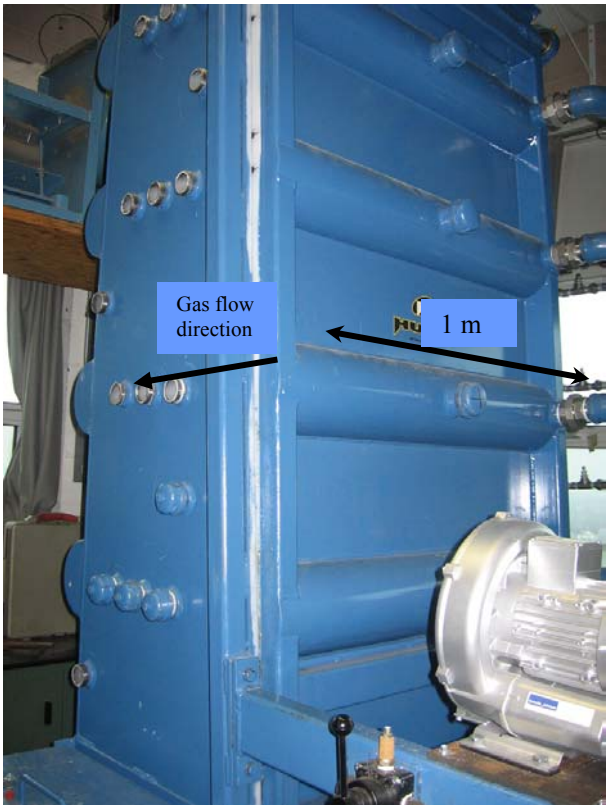

Figure 3.2: Pilot-scale biodrying reactor

Airflow is supplied by forced air and inductive blowers, driving the air in the reactor in a cross-flow direction in each of the four compartments.

In order to generate a variety of results for model verification, two sets of experiments were conducted. Table 3.1 shows the overall experimental program which was performed after reactor troubleshooting and pre-commissioning. The first series was based on design of experiment (DOE) approach and consisted of 8 individual experiments under the following conditions: total air flowrate of 28 and 34 m^3/h, recycle ratio of 15 and 30% (d.b.), and residence

time of 4 and 8 days. The recycling of biodried sludge provides adequate pneumatic conditions in the matrix of the biodrying reactor so that no other bulking agent (e.g. bark) is required. It can also contribute to faster microbial activity of thermophilic bacteria (measured as CFU/g) than that of fresh sludge (Navaee-Ardeh et al., 2008). The chosen range of residence times was recommended by Roy et al. (2006) for an economically feasible batch biodrying reactor, and the range of bulking agent (recycle ratio in this study) was recommended by Frei et al. (2004) for acceptable pneumatic conditions. The second set of experiments was performed at a 6-day residence time, a 30% w/w recycle ratio of biodried sludge, under a controlled outlet relative humidity profile (85-96%) and with a 40-75 m^3/h total air flowrate. Feed and discharge occurred twice a day with a mass flowrate of 10-22 kg (dry basis). The first series of experiments was expected to generate higher temperature and bioheat, which should yield better drying rates and increased larger calorific value losses. The second strategy favors the calorific value of sludge since higher aeration results in less sludge biodegradation.

Table 3.1: Overall experimental program

Run	Case	Residence time (days)	Recycle ratio (% w/w)	Total air flowrate (m^3/h)	Outlet relative humidity (%)
1		4	15	34	
2	3	4	15	28	
3		4	30	28	
4		4	30	34	
5		8	15	34	
6	4	8	15	28	
7		8	30	28	
8		8	30	34	
9	1	6	30	75	85,85,85,85
10	2	6	30	46	96,96,96,96
11	5	6	30	55	85,85,96,96
12	6	6	30	64	96,96,85,85

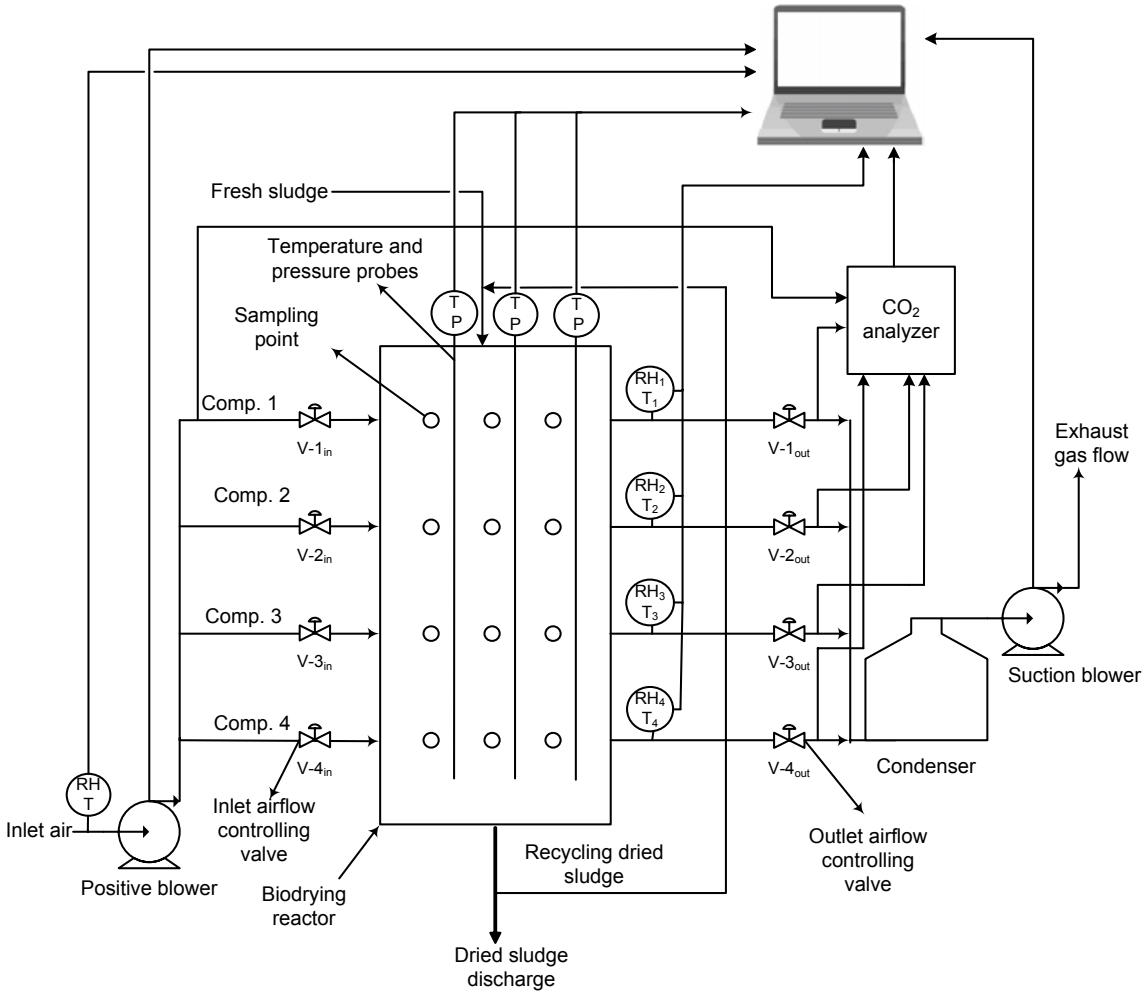

Figure 3.3: Schematic of pilot-scale set-up

3.2. Experimentation

The experimental phase consists of material characterization, screening, and targeted experimentations. The material characterization includes solid and gas phases.

3.2.1. Solid Phase Characterization

Solid biomass characterization is an important step for the process analysis and for understanding the influence of different parameters in the process.

The biomass was a given pulp and paper mixed sludge in a ratio of 45/55 (% w/w) primary to secondary sludges, collected onsite from a typical wastewater treatment plant at an Eastern Canadian TMP pulp and paper mill, and shipped in 25 gallon barrels to our lab. The solid phase consists of dry solids content and water. The solid content is a mixture of microorganisms, fibrous materials, lignin, mineral components such as limestone and phosphorus, and clay. The water itself consists of unbound and bound water.

3.2.1.1. Dry Solids Content

The dry solids content is the water free mass of mixed sludge. This parameter is important as it is one of the objectives of this study to reach economic dry solids level as well as it plays a role in the modeling phase of this study. To measure dry solids content, 16 samples of mixed sludge (each sample approximately 150 g w. b.) taken from different sampling points were oven dried at 105 ^{o}C for 24 h. Two were fresh sludge samples, two were taken at the outlet of the reactor discharge, and twelve were extracted from the designated sampling points illustrated in Figure 3.3.

3.2.1.2. Elemental Analysis

Elemental analyses are needed to determine the C/N ratio and the constant coefficients of the microbial reaction at different compartments (Eq. 2.1).The elemental analyses were conducted by the University of Montreal's independent certified laboratory on a 10-mg representative sample (a mixture of sludge samples extracted at various depths through one of the 12 sampling points) of the dry sludge. The representative samples were ground using a home-style grinder. The model of the elemental analyzer was Fisons AE 1108, and the oxygen, carbon, nitrogen, and hydrogen were measured.

3.2.1.3. Higher Heating Value

The higher heating values (HHV) were measured using an Oxygen Bomb Calorimeter (Parr Instrument Company, Illinois, USA). First the samples were prepared. The preparation of samples included oven-drying, grinding it using a home-style grinder, compressing 1-g of it into a shape of tablet, and transferring it into the Oxygen Bomb Calorimeter for higher heating value measurement. After placing the sample inside the bomb calorimeter, the cylinder was tightly closed and a trace of high pressure pure O_2 (35 atm) was injected into the cylinder already submerged in a water bath. Prior to experiments, the bomb calorimeter was calibrated using a benzoic acid pellet to determine the volume of the water required for the water bath, which is kept constant during all experimental trials. After injecting the oxygen, an ignition was made in order to start the combustion. By tracking the temperature in the water bath, the higher heating value of the solid sample was determined.

3.2.1.4. Density and Porosity

The density and porosity of the mixed sludge in each compartment were measured using an approach adapted from Richard et al. (2004) and Ahn et al. (2008). A 20 liter container was filled with the mixed sludge sample at a given dry solids content, and then a load pressure equal to the pressure that the sludge would have received in the pilot-scale reactor due to the weight of the upper compartments, was applied to the sample. The density was then measured using the ratio of mass to the volume of the sample in the container. The same sample in the container was filled with water to a level such that the solid materials were submerged in the water. The porosity was then reported as the ratio of water added to the total volume of the solid sample. It should be noted that due to the hydrophilic nature of the solid samples, there is a possibility that some water is absorbed into the solid phase, causing slight overestimation of this parameter. Therefore, to verify this, the results were compared to the estimated values determined using a model developed by Richard et al. (2004). The calculated values were slightly higher than the measured values, making the inherent error in the measured values negligible.

3.2.1.5. Microbial Analysis

The microbial analysis of the mixed sludge samples were conducted by Maxxam Analytique Inc., and were reported for both the mesophilic and thermophilic bacteria as CFU/g. The samples were obtained in each compartment at different sampling points illustrated in Figure 3.3.

3.2.1.6. Particle Size Distribution

One of the real complexities with a porous matrix of mixed sludge is the wide range of particle sizes. This makes the study of transport phenomena and the modeling of the biodrying reactor complicated. In this study, particle size distribution was determined for each compartment using a 5-stage sieve. These values are critical for the estimation of Reynolds numbers.

3.2.2. Gas Phase Characterization

The gas phase includes oxygen, nitrogen, carbon dioxide, and water vapor. The ambient air was supplied by two blowers installed underneath the biodrying reactor. Following the school's policy, the lab conditions remained nearly constant, and therefore do not represent the real ambient conditions. Both the relative humidity and the temperature of the gas phase could have a significant impact on the water removal rate and the efficiency of the biodrying process.

3.2.2.1. Relative Humidity and Temperature

Relative humidity and temperature were measured online at the gas inlet and outlet ports, and manually at three points in each compartment in the gas flow direction illustrated in Figure 3.3. However, the temperature was also measured manually to verify the online measurements and to

obtain data from points that are not taken online. These data are critical for the reactor performance as well as for the modeling part of this study.

3.2.2.2. CO_2 and O_2

The CO_2 production was monitored continuously using the data logging system. The concentration of O_2 was measured at the inlet and outlet of each compartment to verify the biological heat generation.

3.2.3. Continuous Biodrying Reactor Commissioning

The reactor commissioning included equipment calibration and reactor troubleshooting issues in order to obtain reliable experimental data. The instrumental calibration is critical for accurate data acquisition and process control.

3.2.3.1. Instrumental Calibration and Precision

The computerized data acquisition system, LabView 8.0.1(National Instrument Inc., USA), gathered much of the raw data in the experimental phase. Calibration of the instruments was performed regularly to determine accuracy, precision, and overall reliability and suitability of the data obtained. Table 3.2 shows the range of precision for each piece of instrumentation. Relative humidity probes were calibrated by Vaisala Inc. once a year, and were checked regularly, whereas CO_2 and O_2 sensors were calibrated regularly in our lab. Temperature and pressure probes were verified by manual temperature measurements on a regular basis. The airflow meters were also checked and controlled.

Table 3.2: Precision and range of measurement of different instruments

Parameter	Range	Precision	Remarks
Air flowrate (m^3/h)	2.7-19	±1	
	20-50	±0.5	
Pressure transducer (kPa)	-0.25-0.25	±0.0004	The range is adjusted automatically
	-2.5-2.5	±0.004	
	-25-25	±0.04	
Pressure probe (kPa)	79-138	±0.2	
Temperature probe (^oC)	-50-200	±0.3	
Temperature sensor in relative humidity probe (^oC)	-20-80	±0.5	
Relative humidity probe (%)	0-90	±0.02	
	90-100	±0.03	
CO_2 (%v/v)	0-5	±0.05	CO_2 production never goes above 5 (%v/v)
O_2 (%v/v)	0-5	±0.05	The range is adjusted automatically
	5-15	±0.03	
	15-21	±0.01	

3.2.3.2. Continuous Biodrying Reactor Troubleshooting Issues

Uniform Residence Time

In order to obtain uniform biodried materials at the discharge of the reactor, it is important to ensure that the particles across the biodrying reactor receive equal treatment and thus have uniform residence times. One way is to check the variability in the dry solids content of the treated materials. In the early phase of the reactor commissioning, a higher variability was noticed in the dry solids content of the biodried mixed sludge. A large cavity was also noticed in the biodrying reactor. Non-uniform residence times could also be the main factor responsible for bridging and cavities in the reactor. Therefore, a series of tests were designed to verify this issue. The reactor was filled with a given mixed sludge, and twelve balls, having nearly the same size and density as the mixed sludge particles, were uniformly distributed at the reactor top. Feed and discharge were followed with 100% recycling in a closed loop. The normalized residence time of each ball was calculated based on the total dry discharge mass measured when each ball was discharged divided by the maximum total dry mass at the discharge of the last ball(s). As can be seen in Figure 3.4, the materials in the back of the reactor (large screw

diameter, y=1m) discharged faster than those in the front (small diameter of screw, y=0). Therefore, the screws were modified accordingly until satisfactory results (Figure 3.4) were achieved. The modified screws did not create any cavities across the reactor.

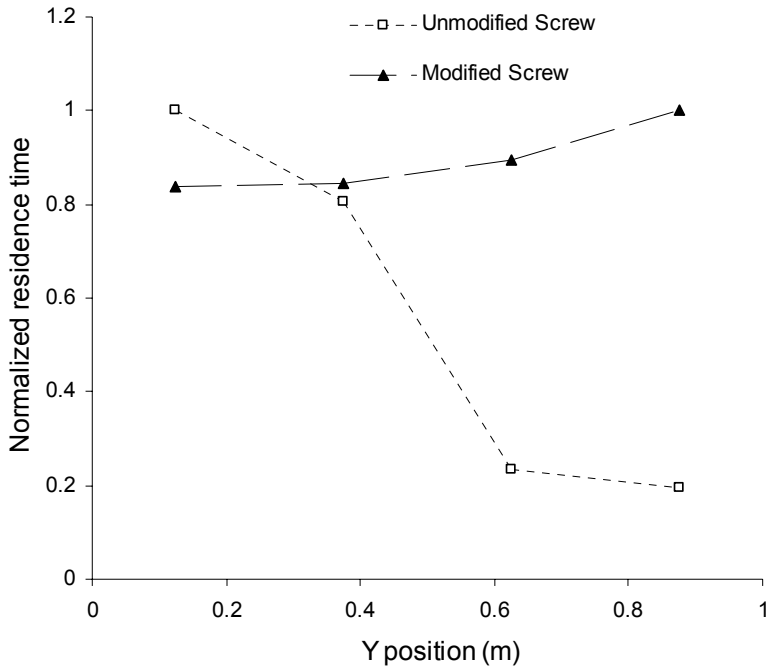

Figure 3.4: Residence time distribution of unmodified and modified screws

Stable Outlet Relative Humidity Control

The relative humidity of the exiting airflow affects the water removal rate as well as control of transport processes in the biodrying reactor. In the early phase of the reactor commissioning, it was noticed that due to the heat exchange between the outlet airflow in the outlet conduits and the surrounding environment, some of the water vapor condensed, generating high variability in the outlet relative humidity profile (Figure 3.5a). To prevent these oscillations, all parts of the conduits were heat-traced with a series of heat tapes and reinsulated. As Figure 3.5b shows, the modified conduits had a stable humidity profile.

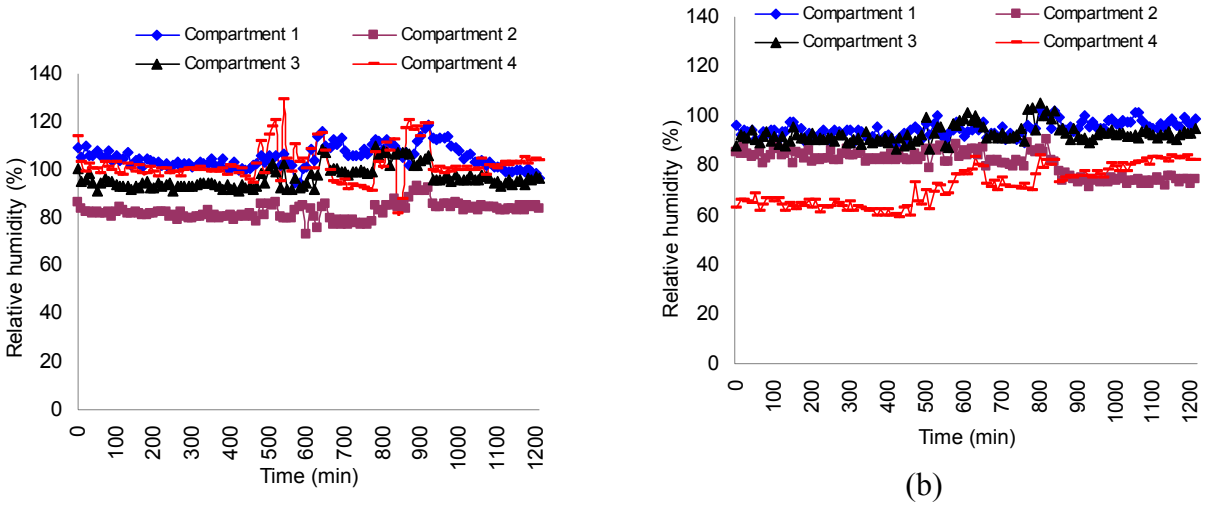

(a) (b)

Figure 3.5: Outlet relative humidity of unmodified (a) and modified (b) conduits

Constant Reactor Dry Weight

It is critical to keep the effective volume of the reactor constant for better process control and data logging. Since it is a vertical reactor, and given the nature of transport processes occurring in the continuous biodrying reactor, several issues could affect the reactor operation: compaction due to loading pressure of the materials, and mass and volume losses due to water and carbon (biodegradation reaction) losses. In the early phase of the reactor commissioning, it was noticed that the volume of the sludge in the biodrying reactor was decreasing over time (Figures 3.6). However, the reason was not clear yet. Therefore, the reactor was emptied, and the total dry weight was measured, which was different from the dry weight at the start-up of the process. It was speculated to be primarily related to the dry mass loss in the form of CO_2 due to the biological reaction and accumulated over time to become significant. By measuring the outlet CO_2 online and the total carbon loss (C loss) in different compartments of the biodrying reactor, the quantity of dry mass loss was estimated, and the equal amount was added to the reactor in the feed. By continuing the new strategy, the total weight of the sludge in the biodrying reactor remained at a constant level.

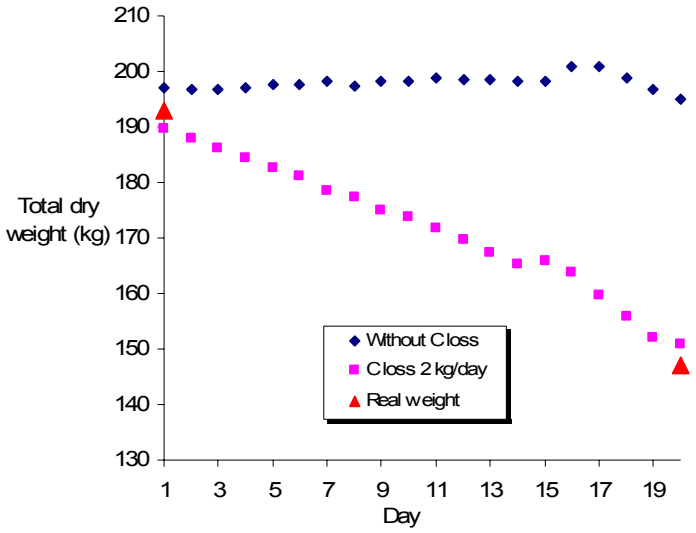

Figure 3.6: Continuous biodrying weight loss

3.2.4. Screening Experimentation and Key Variable Analysis

The goal of these experiments was to identify the key variables that have the most influential effect on the operation and efficiency of the continuous biodrying reactor. Table 3.3 shows different variables, and their ranges and potential impact on the biodrying process.

Table 3.3: Variables investigated in the screening experiments

Biodrying variable	Range	Potential impact on biodrying process
Type of biomass feed	Mill specific	Represents nutrient availability for biodrying operation
pH of biomass	6.4-6.8	Very high (>7) or very low (<5) values could be harmful for the microbial activity and biodrying operation
Nutrient level (C/N ratio)	24-29	Out of range values (<15 or >30) are harmful to microbial activity (Haug, 1993) and biodrying operation
Residence time (day)	4,6,8	Recommended by Roy et al. (2006). This affects reactor performance and economic viability of the process
Recycle ratio (% w/w)	0,15,30	Recommended by Frei et al. (2004). This helps microbial acclimation, and increases porosity and permeability for better air

		flow in the matrix
Outlet relative humidity (%)	85,96	May have significant impact on the transport phenomena in the biodrying reactor as it controls the mechanism of unbound and bound water removal

3.2.5. Targeted Experimentation

Targeted experiments were performed to explore the influence of the key variable(s) already determined from the screening experimental phase on the overall performance of the continuous biodrying reactor. One should note that in this experimental phase only the key variable is altered and the other variables are fixed.

3.3. Modeling

Figure 3.7 describes the different categories and components of the modeling and simulation phase. In the drying process, the most important issue is to provide simultaneous coupling of three major phenomena, i.e., momentum, mass, and heat transfer, which represent the first category. The basic description of these phenomena in drying of porous media is highly complex due to complexities associated with the nature of the feed material, the porous matrix, and the heat source term in the continuous biodrying reactor. Different phases are present and different mechanisms are dominant within the various reactor compartments.

In order to facilitate the modeling task, a thermodynamic analysis of the process can be performed, which represents the second category. This will provide an overall picture of the drying process without having to understand the detail of the process itself. For instance, from previous batch biodrying experimental work (Roy et al., 2006), an accurate insight into the biological heat generation was obtained using thermodynamic analysis of the process. However, this provides only a global insight and understanding of the process of the batch biodrying reactor, and only the total bioheat generated can be extracted. This approach needs to be

modified for the continuous biodrying reactor because each compartment works separately and under different dominant transport phenomena conditions.

The third category of modeling involves empirical models of the process parameters related to mass, heat, or momentum transfer. For instance, the specific heat capacity can be assumed to have a linear relationship with the moisture content and porosity.

By repeatedly working on the four categories that describe the modeling task, models can be constructed. One last step is required before simulations can be performed, which involves accurately determining the constraints and the boundary conditions for the drying process.

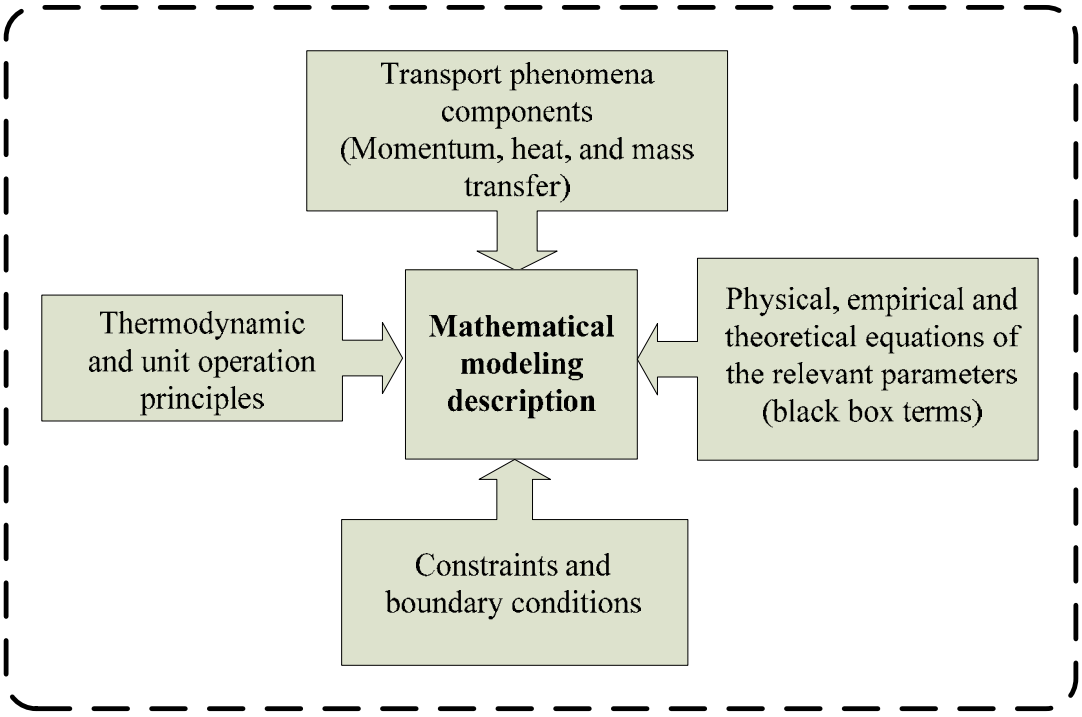

Figure 3.7: Components of a distributed modeling (Navaee-Ardeh et al. (2006a))

3.3.1. Modeling Strategy

The modeling strategy is based on a stepwise approach, starting with simplistic models and adding to the complexity of these models as more insight is gained into the complex transport phenomena involved in this type of process. Figure 3.8 provides more detail on the different phases of the modeling strategy.

The first strategy is modeling based on a lumped parameter approach. In the lumped model, the overall reactor is considered, and the evolution of the dry solids content along the height of the

biodrying reactor is obtained. The second phase of the modeling strategy is a global 1-D distributed model based on chemical and biochemical engineering principles for each compartment. This model includes heat and mass transfer in each of the four compartments. Reasonable assumptions are made to enhance the analytical solution of the differential equations. The model is assessed against the experimental data to identify whether or not a subsequent model is needed. However, it is believed that an adequate and space-dependent description of the transport phenomena governing the continuous biodrying process will ultimately require the development of a 2-D distributed model based on partial differential equations, which constitutes the last phase of modeling. Due to the complexity inherent in modeling of the porous media, the finite element method has been used in the past to obtain the numerical solutions (Vafai et al., 1993; Haghighi et al., 1994). FEMLAB, recently COMSOL Multiphysics, a modeling tool based on the finite element method, is used for the 2-D modeling of this study. The dimensionless analysis is performed on the 1-D as well as the 2-D model. The goal is to explore dimensionless numbers that play a critical role in the transport phenomena in the continuous biodrying reactor.

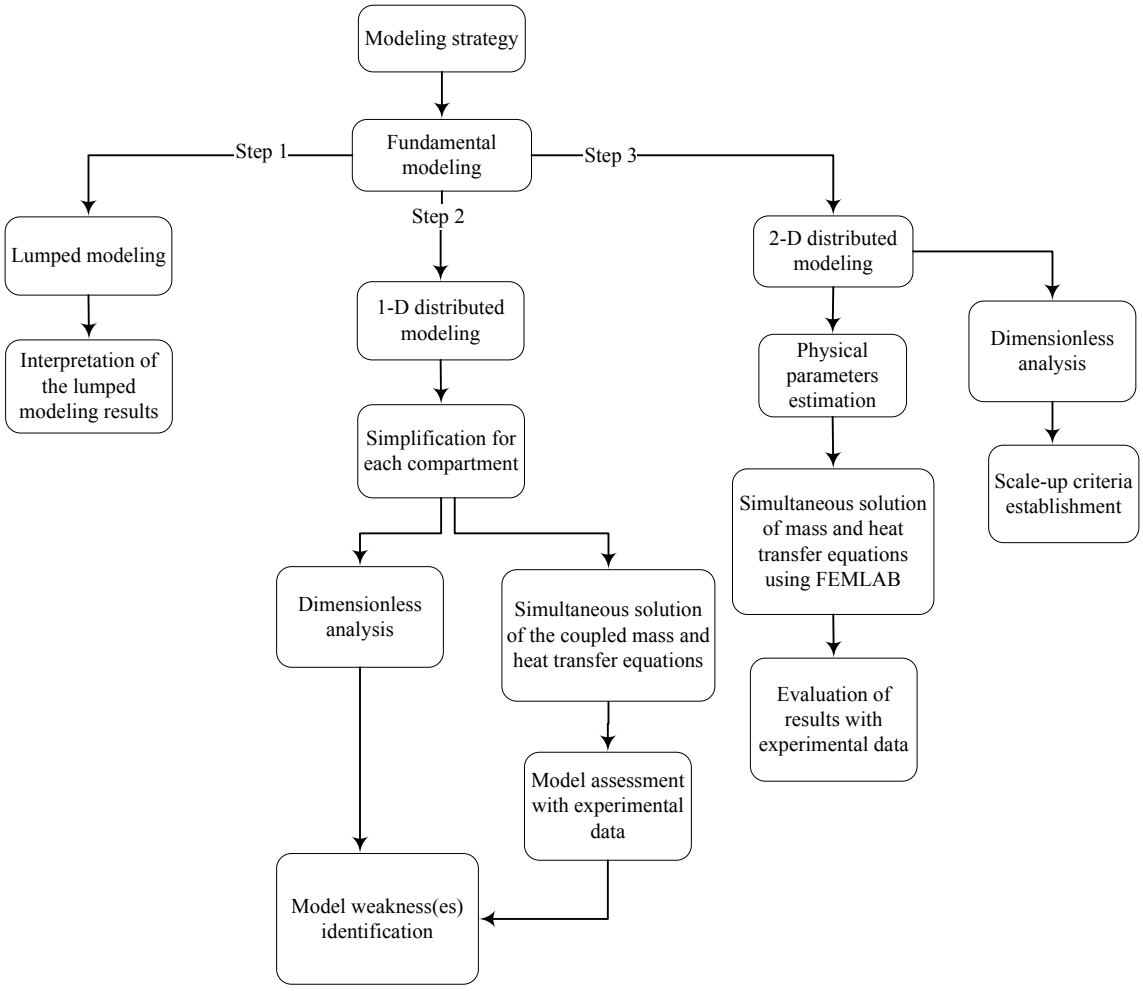

Figure 3.8: Overall methodology of the modeling procedure

CHAPTER 4: PUBLICATION EXECUTIVE SUMMARY

4.1. Presentation of Publications

The following papers that were published in and/or submitted to scientific journals are included in Appendix A of this thesis:

- Navaee-Ardeh, S., Bertrand, F., Stuart, P.R. (2006a). Emerging Biodrying Technology for the Drying of Pulp and Paper Mixed Sludges. *Drying Technology* 24(7), 863-878.
- Navaee-Ardeh, S., Bertrand, F., Stuart, P.R. (2009a). Development and Experimental Evaluation of a 1-D Distributed Model of Transport Phenomena in a Continuous Biodrying Process for Pulp and Paper Mixed Sludge Drying. Accepted at *Drying Technology*.
- Navaee-Ardeh, S., Bertrand, F., Stuart, P.R. (2009b). Key Variables Analysis of a Novel Continuous Biodrying Process for Drying Mixed Sludge. Accepted at *Bioresource Technology*.
- Navaee-Ardeh, S., Bertrand, F., Stuart, P.R. (2009c). A 2-D Distributed Model of Transport Phenomena in a Porous Media Biodrying Reactor for Drying Mixed Sludge. Under review at *Drying Technology*.

Furthermore, the following papers, complementary to the research work done, can be found in Appendix B:

- Navaee-Ardeh, S., Bertrand, F., Stuart, P.R. (2006b). Heat and Mass Transfer Modeling of a Novel Biodrying Process: Lumped System Approach and Preliminary Results, *56th Canadian Chemical Engineering Conference*, Sherbrooke, Canada.
- Navaee-Ardeh, S., Bertrand, F., Stuart, P.R. (2007). 1-D Distributed Modeling of a Novel Continuous Biodrying Reactor. *57th Canadian Chemical Engineering Conference*, Edmonton, Canada.
- Navaee-Ardeh, S., Bertrand, F., Stuart, P.R. (2008a). Distributed Model of a Continuous Biodrying Process for Drying Pulp and Paper Mixed Sludge and Comparison with

Experimental Results. *Proceedings of the Pan-Pacific Conference*, Vancouver, Canada, 51-52.

- Navaee-Ardeh, S., Tchoryk, C., Tolnai, B., Bertrand, F., Stuart, P.R. (2008b). Novel Continuous Biodrying Reactor: Principles, Screening Experiments and Results. 58th *Canadian Chemical Engineering Conference*, Ottawa, Canada.
- Navaee-Ardeh, S., Bertrand, F., Stuart, P.R. (2009d). Modeling and Experimental Verification of a Novel Biodrying Process for Drying Pulp and Paper Sludge. *Inter-American Drying Conference* in 8th World Chemical Engineering Conference, Montreal, Canada.

4.2. Links between Publications

The paper in Appendix A1 discusses the results of a survey on emerging biodrying technology for pulp and paper mixed sludge drying. In this broad survey, several tasks were achieved: recognizing that mixed sludge management in the pulp and paper industry is a big challenge for the industry and the environment, recognizing the existence of four different types of water in the mixed sludge, which exacerbates the complexity of dewatering, a broad review on existing drying technologies for sludge drying, a critical review on the batch biodrying reactors developed previously for the mixed sludge drying, the principle of the continuous biodrying reactor, and a reference to modeling as a useful tool to understand the transport processes in the continuous biodrying reactor. The results of this investigation showed that the majority of drying technologies have technical uncertainty and/or questionable economics. The design and the modeling aspects of the continuous biodrying reactor that are elaborated on in this thesis were inspired by the results of this survey.

The paper in Appendix B1 presents preliminary work on a “lumped model (compartment-wise) analysis”, which involved only mass balances in the lumped model equation systems. This paper showed that the transport phenomena in the continuous biodrying reactor are too complex to be addressed by the lumped model. For instance, a dry solids content predicted by the lumped model was twice as large as the experimental data and indicated that the lumped modeling

approach was inadequate to capture and address the complexity of different types of water and the transport processes involved in the continuous biodrying reactor. It was concluded that the modeling approaches must be re-directed toward the use of distributed models.

The paper in Appendix B2 presents an early theoretical work on the 1-D distributed model inspired by the results of the papers in Appendices A1 and B1. The 1-D model involved distributed parameters in the solid flow direction and lumped parameters in the gas flow direction. The results were promising and indicated that the distributed modeling approach was attractive. However, since the experimental data were not available by the time the model was developed, the weakness and credibility of the 1-D model has not yet been explored.

The papers in Appendices B3 and A2 were an extension of the work done on the 1-D model. More specifically the experimental data were brought into the assessment of the 1-D model. In the paper presented in Appendix B3, the 1-D model was evaluated using one set of experimental data (identical experimental conditions). In the paper presented in Appendix A2, the method of bioheat estimation was modified, and more experimental data were provided through the experimental phase for the assessment of the 1-D model. The 1-D model was solved analytically for each compartment, and as a result of assuming lumped parameters in the gas flow direction, the experimental data were averaged in the gas flow direction for each compartment to represent a single value at a given height (z). The 1-D model was assessed against the experimental data generated under different operating conditions. The dimensionless analysis performed on the 1-D model provided useful information on the interpretation of the experimental data and the modeling results. However, major discrepancies were identified specifically in the bottom compartments, where the temperatures are high. These discrepancies were attributed to averaging the temperatures in the gas flow direction, and complex microbial growth mechanisms, which are strongly temperature dependent. The temperature in the gas flow direction ranges from a mesophilic dominated mechanism (low temperature) to a mixed microbial mechanism, i.e. mesophilic and thermophilic (medium temperatures), and thermophilic mechanism (high temperatures). For the sake of simplicity, this complexity was not addressed in the 1-D model. In other words, the 1-D model, independent of the temperature, uses a uniform bioheat distribution in each compartment. Therefore, it was identified that a 2-D model needs to be developed to incorporate these limitations.

The key variables analysis of the continuous biodrying reactor was performed in papers presented in Appendices B3 and A3. The main task was to identify the key process variable for the continuous biodrying reactor. The outlet relative humidity was identified as the key variable and had the greatest impact on the overall efficiency index and the complexity (two-dimensionality) index of the continuous biodrying reactor. A critical review of the experimental data and the 1-D modeling results were performed in paper A3, which resulted in diagnosing the continuous biodrying reactor's two-dimensionality.

Finally, the last paper, included in Appendix A4, incorporates both the gas and solid flow direction transport processes into a 2-D distributed model. The development of the 2-D model was inspired by the results achieved in the previous papers conducted in this study (Appendices A1, A2, A3, B1, B2, and B3). This paper describes the 2-D modeling of the transport processes in the continuous biodrying reactor that overcame the weaknesses of the 1-D model. These are critical for further exploitation of the continuous biodrying process. The usefulness of the 2-D model is also presented in this paper. The criteria for consideration at a full-scale continuous biodrying process are established and discussed in the last part of the synthesis (section 4.3.3.8).

4.3. Synthesis

The goal of this synthesis is to give an overview of the most pertinent results obtained in this research study that address the hypotheses and objectives of this research. The overall methodology proposed at the outset of the project was systematically addressed as summarized below.

4.3.1. Biodrying Technology for the Drying of Pulp and Paper Mixed Sludges

In the early phase of this study, a broad review was conducted on the most promising technologies for biomass drying. The challenges of mixed sludge disposal in the pulp and paper industry, including current disposal and drying techniques, were reviewed, and combustion of mixed sludge was recognized as an economically viable alternative. The existence of four types

of water in the mixed sludge was highlighted and rigorously discussed. Based on phenomenological understanding of the continuous biodrying reactor, the expected temperature and dry solids content profiles were explored (Navaee-Ardeh et al., 2006a). The fundamentals of the mathematical modeling of the continuous reactor were briefly discussed, and a critical review of the mass and energy balances in aerated composting processes presented. Such a mathematical simulation coupled with experimental verification would yield significant scientific benefits, unique reactor configuration for a given mixed sludge characteristic, and contribute to the goal of advancing the efficient drying of mixed sludge. The design of the continuous biodrying principle was inspired by these findings.

4.3.2. Analysis of the Experimental Results

4.3.2.1. Experimental Data Reliability

A water mass balance, overall energy balance, and assessment of the characteristics of the biodried materials at steady-state regime are critical components that need to be verified for the reliability of the experimental data in the biodrying process.

Overall Water Mass Balance

The water mass balance is important for tracking the main components of the biodrying process as well as for scale-up purposes. Saucedo-Castaneda et al. (1992) showed that a water balance is critical in large scale solid-state fermentation bioreactors. This was confirmed by Von Meien and Mitchell (2002) as well.

Due to some difficulties in measuring the total mass of the sludge exiting each compartment, the water mass balance was not done for each compartment but rather for the overall reactor. The overall water mass balance includes both gas and solid phases. All components, including fresh, recycled, and discharge sludges as well as the inlet and outlet gases were considered for the water mass balance. There are two components involved in the water mass balance, each of

which contains two terms: two streams (gas and solid) for the water inlet and two streams (gas and solid) for the water outlet. These are all connected in the following general equation:

$$Water\ in\text{-}Water\ out + Water\ generation = Water\ Accumulation \quad (4.1)$$

Note that the accumulation term in the right-hand side of Eq. 4.1 vanishes due to steady-state conditions. Table 4.1 summarizes the results of the elemental analyses for a typical experiment under the operating conditions which are summarized in Table 4.2. The results of these elemental analyses are similar to values found in the literature (Larsen and McCartney, 2000). The C/N values are between 15 and 30, indicating the potential for active microbial growth (Haug, 1993).

Table 4.1: Elemental analysis results

From the top to the bottom of the biodrying reactor	% w/w Nitrogen	% w/w Carbon	% w/w Hydrogen	% w/w Oxygen	C/N
Feed	1.48	45.67	4.72	36.60	30.8
Compartment 1	1.58	44.92	5.08	36.10	28.4
Compartment 2	1.64	44.90	4.95	36.25	27.4
Compartment 3	1.81	44.65	4.79	35.80	24.7
Compartment 4	1.85	44.61	4.79	35.80	24.1

Table 4.2:Typical experimental conditions used for the water mass balance

	Q_g (m^3/h)	RH_{out} (%)	T_{out}(°C)	RH_{in}(%)	T_{in}(°C)
Compartment 1	18.2	94	18	14	28.4
Compartment 2	8.5	78	23.6	14	28.4
Compartment 3	16.2	100	16.2	14	28.4
Compartment 4	9.2	80	27.2	14	28.4

Cellular water produced by the microbial aerobic oxidation (Eq. 2.1) of the substrate was calculated based on the results of the elemental analyses in the different compartments (Table 4.1). As can be seen in Table 4.3, cellular water is very small compared to the other components of the water mass balance.

As for the gas phase, the water content was calculated from the relative humidity, temperature and air flowrate according to Eq. 4.7. These will be discussed later. The relative humidity and the temperature of the inlet gas were the same for all compartments, because all lines were connected to a main inlet air stream.

As for the solid phase, the water content was directly obtained from the total mass flowrate of sludge and its dry solids content. Fresh, feed, and discharge sludge dry solids contents were 37, 40, and 51% w/w, respectively. The recycle ratio was 30%w/w.

Table 4.3 shows the results for the corresponding water mass balance. A closed water mass balance was obtained, confirming the reliability of the experimental data and the techniques applied for the parameter measurements.

Table 4.3: Summary of water mass balance

Mass balance components	Value (kg/day)
water In by airflow	5.2
water In by feed	46.8
water generation	0.5
water Out by airflow	25.6
water Out by discharge	28
Total water In	52.5
Total water Out	53.6

Note that the “Total water In” stands for water In and water generated.

Figure 4.1 shows the overall water mass balance for cases 1, 2, 3, and 4. The operating conditions are summarized in Table 4.4. Cases 1and 2 have a residence time of 6-day, a 30% w/w recycle ratio, and controlled outlet relative humidity profiles, whereas cases 3 and 4 have a 15% w/w recycle ratio, total air flowrate 28 m^3/h, and residence times of 4- and 8-day, respectively.

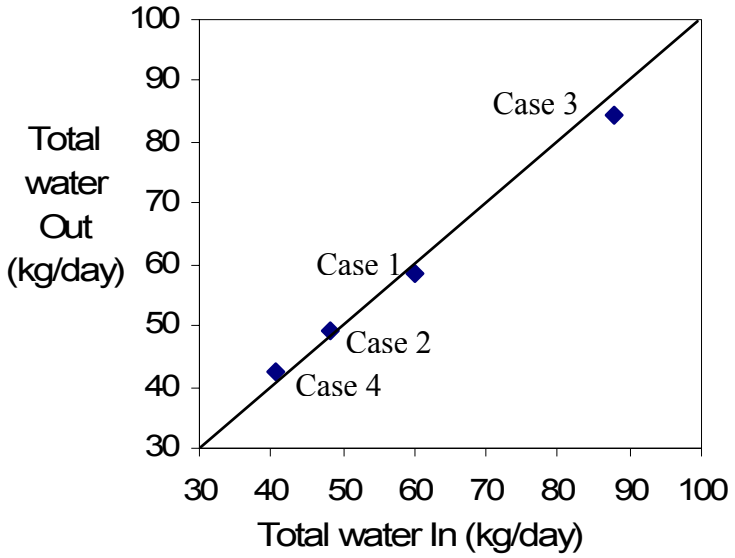

Figure 4.1: Overall water balance for 4 experimental cases

Table 4.4: Operating conditions of four experimental cases used for overall mass and energy balances

	Case 1				Case 2				Case 3				Case 4			
	Comp. 1	Comp. 2	Comp. 3	Comp. 4	Comp. 1	Comp. 2	Comp. 3	Comp. 4	Comp. 1	Comp. 2	Comp. 3	Comp. 4	Comp. 1	Comp. 2	Comp. 3	Comp. 4
$Q_{g,i}$ (m^3/h)	26.40	5.0	26.0	18.0	16.5	8.0	14.0	7.7	7.91	7.41	7.31	7.38	7.04	7.11	7.63	7.65
$\dot{Q}_{bio,i}$ (W/m^3)	0	0	1000	2500	200	400	2200	2400	511	550	1200	2800	0	50	2000	3500
$w_{ms,i}$	0.42	0.43	0.45	0.47	0.42	0.44	0.46	0.50	0.37	0.41	0.42	0.45	0.42	0.44	0.5	0.54
$RH_{out,i}$(%)	73	66	88	89	68	72	92	55	80	97	75	80	41	83	92	100
$T_{out,i}$(^{o}C)	18	20	25.6	27.3	23.5	25	28	42.8	29	30	31	33.8	23	24.3	36	40
RT (days)	6				6				4				8			
RR(%)	30				30				15				15			
RH_{in} (%)	13				14				12				10			
T_{in} (^{o}C)	24				25				27				26			
$\dot{m}_{total}$ (kg/s)	0.001128				0.001128				0.001692				0.000846			

Overall Energy Balance

The energy balance is also critical for the continuous biodrying process. There are several components involved in the energy balance: two energy terms for the gas convection heat transfer (In and Out) and two energy terms for the solid sensible heat transfer (In and Out). Heat generated through metabolic activity counts as "Energy Generated", and energy removed through water evaporation and heat loss through walls are counted as "Energy Consumed". These terms are all connected in the following general equation:

$$Energy\ In + Energy\ Generated - Energy\ Out - Energy\ Consumed = 0 \quad (4.2)$$

The two first terms count for the total Energy In, and the two last terms count for total Energy Out. Figure 4.2 shows the results for cases 1, 2, 3, and 4 (see also Table 4.4). The mathematical expressions for these two terms are as follows:

$$\text{Total Energy In} = 3600\times 24\times W\times L\times D\times Q_{bio} + 24\times \rho_g \times \Delta H_{eva}\times X_{in}\times \sum Q_g + \dot{m}_{total}\times Cp_{mix}\times (T_{in} - T_r) + 24\times \rho_g \times (T_{in} - T_r)\times Cp_{g_{in}}\times \sum Q_g \quad (4.3)$$

$$\text{Total Energy Out} = 24\times \rho_g \times \Delta H_{eva}\times \sum (X_{out}\times Q_g) + \dot{m}_{total}\times Cp_{mix_{out}}\times (T_{bot} - T_r) + 24\times \rho_g \times \sum (Cp_{g_{out}}\times Q_g \times (T_{out} - T_r)) + 0.05\times 3600\times 24\times W\times L\times D\times Q_{bio} \quad (4.4)$$

where $Cp_{mix} = Cp_{H_2O}(1 - w_{ms}) + Cp_{ms}w_{ms}$

where L, D, and W standing for the dimension of each compartment and are 0.4, 0.4, and 1 m, respectively. ρ_g is the density of air (=1.16 kg/m^3).

The data in Tables 4.4 and 4.6 were plugged into Eqs. 4.2, 4.3, and 4.4 for the overall energy balance. The heat loss was estimated as 5% of the total biological heat. As can be seen in Figure 4.2, except in case 2, an acceptable energy balance was achieved for the overall energy balance. Any discrepancies may be due to the variability in the bioheat values that are affected by the online gas measurements and to more heat loss than that assumed in this energy balance. Therefore, for the sensitivity analysis, a 5% variation in the bioheat values resulted in a fairly

acceptable closed energy balance for all cases.

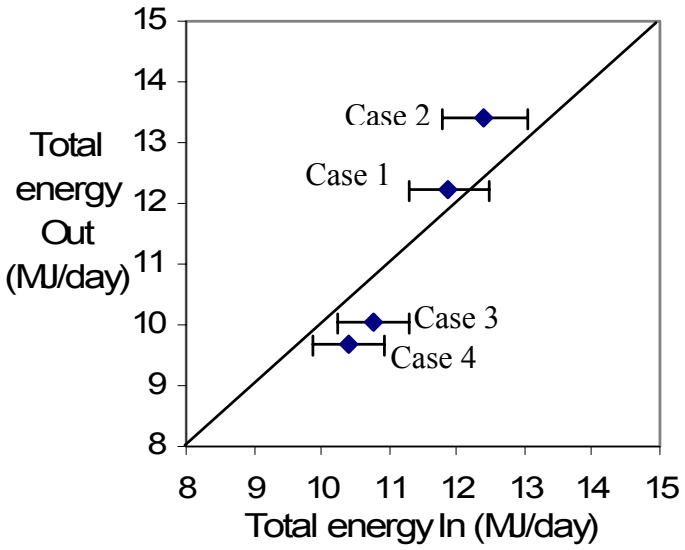

Figure 4.2: Overall energy balance for different experimental cases

Figure 4.3 shows the fraction of each component in the overall energy balance in the continuous biodrying reactor. The total energy fraction is divided into total Energy In and total Energy Out, each of which is 100%. The bioheat in the total Energy In, and the evaporative heat in the total Energy Out are the two fractions that play significant roles in the heat and mass transfer mechanisms, and will be further discussed in the modeling parts (section 4.3.3).

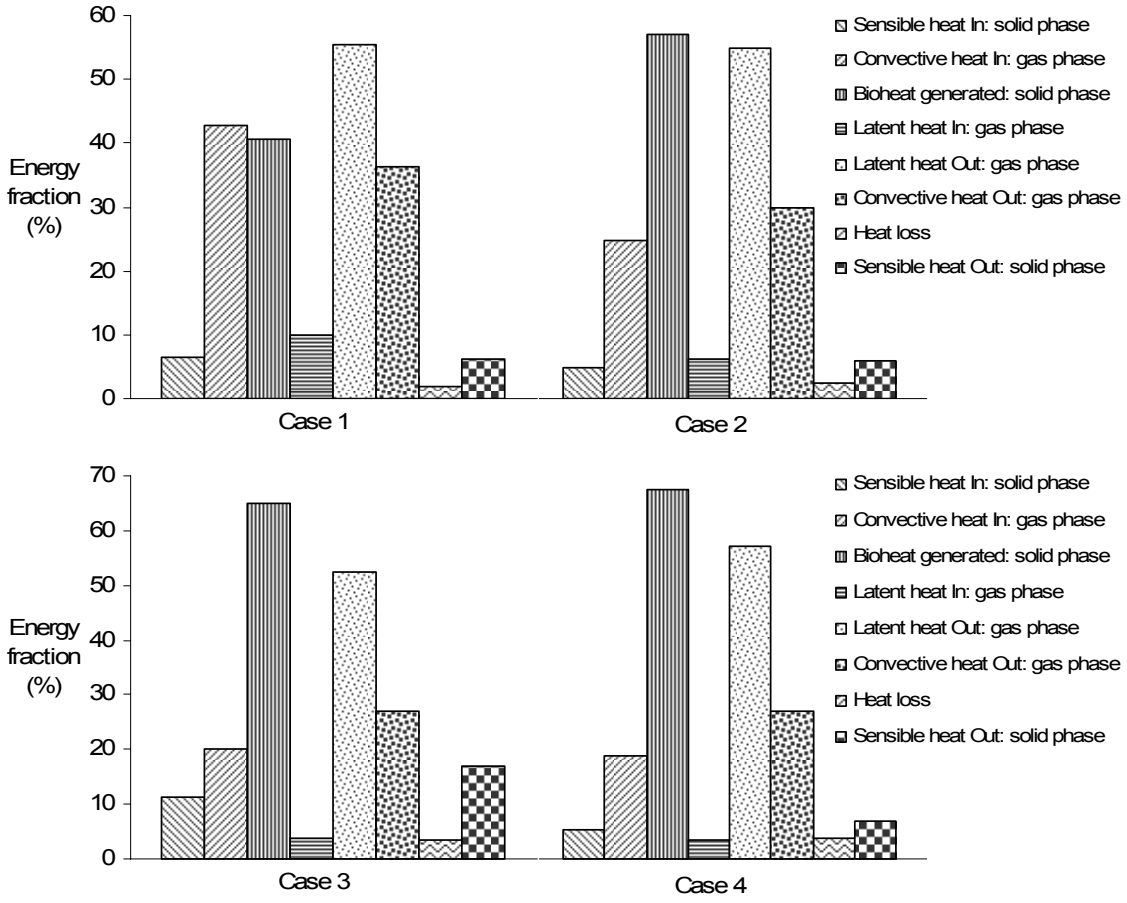

Figure 4.3: Overall energy fraction of different components in the continuous biodrying reactor

4.3.2.2. Process Performance

The continuous biodrying reactor was controlled either at constant air flowrate or controlled outlet relative humidity profile. Despite a different performance in these cases, the experimental results in all cases were acceptable and resulted in an economic dry solids level for mixed sludge. It is important to understand the change in mixed sludge characteristics and properties as the sludge moves downward in the biodrying reactor. Among these properties are the dry solids content and higher heating value (HHV) of the mixed sludge.

Economic dry solids content (w_{ms}) is essential for a safe and economic combustion process. It also explicitly appears in the sensible heat term of the solid phase (in the 1-D and 2-D models)

as well as in the correction factor (a_w) of the evaporation term (Eqs. 4.11 and 4.12) in the 1-D model, which will be discussed later. The higher heating value (HHV), or the calorific value, is a critical factor for the economic feasibility of the combustion as it represents the quantity of energy that can be recovered in a boiler. Note that all these characteristics were obtained in a steady-state regime, when the properties in each compartment remain nearly constant over time. This was verified for all cases (experimental runs) by measuring local temperatures as well as dry solids contents at different positions within the biodrying reactor.

Dry Solids Content

Figure 4.4 shows that the mixed sludge dry solids content increases as the sludge moves downward in the biodrying reactor. The standard error of mean was estimated to be ±2% using 5 measurements on a typical sample. The largest dry solids content gain occurred in the 3rd and 4th compartments. This trend is slightly different from what was expected (Navaee-Ardeh et al., 2006a). Indeed, it was expected that the dry solids content would improve more at the top and reach a flat profile in the 3rd and 4th compartments. However, as shown in Figure 4.4, the dry solids content is nearly flat in the 1st and 2nd compartments in all cases, and increases significantly in the 3rd and 4th compartments. This is due mainly to the significant impact of higher bioheat and higher temperatures in the bottom compartments (Table 4.4). This increases the water holding capacity of the gas phase and the water transfer from the solid phase to the gas phase. As shown in Figure 4.4, all of the dry solids levels are higher than the 45% w/w, which is required for an economically viable combustion process (Kudra et al., 2002; Kraft et al., 1996, and Roy et al., 2006). Indicated by a dashed line, it shows that a shorter residence time (4-day) would be sufficient to achieve this level of dry solids content. Note that in a full-scale reactor this residence time may become even shorter because the feed is already a hot acclimated sludge. There will be further discussed in section 4.3.3.4.

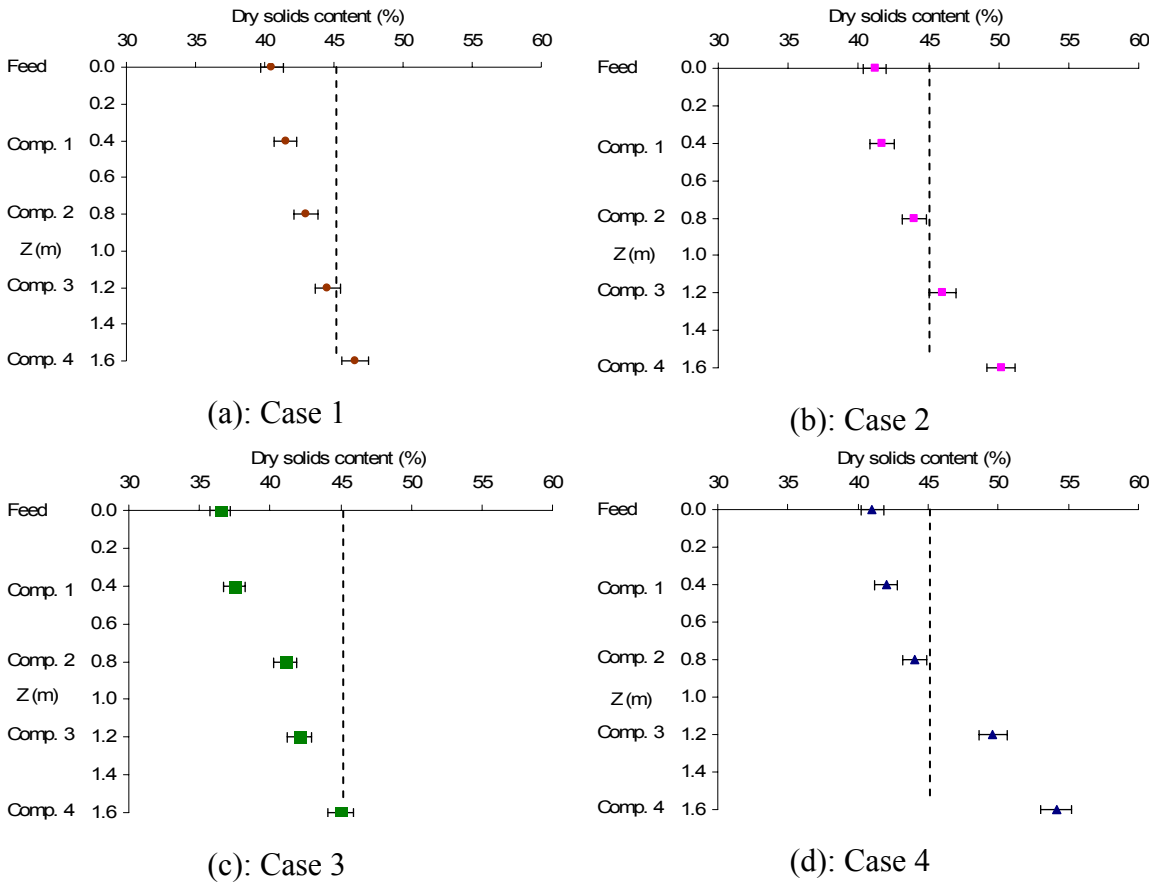

(a): Case 1

(b): Case 2

(c): Case 3

(d): Case 4

Figure 4.4: Dry solids content change in the continuous biodrying reactor

Higher Heating Value

Figure 4.5 illustrates the change in the HHV in the biodrying reactor for case 4 as the data for other cases are not available. As expected, more HHV losses can be observed in the bottom compartments because more bioheat is generated (Table 4.4). The standard error of mean was estimated to be ±1.5% using 5 measurements on a typical sample.

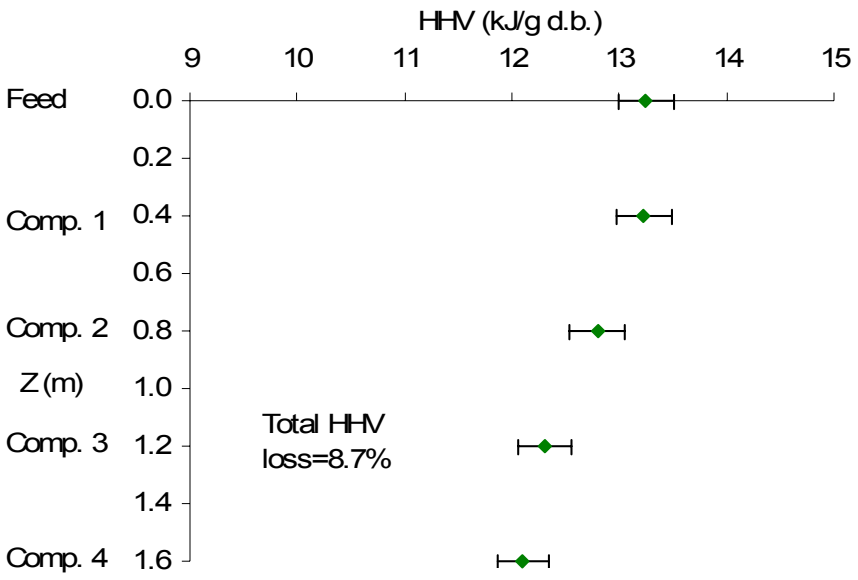

Figure 4.5: Higher heating value (HHV) change in a typical 8-day experiment (case 4)

The goal of an efficient biodrying process is not to achieve a high dry solids content but rather to ensure an adequate dry solids level that yields a safe and economic combustion. In this work, on average the highest dry solids content was achieved for an 8-day residence time (case 4), but the total calorific value loss in this case was the greatest among the four cases. This results in a negative impact on the quantity of energy that can be recovered in a boiler. Therefore, a compromise between the extent of the biodegradation (calorific value loss) and the final dry solids level is required to maximize the energy recovery in the subsequent combustion process. Such a compromise can be determined by optimizing the overall biodrying reactor performance, which will be discussed following the key process variable analysis.

4.3.2.3. Key Variables Analysis

The goal of these experiments was to identify the key variables that affect the operation and efficiency of the biodrying process. The following variables were investigated: biomass feed in terms of pH of mixed sludge and C/N ratio, residence time, recycle ratio of biodried sludge, and outlet relative humidity profile.

Biomass Feed

The type of biomass feed, and hence its properties, could affect the performance of the biodrying process, the extent of the microbial reaction, and the feasibility of the process. Some of these properties are initial feed dry solids content, initial biomass feed temperature, initial active microbial populations of the biomass feed, initial nutrition level in the biomass feed (C/N), and initial pH of the biomass feed. The biomass is mill specific and its properties depend on the pulping and other relevant processes at the mill. Since the biomass feed was obtained from one given thermomechanical (TMP) pulp and paper mill, there were no significant changes in the above-mentioned properties from one experiment to another. Therefore, the feed biomass was assumed to be a fixed parameter for this study. Nevertheless, this is an uncontrollable parameter that could be an essential variable for the biodrying operation, and therefore has to be considered when studying a new type of sludge.

pH of Mixed Sludge

The pH of the mixed sludge was not significantly affected by the process and may be due to the buffer nature of the microbial environment. The pH varied from 6.8 in the fresh feed to about 6.3 in the discharged materials. The impact was considered to be insignificant.

C/N Ratio

The C/N ratio represents the nutrition level of the biomass. This ratio greatly affects microbial activities in the biodrying process and has two impacts on the process. It acts as an inhibitor to the microbial reaction if C/N>30 or <15, and greatly enhances microbial reaction if 15<C/N<30 (Haug, 1993). Roy et al. (2006) reported the C/N ratio as the most influential parameter in the batch biodrying process. Larsen and McCartney (2000) found that bioheat has a negative correlation with the C/N ratio. In the current study, a regular elemental analysis of the mixed sludge was conducted for all compartments. As shown in Table 4.1, the C/N ratios remained

between 15 and 30, indicating the potential for active microbial growth (Haug, 1993). Therefore, it was considered a fixed parameter in this study.
Nevertheless, the C/N ratio of mixed sludge is considered as an independent parameter inherent in the biomass feed, and has to be monitored and controlled for a new type of biomass.

Residence Time

Residence time affects not only the efficiency of the biodrying process, but also its capital cost. Removing unbound water (in the 1st and 2nd compartments) requires less residence time, whereas bound water removal (in the 3rd and 4th compartments) is based on a diffusion mechanism and requires longer residence times. One of the goals of the pilot-scale continuous biodrying reactor was to significantly reduce the residence time required to achieve economic dry solids levels, so as to reduce capital costs. A broad range of residence times were tested: 4, 6 and 8 days, which on average resulted in a 6, 10 and 15% w/w dry solids content increase, starting from an initial dry solids content of 38% w/w. First, an 8-day residence time was tested resulting in a 54 % w/w dry solids content for the discharge sludge. This level of dry solids content is significantly above the economic dry solids content (43-45% w/w in Figure 2.9), and therefore is less attractive (Navaee-Ardeh et al., 2008b). Next, a 4-day residence time was tested. As shown in Figure 4.4c, the economic dry solids level was achieved. However, to ensure that the biodrying operation always receives a 4-day treatment and the microbial activity acclimates well, the residence time was fixed at 6 days.

Recycle Ratio of Biodried Sludge

The recycling of dried sludge into the feed stream may be required for enhanced sludge acclimation, and as well, to ensure that the necessary pneumatic conditions prevail in the porous medium. The microbial lag phase occurs because microbial acclimation is needed when there is a change in environmental conditions (Madigan and Martinko, 2006). 15% of the discharge stream (dry mass basis) was recycled and mixed with 85% of fresh sludge (dry mass basis) and then fed into the bioreactor. This led to an improved matrix temperature in all compartments.

Table 4.5 compares the microbial population counts for three recycle ratios: 0% (100% fresh sludge), 15% w/w (85% fresh feed), and 30% w/w (70% fresh sludge). It can be observed that the population of mesophilic and thermophilic bacteria in the case of a 30% w/w recycle ratio is 200 times and 20 times greater, respectively than those of a 0% recycle ratio.

Table 4.5: Mesophilic and thermophilic populations in fresh and mixed feed

Recycle ratio (% w/w)	Mesophilic (CFU/g)	Thermophilic (CFU/g)
0	4.3×10^{5}	2.1×10^{8}
15	6.05×10^{7}	2.03×10^{9}
30 (first feed)	1.02×10^{8}	4.04×10^{9}
30 (second feed)	9.03×10^{7}	4.04×10^{9}

Another improvement due to the recycling of biodried sludge into the feed stream is the increase of the pneumatic conditions, resulting from a reduction of the pressure drop across the reactor width in each compartment. This can be observed in Figure 4.6, which compares the pressure drops across each compartment between the gas inlet and outlet for 0, 15 and 30% w/w recycle ratios. Increasing recycle ratio reduced the pressure drop in all compartments. As anticipated, the pressure drops in the 1st and 2nd compartments are higher than the pressure drops in the 3rd and 4th compartments and is mainly attributed to the wetness of the sludge. A sharp decrease can also be seen in the pressure drop from the 2nd compartment to the 3rd one. This can be explained by a significant increase of the dry solids content across these compartments, as shown in Figure 4.4. Indeed, the drier the sludge, the smaller the pressure drop. A dryer sludge also has a better resistance toward compaction.

Note that if the pressure drop is too high, it may affect the distribution of air in the matrix, cause the development of unpleasant hot spots, reduce the performance of the biodrying reactor, and result in non-uniform biodried sludge.

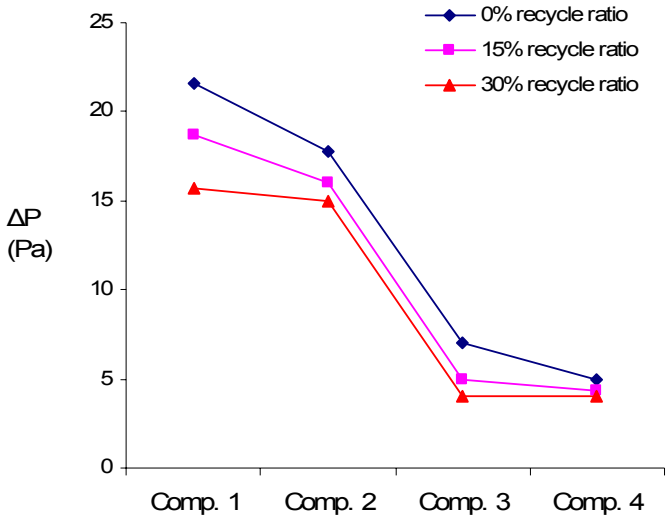

Figure 4.6: Effect of recycle ratio on pressure drops in the reactor

For a full-scale reactor, hot dewatered immediately acclimated sludge will be conveyed directly to it, therefore may not require recycling. This reduces the capital costs of the biodryer. However, recycling may be necessary for those mixed sludges that have a higher proportion of tiny secondary (activated) sludge. Based on this assessment, the recycle ratio was fixed at 30% w/w in this experimental program.

Outlet Relative Humidity Profile

The outlet relative humidity profile along the biodrying height is, a priori, a critical process variable since the air provides oxygen for the aerobic biological activity, cools the matrix when air flowrates are high enough, and transports water vapor and some of the bioheat out of the reactor. Blowing large amounts of air in the upper part of the reactor helps reduce the residence time by accelerating drying, but it cools the matrix of the sludge and prolongs the microbial lag phase period. Adequate combinations of air flowrate and outlet relative humidity profiles may result in optimum conditions for unbound water removal at the top of the reactor, and bound water removal at the bottom. For good biodrying conditions, each sludge type requires a specific combination of outlet relative humidity to prevent excessive biodegradation, and to achieve an adequate water removal rate (drying rate) and an economically feasible residence time. Therefore, various combinations of outlet relative humidity profiles and air flowrates were

investigated in this study. Two outlet relative humidity profiles were investigated following the relevant literature (Mujumdar, 2007) and the controllability of the pilot-scale biodrying reactor: a higher outlet relative humidity (96%) and a lower outlet relative humidity profile (85%). The lower outlet relative humidity profile requires a higher air flowrate and controls the drying process at wet-bulb temperature, therefore, is efficient in a constant drying rate period which corresponds to the removal of unbound (free and interstitial) water (Mujumdar, 2007). The higher outlet relative humidity, however, requires less air flowrate and controls the biodrying process at dry-bulb temperature. This can activate the development of microbial biodegradation (Berg et al., 2002), and is efficient in a falling rate period (Nissan et al., 1959), which corresponds to the bound water removal. This allows the temperature gradient to develop and rise to values that accelerate the internal moisture diffusion and bound water removal. The internal moisture diffusion becomes easier when the temperature level increases.

Various combinations of these outlet relative humidity profiles were investigated to explore a unique profile. These include: a) all compartments at lower outlet humidity profile 85%/85%/85%/85% (case 1), (b) all compartments at higher outlet humidity profile 96%/96%/96%/96% (case 2), (c) the 1^{st} and 2^{nd} compartments at higher (96%) and the 3^{rd} and 4^{th} compartments at lower outlet relative humidity profile (85%) (case 5), and (d) the 1^{st} and 2^{nd} compartments at lower (85%) and the 3^{rd} and 4^{th} compartments at higher outlet relative humidity profile (96%) (case 6) (see Figure 4.7).

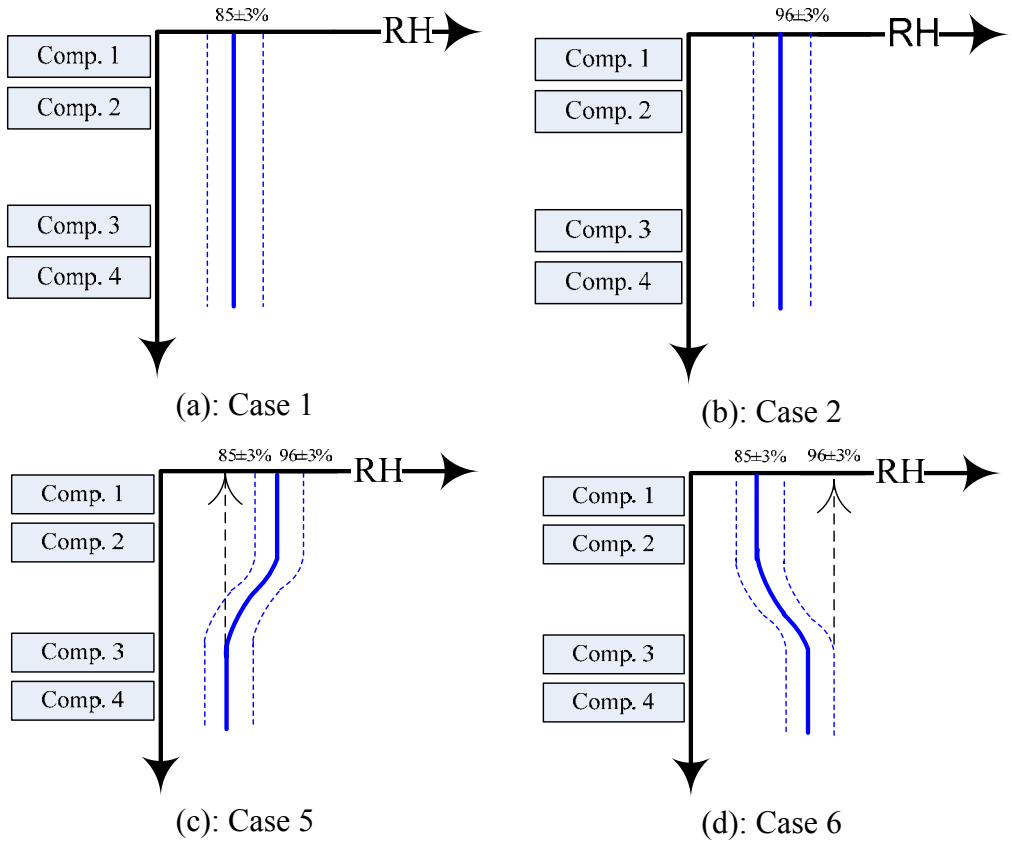

Figure 4.7: Four outlet humidity profiles examined: (a) case 1, (b) case 2, (c) case 5, and (d) case 6

Due to these combinations, the total air flowrate varied from 45 to 75 m^3/h. Therefore, these cases need to be evaluated against a criterion that answers the question "Which case results in a better biodrying operation? "

4.3.2.4. Effects of Outlet Relative Humidity Profiles on Biodrying Performance

In order to find an optimum outlet relative humidity profile, an evaluation criterion is required. Fugere et al. (2007) stated that the biodrying performance could be a critical parameter for assessment of the feasibility of the biodrying process. According to their preliminary assessment, the purchase cost of the biodryer, which is strongly dependent on the efficiency, could be about 35-45% of the total investment costs. Therefore, the efficiency of the biodrying

reactor is an important criterion for the process evaluation. As per the overall energy balance in Figure 4.3, the latent heat of water evaporation and the exothermic biological heat generated through metabolic activity of aerobic microorganisms are the two main components for the biodrying process. These two components are also critical for unbound and bound water removal. Therefore, the biodrying efficiency index (η) is comprised of the biological heat available to bound water diffusion and the latent heat of water evaporation:

$$\eta = \frac{\dot{Q}_{Evaporation}}{\dot{Q}_{Biological}} = \frac{\sum_{1}^{4} \Delta H_{latent} \rho_g Q_{g,i} (X_{out,i} - X_{in})}{\sum_{1}^{4} \dot{Q}_{Biological,i}} \tag{4.5}$$

where η is the biodrying efficiency index and ρ_g is the density of air (= 1.16 kg/m^3) obtained from Perry and Green (1997).

Biological heat ($\dot{Q}_{Biological,i}$) can be directly determined from the CO_2 production rate, or equivalently from the O_2 consumption rate for aerobic processes, as follows (Navaee-Ardeh et al., 2009a):

$$\dot{Q}_{Biological,i} = Q_{bio-standard}\ \rho_{O_2} Q_{g,i} \left(\left(\frac{V_{O_2}}{V_{Air}} \right)_{in} - \left(\frac{V_{O_2}}{V_{Air}} \right)_{out} \right)_i \tag{4.6}$$

where, $Q_{bio\text{-}standard}$, the amount of biological heat generated per gram of oxygen consumed, is equal to 16 kJ/g-O_2 for different microbial species (Bailey and Ollis, 1986), ρ_{O_2} is the density of oxygen (=1.35 kg/m^3) obtained from Perry and Green (1997), and $(V_{O_2}/V_{Air})_{in}$ and $(V_{O_2}/V_{Air})_{out}$ are the volume percentage (absolute value) of oxygen experimentally obtained at the inlet and outlet gas flows, respectively.

$X_{out,i}$–X_{in} represents the net amount of water transferred to the gas phase, that is the difference of absolute humidity between the outlet and inlet gases(kg H_2O/kg air). It is evaluated using the relative humidity and temperature of the inlet and outlet airstreams, and the following modified equation from Geankoplis (1993) and Haug (1993):

$$X_i = 0.622 \times \left(\frac{\frac{RH_i}{100} \times 10^{(8.896 - \frac{2233}{T_i + 273})}}{760 - \frac{RH_i}{100} \times 10^{(8.896 - \frac{2233}{T_i + 273})}} \right) \tag{4.7}$$

Note that the numerical values; 8.896 and 2233 are constant coefficients for partial pressure of water vapor in Antoine's equation obtained from Haug (1993).

As shown in Figure 4.8, blowing more air at the top of the reactor (lower outlet relative humidity (85%)) and slowing it down at the bottom (higher outlet relative humidity (96%)) seems to result in a better biodrying process (case 6). In this case, the amount of evaporative heat is 3 times greater than the biological heat generated. This indicates that the biodrying reactor has performed well with higher water evaporation and less biodegradation.

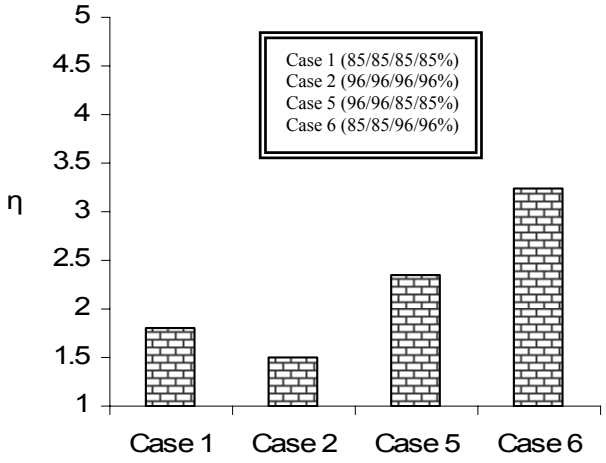

Figure 4.8: Biodrying efficiency index evaluated at four different outlet relative humidity profiles

4.3.2.5. Effects of Outlet Relative Humidity Profiles on the Complexity of Transport Phenomena in the Biodrying Reactor

The temperature of the matrix is one of the key components in the transport phenomena. Another factor that we define in this study is an index that represents the complexity of the transport phenomena in the biodrying reactor. It is a measure of how close/far the biodrying reactor is to/from a 2-dimenional problem. More precisely, we are interested in assessing the impact of the outlet relative humidity profile on the complexity of temperature profile in the biodrying reactor. To do so, the following complexity index (*CI*) is introduced:

$$CI = \sum_{i=1}^{4}\sum_{j=1}^{3}(T_{i,j} - T_{i,in})^2 \qquad (4.8)$$

where, $T_{i,j}$ and $T_{i,\text{in}}$ are the temperatures at local *j* (j=1,2,3 in Figure 3.3) in compartment *i* (i=1,2,3,4) and the inlet gas temperature in compartment *i*, respectively. In fact, it quantifies the importance of the variation of the velocity profile along the gas flow direction.

Figure 4.9 shows the values of the complexity index for cases 1, 2, 5, and 6. In cases 1, 5, and 6, where higher air flowrates were applied (lower outlet relative humidity along the reactor height), the temperature variation in the gas flow direction was not significant, indicating a less complex transport phenomena in the biodrying reactor that can be described, depending on the accuracy, approximately with a 1-D model. In fact, our 1-D modeling results confirmed acceptable accuracy for these cases (Navaee-Ardeh et al., 2009a). In case 2, however, the complexity index is very large indicating a more complex biodrying reactor that requires a sophisticated model (e.g. a 2-D model) for the description of the transport phenomena. The large complexity in this case is attributed to a lower air flowrate (higher outlet relative humidity profiles (96%)) that favors the development of higher temperatures in the biodrying reactor and results in a higher aerobic exothermicity in the reactor. In fact, it was found that the 1-D model poorly predicted the 2-D transport phenomena governing in the reactor (Navaee-Ardeh et al., 2009a).

Interestingly, the complexity index (*CI*) in cases 5 (blowing low at the top and high at the bottom) and 6 (blowing high at the top and low at the bottom) are equal, even though the biodrying efficiency index in case 6 is higher than that of case 5. This indicates that *CI* alone is not sufficient to fully grasp the complexity of the heat transfer mechanisms prevailing in the reactor. It appears that combining *CI* and biodrying efficiency index (η) would be more appropriate.

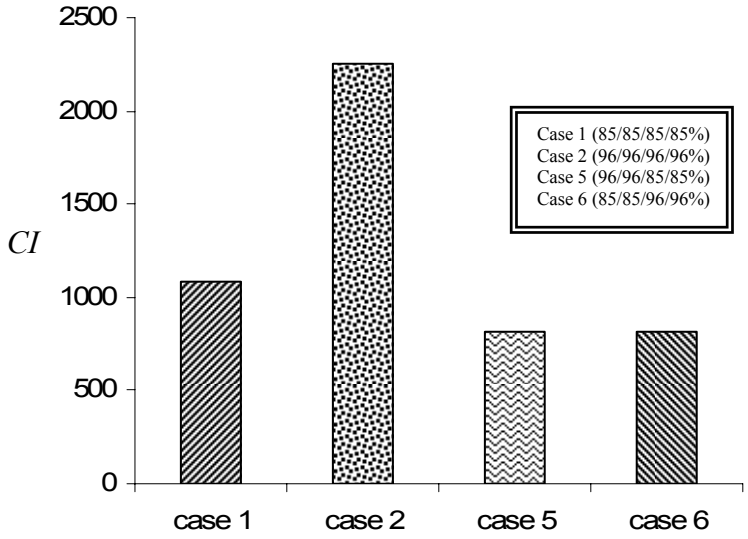

Figure 4.9: Complexity index versus outlet relative humidity profiles

4.3.3. Modeling of the Continuous Biodrying Reactor

Although there have been several studies on biodrying of municipal sludge, little information is available on the modeling aspects of a biodrying reactor. To better understand the transport phenomena inside the biodrying reactor, modeling is a critical step. The insights gained through modeling can also result in a more efficient reactor design, better control, and establishing scale-up criteria. The modeling strategy, and hence the results, follow the methodology discussed in section 3.3.

4.3.3.1. Lumped Modeling Results

The lumped model was developed in such an early phase of this study that no experimental data were available at the time. As can be seen in Figure 4.10, the dry solids content increases from the top to the bottom and reaches a flat profile at the bottom of the biodrying reactor. Different residence times were examined, and the results for 5- and 6-day residence times indicate dry solids content of above 60% at the bottom of the biodrying reactor. Later, the experimental data revealed that such dry solids content can not be achieved in a 4-day residence time. The main reason was attributed to the lumped model, which assumed the same drying mechanisms for

removing different types of water. In other words, in the lumped model there was no distinction between the unbound and bound water. Despite its simplicity the results were unrealistic and no further improvement was made on the lumped model. Therefore, the distributed model was built to better represent the transport phenomena in the biodrying reactor.

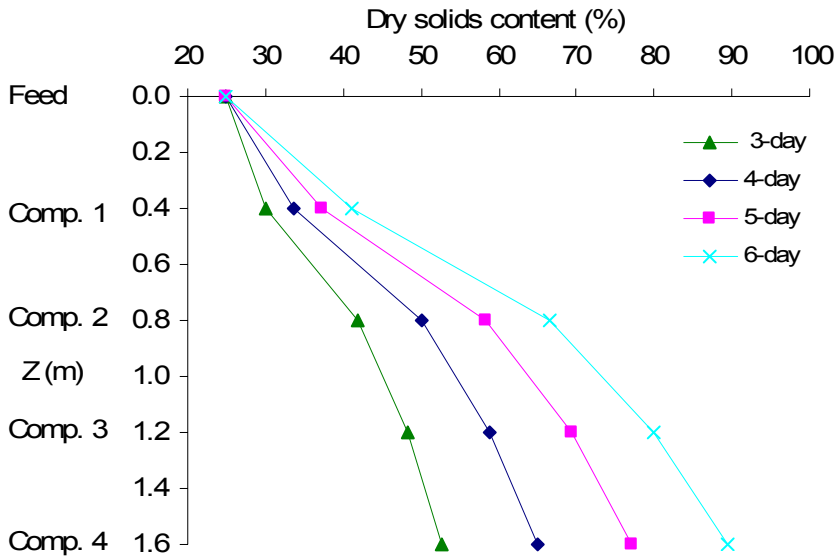

Figure 4.10: Lumped modeling results- dry solids content vs. residence times (Navaee-Ardeh et al., 2006b)

4.3.3.2. 1-D Distributed Modeling

The 1-D distributed model is a global heat transfer based on the principles of chemical and biochemical reactions in porous media. The model includes biological heat production, an evaporation sink term, and convective and conductive heat transfer. Two types of convective heat transfer are represented: convection due to the solid phase, which brings into play the sensible heat, and convection due to the gas phase. The model incorporates these heat transfer terms into a single equation solved for each compartment separately using the boundary conditions as a term linking any two adjacent compartments. The model assumes lumped parameters in the gas flow direction and distributed parameters in the solid flow direction, as shown in Figure 4.11a.

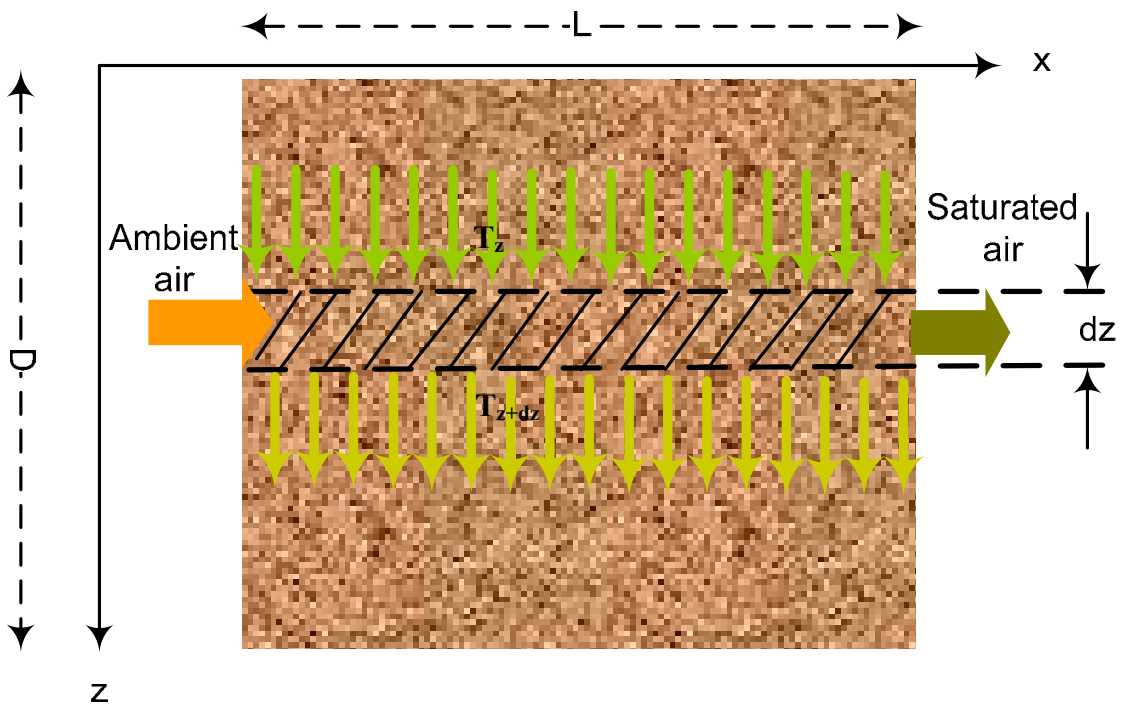

(a)

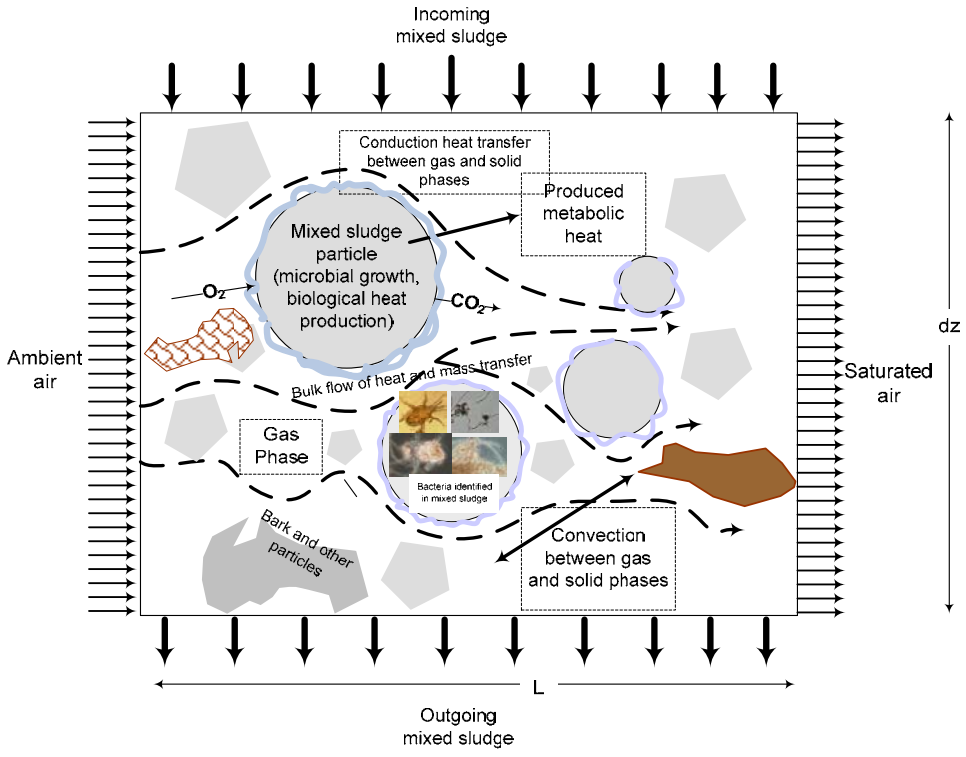

(b)

Figure 4.11: Schematic of one compartment in (a) macroscopic and (b) microscopic scales

For the 1-D modeling, the following simplifications and/or assumptions are made:

- For each compartment, air mass flowrates conservation is assumed;
- All phases (solid and gas) in the matrix are at equal temperature (thermal equilibrium among phases). Du and Wang (2001) found that for porous media with forced convection, local thermal equilibrium is a reasonable assumption if Re>10. In this study as shown in Table 4.7, all Reynolds numbers are higher than 10. Note that the difference in water concentration between the solid and the gas phase provides the driving force for the mass transfer of water between these two phases;
- The process is at steady-state. This assumption is justified by the fact that a stable matrix temperature and drying rate have been observed experimentally;
- The heat loss through the walls of the reactor is assumed to be negligible. The reactor is insulated with UHMW (ultra high molecular weight) polyethylene on the inside and regular insulation materials on the outer surface. This assumption has been shown to be valid for large scale systems that have a small surface/volume ratio (Mason and Milke, 2005a), as is the case for the current biodrying reactor;
- There is enough oxygen in the porous matrix for microbial biodegradation. This assumption is particularly valid for processes under forced aeration such as solid-state fermentation (Gowthman et al., 1993);
- The specific thermal heat capacity of the solid phase is constant for each compartment;
- For aerobic processes such as biodrying, it is essential to have sufficient pneumatic conditions along the reactor to ensure that oxygen in the air reaches the microorganisms and that anaerobic hot spots are minimized. The pilot-scale biodrying reactor was designed so that the air is uniformly distributed in each compartment through a series of perforated plates installed at the gas inlet and outlet of each compartment. Therefore, a uniform gas flow distribution is assumed for each compartment;
- The biological heat ($\dot{Q}_{bio}$) is obtained from the following correlation (details were described in Eq. (4.6)):

$$\dot{Q}_{bio} = Q_{bio-standard}\ \rho_{O_2}\left(\left(\frac{V_{O_2}}{V_{Air}}\right)_{in} - \left(\frac{V_{O_2}}{V_{Air}}\right)_{out}\right)\frac{Q_g}{WLD} \tag{4.9}$$

Based on these assumptions, and the control volume and heat transfer mechanisms illustrated in Figure 4.11, the following overall heat transfer balance is obtained for each compartment:

$$
\begin{aligned}
&-\dot{m}_{total,i}\left(w_{ms,i}Cp_{ms,i}+(1-w_{ms,i})Cp_{H_2O}\right)(T_i-T_r)\Big|_z^{z+dz} \quad \leftarrow\text{---- Sensible heat transfer due to solid phase}\\
&+k_s(1-\varepsilon_i)LW\left.\frac{dT_i}{dz}\right|_z^{z+dz} \quad \leftarrow\text{---- Conductive heat transfer due to solid phase}\\
&+(d\dot{m}_{g,i})Cp_{g,i}(T_{in}-T_r)-(d\dot{m}_{g,i})Cp_{g,i}(T_i-T_r) \quad \leftarrow\text{---- Convective heat transfer due to gas phase}\\
&+\dot{Q}_{bio,i}(1-\varepsilon_i)LWdz-\Delta H_{eva}a_{w,i}(X_{out,i}-X_{in})d\dot{m}_{g,i}=0
\end{aligned}
\qquad (4.10)
$$

↑ Biological heat source term ↑ Evaporative heat sink term

for i=1,2,3,4

The first term represents the sensible heat change due to the solid flow in the reactor. The second and third terms represent the conductive heat transfer due to the solid phase and the convective heat transfer due to the gas phase, respectively. The fourth term represents the bioheat generated through the exothermic metabolic microbial activity, and the last term is a sink term representing the quantity of energy removed from the matrix through water evaporation.

The values of the physical parameters in Eq. (4.10) are given in Tables 4.6 and 4.7. The following comments are in order:

- The uniform gas flow distribution assumption, as discussed earlier, leads to

$$d\dot{m}_{g,i}=\frac{\dot{m}_{g,i}}{D}dz\ ;$$

- $X_{out,i}$-X_{in} represents the net amount of water transferred to the gas phase, which is the difference of absolute humidity between the outlet and the inlet gas (kg H_2O/kg air). It is evaluated using Eq. (4.7).
- The evaporation heat of water, ΔH_{eva}, has a negative correlation with the temperature. In order to incorporate this in Eq. (4.10), a constant value of ΔH_{eva}=2270000 J/kg H_2O (Perry

and Green, 1997) was used along with a correction factor, $a_{w,i}$, so that the last term in Eq. (4.10) remains constant for each compartment but varies from one compartment to another as the dry solids content varies. The correction factor, $a_{w,i}$, was fitted using data obtained from isotherm experiments on mixed sludge with saturated salt solutions, by means of a procedure adapted from Rowley and Mackin (2003) and Labuza (1984):

$$a_{w,i} = 4.286 w_{ms,i}^2 - 4.74 w_{ms,i} + 2.009 \quad (4.11)$$

A similar model was also reported for solid-state fermentation by Von Meien and Mitchell (2002);

- The heat capacity of the gas phase ($Cp_{g,i}$) is determined from the following correlation (Geankoplis (1993)): $Cp_{g,i} = 1005 + 1880 X_{out,i}$;
- The reference temperature, T_r, is assumed to be equal to T_{in}.

Based on these comments, Eq. (4.10) leads to the following differential equation:

$$\frac{d^2 T_i}{dz^2} - \frac{\alpha_i}{k_s(1-\varepsilon_i)LW}\frac{dT_i}{dz} - \frac{\dot{m}_{g,i} Cp_{g,i}}{k_s(1-\varepsilon_i)LWD} T_i = -\frac{\dot{m}_{g,i} Cp_{g,i} T_{in} + \dot{Q}_{bio,i}(1-\varepsilon_i)LWD - \Delta H_{eva} a_{w,i}(X_{out,i} - X_{in})\dot{m}_{g,i}}{k_s(1-\varepsilon_i)LWD} \quad (4.12)$$

where $\alpha_i = \dot{m}_{total}(w_{ms,i} Cp_{ms,i} + (1 - w_{ms,i}) Cp_{H_2O})$. Note that Eq. (4.12) is a convection-diffusion ordinary differential equation for each compartment (i=1,2,3,4) that, along with boundary conditions, can be solved analytically. For the boundary conditions, the inlet temperature in the 1st compartment is equal to T_{in}, and the inlet temperature in the other compartments is equal to the temperature at the outlet of the previous compartment. Note that one of the exponential terms in the analytical solution vanishes due mainly to a highly convective dominated problem, therefore, only one boundary condition is required to satisfy the analytical solution. The analytical solution for each compartment is given in Appendix A (paper A2).

4.3.3.3. Dimensionless Analysis on 1-D Model

Dimensionless analysis can provide basic insights into the mechanisms that govern the transport phenomena taking place in a process. A dimensionless form of Eq. (4.11) was derived, which brings into play dimensionless groups:

$$\frac{d^2T_i^*}{dz^{*2}} - A_i\frac{dT_i^*}{dz^*} - Pe_iT_i^* + B_i = 0 \text{ , for } i=1, 2, 3, 4 \tag{4.13}$$

where $T_i^* = \frac{T_i - T_{in}}{T_{bot} - T_{in}}$ is the dimensionless temperature, $z^* = \frac{z}{D}$ is the dimensionless height, and A_i, B_i and Pe_i are:

$$A_i = \frac{D\alpha_i}{k_s(1-\varepsilon_i)LW} \tag{4.14}$$

$$B_i = \frac{\dot{Q}_{bio,i}(1-\varepsilon_i)LWD^2 - \Delta H_{eva}a_{w,i}(X_{out,i} - X_{in})\dot{m}_{g,i}D}{k_s(1-\varepsilon_i)(T_{bot} - T_{in})LW} = E_{1,i}(E_{2,i} - 1) \tag{4.15}$$

$$E_{1,i} = \frac{\Delta H_{eva}a_{w,i}(X_{out,i} - X_{in})\dot{m}_{g,i}D}{k_s(1-\varepsilon_i)(T_{bot} - T_{in})LW} \tag{4.16}$$

$$E_{2,i} = \frac{\dot{Q}_{bio,i}(1-\varepsilon_i)LWD^2}{\Delta H_{eva}a_{w,i}(X_{out,i} - X_{in})\dot{m}_{g,i}D} \tag{4.17}$$

$$Pe_i = \frac{\dot{m}_{g,i}Cp_{g,i}D}{k_s(1-\varepsilon_i)LW} \tag{4.18}$$

A_i represents the ratio of the mixed sludge sensible heat to the conductive heat, and Pe_i, the Peclet number, is the ratio of convective heat to conductive heat. B_i, which brings into play two dimensionless numbers, $E_{1,i}$ and $E_{2,i}$, is the ratio of net heat generated to conductive heat. The net heat generated is the amount of the biological heat generated minus the heat lost through evaporation. $E_{1,i}$ is the ratio of evaporative heat to conductive heat, and $E_{2,i}$ is the ratio of bioheat to evaporative heat. $E_{2,i}$ is similar to the Damkohler number (Da), the ratio of the metabolic reaction rate to the convective rate. Da is used frequently in aerobic composting processes to control the biodegradation rate (Nakayama et al., 2007). All three of these terms (A_i, Pe_i and B_i) are important, and their relative values may vary in the four compartments of the biodrying reactor. The effect of these dimensionless parameters will be discussed in the next section.

4.3.3.4. 1-D Distributed Modeling Results

Experimental Data Presentation

In order to investigate different scenarios for the biodrying process and identify the 1-D model flexibility and limitations, four experimental cases were considered for this assessment. These cases represent diversity of the overall experimental program (Table 3.1) and involve two types of physical parameters, some with fixed values that remain the same for all cases (Table 4.6), and some that vary from one experiment to another (Table 4.7). Note that some of the fixed values in Table 4.6 were obtained from the literature.

Table 4.6: Fixed values of the physical parameters used for the 1-D model

	Comp. 1	Comp. 2	Comp. 3	Comp. 4	Reference
Cp_{H_2O} (J/(kg ^oC))	4200	4200	4200	4200	Bird et al. (2002)
$Cp_{ms,i}$ (J/(kg ^oC))	2360	2000	1800	1700	Perry and Green (1997)
D(m)	0.4	0.4	0.4	0.4	Pilot-scale set-up
d_p(mm)	1.5	1.3	1	0.8	Biodrying experiments
k_s (W/(m ^oC))	0.15	0.15	0.15	0.15	Geankoplis (1993)
L(m)	0.4	0.4	0.4	0.4	Pilot-scale set-up
W (m)	1	1	1	1	Pilot-scale set-up
ΔH_{eva} (J/kg H_2O)	2.27×10^6	2.27×10^6	2.27×10^6	2.27×10^6	Geankoplis (1993)
ρ_g (kg/m^3)	1.16	1.16	1.16	1.16	Geankoplis (1993)
ε_i	0.4	0.45	0.5	0.55	Biodrying experiments
μ(Pa.s)	1.5×10^{-5}	1.5×10^{-5}	1.5×10^{-5}	1.5×10^{-5}	Bird et al. (2002)

Table 4.7: Experimental parameters for 1-D model

	Case 1				Case 2				Case 3				Case 4			
	Comp. 1	Comp. 2	Comp. 3	Comp. 4	Comp. 1	Comp. 2	Comp. 3	Comp. 4	Comp. 1	Comp. 2	Comp. 3	Comp. 4	Comp. 1	Comp. 2	Comp. 3	Comp. 4
$Q_{g,i}$ (m^3/h)	26.40	5.0	26.0	18.0	16.5	8.0	14.0	7.7	7.91	7.41	7.31	7.38	7.04	7.11	7.63	7.65
$\dot{Q}_{bio,i}$ (W/m^3)	0	0	1000	2500	200	400	2200	2400	511	550	1200	2800	0	50	2000	3500
$w_{ms,i}$	0.42	0.43	0.45	0.47	0.42	0.44	0.46	0.50	0.37	0.41	0.42	0.45	0.42	0.44	0.5	0.54
$a_{w,i}$	0.78	0.76	0.75	0.73	0.78	0.75	0.74	0.71	0.84	0.79	0.77	0.76	0.78	0.75	0.71	0.7
$RH_{out,i}$(%)	73	66	88	89	68	72	92	55	80	97	75	80	41	83	92	100
$T_{out,i}$(^{o}C)	18	20	25.6	27.3	23.5	25	28	42.8	29	30	31	33.8	23	24.3	36	40
Pe_i	101	20	117	90	63	33	63	39	30	30	33	37	27	29	34	38
$Re_i = \frac{u_{g,i}\rho_g d_p}{\varepsilon_i \mu}$	468	68	246	124	291	109	133	53	140	101	69	51	125	97	72	53
$E_{2,i}$	0	0	0.54	1	0.2	0.65	1.13	1.5	0.53	0.45	1.17	1.96	0	0.07	1.15	1.32
RT (days)	6				6				4				8			
RR(%)	30				30				15				15			
RH_{in} (%)	13				14				12				10			
T_{in} (^{o}C)	24				25				27				26			
$\dot{m}_{total}$ (kg/s)	0.001128				0.001128				0.001692				0.000846			

In this section, the accuracy of the 1-D model is assessed against the experimental data. Note that the temperatures in the gas flow direction are averaged in each compartment (last column in Table 4.8), and are used for the mode accuracy assessment. Note that the T_{out} values are the average of internal temperatures near the wall and the ambient temperature. This is mainly related to the effect of ambient conditions on the external conduits of each compartment in Figure 3.2.

Table 4.8: Experimental temperatures in the continuous biodrying reactor*

		T_{in} (°C)	x=7.5 cm	x=17.5 cm	x=27.5 cm	T_{out} (°C)	Averaged Temperature
Case 1	Comp. 1	24	13	13	14	18	13
	Comp. 2	24	13	15	16	20	15
	Comp. 3	24	15	15	20	26	17
	Comp. 4	24	19	20	27	27	22
Case 2	Comp. 1	24	15	16	17	24	16
	Comp. 2	24	17	18	23	25	19
	Comp. 3	24	19	28	38	28	28
	Comp. 4	24	30	38	47	43	38
Case 3	Comp. 1	26	12	20	30	29	21
	Comp. 2	26	14	16	23	30	18
	Comp. 3	26	18	26	30	31	25
	Comp. 4	26	29	44	50	34	41
Case 4	Comp. 1	26	18	20	23	23	20
	Comp. 2	26	13	14	20	24	16
	Comp. 3	26	22	30	42	36	31
	Comp. 4	26	43	50	55	45	49

* The average temperature represents an arithmetic average of the bed temperature (excluding inlet and outlet temperatures)

The accuracy of the 1-D model is compared to the average values of experimental temperature in Figure 4.12. Although different operating conditions result in different temperature profiles in all four compartments, the overall trend is fairly similar for all cases. The standard error of mean was estimated to be ±3% using 5 temperature measurements on a typical point illustrated in Figure 3.3. Overall, the predicted temperatures are in good agreement with the experimental data, although larger differences can be noticed in the 4th compartment for cases 3 and 4. We believe these discrepancies are due to the growth behavior of the mesophilic and thermophilic microorganisms, which depend strongly on temperature (see section 2.4.1.2 for the effect of temperature on microbial activity). In both cases 3 and 4, the higher temperature in the 4th

compartment favors a higher growth rate of thermophilic bacteria, giving a higher bioheat release into the matrix of the mixed sludge. This contradicts the assumption of a uniform bioheat release and distribution that was made for the development of the 1-D model (see section 4.3.3.2). Note, however, that such an assumption simplified the 1-D model resulting in obtaining an analytical solution.

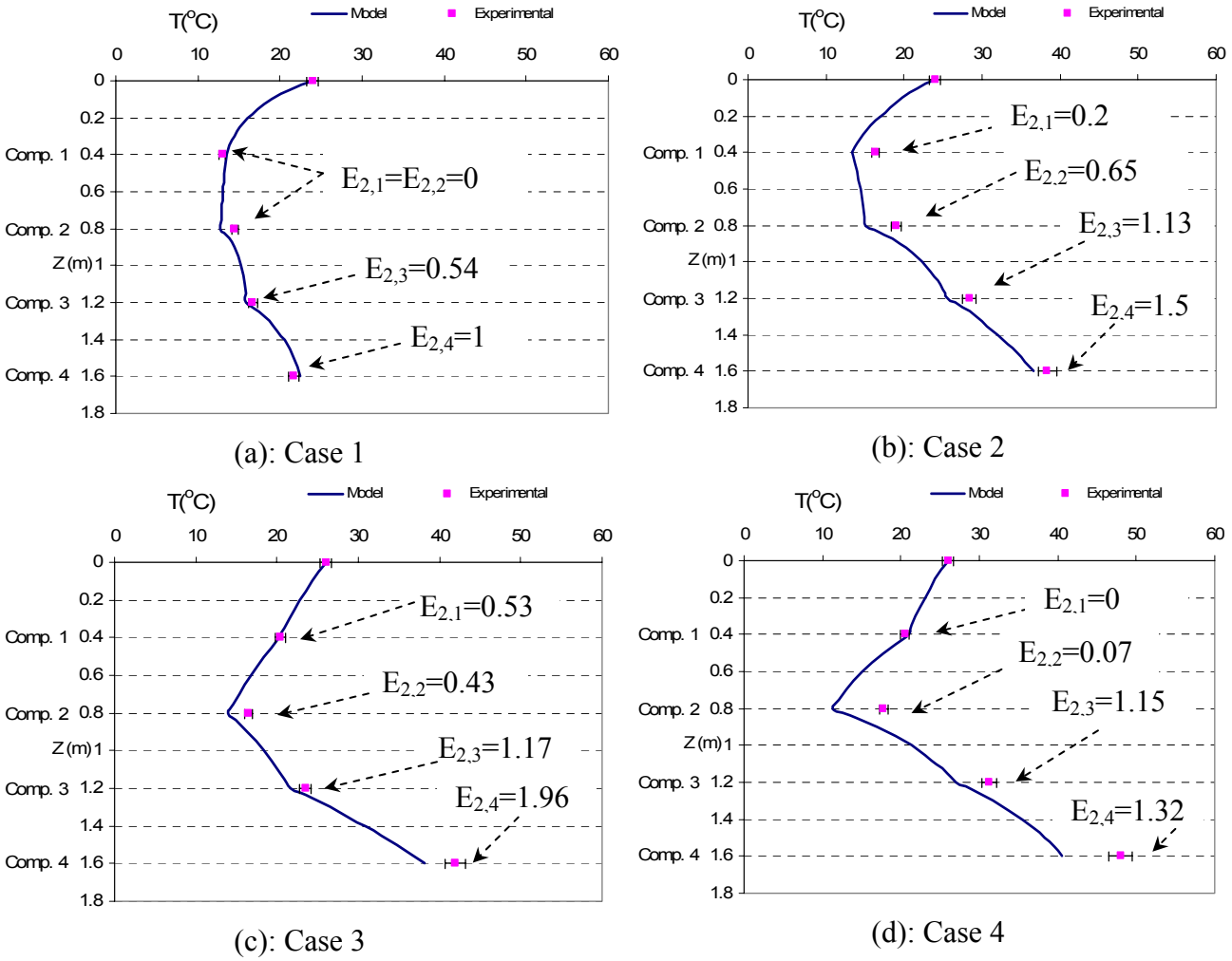

Figure 4.12: Comparison of the predicted temperatures to the experimental data

Analysis of the Temperature Profiles

Figure 4.13 displays the temperature profiles for all four cases. One may readily see that there are two zones: a convection-dominated zone that includes the 1st and 2nd compartments (first

zone) and a bioheat- and diffusion-dominated zone that includes the 3rd and 4th compartments (second zone). In the first zone, a dramatic drop in the matrix temperature can be observed in all cases. In this zone, as shown in Figure 4.4, the dry solids content does not significantly increase as the matrix temperature is quite low, resulting in less water transfer to the gas phase. The temperature in the first zone is slightly different from what was expected by Navaee-Ardeh et al. (2006a). Indeed, it was expected that the temperature would gradually increase from the top to the bottom compartments. Two phenomena occur simultaneously here. One is the very low bioheat generation in the 1st and 2nd compartments due mainly to the delay in the microbial start-up caused by the microbial lag phase that is longer at low temperatures. The other one is the cooling effect of the evaporation of the unbound water, which occurs at wet-bulb temperature. It also follows from the values of the ratio of bioheat to evaporative heat ($E_{2,i}$) (see Table 4.7) that the biological heat is not large enough to overcome the effect of evaporative heat. The decline of the matrix temperature is sharper in cases 1 and 2, which can also be inferred from the *Re* and *Pe* values in Table 4.7. The higher air flowrates, and hence the higher *Re* and *Pe* values, cause convection to dominate diffusion and, since the evaporation of unbound water takes place at wet-bulb temperature, the matrix temperature declines.

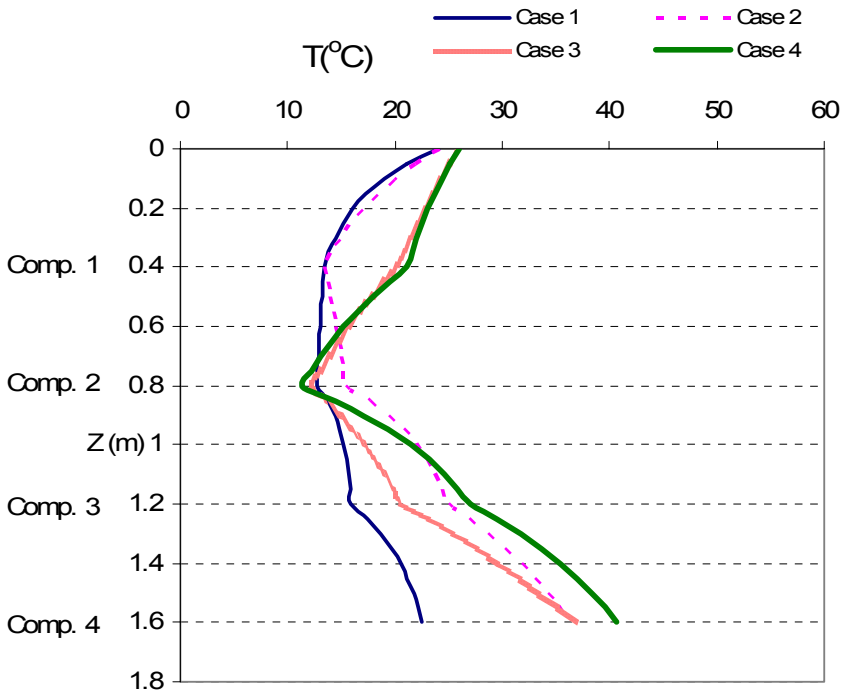

Figure 4.13: Predicted temperature profiles

In the second zone, the 3rd and 4th compartments, the temperature gradient quickly becomes positive, promoting the diffusion and evaporation of bound water, resulting in an increase of the matrix temperature and the dry solids content (Figure 4.4). This occurs because the bioheat released to the gas phase increases the gas phase moisture holding capacity as already discussed in section 4.3.2.2 (RH_{out} in Table 4.7), which then results in the transfer of more water to the gas phase and the diffusion of more bound water from the particle interior to its surface. As a result, mixed sludge drying improves. As can be seen in Table 4.7, the ratio of bioheat to evaporative heat ($E_{2,i}$) significantly jumps in the 3rd and 4th compartments, yielding a steep rise in the matrix temperature in Figure 4.13.

An optimum range for the moisture level (1-w_{ms}) under aerobic conditions of 45-55 (%w/w) was reported by Nakasaki et al. (1994), resulting in a maximum biological reaction rate and higher bioheat production. This was also confirmed by Liang et al. (2003). Consequently, Figure 4.4 shows that the dry solids content in the 3rd and 4th compartments provides optimum conditions for the microbial reactions. The diffusion and capillary forces create a water gradient between the interior and the exterior of the particles (Stanish et al., 1986). Although bound water diffusion is the controlling mechanism in the 3rd and 4th compartments, the higher temperatures related to the bioheat release enhance the drying rates significantly, as discussed above. Under these conditions, the bioheat surpasses the cooling effect of water evaporation ($E_{2,i}$ values >1 in Figure 4.12 and Table 4.7) . The *Re* and *Pe* numbers in the 3rd and 4th compartments for cases 3 and 4 are less than those for cases 1 and 2, which caused a sharp increase in the matrix temperature (Figure 4.13).

Finally, the highest temperature was found at the end of the 4th compartment for case 4. This is attributed to a higher level of biodegradation ($Q_{bio,4}$=3500W/m^3, Table 4.7). Due to the low air flowrate in this case, the rate of bioheat released in the matrix of mixed sludge is higher than the rate of heat removed by convection ($E_{2,i}$ >1). As a result, the accumulated heat leads to a higher temperature of the matrix.

Sensitivity Analysis on the 1-D Model

Sensitivity analyses were performed on the temperature of the porous matrix (results not shown due to lengthy mathematical formulations) with respect to the matrix porosity (ε), oxygen consumption (ΔO_2% v/v), air flowrate (Q_g), mixed sludge dry solids content (w_{ms}), and water removal rate including the combined effect of inlet and outlet air temperatures and relative humidity (X_{out}-X_{in}). It was found that the most influential parameters are the oxygen consumption rate (related to the aerobic exothermic biological heat), the air flowrate and the water removal rate (related to the outlet relative humidity profile).

4.3.3.5. Two-Dimensionality of the Transport Phenomena in the Continuous Biodrying Reactor

Usefulness and Shortcomings of the 1-D Model: Critical Review

Sludge drying rate in the continuous biodrying reactor can be used to estimate the final dry solids level. It is also critical for the design of a biodryer. As discussed earlier, the dry solids level is also essential for an economically feasible combustion operation in a biomass boiler.

The model-predicted temperatures were used to calculate the water removal rate (drying rate) for different cases. The total water removal rate is $\sum \rho_g Q_{g,i}(X_{out,i} - X_{in})$, which can be determined using Eq. (4.7) and the data in Tables 4.7 and 4.8. These results were compared to experimental data. As shown in Figure 4.14, the 1-D model is good only if the temperature variation in a given compartment does not vary significantly from the gas inlet to the gas outlet (see Table 4.8). For instance, the temperature variation in each compartment for case 1, and the 1st and 2nd compartments of all other cases is very small, and hence a good agreement can be observed between the model predicted drying rates and the experimental values. However, the agreement is not as good for the 3rd and 4th compartments in cases 2, 3, and 4, in which the exothermic aerobic bioenergy is the dominating mechanism. The usefulness of the 1-D model is then limited in such cases, because it poorly predicts the 2-D transport phenomena governing the higher aerobic exothermicity in the reactor, a situation that might arise in an industrial biodrying reactor.

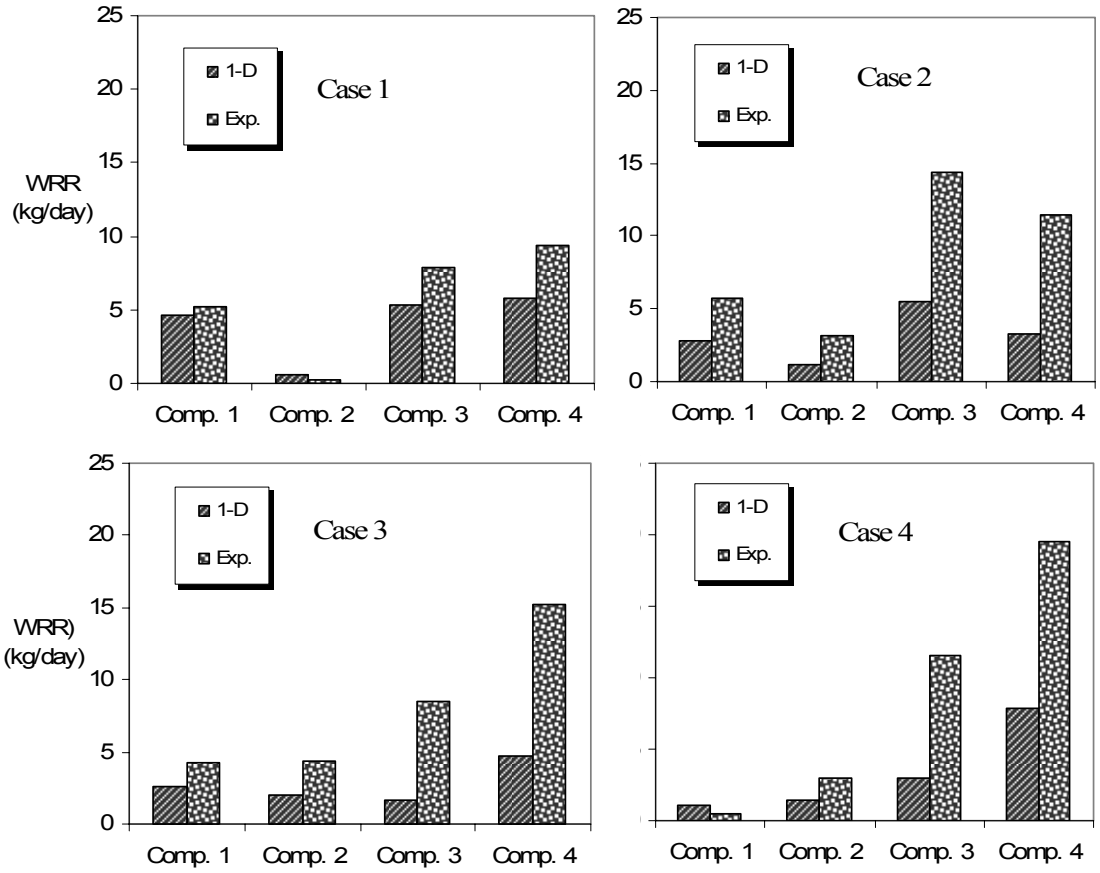

Figure 4.14: Comparison of 1-D model versus experimental data for sludge drying rate

Two-dimensional Profile of Experimental Temperatures

In contrast to our initial thought that a thin reactor (L=40 cm) would result in a one-dimensional temperature variation in the biodrying reactor, the temperature in each compartment has a different variation in the gas flow direction (Figures 4.15a, 4.16a, 4.17a, and 4.18a). Except in the 4th compartment, the experimental data show a sharp temperature decline in the first section of each compartment (x<7.5 cm). This is because of a rapid heat exchange between the gas and the solid phases in the front line of the gas entrance to each compartment. In fact, despite the complexity of porous media, it is known as one of the most efficient heat exchangers in the category of porous media heat exchangers (PMHE) (Hayes et al., 2008; and Pavel et al., 2004). In the 1st and 2nd compartments, due to the absence of bioheat on the one hand and the evaporation of unbound water at wet-bulb temperature on the other hand, the matrix temperature

faces a rapid initial decline. It tends to recover in the second section (x>7.5 cm) yet stays below the inlet gas temperature. As can be seen in Figures 4.15a, 4.16a, 4.17a, and 4.18a, due to this cold environment in the first zone (the 1st and 2nd compartments), the drying rate is very small, and accounts for less than one third of the total mass transfer (Figure 4.25). Nevertheless, the evaporation of the unbound water still progresses because the reactor is under vacuum conditions, controlled by the positive and negative blowers (see Figure 3.3). This can also be inferred from the X (kg H_2O/kg Air) values in Figures 4.15a, 4.16a, 4.17a, and 4.18a. The profile of X shows that regardless of the temperature decline in the first section (x<7.5 cm), there is always some mass transfer. This is why, despite our initial expectation that the front line in the gas flow direction (x< 7.5 cm) may dry more than the back, a uniform dry solids level was observed across each compartment at a given reactor height (z). This brings a great advantage to the biodrying reactor, and despite a two-dimensional mass and heat transfer phenomena, the mixed sludge across each compartment dries uniformly. This is related to the uniform transfer rate of moisture from the solid phase to the gas phase as the gas proceeds toward the exit in each compartment, which is related not only to the matrix temperature, but also to the relative humidity of the gas phase.

The temperature reestablishment strongly depends on the quantity of the bioheat generated in each particular compartment. For example, in the 3rd compartment, after a slight decrease (up to x=7.5 cm), the temperature increases along the rest of the reactor length. This is the point at which biological heat dominates the cooling effect of water evaporation. There is no decline in the matrix temperature in the 4th compartment except in case 1 which can be attributed to the extreme aeration in that compartment. This can be attributed to the moisture contents in the 3rd and 4th compartments (Table 4.7, Figure 4.4) that are in favor of increased metabolic activity of thermophilic bacteria. Such an activity generates substantial bioheat, which indeed increases the matrix temperatures and the water holding capacity of the gas phase.

A similar trend can also be seen in the solid flow direction (Figures 4.15b, 4.16b, 4.17b, and 4.18b). The description is similar to the transport phenomena discussed in the 1-D model (section 4.3.3.4).

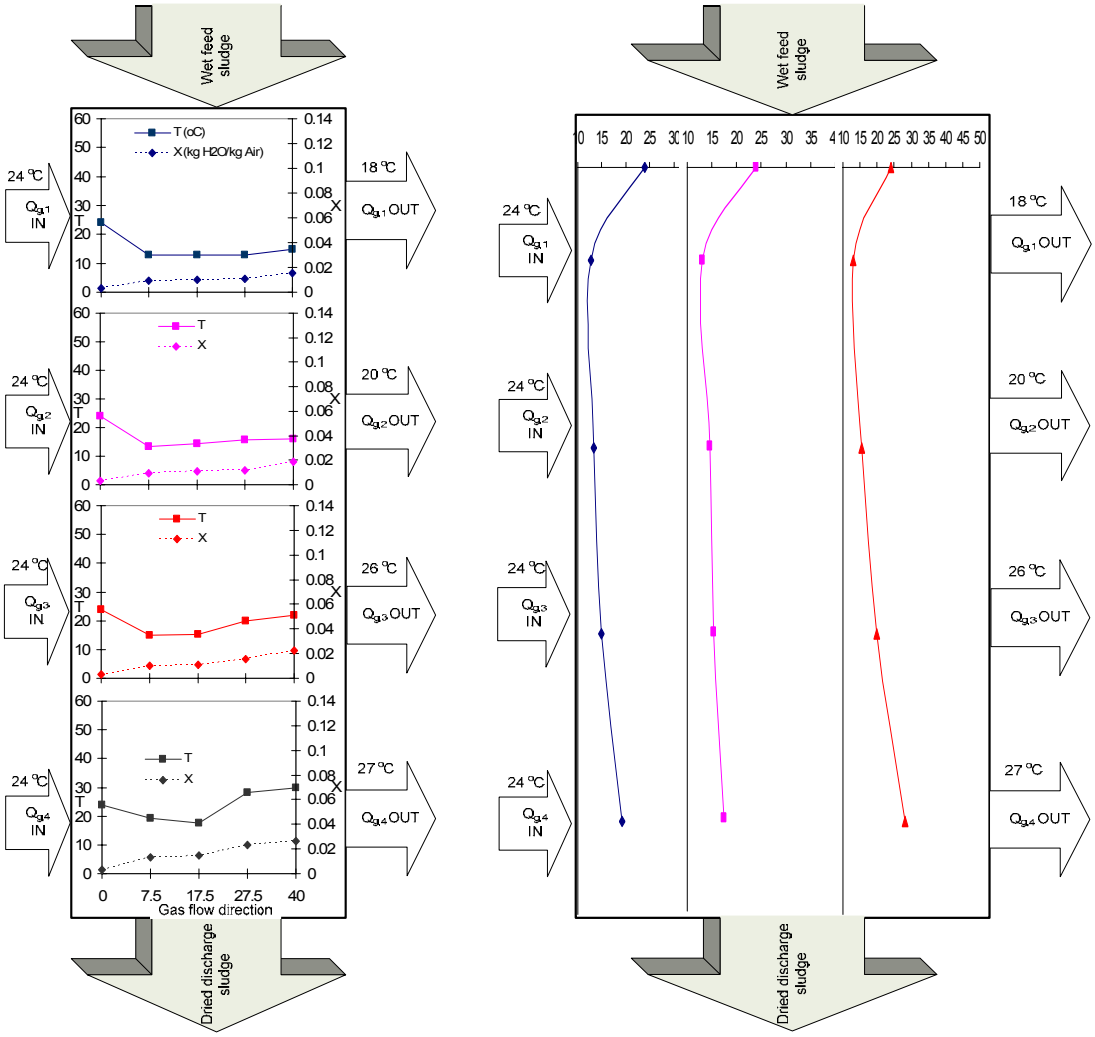

(a) (b)

Figure 4.15: Experimental *T* and *X* profiles in the gas (a) and *T* profiles in the solid (b) flow directions: case 1

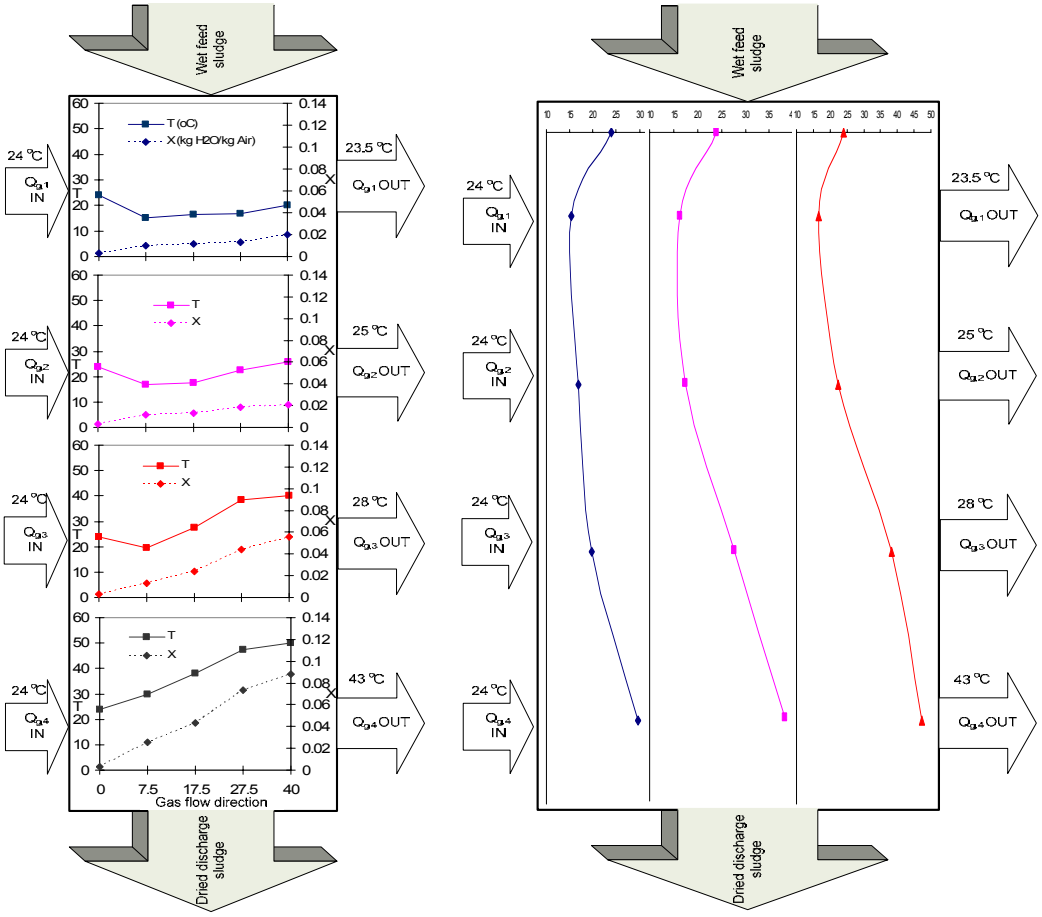

Figure 4.16: Experimental *T* and *X* profiles in the gas (a) and *T* profiles in the solid (b) flow directions: case 2

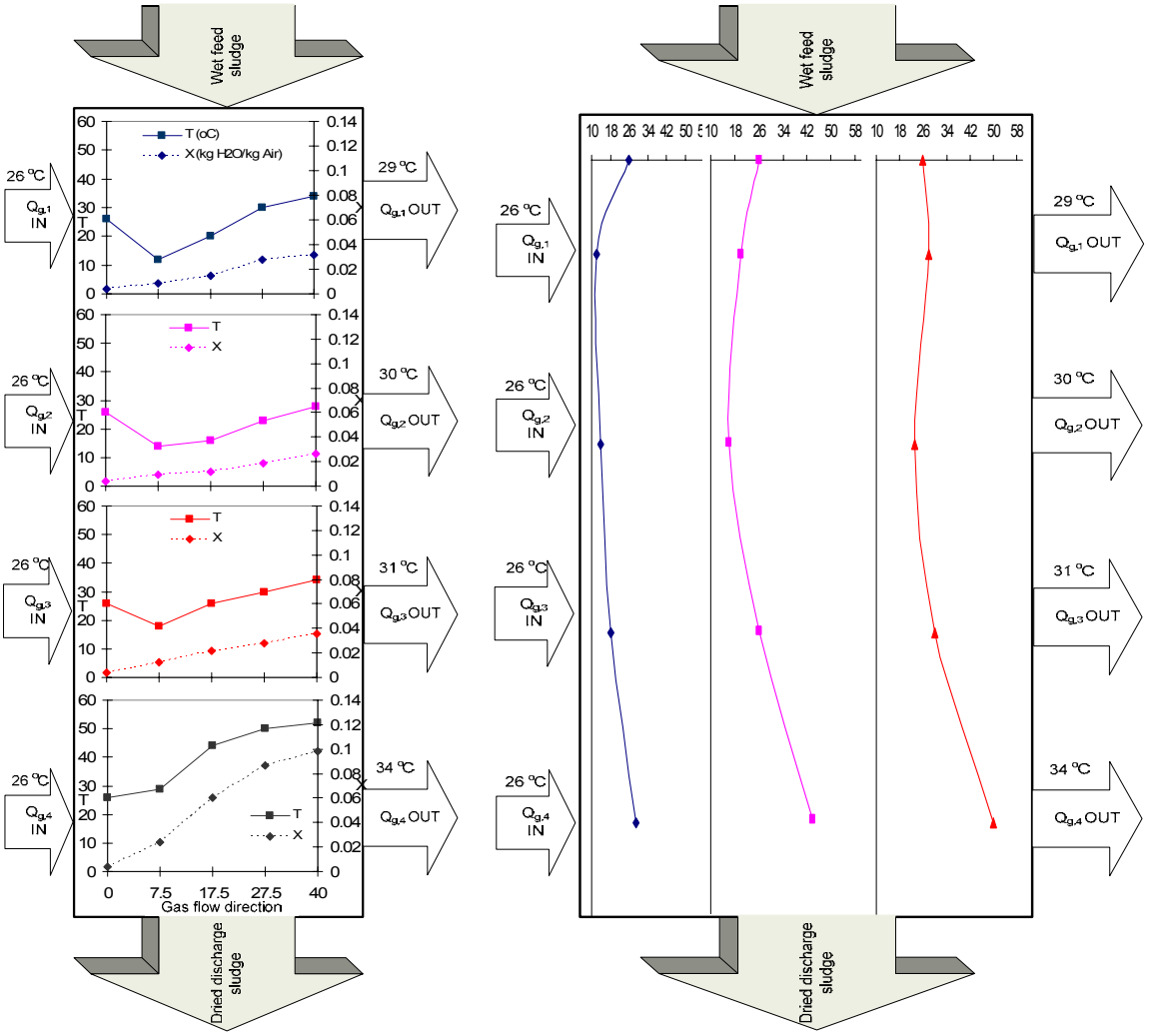

(a): case 3 (b): case 3

Figure 4.17: Experimental *T* and *X* profiles in the gas (a) and *T* profiles in the solid (b) flow directions: case 3

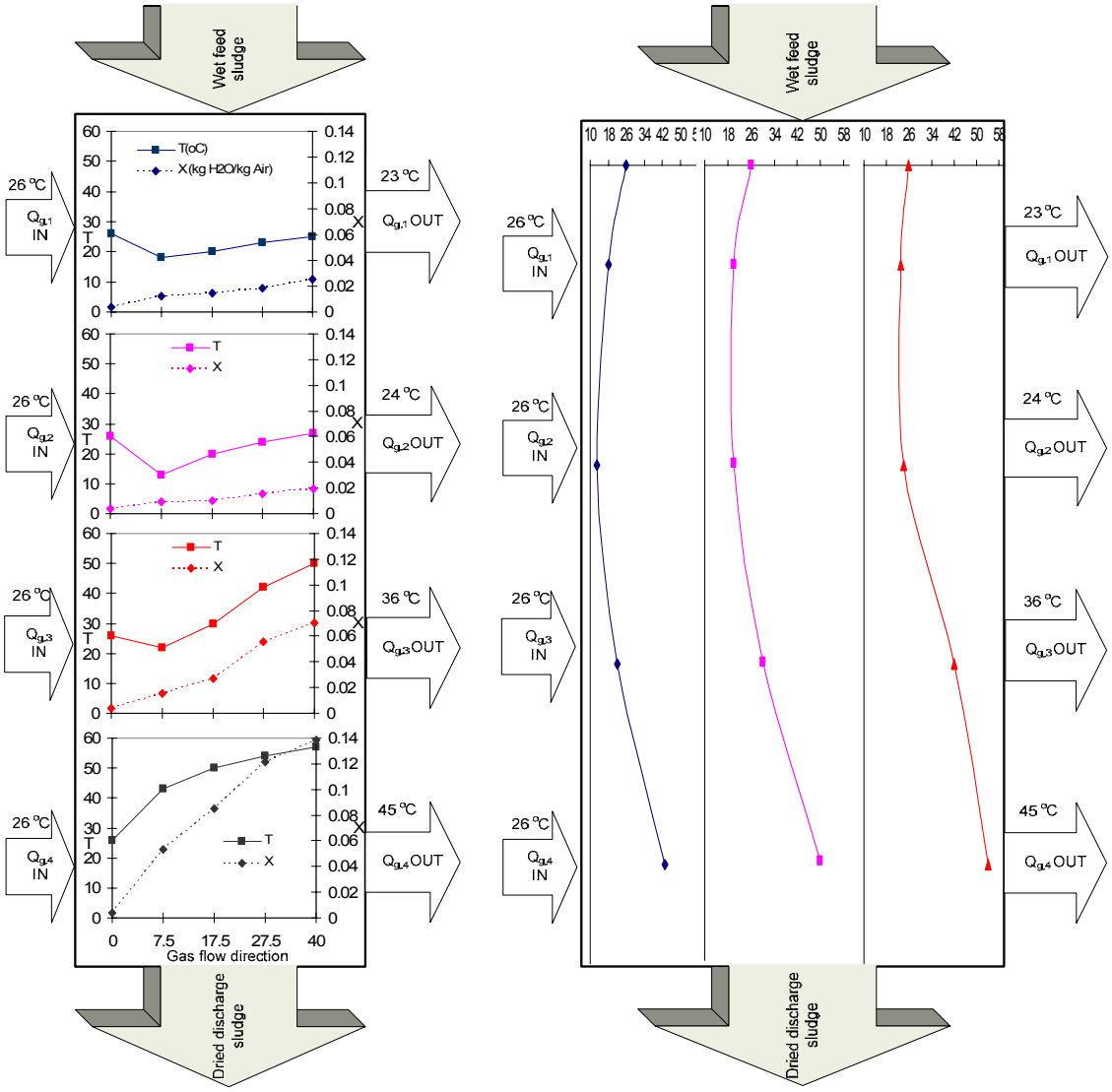

Figure 4.18: Experimental *T* and *X* profiles in the gas (a) and *T* profiles in the solid (b) flow directions: case 4

In conclusion, it is evident that these trends support a two-dimensional transport phenomenon in the continuous biodrying reactor, which can not be accounted for within the 1-D model.

The 1-D model was based on lumped parameters in the gas flow direction and distributed parameters in the solid flow direction. The discrepancies between the predicted and experimental results are attributed to the following:

- The biological heat release was assumed to be uniform in a given compartment. In reality, it may vary due to the effect of temperature in the gas flow direction on microbial activity of mesophilic and thermophilic bacteria;
- Most of the physical parameters used for the 1-D model are temperature dependent. However, due to the nature of the 1-D model, the physical parameters were assumed constant, whereas these properties may vary both in the gas and solid flow directions;
- The 1-D model assumes a flat air velocity profile in each compartment, making it impossible to take into account the effect of possible hot spots that are likely in full-scales in the matrix of mixed sludge. This may lead to unexpected results such as instantaneous firing and non-uniform final materials;
- Experimental results confirmed the expected disagreement between the predicted water removal rate and the experimental data from the 3^{rd} and 4^{th} compartments. This is mainly related to the exothermic bioheat generated in the 3^{rd} and 4^{th} compartments, which results in a large temperature variation from the gas inlet to its outlet.

Although good mathematical agreement was obtained between the model-predicted temperature and the averaged experimental data, the water removal rate for the 3^{rd} and 4^{th} compartments shows large model-data mismatch. Therefore, despite the simplicity of the 1-D distributed model, a 2-D distributed model is required to overcome the above-mentioned limitations and to improve the prediction capability of the model not only in the solid flow direction but also in the gas flow direction.

4.3.3.6. 2-D Distributed Modeling

The approach developed for the 1-D model is used for the development of the 2-D model. However, the 2-D model attempts to address and eliminate the limitations of the 1-D model. Based on concepts of chemical and biochemical reaction engineering in porous media, it includes biological heat, evaporative heat, and convective and conductive heat transfer due to the solid and gas phases. Two types of convective heat transfer are represented: convection due to the solid phase, which brings into play sensible heat, and convection due to the gas phase.

All assumptions made for the 1-D model and described in Navaee-Ardeh et al. (2009a) are valid except:

- Specific heat capacities of the solid and gas phases are not constant;
- Heat conduction due to gas phase is negligible and only heat conduction in solid phase in both directions is considered;
- Gas flow distribution is not uniform and follows the ideal gas law (see Table 4.9).
  Each compartment is discretized in the *x* and *z* directions as illustrated in Figure 4.19

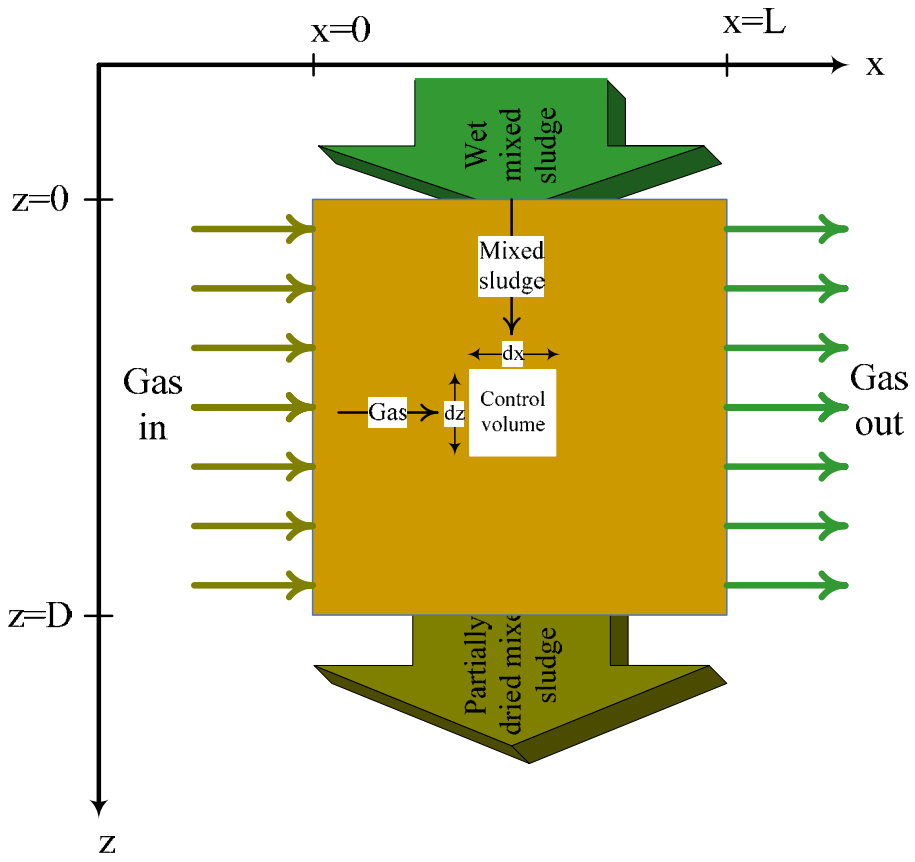

Figure 4.19: Schematic of a control volume in macroscopic scales for each compartment

Based on the assumptions and the control volume, and the heat transfer mechanisms illustrated in Figures 4.11b and 4.19, the following energy balance is obtained for the control volume in each compartment:

Solid phase conductive heat transfer in vertical direction

Solid phase conductive heat transfer in gas flow direction

$$W\frac{\partial}{\partial z}((1-\varepsilon_i)k_s\frac{\partial T_i}{\partial z})dzdx + W\frac{\partial}{\partial x}((1-\varepsilon_i)k_s\frac{\partial T_i}{\partial x})dzdx$$
$$-\frac{\partial(\Delta H_{eva.i}(T_i)X_i(x)d\dot{m}_{g,i})}{\partial x}dx \leftarrow \text{Evaporative heat sink term} \qquad (4.19)$$
$$-\frac{\partial(Cp_{g,i}d\dot{m}_{g,i}(T_i - T_r))}{\partial x}dx \leftarrow \text{Convective heat transfer due to gas phase}$$
$$-\frac{\partial}{\partial z}\left(d\dot{m}_s Cp_{mix,i}(T_i - T_r)\right)dz + \dot{Q}_{bio.,i}W(1-\varepsilon_i)dxdz = 0$$

Convective heat transfer due to solid phase

Biological heat source term

i=1,2,3,4

where i stands for control volume in compartment i and T_r is the reference temperature, which was chosen to be T_{in}.

The first and second terms represent the conductive heat transfer due to solid phase in x and z-direction, respectively. The third term is the thermal sink term representing the quantity of heat removed from the matrix through water evaporation. The fourth and fifth terms are convective heat transfers due to gas and solid phases, respectively, and the last term represents the bioheat generated through the aerobic exothermic microbial activity.

The following comments are in order:

- The mass flowrate of solid phase obtained from $d\dot{m}_{s,i} = \frac{\dot{m}_{total}}{LW}dx$;
- The mass flowrate of gas phase is given by $d\dot{m}_{g,i} = u_{g,i}\varepsilon_i\rho_{g,i}Wdz$;
- The biological heat was determined using the same approach as described in Navaee-Ardeh et al. (2009a);
- Reference temperature (T_r) is chosen to be that at the inlet (T_{in});
- Cp_{mix} is modeled as function of the reactor height $Cp_{mix} = az^2 + bz + c$, where coefficients *a, b,* and *c* are set from experimental data (see Table 4.9);

Due to the difficulty of finding an appropriate global bioheat model for the entire biodrying reactor, experimental bioheat values were used for the 1st and 2nd compartments (see Table 4.10), and correlation in Table 4.9 was employed for the other compartments.

Based on these assumptions, Eq. (1) leads to the following differential equation:

$$
\begin{aligned}
&-\frac{\partial}{\partial x}((1-\varepsilon_i)k_s\frac{\partial T_i}{\partial x})-\frac{\partial}{\partial z}((1-\varepsilon_i)k_s\frac{\partial T_i}{\partial z})\\
&=\dot{Q}_{bio.,i}(1-\varepsilon_i)-(T_i-T_{in})\frac{\dot{m}_{total}}{LW}\frac{\partial Cp_{mix.i}}{\partial z}\\
&-u_{g,i}\varepsilon_i\rho_{g,i}\left((T_i-T_{in})\frac{\partial Cp_{g,i}}{\partial X_i}\frac{\partial X_i}{\partial T_i}+Cp_{g,i}+X_i\frac{\partial \Delta H_{eva.i}}{\partial T_i}+\Delta H_{eva.i}\frac{\partial X_i}{\partial T_i}\right)\frac{\partial T_i}{\partial x}\\
&-Cp_{mix,i}\frac{\dot{m}_{total}}{LW}\frac{\partial T_i}{\partial z}
\end{aligned}
\tag{4.20}
$$

This equation is now according to the general form of the equation available in COMSOL Multiphysics (Version 3.5, USA) under the convection-conduction module:

$$
\vec{\nabla}.(-k\vec{\nabla}T)=Q-\rho Cp\vec{\mathbf{u}}.\vec{\nabla}T \tag{4.21}
$$

where

$$
k=\begin{pmatrix}k_s(1-\varepsilon_i) & 0\\ 0 & k_s(1-\varepsilon_i)\end{pmatrix}
$$

$$
\rho\mathrm{Cp}\vec{\mathbf{u}}=\begin{pmatrix}u_{g,i}\varepsilon_i\rho_{g,i}\left((T_i-T_{in})\frac{\partial Cp_{g,i}}{\partial T_i}+Cp_{g,i}+X_i\frac{\partial \Delta H_{eva,i}}{\partial T_i}+\Delta H_{eva,i}\frac{\partial X_i}{\partial T_i}\right) & 0\\ 0 & Cp_{mix,i}\frac{\dot{m}_{total}}{LW}\end{pmatrix}
$$

$$
Q=\dot{Q}_{bio.,i}(1-\varepsilon_i)-\frac{\dot{m}_{total}}{LW}(T_i-T_{in})\frac{\partial Cp_{mix,i}}{\partial z}
$$

where, $\frac{\partial X_i}{\partial T_i}=\frac{5141.7}{T_i^2}X_i(1+1.6X_i)\approx\frac{5142X_i}{T_i^2}$

Using the boundary conditions, $T(0, z)=T_{in}$ and $T(x,0)=T_{in}$, the set of four partial differential equations given in Eq. (4.20) were solved numerically using the convection-conduction heat transfer module in COMSOL Multi-physics (Version 3.5). Navaee-Ardeh et al.

(2009a) found that in the continuous biodrying reactor the convection heat transfer is greater than the conduction one. Therefore, a convective flux boundary condition, $\mathbf{n}.(-k\nabla T)=0$, was prescribed along the other two sides of the computational domain.

Preliminary simulations were done with coarse and fine meshes of P_2 Lagrange- quadratic triangular elements, which showed that the use of a 182 finite element mesh was adequate. Consequently, all simulations discussed in the next section were carried out with this mesh.

4.3.3.7. 2-D Modeling Results

In order to investigate different scenarios for the continuous biodrying process and identify model flexibility and limitations, three cases, differing in operating conditions, were considered and discussed in this study.

Cases 2, 3, and 4 were a series of experiments selected from the overall experimental program (Table 3.1) conducted at 6-, 4-, and 8-day residence times, respectively. All data presented in Tables 4.9 and 4.10 were obtained under a steady-state regime.

Table 4.9: Parameters involved in 2-D model

Parameter	Correlation or value	Reference
$\Delta H_{eva.,i}$ (J/kg H_2O)	$2982797-2427T_i$	Geankoplis (1993)
ε_i	$0.125z_i+0.375$	Biodrying experiment
$u_{g,i}$(m/s)	$\frac{T_i+273}{T_{in}+273}\frac{Q_{g,i}(m^3/h)}{16.25}$ (flat flow)	Biodrying experiment
RH(%)	$16.06+\frac{84.4(100x)}{1.24+(100x)}$	Biodrying experiment
$\dot{Q}_{bio,i}$ (W/m^3)	$\delta_1(\frac{T_i+273}{T_{in}+273})e^{\delta_2 z_i}$	Biodrying experiment
k_s (W/kg-ds)	0.15	Geankoplis (1993)
$z_{0,1}$(m)	0.2	Biodrying reactor
$z_{0,2}$(m)	0.6	Biodrying reactor
$z_{0,3}$(m)	1	Biodrying reactor
$z_{0,4}$(m)	1.4	Biodrying reactor

Table 4.10: Experimental parameters required for modeling

	Case 2				Case 3				Case 4			
	Comp 1	Comp 2	Comp 3	Comp 4	Comp 1	Comp 2	Comp 3	Comp 4	Comp 1	Comp 2	Comp 3	Comp 4
$Q_{g,i}$ (m^3/h)	16.5	8.0	14.0	7.7	7.91	7.41	7.31	7.38	7.04	7.11	7.63	7.65
$\dot{Q}_{bio,i}$ (W/m^3)	494	511	1770	2000	511	402	1200	2800	0	50	2000	3500
$w_{ms,i}$	0.42	0.44	0.46	0.50	0.37	0.41	0.42	0.45	0.42	0.44	0.5	0.54
RT (days)	6				4				8			
RR (% w/w)	30				15				15			
T_{in} (^{o}C)	24				26				26			
RH_{in} (%)	14				12				10			
d	78.1				156.8				51.6			
e	274.7				102.5				408			
f	2891				3054				2759			
δ_1(m^{-1})	1.56				1.38				1.68			
δ_2(W/m^3)	322.5				210				336.7			

The experimental temperature values are available in Table 4.8.

Temperature Profile in the Gas Flow Direction

The accuracy of the 2-D model is first assessed by comparing the numerical results to the experimental data in the gas flow direction. Although different operating conditions are expected to result in different temperature profiles in all four compartments, Figures 4.20, 4.21, and 4.22 show that the overall trend is fairly similar for all cases. The experimental error was estimated at ±3% using 5 temperature measurements taken at a typical location in the reactor. Overall, the predicted temperatures are in good agreement with the experimental data. The largest discrepancies were observed in the 4th compartment (about 30%). This is believed to be due to the complexity of the microbial growth behavior of the mesophilic and thermophilic microorganisms, which are not only space- and temperature-dependent but are also influenced by the moisture and nutrient availability in the matrix. In fact, the bioheat model (Table 4.9) does not take into account the effect of C/N ratio and moisture content. It was reported elsewhere that these two parameters also have a strong impact on the microbial growth in the

aerobic composting processes (Haug, 1993). Several global empirical bioheat models were developed and tested in this study, but were not accurate enough to estimate the bioheat in different compartments.

Note that a thorough investigation of the velocity profile would require adding momentum equation to the current set of equations, which would result in a more complex system to be solved. Therefore, only a flat velocity profile based on ideal gas law was used in all simulations.

The numerical results in the gas flow direction are presented in Figures 4.20, 4.21, and 4.22. Due to a rapid exchange between the gas and the solid phases, a sharp decrease can be noticed in every compartment when it enters the reactor ($x<7.5$ cm). In fact, this type of porous medium is known to be a very efficient heat exchanger (Hayes et al. (2008); Pavel et al. (2004)). However, one may observe that the temperature tends to increase in the second section ($x>7.5$ cm) of each compartment. The extent of this temperature rise depends on the quantity of bioheat generated in each compartment. More precisely, in the 3rd and 4th compartments, after a slight decrease (up to $x=7.5$ cm), the temperature increases all the way to the gas outlet in the reactor. This is mainly due to the availability of higher biological heat and exothermic activity of thermophilic bacteria (see Table 4.10). In the 1st and 2nd compartments, because of an evaporative heat dominating mechanism, the matrix temperature does not recover as much and stays below the inlet gas temperature.

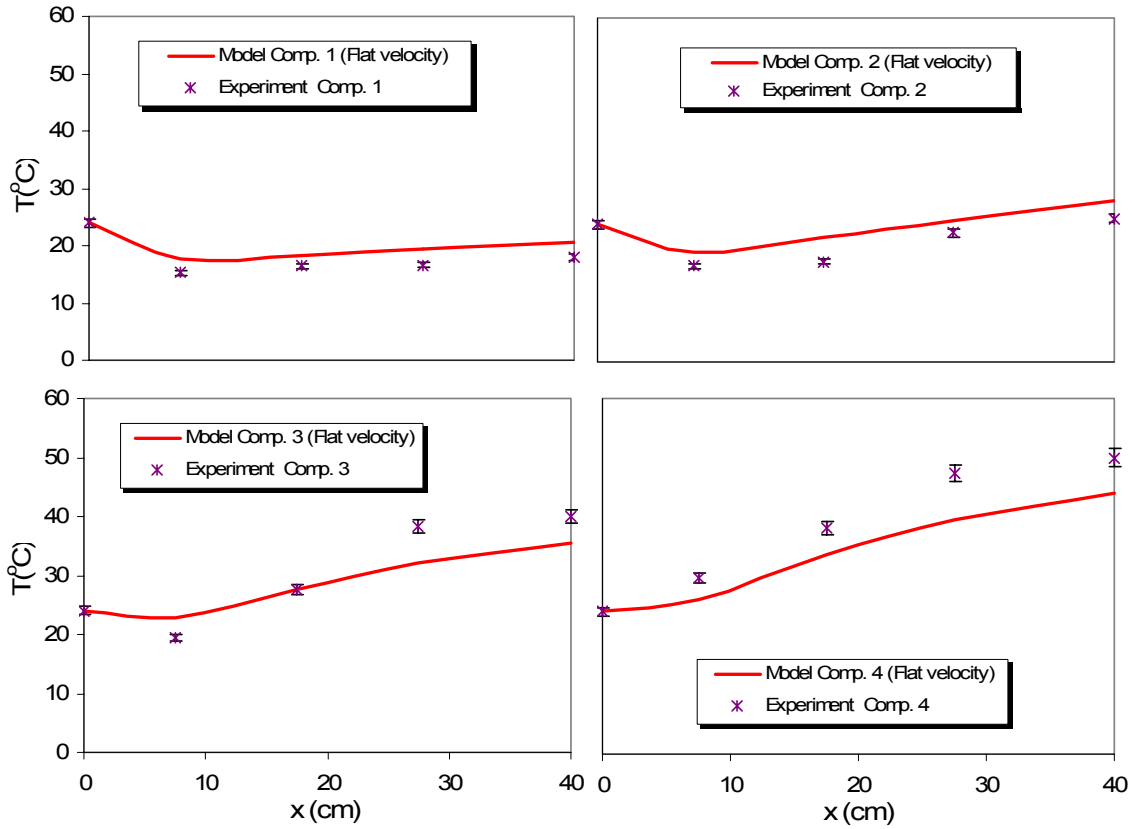

Figure 4.20: Comparison of the predicted temperatures to the experimental data in the gas flow direction (case 2)

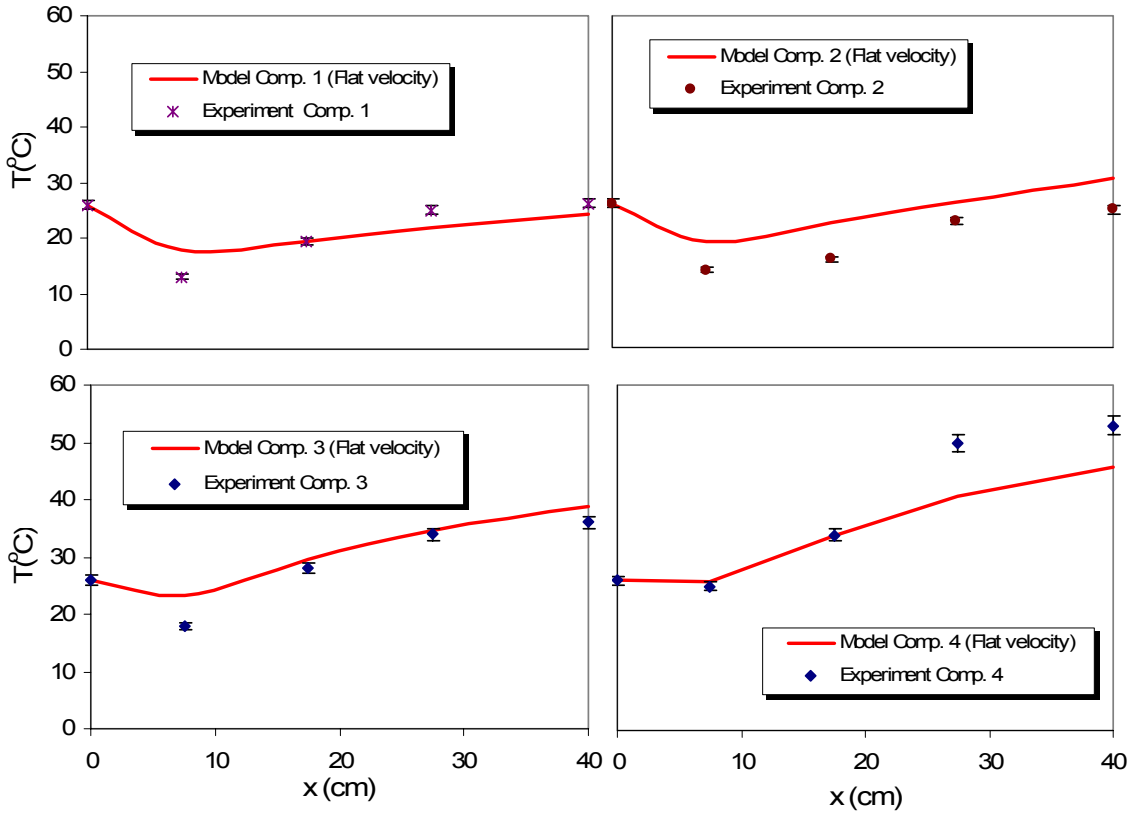

Figure 4.21: Comparison of the predicted temperatures to the experimental data in the gas flow direction (case 3)

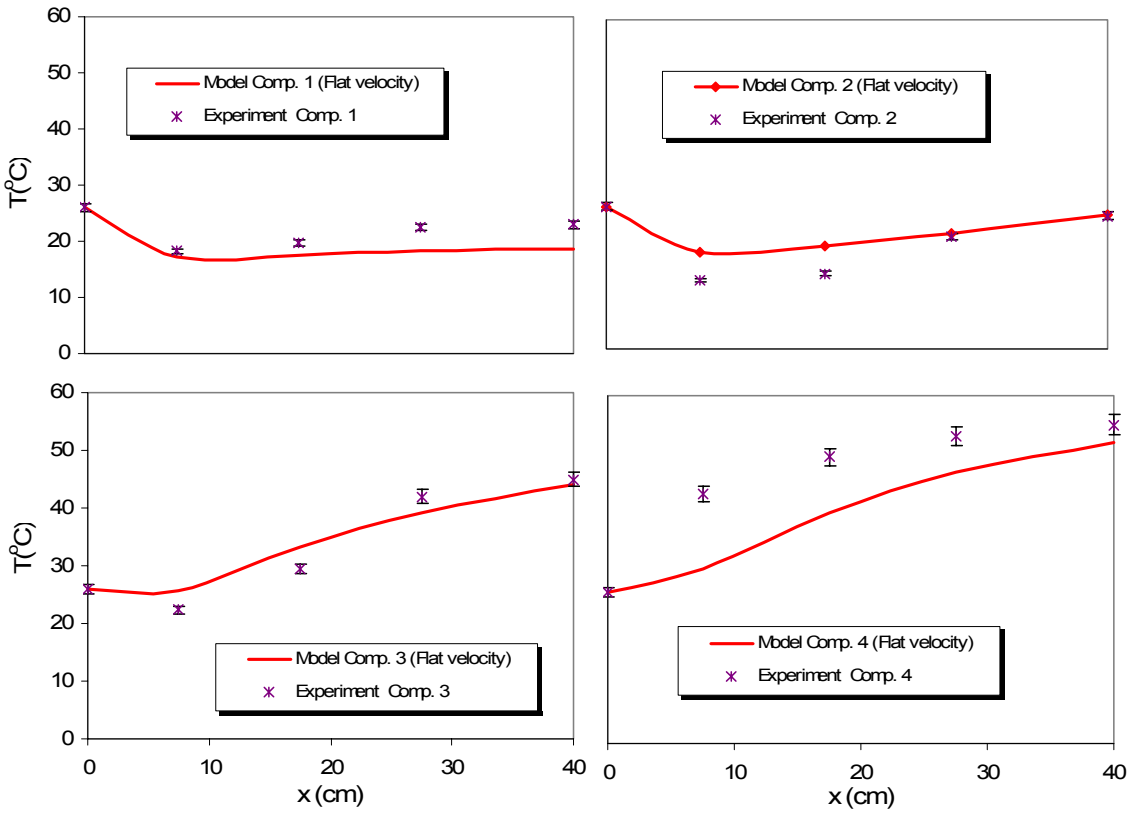

Figure 4.22: Comparison of the predicted temperatures to the experimental data in the gas flow direction (case 4)

Temperature Profile in the Solid Flow Direction

Figure 4.23 compares the numerical results obtained with the 2-D model to the experimental data. Only case 4 is considered here because similar behavior was observed in the other two cases. As can be seen in Figure 4.23, there is a good agreement between the experimental data and these numerical results. The upper bound discrepancy observed in the first section (x<7.5 cm) of the 4th compartment is 30%. However, this discrepancy decreases when approaching to the gas outlet. Possible explanations are due to the gas flow pattern at the entrance of each compartment or the dependency of the biological heat on the mixed sludge moisture content and nutrition level (C/N). The higher temperature in the 4th compartment favors the exponential growth rate of thermophilic bacteria, resulting in higher bioheat release into the matrix of mixed sludge and more bound water diffusion toward the surface of the particles.

In all cases, two zones can be recognized for the temperature profile in the biodrying reactor: a convection-dominated zone that is comprised of the 1st and 2nd compartments, and a diffusion- and bioheat-dominated zone that is comprised of the 3rd and 4th compartments. Consistent with the results of the 1-D model in the first zone, a large drop in the matrix temperature can be observed. This can be explained by the values of the bioheat to evaporative heat ratio (E_i) (see Table 4.7) that are smaller in the first zone, which means that the biological heat is not large enough to raise the temperature of the matrix. The dependence of this ratio on the temperature profile was observed in one of the related papers (Navaee-Ardeh, et al. (2009a)). It was then established that the temperature decreases when $E_i<1$ and increases when $E_i>1$.

In the second zone (the 3rd and 4th compartments) the higher bioheat results in a significant temperature rise in the matrix of mixed sludge. Navaee-Ardeh et al. (2009a) stated that the moisture content in these compartments leads to enhanced microbial activity. The diffusion of bound water out of the sludge particles is favored by higher temperature, which also speeds up drying. In the biodrying reactor, water removal mainly takes place in the second zone, because of the higher matrix temperature in this zone. This can be inferred from Figure 4.25 where it shows that more than 70% of the total water removal takes place in the second zone. Note that, as a rule of thumb, an increase of 11^{o}C in temperature causes a 50% drop in the air relative humidity, which improves mass transfer from the solid phase to the gas phase (Geankoplis, 1993).

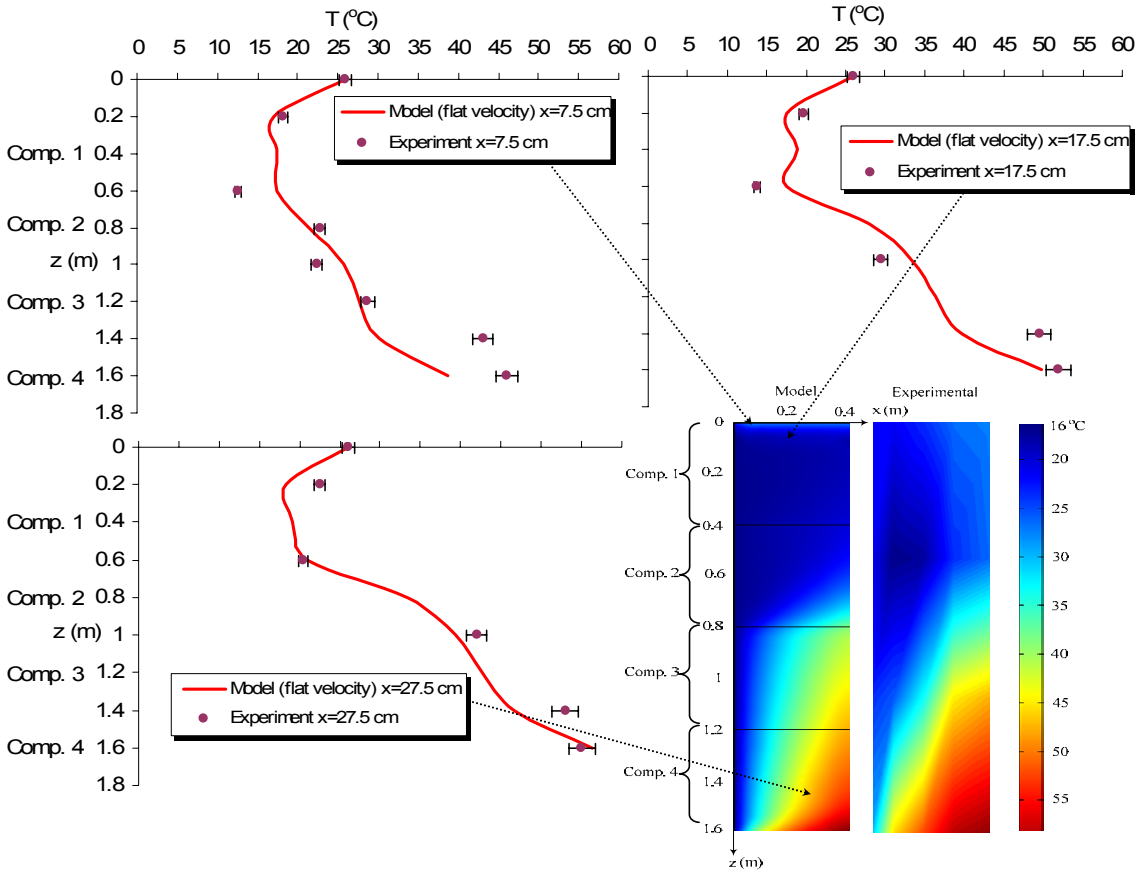

Figure 4.23: Comparison of the predicted temperatures to the experimental data in the solid flow direction (case 4)

Similar trends were observed for cases 2 and 3, as shown in Figure 4.24. In the first zone, the 1st and 2nd compartments, the matrix temperatures in cases 2 and 3 are higher than that of case 4, which is attributed to the bioheat values in cases 2 and 3 (Table 4.7). However, in the second zone, the 3rd and 4th compartments, the higher bioheat in case 4 results in the temperature profile rising faster than those of cases 2 and 3. The main difference between the first zone (the 1st and 2nd compartments) and the second zone (the 3rd and 4th compartments) in the biodrying reactor is that the major water removal takes place in the second zone, because of the higher matrix temperature in this zone. This can be inferred from Figure 4.25 where about 32% w/w and 40% w/w of the total water removal takes place in the 3rd and 4th compartments, respectively, and only 30 % w/w of the total water removal takes place in the 1st and 2nd compartments.

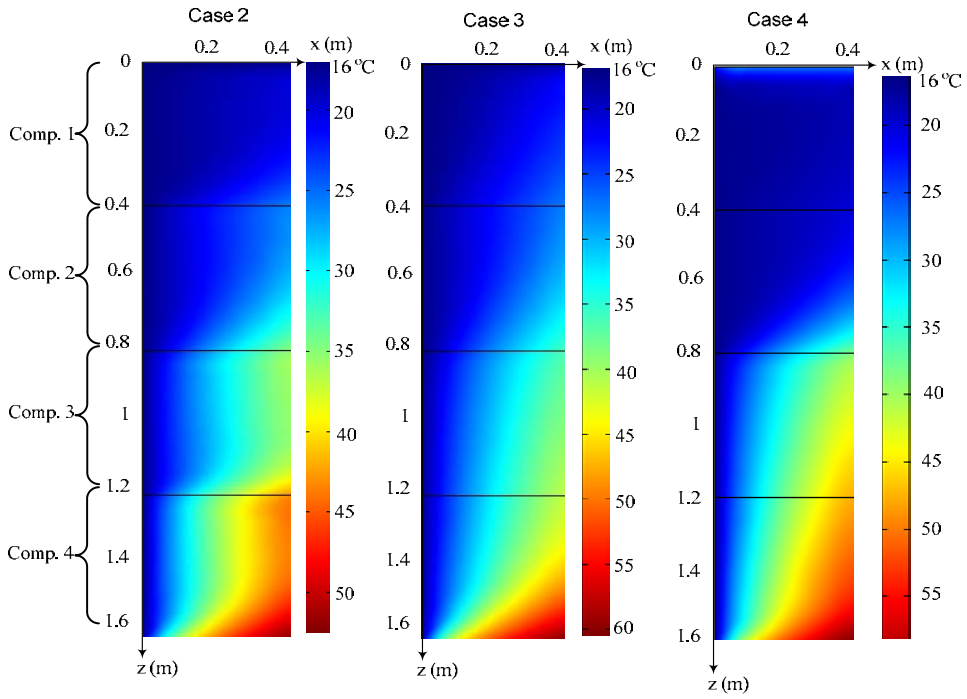

Figure 4.24: Two-dimensional profile of predicted temperatures for case 2 (6 days), case 3 (4 days), and case 4 (8 days)

The discrepancies between the experimental data and the model predicted values in the gas and solid flow directions are not only due to the experimental error. Other possible causes are: (1) the presence of anaerobic zones due to uneven distribution of gas velocity profile which were not investigated, (2) the complex mechanisms of water diffusion out of the particles in the mixed sludge which was not taken into account, (3) the numerical error inherent to the estimation of bioheat, and (4) the possibility of local thermal non-equilibrium which was not considered.

4.3.3.8. Dimensionless Analysis and Scale-Up Criteria

In addition to the water removal rate estimation using the 2-D model, the prevailing transport phenomena in the continuous biodrying reactor relevant to the unbound and bound water in the mixed sludge can be understood by means of dimensionless analysis and the key dimensionless numbers.

By performing dimensionless analysis on Eq. (4.19), the following equation was obtained:

$$\begin{aligned}
&\frac{k_s(T_{bot}-T_{in})}{L^2}\frac{\partial}{\partial x^*}((1-\varepsilon_i)\frac{\partial T_i^*}{\partial x^*})+\frac{k_s(T_{bot}-T_{in})}{D^2}\frac{\partial}{\partial z^*}((1-\varepsilon_i)\frac{\partial T_i^*}{\partial z^*})\\
&-\frac{\rho_g u_{g,in}(X_{out}-X_{in})\Delta H_{eva,in}}{L}u_{g,i}^*\varepsilon_i\frac{\partial(\Delta H_{eva,i}^* X_i^*)}{\partial x^*}\\
&-\frac{\rho_s u_{s,in} Cp_{s,in}(T_{bot}-T_{in})}{D}u_s^*\frac{\partial}{\partial z^*}\left(Cp_{mix,i}^* T_i^*\right)\\
&-\frac{\rho_g u_{g,in} Cp_{g,in}(T_{bot}-T_{in})}{L}u_{g,i}^*\varepsilon_i\frac{\partial(Cp_{g,i}^* T_i^*)}{\partial x^*}\\
&+\dot{Q}_{bio,i}(1-\varepsilon_i)=0
\end{aligned} \tag{4.22}$$

Rearranging Eq. (4.22) gives:

$$\begin{aligned}
&\frac{\partial}{\partial x^*}((1-\varepsilon_i)\frac{\partial T_i^*}{\partial x^*})+\frac{\frac{k_s(T_{bot}-T_{in})}{D^2}}{\frac{k_s(T_{bot}-T_{in})}{L^2}}\frac{\partial}{\partial z^*}((1-\varepsilon_i)\frac{\partial T_i^*}{\partial z^*})\\
&-\frac{\frac{\rho_g u_{g,in}(X_{out}-X_{in})\Delta H_{eva,in}}{L}}{\frac{k_s(T_{bot}-T_{in})}{L^2}}u_{g,i}^*\varepsilon_i\frac{\partial(\Delta H_{eva,i}^* X_i^*)}{\partial x^*}-\frac{\frac{\rho_s u_{s,in} Cp_{s,in}(T_{bot}-T_{in})}{D}}{\frac{k_s(T_{bot}-T_{in})}{L^2}}u_s^*\frac{\partial}{\partial z^*}\left(Cp_{mix,i}^* T_i^*\right)\\
&-\frac{\frac{\rho_g u_{g,in} Cp_{g,in}(T_{bot}-T_{in})}{L}}{\frac{k_s(T_{bot}-T_{in})}{L^2}}u_{g,i}^*\varepsilon_i\frac{\partial(Cp_{g,i}^* T_i^*)}{\partial x^*}+\frac{\dot{Q}_{bio.,i}}{\frac{k_s(T_{bot}-T_{in})}{L^2}}(1-\varepsilon_i)=0
\end{aligned} \tag{4.23}$$

Four dimensionless groups can be identified, which are defined below:

$$Pe_s=\frac{\frac{\rho_s u_{s,in} Cp_{s,in}(T_{bot}-T_{in})}{D}}{\frac{k_s(T_{bot}-T_{in})}{L^2}},\ \Pi_1=\frac{\frac{\rho_g u_{g,in}(X_{out}-X_{in})\Delta H_{eva,in}}{L}}{\frac{k_s(T_{bot}-T_{in})}{L^2}},\ Pe_g=\frac{\frac{\rho_g u_{g,in} Cp_{g,in}(T_{bot}-T_{in})}{L}}{\frac{k_s(T_{bot}-T_{in})}{L^2}},$$

$$\Pi_2=\frac{\dot{Q}_{bio,i}}{\frac{k_s(T_{bot}-T_{in})}{L^2}}$$

The unknown parameter for the continuous biodrying reactor, which has a key role in the transport phenomena, is the quantity of the bioheat. The bioheat in Π_2 can be correlated to the other three dimensionless numbers as follows:

$$\frac{\dot{Q}_{bio,i}}{\frac{k_s(T_{bot}-T_{in})}{L^2}} = \alpha_1\left(\Pi_1 Pe_s Pe_g\right) + \alpha_2 \tag{4.24}$$

Using the experimental data of the pilot-scale continuous biodrying reactor, the unknown constant coefficients were determined:

$$\dot{Q}_{bio,i} = 5\times10^{-10}\left(\frac{\rho_g u_{g,in}(X_{out}-X_{in})\Delta H_{eva,in}}{L}\right)Pe_s Pe_g + 92.2k_s\frac{T_{bot}-T_{in}}{L^2} \tag{4.25}$$

Besides obtaining a correlation for the estimation of the bioheat, two scale-up criteria can be established: a) Peclet number of the solid phase, and b) Peclet number of the gas phase. The former is related to the sludge residence time in the continuous biodrying reactor, whereas the latter is related to gas flowrate and how the outlet relative humidity is controlled. This shows how the 2-D model is relevant for designing a full-scale continuous biodrying process.

Eq. (4.25) considers the effect of outlet relative humidity profile, the inlet air conditions, the velocity of the gas phase, the reactor design parameters (*L*, *W*, *H*), and the initial temperature of the feed sludge. The latter is an important issue for a full-scale process because the sludge being fed to the biodrying reactor will be at a higher temperature and will already be acclimated. By estimating the quantity of the biological heat (Eq. 4.25) and using the 2-D model, the temperature profile and the water removal rate (drying rate) can be estimated for a full-scale process. This provides a significant advantage for the design of a full-scale biodrying process prior to any expensive experimentation and/or reactor installation. The results of this step can be merged with the techno-economic consideration, and provide the answer and guide to "Is the biodrying process feasible for a given pulp and paper mill?"

4.3.3.9. Comparison between the 1-D and 2-D Models

Predicting Water Removal Rate by Means of the 1-D and 2-D Models

To achieve an appropriate level of final dry solids content, all of these complex transport phenomena must work together, and by knowing the amount of water removal that can be

controlled by the outlet relative humidity profile, it is possible to have better control and design of the continuous biodrying reactor. This is why the temperature profiles in the continuous biodrying reactor play a significant role for the estimation of the water removal rate.

Figure 4.25 compares the drying rate calculated from the 1-D and 2-D models with the experimental data. Despite some discrepancies between the predicted temperatures in the 2-D model and the experimental data (Figures 4.20, 4.21, and 4.22), the predicted water removal rates (drying rates) are in good agreement with the experimental data. Whereas, the 1-D model poorly can predict the water removal rate for the diffusion zone (the 3rd and 4th compartments), in which the aerobic exothermicity dominates. Therefore, the 1-D model can not accurately address the transport phenomena (see section 4.3.3.4). This illustrates the significant advantage of the 2-D model over the 1-D model.

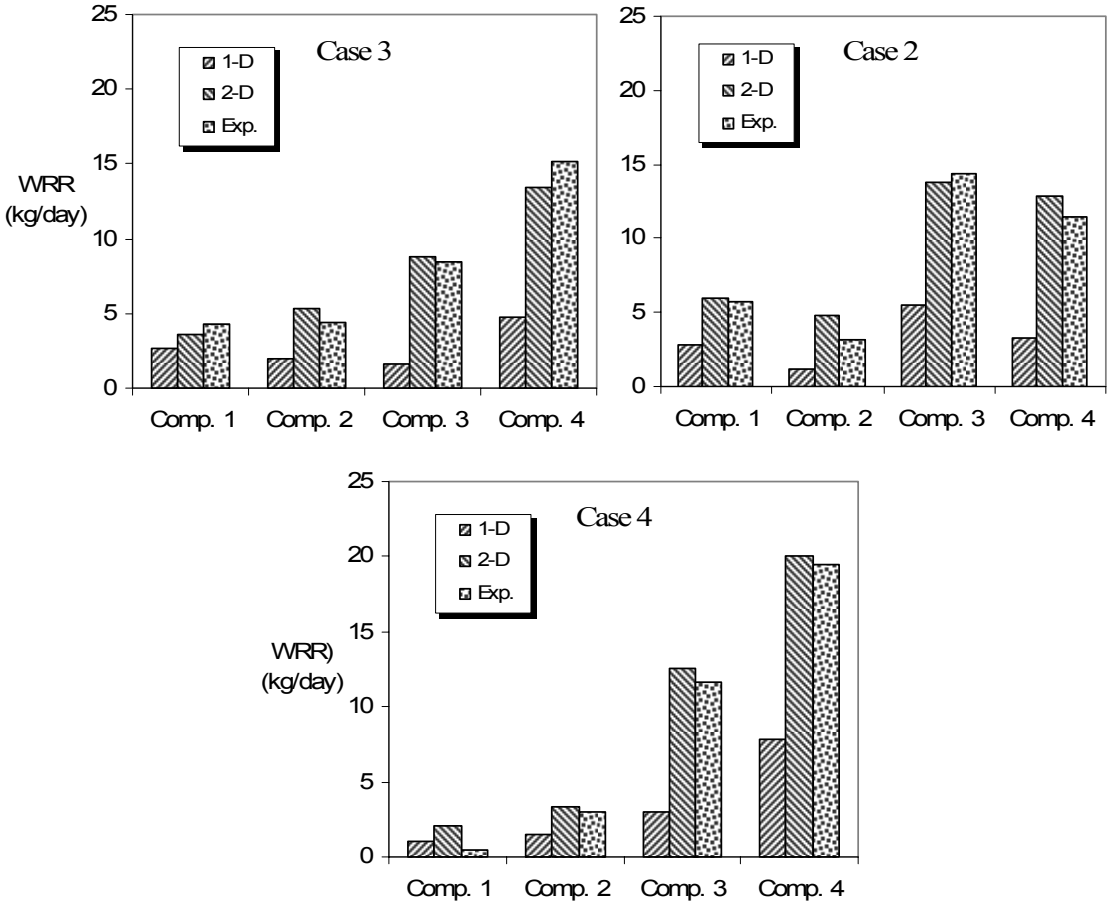

Figure 4.25: Water removal rate: 1-D and 2-D models vs. experimental data

More specifically, Table 4.11 summarizes the advantages and disadvantage of the 1-D and 2-D models.

Table 4.11: Comparison between the 1-D and 2-D models

	Advantage	Disadvantage
1-D model	- Analytical solution (explicit solution) can be obtained - Easy to perform sensitivity analysis - Good agreement with the averaged temperature - Dimensionless analysis is simple to follow	- Unable to predict temperature variation in the gas flow direction - Uses only constant physical parameters - Uses averaged temperature for model verification - Can not incorporate complex microbial growth mechanisms into the equation system - Uses only constant values of bioheat for each compartment - Unable to predict higher temperatures such as in the 4^{th} compartment - Lacks to adequately estimate the drying rate - Unable to apply gas different velocities into the equation
2-D model	- Predicts the temperature profile for both solid and gas flow directions - Capable to incorporate momentum transfer into the mass and heat transfer equations (gas different velocities) - Uses variable physical parameters (more realistic values) - Uses actual experimental data for model assessment - Good agreement with actual experimental data both for the solid and gas flow direction - Dimensionless analysis considers both directions (solid and gas) and provides basis for scale-up - Capable to incorporate nonlinear terms into the equation systems - Incorporates variable bioheat model into the equation - Predicts better the water removal rate	- Advanced tool needed to obtain numerical solution - Solution is not explicit - Difficult to perform sensitivity analysis - Nonlinear terms increase convergence time - Solution is sensitive to implement each term correctly into the programming - Bioheat model does not take into account the moisture content and C/N ratio

4.3.4. Conclusion

A novel continuous biodrying reactor was designed and used to test the drying of pulp and paper mixed sludge. The process operates under forced convection and the drying rates are enhanced by the biological heat generated through metabolic activity of the mesophilic and thermophilic bacteria naturally present in the mixed sludge. An adequate dry solids level was obtained in

much shorter residence times in the continuous biodrying reactor compared to the batch biodrying reactor, which underlines the economic viability of the developed continuous biodrying reactor. The experimental results obtained indicate a better process performance and is mainly attributed to the flexibility inherent in the continuous biodrying reactor for removal of different types of water under different outlet relative humidity profiles.

The key variable analysis for the continuous biodrying reactor revealed that the type of biomass feed, the nutrition level, and the outlet relative humidity profile were critical variables for the process. Since the type of biomass feed was fixed by choice and the nutrition level was in the active range for microbial growth, the influence of the outlet relative humidity profile on overall efficiency and the complexity of the continuous biodrying reactor were investigated. It was found that the best process performance was under the following outlet relative humidity profiles:

- Controlling the biodrying reactor at lower (85%) outlet relative humidity at the top (1^{st} and 2^{nd} compartments) where more unbound water exists;
- Controlling the biodrying reactor at higher (96%) outlet relative humidity profile at the bottom (3^{rd} and 4^{th} compartments) in which there is more bound water.

A systematic modeling approach was developed and executed for the continuous biodrying. This helps to better understand the prevailing transport phenomena in different compartments of the continuous biodrying reactor, establishing scale-up criteria for implication to a full-scale process, and improving control alternatives of the continuous biodrying reactor.

CHAPTER 5: GENERAL DISCUSSION

5.1. Overall Evaluation of the Project

Figure 5.1 illustrates the integration of a combined wastewater plant with the biodrying and combustion facilities. The pilot-scale continuous biodrying reactor was proven to be a successful solution to a major industrial problem associated with the mixed sludge management. As can be seen in Figure 5.1 (and compared to Figure 2.1) the landfilling, landspreading, and other land applications of the mixed sludge can be eliminated and/or minimized. The key process variable, the outlet relative humidity profile, provides an opportunity to have optimum and more cost effective operation for a target dry solids level within a short period of time. The outlet relative humidity profile is easy to control through a feedback loop. Better biodrying performance in a shorter period of time was achieved in the continuous biodrying reactor compared to batch one.

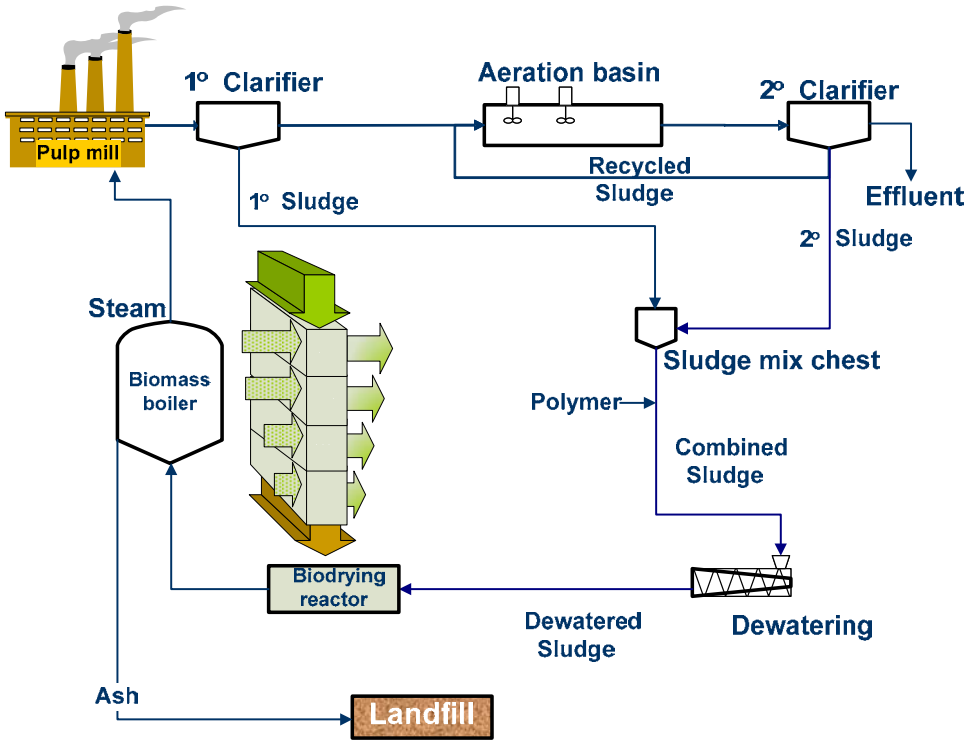

Figure 5.1: Integrated continuous biodrying process into a energy recovery process

The pilot-scale continuous biodrying reactor is a self-biofiltering system. Odorous gases that may be produced in parts of the reactor due to possible anaerobic conditions are consumed by microbes before reaching the exhaust outlet. The aerobic conditions prevent malodors. The exhaust gas is primarily made up of carbon dioxide, water vapor, and nitrogen. Some of the water vapor condensed on the walls of the exhaust ducts is collected in a PVC pipe. The condensate is usually benign due to the dynamics of the process and suitable for irrigation or can be re-used in the process after some minor treatment.

5.2. Implication of the Modeling for the Pilot-Scale Biodrying Reactor and Full-Scale Biodrying Process

Through a systematic modeling approach, evaluated by experimental data, it was possible to understand the prevailing transport phenomena in the continuous biodrying reactor. One of the greatest advantages of the 2-D model developed in the modeling phase of this study is its ability to address the two-dimensionality of transport phenomena in the pilot-scale biodrying reactor.

This not only helps to control and better understand the drying mechanisms of a complex mixture containing different types of water, but it also enhances development of a simple design tool.

The dimensionless analysis performed on the 2-D model is an approach for scale-up, and hence provides key information, a priori, for designing a continuous biodrying reactor for a specific need and/or condition. This yields significant scientific and engineering benefits, a unique reactor configuration for given mixed sludge characteristics, and contributes to the goal of advancing the efficient drying of mixed sludge.

5.3. Economic Viability of the Biodrying Process Compared to Competitive Drying Techniques

In the next sections, techno-economic indices for the biodrying process are compared to those of other drying techniques.

5.3.1. Technical Performance Indices for Sludge Drying Technologies

A comparison of the drying processes requires an understanding of their separate benefits and drawbacks, their applicability to dry a given material, as well as specific performance ratings. Table 5.1 compares several drying techniques, which are reported to be applicable for sludge drying, in terms of specific thermal rate and energy consumption rate. As can be seen from this table, the continuous biodrying process is among those that have a low energy consumption rate. However, a better conclusion can be made when both economic and technical aspects are considered simultaneously.

Table 5.1: The biodrying process versus other drying technologies for drying one tonne of wet sludge

Drying technology		Specific thermal rate (kJ/kg H_2O)	Dry solids content (%w/w) from initial value	Water removed (kg H_2O)/wet tonne	Energy consumption (GJ/wet tonne)
Alternative dryer system*	Rotary	3600-9200	55→ 95	400	1.44-2.51
	Conveyor	5500-6000	25→95	700	3.85-4.2
	Fluidized bed	4000-6000	50→100	500	2-3
	Superheated steam dryer (SSD)	1750	30→95	685	1.2
	AGES	317-793	50→90	400	0.12-0.32
Dry-Rex**		180-540	25→80	550	0.1-0.3
Continuous Biodryer		1176	30→60	510	0.6

*Frei et al. (2004), **Barre & Bilodeau. (2001).

5.3.2. Techno-Economic Assessment for Sludge Drying Technologies

Two Eastern Canadian Pulp mills were considered as case studies for the techno-economic analysis. Their characteristics are listed in Table 5.2. As can be seen in Tables 5.3 and 5.4, from an economic point of view, the rotary dryer seems more attractive for mill A, whereas the biodryer is more feasible for mill B, since it produces more mixed sludge. However, the technical issues associated with the sludge drying are relevant enough to be considered obstacles in the implementation of a rotary dryer for mixed sludge drying. For instance, due to its sticky characteristic behavior, the sludge could build up inside the rotary dryer, resulting in a significant decline in overall performance and heat transfer, and substantial technical difficulties such as lengthy periodic maintenance. Besides, one should note that the energy consumption rate in the rotary dryer is 2-3 fold of the energy consumption in the biodryer (Table 5.1). As well, there is currently no application available related to the technical performance of a super steam dryer (SSD) for sludge drying.

Table 5.2: Characteristics of two cases for techno-economic assessment of the biodrying process

Characteristics	Mill A	Mill B
Sludge production (tonne/day)	125	200
Wood waste burned in boiler (tonne/day)	720	100
Boiler type	Fluidized bed	Fluidized bed
Initial dry solids level (%w/w)	35	28
Current sludge usage	Combustion	Landfilled
Oil price ($/barrel)	100	100
CO_2 credit ($/tonne)	15	15
Transportation cost ($/tonne)	11	11

Table 5.3: Costs items and techno-economic assessment results of Mill A

	Base case	Biodrying	SSD	Rotary dryer
Landfilling and transportation costs ($)	3.85×10^4	3.84×10^4	3.83×10^4	3.82×10^4
Fuel costs ($)	1.41×10^7	1.34×10^7	1.23×10^7	1.20×10^7
Operation costs ($)	0	1.09×10^5	2.01×10^5	6.45×10^5
CO_2 credit ($)	0	-5.35×10^4	-1.27×10^5	-1.44×10^5
Annual operation costs ($)	1.41×10^7	1.35×10^7	1.24×10^7	1.25×10^7
Capital costs ($)	0	1.95×10^6	4.42×10^6	2.67×10^6
Payback time (year)	0	2.9	2.5	1.7

Table 5.4: Costs items and techno-economic assessment results of Mill B

	Base case	Biodrying	SSD	Rotary dryer
Landfilling and transportation costs ($)	9.42×10^5	6.00×10^5	2.87×10^5	2.87×10^5
Fuel costs ($)	1.06×10^7	7.00×10^6	5.25×10^6	4.91×10^6
Operation costs ($)	0	1.16×10^5	2.44×10^5	1.08×10^6
CO_2 credit	0	-2.61×10^5	-3.81×10^5	-4.06×10^5
Annual operation costs ($)	1.15×10^7	7.45×10^6	5.40×10^6	5.87×10^6
Capital costs ($)	0	2.30×10^6	5.10×10^6	3.82×10^6
Payback time (year)		0.56	0.83	0.67

Mills that are more likely to find the biodrying process economically attractive include those that:

- have biomass combustion facilities and related material handling operations already in place
- pay to send their sludge offsite (for either landfilling or landspreading)
- have space available for multiple biodrying reactors, especially located near existing boiler facilities
- would displace fossil fuels for steam production within the process.

5.4. Environmental Aspects of the Biodrying Process

Table 5.5 shows the reduction of CO_2 emissions due to sludge drying and combustion in the boiler by reducing the fossil fuel consumption.

Table 5.5: CO_2 emissions reduction

	Biodrying	SSD	Rotary dryer
Mill A	1.08	2.56	2.91
Mill B	6.06	8.85	9.44

It was found that the reduction in fossil fuel consumption for mill A and B are 5 and 35%, respectively. This shows that the biodrying process not only provides competitive techno-economic results, but it also results in long term environmental benefits for the pulp and paper industry.

5.5. Biodrying Reactor Scale-up and Process Risks

The scale up of the biodrying reactor is the ultimate goal so that the criteria for an industrial biodrying reactor can be established. The biodrying reactor developed for this study can easily be scaled up to construct a flexible plant capable of processing a higher tonnage of mixed

sludge. The biodrying modularity means that multiple units can be installed and results in a flexible plant capable of processing larger quantities of mixed sludge.

Following are a few considerations for the scale-up of the biodrying reactor:

- Simple control of the relative humidity profile
- Fitting it into a crowded mill site
- Minimum moving parts

Figure 5.2 illustrates an example of how the continuous biodrying reactor can be scaled up for larger quantities of mixed sludge.

Figure 5.2: Full-scale continuous biodrying reactor

However, the following process risks must be considered in a full-scale biodrying design:

Odor Management

The pilot-scale continuous biodrying reactor demonstrated that the reactor is a self-biofiltering system. As mentioned earlier, odor management was not recognized to be a problem in the pilot-scale biodrying reactor. However, in a full-scale process, where the distances between two adjacent compartments could be larger than that of the pilot-scale, anaerobic conditions may occur that lead to the generation of anaerobic gases. Therefore, outlet gas treatment may be required before gases are released as exhaust.

Compaction

The effect of compaction was not significant in the pilot-scale biodrying reactor due mainly to the strong impact of increased dry solids level in the bottom compartments, which increased porosity of the matrix and overcame the effect of compaction (ε_i values in Table 4.7). However, in a full-scale process, it may be favorable to design a taller reactor in order to reduce the capital costs and footprint of the installation. Excessive loading pressure might, at some point, overcome the effect of the dry materials' increased porosity and forcefully create a plug flow that is less permeable to the air flow. Therefore, an increased recycle ratio or addition of bulking agent may be required, offsetting the effect of reduced capital costs due to taller biodrying reactor.

There are other design issues such as bridging as a function of geometry and sludge characteristics and hot sludge being fed to the reactor, which all have to be taken into account for a large scale design and installation.

In conclusion, the length (L) of the biodryer at full-scale may be limited by the mass transfer mechanism in the gas flow direction, and the height (H) by compaction due to the loading pressure. Therefore, the scale up is mainly in the reactor depth (W) that can be extended per required volume for the treatment of mixed sludge (see Figure 5.2).

CHAPTER 6: CONCLUSIONS AND RECOMMENDATIONS

The potential for this technology is promising, particularly in Canada, where there are many opportunities to treat biomass streams. Wastewater sludge is as much a problem in the pulp and paper industry as it is in the municipal sector. Biomass waste streams in the form of wood waste, forest floor biomass, and agricultural residues are identified as usable energy sources. More and more, drying of these new energy sources will be the key to extracting maximum value. Having such an environmentally friendly solution in place increases the sustainability of the pulp and paper industry, and not only enhances recovery of energy from wastes but also is economically feasible.

6.1. Contributions to the Body of Knowledge

The novel continuous biodrying reactor designed and examined in this study contributes to the advancement of the scientific knowledge as follows:

Application of a novel pilot-scale continuous biodrying reactor

Through this research work, a continuous biodrying reactor was designed and tested for the drying of mixed sludge. The continuous biodrying reactor with minimum moving parts and reduced footprint addresses a major industrial problem associated with mixed sludge management. The main advantage of the continuous biodrying reactor is the shortened residence time to achieve an economic dry solids level. A residence time 2-3 times shorter in the continuous biodrying reactor compared to the batch one results in significant economic benefits. This is because the removal of different types of water is faster mainly attributed to the flexibility and higher efficiency of the continuous biodrying reactor.

Identification of the key process variable(s) for the continuous biodrying process

Two key process variables were identified for the continuous biodrying reactor: the nutrition level of the biomass feed (C/N ratio), and the outlet relative humidity profile along the height of the biodrying reactor. Despite the fact that only one type of mixed sludge was examined in this research work, it is speculated that the nutrition level of the biomass could play an important role on the operation and performance level of the continuous biodrying reactor. The outlet relative humidity profile was found to be the key variable in the continuous biodrying reactor controlling the transport phenomena and the complexity of the system as well as affecting the reactor performance. It was found that controlling the biodrying process at wet-bulb temperature is efficient only at the top of the reactor, where more unbound water present attributed to the limitation related to the external heat transfer. It was also found that drying the mixed sludge at dry-bulb temperature is feasible for bound water removal, which takes place in the bottom of the biodrying reactor (3^{rd} and 4^{th} compartments). The outlet relative humidity profile is a unique variable that can be controlled using a regulated feedback control strategy.

Application of the developed modeling approach for better understanding of the transport processes and process control

The modeling approach developed in this study is capable of identifying favorable operating conditions and/or strategies for the implementation of the biodrying process in the pulp and paper industry for mixed sludge drying. The 2-D model may be utilized for both a pilot-scale reactor and a full-scale biodrying process.

Implication of the 2-D model to the pilot-scale biodrying reactor

The main implication of the 2-D model to the pilot-scale biodrying reactor is the capability of the model in recognizing the two-dimensionality of the transport phenomena in the reactor, and the impact of each transport processes on the overall performance of the biodrying reactor. The

2-D model was found to be a more accurate tool to estimate the total water removal rate, which is a critical design parameter.

Implication of the 2-D model to a full-scale biodrying process

Through a dimensionless analysis performed on the 2-D model a few key number of dimensionless groups were identified which could be used for the design of a full-scale biodrying process. The key dimensionless groups were the Peclet numbers (*Pe*) for the gas and solid phases, and the ratio of exothermic biological heat and evaporative heat. These numbers help to better understand and interpret the prevailing transport phenomena relevant to the different types of water removal in the continuous biodrying reactor. These numbers are also useful tools to extrapolate the results of the pilot-scale biodrying reactor for a large-scale biodrying process.

6.2. Future Work

Despite several major goals accomplished in this study, there are other aspects that remained untouched:

- In this research work, we were not able to cover a full range of biomasses for different pulp and paper mills and identify possible inflexibilities and limitations of the current biodrying process as well as modeling drawbacks. It is recommended to extend the experimental phase to testing other types of biomasses and/or sludges so that the effect of nutrient availability (C/N ratio) on the performance of the continuous biodrying process can be thoroughly investigated. How will nutrient level impact the performance of the biodryer? Such a task could be critical for other biomass drying as suitable feedstocks for the viability of upcoming biorefinery processes.
- Since biological heat plays a critical role in the process performance and drying mechanism, it is required to perform a comprehensive study on the microbiological level in terms of kinetics of the microbial biodegradation for different biomasses under

different operating conditions and explore under which optimal conditions the reactor performs even better. This study can be done using a small scale batch biodrying reactor.

- Performance of the biodrying experimentation under real ambient conditions was not investigated as the lab conditions were out of control and dictated by school policy. This is important because the driving forces for the mass transfer are temperature and relative humidity. The mass transfer rate would be obviously high if the inlet air is dry and hot. If the relative humidity of inlet air is already very high, for instance in tropical countries, then the mass transfer will be decreased and consequently, the drying rates will decline. If the temperature is very cold, such as in Canada during winter, certainly pre-heating the inlet air would be necessary if the air is directly taken from the ambient conditions. Therefore, in both cases pre-treatment of the inlet air is required in order to increase the efficiency of the biodrying operation and maximize the mass transfer and water removal rate.
- Optimization of the current biodrying process was not performed. Hence it is recommended this part be covered so that possible optimal geometric configurations may be explored.
- Given the complexity of the 2-D model and its advantages, and the simplicity of the 1-D model and its disadvantages, it may be appropriate to develop a modified 1-D model that can be used as a design tool.

REFERENCES

Adani, F., Baido, D., Calcaterra, E., and Genevini, P. (2002). The influence of biomass temperature on biostabilization–biodrying of municipal solid waste, *Bioresource Technology* 83(3), 173-179.

Bach, P.D., Nakasaki, K., Shoda, M., and Kubota, H. (1987). Thermal balance in composting operations. *Journal of Fermentation Technology* 65(2), 199-209.

Banerjee, S., Mahmood, T., Phelan, P. M., and Fouke, R. W. (1998). Impulse drying sludge. *Water Research*, 32(1), 258-260.

Bari, Q.H., Koenig, A., and Guihe, T. (2000). Kinetic analysis of forced aeration composting: I. Reaction rates and temperature. *Waste Management & Research* 18(4), 303-312.

Barre, L., and Bilodeau, M. (2001). Drying residuals at low temperature with the Dry-Rex^{TM} dryer. *Pulp & Paper Canada* 100(12), 132-138.

Basu, S., Shivhare, U.S., and Mujumdar, A.S. (2006). Models for sorption isotherms for foods: a review. *Drying Technology* 24, 917–930.

Batista, J.G.F., van Lier, J.J.C., Gerrits, J.P.G., Straatsma, G., and Griensven, L.J.L.D. (1995). Spreadsheet calculations of physical parameters of phase II composting in a tunnel. *Mushroom Science* 14, 189-194.

Beckley, J.; and Banerjee, S. (1999). Operational issues with impulse drying sludge. *Water Science & Technology* 40(11-12), 163-168.

Berg, C.G., Kemp, I.C., Stenström, S., and Wimmerstedt, R. (2002). Transport equations for moist air at elevated wet bulb temperatures. *13th International Drying Symposium, Beijing, China, Conference Proceedings*, 135–144.

Brazier, K.J. (1996). *Verification and parameter optimisation of a simulation of near-ambient grain drying*. Ph.D. Thesis, Cranfield University, Silsoe, UK, p. 224

Campbell, A.G., Engebretson, R.R., and Tripepi, R.R. (1991). Composting a combined RMP/CMP pulp and paper sludge. *Tappi Journal* 74, (9), 183-191.

CANMET Energy Technology Center (2005). *Pulp and Paper Sludge to Energy-Preliminary Assessment of Technologies*. ADI Limited Report, Canada.

Chen, G., Yue, P.L., and Mujumdar, A.S. (2002). Sludge dewatering and drying. *Drying Technology* 20(4-5), 883-916.

Choi, H.L., Richard, T.L., and Ahn, H.K. (2001). Composting high moisture materials: biodrying poultry manure in a sequentially fed reactor. *Compost Science & Utilization* 9(4), p. 303.

Durai-Swamy, K., Warren, D.W., and Mansour, M.N. (1991). Indirect steam gasification of paper mill sludge waste. *Tappi Journal* 74(10), 137-143.

Dufour, P. (2006). Control engineering in drying technology: review and trends. *Drying Technology* 24(7), 889-903.

Du, J.H., and Wang, B.X, 2001. Forced convective heat transfer for fluid flowing through a porous medium with internal heat generation. *Heat Transfer-Asian Research* 30(3), 213-221.

Elliott, A., and Mahmood, T. (2005). Survey benchmarks generation: management of solid residues. *Pulp and Paper* 79(12), 49-55.

Finstein, M.S., Miller, F.C., and Strom, P.F. (1986). *Waste treatment composting as a controlled system.* In: Biotechnology, a Comprehensive Treatise. New York: VCH Inc.

Frei, K.M., Cameron, D., Stuart, P.R. (2004). Novel drying process using forced aeration through a porous biomass matrix. *Drying Technology* 22(5), 1191-1215.

Frei, K.M., Cameron, D., Jasmin, S., Stuart, P.R. (2006). Novel sludge drying process for cost-effective on-site sludge management. *Pulp and Paper Canada* 107(4), 47-53.

Fugere, M., Farand, P., Chabot, R., Stuart, P.R. (2007). Design and techno-economic analysis of a process for transforming pig manure into a value-added product. *The Canadian Journal of Chemical Engineering* 85(6), 360-368.

Gatica, J.E., Viljoen, H.J., and Hlavacek, V. (1987a). Thermal instability of nonlinear stratified fluids. *International Communications in Heat and Mass Transfer* 14, 673–686.

Gatica, J.E., Viljoen, H.J., and Hlavacek, V. (1987b). Stability analysis of chemical reaction and free convection in porous media. *International Communications in Heat and Mass Transfer* 14, 391–403.

Geankoplis, C. J. (1993). *Transport processes and unit operations*. 3rd edition. Prentice Hall, NJ, USA.

Gowthman, M.K., Ghildyal, N.P., Raghava Rao, K.S.M.S., and Karanth, N.G. (1993). Interaction of transport resistances with biochemical reaction in packed-bed solid state fermenters: the effect of gaseous concentration gradients. *Journal of Chemical Technology*

and Biotechnology 56, 233-239.

Hackett, G.A.R., Waston, C.A., Duff, S. (1999). Composting of pulp and paper mill fly ash with wastewater treatment sludge. *Bioresource Technology*70, 217-224.

Haghighi, M. (1994). *Visualization and simulation of immiscible displacement in fractured systems using micromodels: drainage, imbibition and steam injection*. PhD Thesis, University of Southern California, Los Angeles (CA), USA.

Hansjoerg, H., Hans-Joachim, B., Gurudas, S., Kurt, S., Barbara, R., and Juergen, R. (2004). *Process and apparatus for biological drying of residual waste, sewage sludge and/or biomass*. European Patent, EP1408021.

Haug, R.T. (1993). *The Practical Handbook of Compost Engineering*. 1st edition, Lewis Publishers, Boca Raton, FL, USA.

Harper, E., Miller, F.C., and Macauley, B.J. (1992). Physical management and interpretation of an environmentally controlled composting ecosystem. *Australian Journal of Experimental Agriculture* 32(5), 657-667.

Hayes, A.M., Khan, J.A., Shaaban, A.H., and Spearing, I. G. (2008). The thermal modeling of a matrix heat exchanger using a porous medium and the thermal non-equilibrium model, *International Journal of Thermal Science* 47, 1306-1315.

Hippinen, I., and Ahtila, P. (2002). Activated sludge drying in the pulp and paper industry by means of secondary energies, *1st International Conference on Sustainable Energy Technologies*, Porto, Portugal, paper EES4.

Hippinen, I. and Ahtila, P. (2004). Drying of activated sludge under partial vacuum conditions-An experimental study. *Drying Technology* 22(9), 2119-2134.

Huang, C.H., and Kim, S. (2005). An inverse problem for estimating the time-dependent reaction coefficient in an autocatalytic reaction pathway. *Chemical Engineering Science* 60(2), 447-457.

Huang, C.H., Yen, C.Y., and Orlande, H.R.B. (2003). A nonlinear inverse problem in simultaneously estimating the heat and mass production rates for a chemically reacting fluid. *Chemical Engineering Science* 58, 3741–3752.

Hynninen, P., and Laine, P. (1998). *Environmental Control, Papermaking Science and Technology* (19). 1st edition, Helsinki, Finland, Fapet Oy.

Ilic, M., and Turner, .I.W. (1986). Drying of a Wet Porous Material. *Journal of Applied Mathematical Modelling* 10, 16-24.

James, B.A., and Kane, P.W. (1991). Sludge dewatering and incineration at Westvaco, North Charleston, SC. *Tappi Journal* 74(5), 131-137.

Jewell, W.J., Dondero, N.C., van Soest, P.J., Cummings, R.T., Vegara, W.W., and Linkenheil, R. (1984). *High temperature stabilization and moisture removal from animal wastes for by-product recovery*. Final Report for the Cooperative State Research Service, SEA/CR 616-15-168, USDA, Washington, DC, USA, p. 169.

Kara, M. (1994). Thermal recycling of used fiber, *Paperi ja Puu* 76(1-2), 44-49.

Klaus, H. (1992a). Process for the biological drying of sewage sludge. *European Patent*, EP0508382.

Klaus, H. (1992b). Control and measurement method for the biological drying of sewage sludge. *European Patent*, EP0508383.

Koenig, A. and Tao, G. H. (1996). Accelerated forced aeration composting of solid waste. *In Proceedings of the Asia-Pacific Conference on Sustainable Energy and Environmental Technology*, 450-457.

Konovalov, V.I. (2005). Drying R&D needs: basic research in drying of capillary porous materials. *Drying Technology* 23, 2307–2311.

Kraft, D.L., and Orender, H.C. (1993). Considerations for using sludge as a fuel, *Tappi Journal* 76(3), 175-183.

Kordlewski, W., and Krajewski, Z. (1984). Convection effects on thermal ignition in porous media. *Chemical Engineering Science* 39, 610–612.

Krupinska, B., Strømmen, I., Pakowski, Z., and Eikevik, T.M. (2007). Modelling of sorption isotherms of various kinds of wood at different temperature conditions. *Drying Technology* 25, 1463–1470.

Kudra, T., Gawrzynski, Z., Glaser, R., Stanislawski, J., and Poirier, M. (2002). Drying of pulp and paper sludge in a pulsed fluid bed dryer, *Drying Technology* 20(4-5), 917–933.

Kulasiri, D., and Samarasinghe, S. (1996). Modelling heat and mass transfer in drying of biological materials: a simplified approach to materials with small dimensions. *Ecological Modelling* 86, 163-167.

Kulcu, R., Sonmez, I., Yaldiz, O., and Kaplan, M. (2008). Composting of spent mushroom compost, carnation wastes, chicken and cattle manures. *Bioresource Technology* 99, 8259-8264.

Labuza, T.P. (1984). *Moisture sorption: Practical aspects of isotherm measurement and use*. In: American Association of Cereal Chemists, USA.

Laflamme-Mayer, M., Bellec, S., Gaudreault, C., Thibodeau, J.-B., and Stuart, P.R. (2004). Techno-economic evaluation of some emerging sludge management options for mills with activated sludge treatment, *Pulp & Paper Canada* 105(6), 33-37.

Lagace´, P., Stuart, P.R., Miner, R.A., and Barton, D.A. (2000). Costs associated with implementation of zero effluent discharge at recycled fiber paperboard mills. *Pulp and Paper Canada* 101(7), 200-204.

Lagace´, P., Bourdages, G., Steinback, B., and Levis, C. (1998). Exploring the value of sludge. *Proceedings of the 84th Annual Meeting of the Technical Section*, CPPA, vol. 2. pp. 331–335.

Larsen, K.L. and McCartney D.M. (2000). Effect of C/N ratio on microbial activity and N retention: bench scale study using pulp and paper biosolids. *Compost Science & Utilization* 8(2), 147-159.

Léonard, A., Blacher, S., Marchot, P., Pirard, J.P., and Crine, M. (2005). Convective drying of wastewater sludges: influence of air temperature, superficial velocity, and humidity on the kinetics. *Drying Technology* 23(8), 1667–1679.

Liang, C., Das, K.C., and McClendon, R.W. (2003). The influence of temperature and moisture contents regimes on the aerobic microbial activity of a biosolids composting blend. *Bioresource Technology* 86(2), 131-137.

Madigan, M.T., and Martinko, J.M. (2006). *Brock Biology of Microorganisms*. 6th edition, Upper Saddle River, NJ: Prentice Hall.

Mahmood, T., and Elliott, A. (2006). A review of secondary sludge reduction technologies for the pulp and paper industry. *Water Research* 40, 2093-2112.

Manser, A.G.R., and Keeling, A.A. (1996). *Practical Handbook of Processing and Recycling Municipal Waste.* CRC Press, Lewis Publishers.

Mason, I.G. and Milke, M.W. (2005a). Physical modeling of the composting environment: A review. Part 1: Reactor systems. *Waste Management* 25(5), 481-500.

Mason, I.G. and Milke, M.W. (2005b). Physical modeling of the composting environment: A review. Part 2: Simulation performance. *Waste Management* 25(5), 501-509.

Mason, I.G. (2006). Mathematical modeling of the composting process: A review. *Waste Management* 26(1), 3-21.

McBurney, B. (1993). Wood refuse/biomass fuel specification guidelines. *Tappi Proceedings-Engineering Conference*, 1141-1152.

Metcalf and Eddy (1991). *Wastewater engineering: treatment, disposal and reuse*. 3rd Edition, McGraw-Hill.

Morales, M., Hernandez, S., Cornabe, T., Revah, S., and Auria, R. (2003). Effect of drying parameters on biofilter performance. *Environmental Science and Technology* 37, 985-992.

Mujumdar, A.S. (2004). Research and development in drying: recent trends and future prospects. *Drying Technology* 22, 1–26.

Mujumdar, A.S. (2007). *Handbook of Industrial Drying CRC Press*. Taylor & Francis Group, Boca Raton, 3rd edition, FL, USA.

Mujumdar, A.S., and Beke, J. (2003). *Grain drying: basic principles. In Handbook of Postharvest Technology*. Marcel Dekker, New York, pp. 119–138.

Nakasaki, K., Aoki, N., and Kubota, H. (1994). Accelerated composting of grass clippings by controlling moisture level. *Waste Management & Research* 12 (1), 13-20.

Nakayama, A., Nanasaki, K., Kuwahara, F., and Sano, Y. (2007). A lumped parameter heat transfer analysis for composting processes with aeration. *Transactions of the ASME* 129(7), 902-906.

National Council of the Paper Industry for Air and Stream Improvement Inc (NCASI) (1992). *Solid waste management and disposal practices in the U.S. paper industry*. Technical Bulletin No. 641. New York, N.Y.

Navaee-Ardeh, S., Bertrand, F., and Stuart, P.R. (2006a). Emerging biodrying technology for the drying of pulp and paper mixed sludges. *Drying Technology* 24(7), 863-878.

Navaee-Ardeh, S., Bertrand, F., and Stuart, P.R. (2006b). Lumped modeling of a novel continuous biodrying reactor. *56th Canadian Chemical Engineering Conference*, Sherbrooke, Canada.

Navaee-Ardeh, S., Tchoryk, C., Bertrand, F., Stuart, P., and Tolnai, B. (2008b). Novel continuous biodrying reactor: principles, screening experiments and results, *58th Canadian*

Chemical Engineering Conference, Ottawa, Canada.

Navaee-Ardeh, S., Bertrand, F., and Stuart, P.R. (2009a). Development and experimental evaluation of a 1-D distributed model of transport phenomena in a continuous biodrying process for pulp and paper mixed sludge. Accepted at *Drying Technology*.

Naylor, L.M. (1996). Biosolids treatment and management: processes for beneficial use, Edited by Girovich, M., Marcel Dekker Inc., New York.

Nellist, M.E., Lamond, W.J., Pringle, R.T., and Burfort, D. (1993). Storage and drying of comminuted forest residues, Vol. 1, *AFRC Sisloe Research Institute*, 1–82.

Nellist, M.E. (1997). Storage and drying of arable coppice. Aspects of Applied Biology–*Biomass and Energy Crops* 49, 349–359.

Nield, D.A., and Kuznetsov, A.V. (2008). A bioheat transfer model: forced convection in a channel occupied by a porous medium with counterflow. *International Journal of Heat and Mass Transfer* 51 923-24), 5534-5541.

Niessen, W.R. (2002). *Combustion and incineration processes*. 3rd edition, Marcel Dekker Inc., NY, USA.

Nissan, A.H., Kaye, W.G., and Bell, J.R. (1959). Mechanism of drying thick porous bodies during the falling rate period. I. The pseudo-wet-bulb temperature, *AIChemE J.* 5(1), 103–110.

PAPTAC (Pulp and Paper Technical Association of Canada) (1999). *Environment committee, subcommittee for the survey of Canadian activated sludge treatment plants in pulp and paper mills*. Montreal, Canada.

Pavel, B., Mohamad, I., Abdulmajeed, A. (2004). An experimental and numerical study on heat transfer enhancement for gas heat exchangers fitted with porous media. *International Journal of Heat and Mass Transfer* 47, 4939-4952.

Perry, R. H. and Green, D. W. (1997). *Perry's chemical engineers' handbook*. 6th edition, McGraw-Hill, USA.

Prud'homme, M. and Jasmin , S. (2006). Inverse solution for a biochemical heat source in a porous medium in the presence of natural convection. *Chemical Engineering Science* 61, 1667-1675.

Rajagopalan, S., and Modak J.M. (1994a). Heat and mass transfer simulating studies for solid-state fermentation processes. *Chemical Engineering Science* 49, 2187-2193.

Rajagopalan, S., and Modak J.M. (1994b). Modeling of heat and mass transfer for solid state fermentation process in tray bioreactor. *Bioprocess Engineering* 13, 161-169.

Reid, I. (1998). Solid residues generation and management at Canadian pulp and paper mills in 1999 and 1995. *Pulp Paper Canada* 99 (4), 49–53.

Richard, T. (1997). *The Kinetics of Solid-State Aerobic Biodegradation*, PhD Dissertation, Cornel University, USA.

Richard, T.L., Veeken, A.H.M., De Wilde, V., and Hamelers, H.V.M. (2004). Air-filled porosity and permeability relationships during solid-state fermentation. *Biotechnology Progress* 20, 1372–1381.

Robinzon, R., Kimmel, E., and Avnimelech, Y. (2000). Energy and mass balances of windrow composting system. *Transactions of ASAE* 43(5), 1253-1259.

Rouleau, G., and Sasseville, M. (1996). Waste reduction: a sound business decision. *Pulp Paper Canada* 97 (12), 114–116.

Roy, G., Jasmin, S., and Stuart, P. R. (2006). Technical modeling of a batch biodrying reactor for pulp and paper mill sludge. *17th CHISA International Congress of Chemical and Process Engineering*. Prague, Czech Republic.

Rowley, G. and Mackin L.A., 2003. The effect of moisture sorption on electrostatic charging of selected pharmaceutical excipient powders. *Powder Technology* 135-136 50-58.

Ruzicka, M.C. (2008). Review on dimensionless numbers. *Chemical Engineering Research and Design* 86, 835-868.

Saucedo-Castaneda, G., Lonsane, B.K., Krishnaiah, M.M., Navarro, J.M., Roussos, S., and Raimbault, M. (1992). Maintenance of heat and water balances as a scale-up criteria for the production of ethanol by Schwannimyces castelli in a solid state fermentation system. *Process Biochemistry* 27, 97-107.

Scott, G.M., Abubakr, S., and Smith, A. (1995). Sludge characteristics and disposal alternatives for the pulp & paper industry. *Tappi – International Environmental Conference Proceedings*, 269-279.

Shimek, S., Nessman, M., Charles, T., and Ulrich, D. (1988). Paper sludge land application studies for three Wisconsin mills. *Tappi Journal* 71(9), 261-264.

Smith, J.K., Vesilind, P.A. (1995). Dilatometric measurement of bound water in wastewater sludge. *Water Research* 29(12), 2621–2626.

Stanish, M.A., Schajer, G.S., and Kayihan, F. (1986). A mathematical model of drying for hygroscopic porous media. *AIChE Journal* 32(8), 1301-1311.

Straatsma, G., Gerrits, J.P.G., Thissen, J.T.N.M., Amsing, J.G.M., Loffen, H., and van Griensven, L.J.L.D. (2000). Adjustment of the composting process for mushroom cultivation based on initial substrate composition. *Bioresource Technology* 72(1), 67-74.

Sugni, M., Calcaterra, E., and Adani, F. (2005). Biostabilization–biodrying of municipal solid waste by inverting air-flow, *Bioresource Technology* 96(12), 1331-1337.

Thaker, W.E. (1985). *Silvicultural land application of wastewater and sludge from the pulp and paper industry*. The Forest Alternative for Treatment and Utilization of Municipal and Industrial Waste, University of Washington Press, Seattle, USA, pages 41-54.

Tsang, K.R., and Vesilind, P.A. (1990). Moisture distribution in sludges. *Water Science and Technology* 22 (12). 135-142.

Vafai, K., Desai, C.P., Chen, S.C. (1993). An investigation of heat transfer process in a chemically reacting packed bed. *Numerical Heat Transfer* 24, 127–142.

Vanhatalo, A., and Ahtila, P. (2001). Drying of Forest Industry Sludge for Energy Production with Partial Vacuum Technology. *ACEEE summer study on Energy Efficient in Industry*, New York, USA.

Vaxelaire, J., Bongiovanni, J. M., Mousques, P., and Puiggali, J. R. (2000). Thermal drying of residual sludge. *Water Research* 34(17), 4318-4323.

Vaxelaire, J., and Cezac, P. (2004). Moisture distribution in activated sludges: a review, *Water Research* 38, 2215–2230.

VCU technology Ltd. (2005). *Vertical Composting Unit*. http://www.vcutechnology.com.

Velis, C.A., Longhurst, P.J., Drew, G.H., Smith, R., and Pollard, S.J.T. (2009). Biodrying for mechanical–biological treatment of wastes: A review of process science and engineering. *Bioresource Technology* 100, 2747–2761

Von Meien, O.F., and Mitchell, D.A. (2002). A two-phase model for water and heat transfer within an intermittently-mixed solid-state fermentation bioreactor with forced aeration. *Biotechnology and Bioengineering* 79(4), 416-428.

APPENDIX A: Journal Papers

A1. Emerging Biodrying Technology for the Drying of Pulp and Paper Mixed Sludges

Drying Technology, 24: 863–878, 2006
Copyright © 2006 Taylor & Francis Group, LLC
ISSN: 0737-3937 print/1532-2300 online
DOI: 10.1080/07373930600734026

Emerging Biodrying Technology for the Drying of Pulp and Paper Mixed Sludges

Shahram Navaee-Ardeh, François Bertrand, and Paul R. Stuart
Chemical Engineering Department, École Polytechnique de Montréal, Montréal, Québec, Canada

Effective sludge management is increasingly critical for pulp and paper mills due to high landfill costs and complex regulatory frameworks for options such as sludge landspreading and composting. Sludge dewatering challenges are exacerbated at many mills due to improved in-plant fiber recovery coupled with increased production of secondary sludge, leading to a mixed sludge with a high proportion of biological matter that is difficult to dewater. Various drying technologies have emerged to address this challenge of sludge management, whose objective is to increase the dryness of mixed sludge to above critical levels (≈42% dryness) for efficient and economic combustion in the boiler for steam generation. The advantages and disadvantages of these technologies are reviewed in this article, and it is found that many have significant technical uncertainties and/or questionable economics. A biodrying process, enhanced by biological heat generation under forced aeration, is introduced that has significant promise. A techno-economic analysis of the batch biodrying process at a case study mill showed an annual operating cost savings of about $2 million, including the elimination of landfilling practices and supplemental fuel requirements in the boiler. It was shown that if a biodrying residence time of less than 4 days can be achieved, payback periods of 2 years or less can result in many mills. The potential for the development of a continuous biodrying reactor and the fundamentals of its mathematical modeling are thus presented. Compared to the batch reactor configuration, it is expected that the continuous process would result in improved process flexibility and controllability, lower investment and operating costs due to shorter residence times, and an improved potential to fit into the crowed pulp and paper mill site.

Keywords Biological drying; Combustion; Mixed sludge management; Pulp and paper industry; Techno-economic analysis

INTRODUCTION

Pulp and paper mills produce large quantities of mixed sludge, especially mills that have implemented activated sludge treatment (AST). The two main alternatives for dealing with mixed sludge from pulp and paper mills include (a) increasing sludge dryness by mechanical dewatering and combusting it in a boiler to generate steam and/or power and (b) landfilling. In recent years, landfilling of mixed sludge has dramatically decreased. A survey of the Canadian pulp and paper industry sector in 1995 and 2002 indicated that landfilling of pulp and paper mixed sludge and solid residues in 2002 had decreased by 50% compared to 1995 values.[1] Landspreading and composting have been selected as the preferred sludge management strategies at some mills. For various reasons, including in particular rising energy costs and complex regulations related to landspreading and composting, many mills are currently seeking to dispose of their sludge by combustion, and mills already employing this method want to improve their operating efficiencies.

With improvements in fiber recovery processes in recent years and incremental increases in pulp production, mills are generating less primary (fibrous) sludge and more secondary (biological) sludge. The mixture of primary and secondary sludge is called "mixed sludge." The mechanical dewatering of mixed sludge with a high proportion of secondary sludge is difficult and can result in lower and variable dewatered sludge drynesses. This results in operating challenges and increased costs for all sludge management options, particularly at mills that combust sludge.

Canada has promulgated the Kyoto protocol and has targeted significant reductions in greenhouse gas (GHG) emissions. Mixed sludge from the pulp and paper industry is an important source of GHG emissions when landfilled. However, mixed sludge can reduce fossil fuel requirements and GHG emissions if combusted to produce steam and/or power. With the emergence of GHG trading markets, it is expected that there will be additional economic driving forces for efficient sludge combustion at pulp and paper mills.

It is critical, therefore, to develop an efficient way to increase the dry matter content of mixed sludge from pulp and paper mills to values above critical levels for safe and economic combustion.

Biological drying ("biodrying") represents an important opportunity for the treatment of mixed sludge to consistently

Correspondence: Paul R. Stuart, École Polytechnique de Montréal, Chemical Engineering Department, C.P. 6079, Succ. Centre-ville, Montréal, Québec, Canada H3C 3A7; E-mail: paul.stuart@polymtl.ca

raise the dry solids content so that the sludge can be economically disposed of in boilers for the generation of steam and/or power. In this article, the biodrying technologies that have been employed for other types of sludges are reviewed, and the key issues relevant to the biodrying of pulp and paper mixed sludge are presented.

MATERIAL CHARACTERISTICS AND TREATMENT METHODS

Pulp and Paper Mill Mixed Sludge

A typical pulp and paper mill wastewater treatment system consists of two treatment systems: primary (mechanical) and secondary (biological) treatments. In the primary wastewater treatment system, solid particles are removed by gravity, settling/clarification, and flotation.[2] The primary sludge mainly contains fibers (cellulose, hemicellulose) and fillers. Primary treatment is followed by biological treatment, often an activated sludge treatment (AST) system, in which wastewater organic matter is broken down by means of aerobic biodegradation.[2] The combined sludge from primary and secondary treatment consists of a muddy mass of microorganisms, fibrous materials, lignin, mineral components (limestone and phosphorous), clay, inert solids rejected during the recovery process, ash, and water.[3,4] The possibility of recycling this sludge to the process is limited, and landfilling is increasingly restricted due to mounting environmental pressures and high costs. Therefore, combustion can provide a competitive disposal method, as long as the dry solids content of the sludge is maintained above the critical level for good combustion. Previous publications have reported that the critical level of dryness of combustible materials in order to guarantee stable conditions in the boiler is about 42%.[5,6]

At most mills, the mechanical dewatering process (alone) is neither feasible nor economically viable for the target dryness levels sought for efficient sludge disposal by combustion.[7] Figure 1 qualitatively describes the four types of water that can be present in mixed sludge. The constant drying rate (free water removal) is followed by the first (interstitial water removal) and second (surface water removal) falling rates. In the falling rate periods, a much higher external heat/mass transfer coefficient is required to remove the moisture arriving at the surface of the sludge. Free and interstitial water can be mechanically removed by an efficient dewatering process, but surface and intercellular (bound) water require more extensive treatment techniques.

The heating value of mixed sludge on dry basis is 14–19 MJ/kg, which is relatively close to the values of wood or peat,[8] although the sludge must be dried to above critical values for good combustion. Table 1 summarizes typical characteristics of mixed sludge produced in a kraft pulp mill.

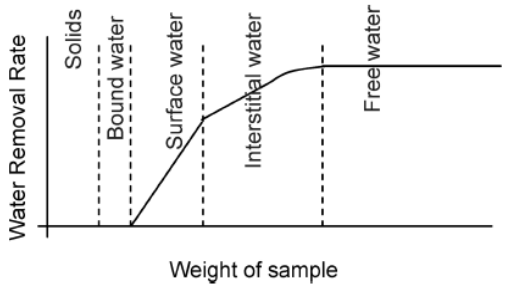

FIG. 1. Typical drying curve for sludge (adapted from Tsang and Vesilind[7]).

Mixed Sludge Disposal Techniques

Table 2 provides a summary of the advantages and disadvantages of sludge management techniques commonly used by pulp and paper mills.

A benchmark survey of Canadian pulp and paper solid waste residues management revealed that the amount of ash generated in power boilers in 2002 was 37% greater than in 1995. This is an indication that sludge landfilling has dramatically decreased, and mills have become increasingly reliant on on-site energy sources, such as burning bark and mixed sludge.[1]

Sludge Combustion

Exponentially increasing fossil fuel prices are increasingly driving pulp and paper mills to valorize mixed sludge and burn it in power boilers for steam and/or power generation. To some extent, the acceptance of sludge to energy is related to the development of renewable energy alternatives, fuels, and the subsequent reduction of greenhouse gases. Carbon dioxide emissions from the pulp and paper biomass combustion are considered neutral and are not counted in greenhouse gas emissions.[9]

A 4% increase in moisture content of the fuel in a boiler can result in a 38°C drop in boiler combustion temperature, which in turn greatly affects boiler performance.[5,6] Thus,

TABLE 1
Characteristics of mixed sludge from a typical kraft mill (mixed sludge/bark ratio = 2)

		Sludge elemental analysis (%)			
Sludge dryness (%)	Bark dryness (%)	%C	%H	%N	C/N ratio
19–25	33–50	33–43	4.9–6.3	1.6–3.2	15–26

TABLE 2
Pulp and paper industry sludge disposal techniques

Disposal technique	Advantages	Disadvantages
Landfilling	–Established	–Greenhouse gas emissions
	–Simple disposal	–Transport offsite
	–No complex treatment	–Increasing environmental restrictions
		–Increasing high cost
		–Odor problem
		–Needs suitable sites
Landspreading	–Improves soil characteristics	–Potential liabilities (metals, pathogens and non-elemental particles)
	–Returns some nutrients and carbon to environment	–Odor problem
		–Transportation & spreading equipment
		–Regulatory complexity and requirements
Composting	–Produces saleable product	–Capital costs associated with facilities
	–Destroys pathogens	–Reliable market for product
	–Low energy consumption	–Long residence time required for treatment
	–Well established at the full scale	–Mostly batch operation (except VCU technology)
		–Transportation of the product
Recycling to the process	–Reclaims value in new products	–Reduces product quality (mostly paper quality)
	–Reduces burden on other sludge disposal techniques	–Limited to specific board and paper products
		–Sludge pretreatment process sometimes required
Combustion	–Energy recovery	–High capital costs (if the boiler does not already exist in the mill)
	–Significant volume reduction of wastes	–Operating risk (if moisture content is too high)
	–Displaces fossil fuels (at appropriate dryness level)	–High maintenance cost
	–Reduces GHG emissions	–Ash management required
		–Equipment corrosion
Thermal processes	–Energy is derived from waste heat sources	–Complex technology (due to process integration)
	–Potential for profitable operation	–Not yet proven commercially
	–Sludge kept onsite	–High capital cost

at mills where mixed sludge is burned, supplementary fuel (natural gas, oil, or coal) is typically required. The calorific value of mixed sludge could be similar to some wood species and peat if it is dried to above 40% dryness.[6,8,10] It has been reported that for an average size mill producing 850 dry tons of product, about 34% of the purchased fossil fuel could theoretically be substituted by the effective heating value of mixed sludge of sufficient dryness. This estimate was based on a sludge generation rate equivalent to 128 tons of dry sludge per day, the effective heat value of sludge at 5.5 MJ/kg and mill energy consumption of fossil fuel at 6.0 GJ/ton dry product.[11]

The energy content of pulp and paper mixed sludge is doubled when the dry solids content is increased from 20 to about 50%. As can be observed from Fig. 2, further drying (to >50% dryness) brings little value to the energy content of the sludge. Therefore, if drying of sludge to about 50% can be accomplished in an efficient way, it can result in significant economic benefit to boiler operations.[12] Figure 3 describes the inverse relationship between the efficiency of the boiler and the moisture content of the biomass being burned.[13]

DRYING OF PULP AND PAPER MIXED SLUDGE

Conventional Drying Technologies

For the various reasons cited above, the pulp and paper industry is seeking to develop efficient techniques to dry

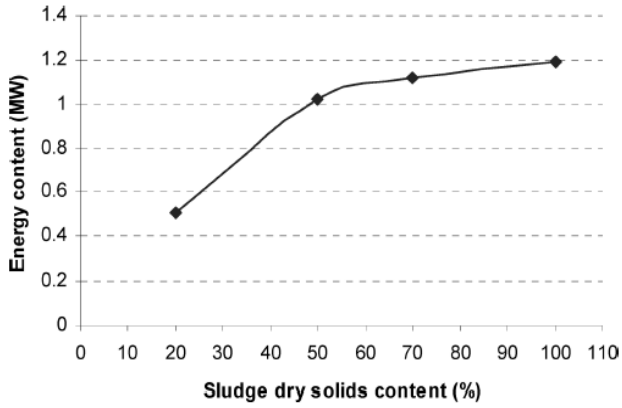

FIG. 2. Energy content of mixed sludge vs. dry solids content (adapted from Hippinen and Ahtila[12]).

mixed sludge that can guarantee the economic viability of sludge combustion. In recent years, a number of sludge drying innovations have entered the market whose objective is to provide economic solutions that address the problem of low and variable solids content of dewatered mixed sludge in the pulp and paper industry. Following is a critical review of mixed sludge drying techniques and relevant studies.

Chen et al.[3] provided an overview of pulp and paper sludge dewatering and possible drying alternatives. Direct, indirect, and combined drying alternatives were reviewed for the drying of activated sludge from the pulp and paper industry. However, based on the preliminary assessment, it was concluded that it is necessary to develop a new drying process that can be economically feasible and thermally efficient.[3] Banerjee et al.[14] and Beckley and Banerjee[15] developed an impulse drying method to dry mixed sludge from pulp and paper mills. The mixed sludge is briefly exposed under pressure to a hot surface. This technique

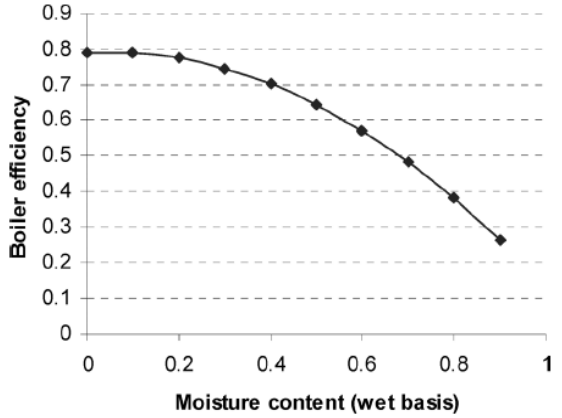

FIG. 3. Boiler efficiency vs. moisture content of biomass (adapted from Liang et al.[13]).

enhanced drying compared to a pure thermal drying approach but implies high temperatures and a complex technology.[14,15] Vaxelaire et al.[16] studied the convective drying of activated sludge and PVC with ambient air at temperatures of 41–60°C. The results showed that the activated sludge was very difficult to dry compared to PVC because of a crust that forms.[16] Kudra et al.[5] studied the hydrodynamics and drying kinetics of pulp and paper sludge via a lab-scale batch pulsed fluid bed dryer, where high drynesses (88% w/w) of the disintegrated mixed sludge was achieved. The hydrodynamics considered included the development of pressure drop, minimum pulsed-fluidization velocity, dynamic bed height, and mass flow rate coefficient equations. However, there is no information available at full scale. Hippinen and Ahtila[4] reported an experimental approach for the drying of activated sludge under partial vacuum by means of waste energy streams. Waste heat sources are widely available in pulp and paper mills, particularly since recent environmental legislation and restrictions have prompted mills to minimize water consumption, which leads to an increase in the temperature of water in the system. The warm water needs to be cooled in order to be reused in the process, and one possibility would be to use this energy to dry activated sludge. It was concluded that partial vacuum drying of mixed pulp and paper sludge can provide a competitive solution to this challenge. However, this conclusion was made based on laboratory-scale experimentation.[4] Leonard et al.[17] investigated the influence of three operating variables, i.e., inlet air temperature, superficial velocity, and humidity, on wastewater sludge drying kinetics, and concluded that the temperature of the inlet air was the main operating parameter affecting the kinetics of drying. It was also reported that the drying of activated sludge was mainly controlled by external limitations. It is worth mentioning that all the above-mentioned conclusions of various studies were made either in lab scale or without economic consideration.

A comprehensive review of available drying technologies was conducted for the CANMET Energy Technology Centre in Canada including fluidized bed dryers, rotary dryers, paddle dryers, superheated steam pneumatic dryers (GEA exergy steam dryer), belt dryers, integrated sludge dewatering and drying systems (J-VAP and DryVac), integrated sludge drying and combustion systems, the TLG sludge drying process, the Dry-Rex dryer, the SmartSoil Biodrying technology, solar dryers, and cyclonic dryers.[11] The main advantages and disadvantages of each are summarized in Table 3 and suggest that the majority of these technologies suffer from technical uncertainty and offer questionable economic benefits. Therefore, new efficient drying technologies for mixed sludge continue to be sought. One such innovation is biodrying technology, which provides both economic and environmental benefits.

TABLE 3
Advantages and disadvantages of conventional drying technologies

Disposal technique	Advantages	Disadvantages
Fluidized bed dryers	–Direct drying –Gentle, fast and uniform drying at low temperature –Low space requirements –High degree of product dryness	–High initial capital costs –Requires off-gas handling and cleaning equipment –High degree of auxiliary equipment required
Rotary dryers	–Provides for drying and granulation in one step –Allows for reclamation of waste heat –Versatile in configuration –Well-suited for heavy products	–Large floor space requirement –High capital and maintenance costs –Back-mixing to avoid sludge agglomeration required
Paddle dryers	–High ratio of heat transfer surface area to overall dryer volume –Self-cleaning of the intermeshing paddles –Low space requirement –Low capital and installation costs –Well-proven, commercially available technology	–Relatively high complexity of equipment –High maintenance costs –Sensitivity to large agglomerates, grit, or rocks in the sludge –Jamming or premature wear of the paddles
Superheated steam pneumatic dryer	–Compact design –Short product residence time –Low floor space requirements –80–90% energy recovery from the drying process possible –Closed-loop steam cycle	–Back-mixing of dried product with wet feed –Relatively high specific energy consumption –Turbulent drying conditions and high capital cost
Belt dryers	–Ability for low-grade energy usage –Low air temperatures required (30°C to 90°C) –No back-mixing of dried product with wet feed required	–Large floor space requirement –Relatively high degree of auxiliary equipment –High complexity of equipment –High maintenance and long residence time
Integrated sludge dewatering and drying systems	–Indirect sludge drying	–New technology –No installation for pulp and paper mixed sludge
Integrated sludge drying and combustion systems	–Surplus heat generation –Cyclone furnace is used for incineration	–Treatment of boiler flue gas required –High degree of auxiliary equipment –Large floor space requirement
TLG dryer	–Low-temperature drying –No loss of energy –Surplus heat generation –Low degree of auxiliary equipment required	–Relatively high floor space requirements –Manufactured in only two sizes (1.6 and 20 tons per day)

(*Continued*)

TABLE 3
Continued

Disposal technique	Advantages	Disadvantages
Dry-Rex dryer	–Low-temperature air (30°C to 90°C)	–Powerful vacuum system required for large air volumes
	–Accelerated drying process	–Many moving parts
SmartSoil™ Biopile	–Fully automated process	–Long residence times result in higher capital cost
	–Very little process equipment	–Economically feasible for mills having large sludge production
	–Bi-directional aeration through forced convection	
	–Enhanced by biologically heat generation	
Carver-Greenfield	–Efficient heat transfer rates	–Very high capital cost
	–Dries difficult (very wet) substrates	–Complex system
		–Not generally applied in the P&P industry
Solar dryers[67]	–Natural energy from sun	–Large space requirement
		–Odor problem
		–Regional and seasonal
Cyclonic dryers[68]	–Direct drying	–Not proven commercially
	–Better contact	–Wet sludge feeding problem
	–Short residence time	

Biologically Enhanced Drying

In biodrying processes, the drying of sludge is augmented by biological heat in addition to forced aeration. The major portion of biological heat, naturally available through the aerobic degradation of organic matter, is utilized to evaporate surface and bound water associated with the mixed sludge. This heat generation assists in reducing the moisture content of the biomass without the need for supplementary fossil fuels, and with minimal electricity consumption. The advantages of employing sludge as a fuel include low cost, displacement of fossil fuels, and supply dependability (not seasonal or variable).

Two prominent parameters must be considered relative to moisture removal rate in the biodrying process: inlet air flow rate and exit air temperature. Airflow is necessary to remove water from the matrix, and air temperature affects the moisture holding capacity of air.[18–20]

Microbial activity produces a rise in temperature within the porous matrix. Biological activity is mostly due to the presence of bacteria categorized into three major groups;[21] i.e., psychrophiles (active at −5 to 20°C), mesophiles (active at 5 to 48°C), and thermophiles (active at 42 to 68°C). Forty to 50% of the biologically generated heat in the solid matrix is utilized by microorganisms to guarantee their preservation, growth, and multiplication. The rest is distributed throughout the porous matrix, and serves to enhance the evaporation of interstitial and bound water.[22] The metabolic reaction can theoretically proceed at high moisture levels, but the oxygen supply that sustains the microbial activity necessary for aerobic decomposition can be diminished under high moisture conditions. Nakasaki et al.[23] reported that optimum moisture content for microbial activity is 45–65% w/w. This has been confirmed elsewhere.[24] In contrast to the composting process, in the biodrying process a compromise is made between the rate microbial activity and preserving the heating value of the remaining dried sludge.

Recent Studies on Biodrying Processes

Klaus[25] studied the effect of operating variables on the biodrying process for municipal sludge, i.e., the ratio of sewage sludge to flocculating agent, the throughput of the sludge, the temperature of the inlet air, as well as the residence time on the controllability of the biodrying process. By controlling these variables, it was possible to optimize the biodrying operation. Additives were added as conditioning agents to the sludge.[25,26] Nellist et al.[27,28] reported that fast biodrying determines low biological stability and vice versa. A similar result was confirmed by Adani et al.[19] Choi et al.[29] concluded that high moisture removal can be achieved in a full-scale, well-insulated biodrying reactor.[29] Adani et al.[19] reported that the biological stability provided by the biodrying process could minimize odors and biogas production of municipal waste sludge. Hansjoer et al.[30] developed a method for the continuous biological drying of garbage residues and sewage sludge. The technique involved continuous measurement of the carbon dioxide gas content in the exhaust air along

a closed transport track in order to control the air supply, so that the carbon dioxide gas content in the exhaust air was kept within a range of 0.05 to 0.4% by volume.[30] Sugni et al.[31] reported that biodrying could be a good solution for municipal solid waste management, allowing for the production of fuel with attractive energy content. It was possible to mitigate the heterogeneity and temperature gradient of the dried sludge by inverting the airflow direction.[31] Lhadi et al.[32] studied the evolution of organic matter and the humification process during the co-composting of the organic fraction of municipal solid waste and poultry manure with two different particle sizes (0.2 and 1 cm). The results suggested that hemicelluloses were readily degradable compared to cellulose and lipids. It was also pointed out that degradation phenomena were more marked for mixtures with lower particle sizes.[32] The techno-economic analysis of Laflamme-Mayer et al.[33] illustrated that biodrying could be an attractive alternative for those pulp and paper mills that are seeking to eventually achieve zero-effluent operations when compared with other alternatives such as low sludge production and retrofit of hollow-fiber membranes into the aeration basin.[33]

Therefore, biodrying shows considerable potential as a management strategy for high-moisture organic residuals. To our knowledge, to date there is no literature regarding implementation of biodrying processes for treating pulp and paper mixed sludge. Certainly, the complexity of the mixed sludge is one of the formidable challenges, which requires a specific reactor configuration with a precise control system that needs to be carefully addressed in any technology development.

BIODRYING PROCESS UNDER DEVELOPMENT AT ÉCOLE POLYTECHNIQUE

The concept of biodrying is explored by examining the fundamentals of modeling and transport phenomena, with an emphasis on the advantages of a continuous biodrying reactor configuration versus batch operation. A novel biodrying technology has been under development over the last few years.[34] The novelty of the biodrying process lies in the fact that the driving force for drying is naturally present in the porous matrix (self-heating process) due to the metabolic degradation that differs this technology from the conventional drying technologies.

Batch Biodrying Process

Frei[18] studied the drying of mixed sludge using a 1-m^3 batch biodrying reactor (1.75 m × 0.75 m × 0.75 m) for three mixed sludge/woodwaste dry mass ratios (1:1, 1:0.5, and 1:0.25). The optimum pneumatic condition for the biodrying process performance was achieved using a ratio of 1:0.5 of mixed sludge/wood waste. Measured

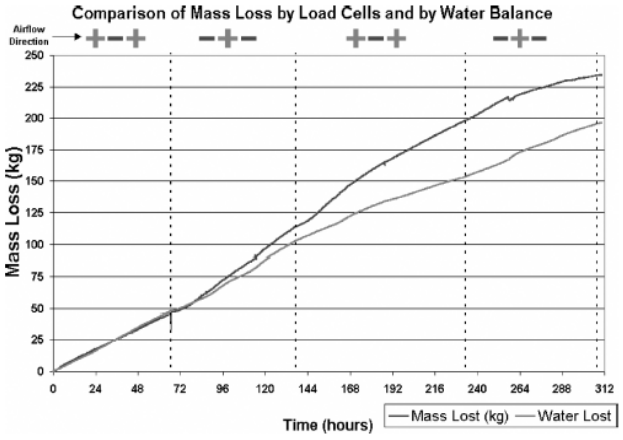

FIG. 4. Mass loss of porous matrix vs. biodrying time (adapted from Frei et al.[34]).

temperatures and pressures in the porous matrix were used to estimate permeability using Darcy's law. The maximum matrix temperature reached was around 65°C, and sludge carbon losses were estimated at between 5.5% and 18% over the three experimental runs. As biodrying progressed, the carbon loss increased linearly to about 20% (Fig. 4).

The matrix permeability (ability of the porous matrix to transmit air flow through pore spaces) increased significantly during forced aeration periods [− + −, when the center conduit was injecting (+) air, the two side conduits would be extracting (−) air] as drying progressed, and conversely, the permeability decreased during extracted air periods (+ − +), due to the rewetting phenomenon (Fig. 5), where reversing the air flow direction rewetted the sludge, resulting in the rehydration of solids by humid air, which increased microbial activity and subsequently led to a high drying rate.

Furthermore, the drying rate more or less followed the same trend as the average internal temperature (Fig. 6). The increased outlet air temperature (as a consequence of the microbial activity) allowed the air to hold greater quantities of moisture, thus increasing the drying rate.

Roy[20] performed batch biodrying experiments with the goal of optimizing the batch biodrying process. It was concluded that low air flow rates favor biodegradation, although less progress on biodrying can be achieved, whereas at higher air flow rates, biodegradation is limited due to the fact that the biomass is cooled. The natural biological heat provided by microbial activity was recognized to be the major source of energy in the novel biodrying system. It was found that the biological energy produced in a batch biodrying system for mixed sludge varies from 23 to 39 W/kg. Similar results have been reported by Mote and Griffis[35] (20–28 W/kg-DM)[35] and Harper et al.[36] (20–38 W/kg-DM).

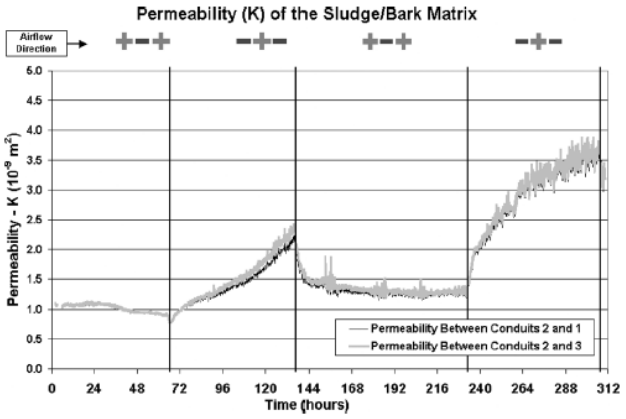

FIG. 5. Permeability of porous matrix vs. biodrying time.[18]

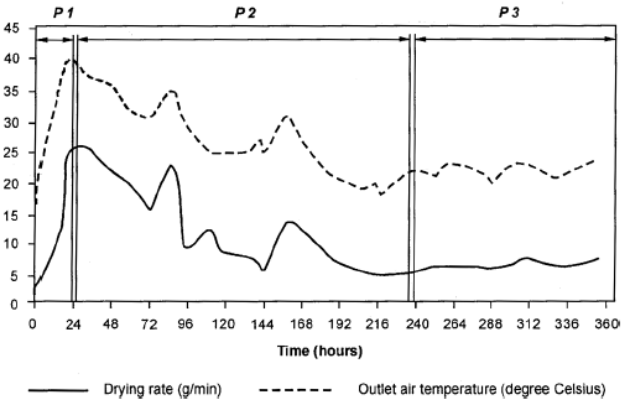

FIG. 7. Drying rate and outlet air temperature for a typical run.[20]

Performance variations were attributed largely to the initial sludge properties. It was determined that the drying rate was mostly a function of air flowrate and of outlet air temperature. The outlet air temperature was a function of biological activity close to the air outlets. Three distinct drying periods were identified and correlated to the microbial population growth periods (Fig. 7).

- The exponential rate period (P1), characterized by an exponential increase in the drying rate, was mostly a function of the acclimatization of the microbial mass (increase of cell counts from 10^6 CUF/g to 10^8 CUF/g) comparable to microbial populations reported by Haug.[37]
- The declining rate period (P2), characterized by an exponential decrease in the drying rate triggered by a lack of organic substrate/nutrient availability.
- The stable rate period (P3), which began following nine days of the biodrying process and was characterized by a stable drying rate, was mostly a function of the air flow rate.

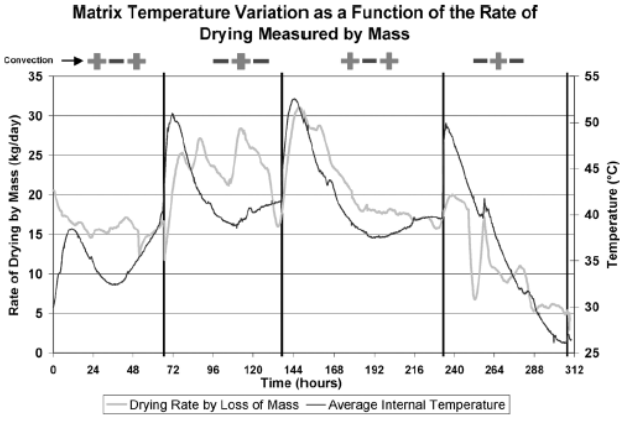

FIG. 6. Rate of drying and porous matrix temperature vs. time for a typical run.[18]

It was also found that in the batch reactor configuration, air flow inversion favored biodegradation rather than biodrying. Inverting the air flow direction causes the water front to switch direction, and water removed from the wet portion of the matrix is deposited in the dry area.[18,20,31,35]

Techno-Economic Analysis of the Batch Biodrying Process

In most cases, the economics of biomass to energy conversion is sensitive to the size and configuration of the main process from which the waste is generated, as well as to the value of the fuel used to produce steam and electricity for the main process. The value of the mixed sludge relative to its thermal content, and the overall efficiency of energy recovery inherent to the mixed sludge to energy process will dictate the economic viability of a particular technology.

Frei et al.[38] considered the techno-economic analysis of a 7 m × 18 m (height and width, respectively) batch biodrying system applied to the drying of pulp and paper mixed sludge. The length of the reactor can be modified because there is little variation in drying with length. The residence time was assumed to be 7 days. The sensitivity analysis of three scenarios showed that in the worst case, the long residence times required for biodrying would allow the dryness of the sludge to reach 45%, while the ratio of mixed sludge/woodwaste was 1:1. The implementation of the best scenario can yield 60% dryness when the ratio of mixed sludge/woodwaste is 4. A short residence time and a short investment payback period were the main advantages of this scenario. A savings of more than $2 million in annual operating costs was realized for the base case model, whereas the payback period was about 2.5 years. It was also

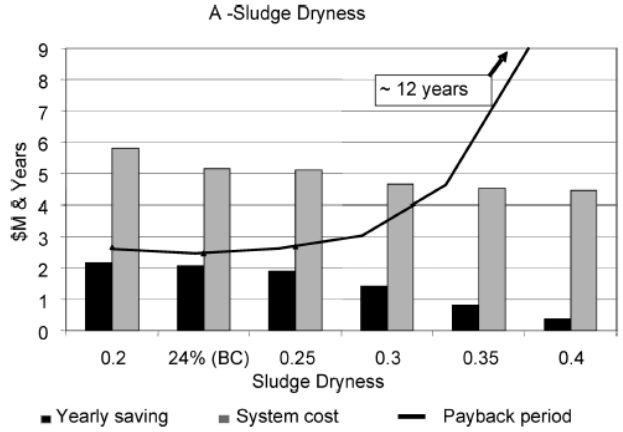

FIG. 8. Effect of sludge dryness on annual saving, system cost and payback period.[38]

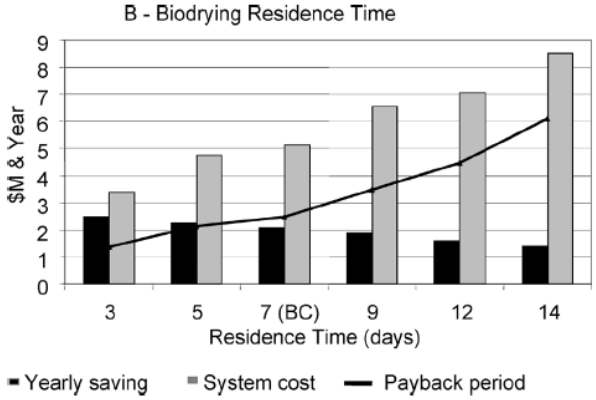

FIG. 9. Effect of biodrying residence time on annual saving, system cost, and payback period.[38]

concluded that the feed dryness and the residence time have the greatest effect on the performance of the system. Moreover, the mixed sludge/woodwaste ratio and the porous matrix temperature were other influential factors.

As can be seen in Fig. 8, the feed dryness had the largest impact on the yearly saving and the project payback. While performing the sensitivity analysis, other variables, such as residence time and sludge/woodwaste ratio, were kept constant at values of 7 days and 2, respectively. The minimum payback period was observed to occur at 24% of feed dryness.

Figure 9 illustrates the effect of residence time on the annual savings and payback period. Long residence times yielded little annual savings but greatly increased the payback period. For instance, by tripling the residence time, the system installation cost was doubled.

Roy et al.[39] considered a full-scale biodrying system comprising two 625-m^3 reactors of 5 m in height, 5 m in width, and 25 m in length. The effect of final material dryness on capital and operational costs as well as on the system performance was investigated. Among three scenarios with different types of bulking agents and air flow rates, the best scenario was found to be the one with the maximum aeration (32 cfm), with dried mixed sludge as the bulking agent.

Aeration rate had an influential effect on the capital costs of the biodrying system. For instance, doubling the air flow rate (from 16 cfm to 32 cfm) reduced the capital cost of the system by half. Utilizing treated sludge as bulking agent instead of bark also reduced capital costs for final material dryness values greater than 43%.

Greater air flow rates, such as 32 cfm/m^3, provided acceptable payback periods that could eventually minimize mill-specific system sizing. Proper sizing of the biodrying system would significantly lower capital costs to achieve payback periods in the range of 1.5–2 years, which, in the current economic context, appears to be the industrial standard for this type of project.

Figure 10 represents the trend of system performance for different scenarios. It can be observed that after 4 days of biodrying process, using treated material as bulking agent provides greater final dryness. However, this will not have a significant impact on the viability of the biodrying process. Furthermore, doubling the air flowrate (from 16 cfm to 32 cfm) doubled the return on investment.

From the results discussed above, it is clear that batch biodrying is a process that is technically sound and economically viable. Some of the promising achievements that encourage further consideration of biodrying include the short payback period, high annual savings, significant reduction in fossil fuel consumption, environmental benefits, and self-heating system. Although the results confirm the applicability and operability of the batch biodrying technology, a number of shortcomings were identified,

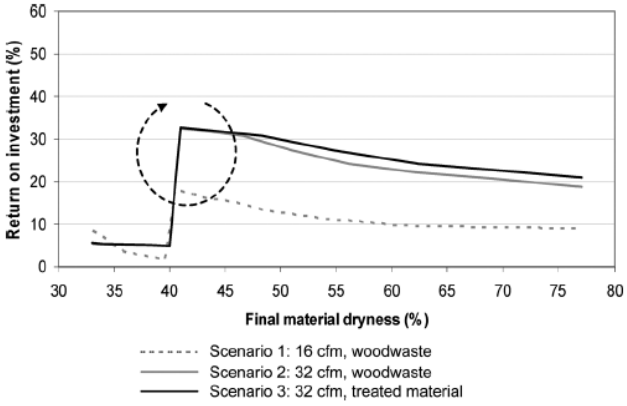

FIG. 10. Three scenarios of return on investment vs. final dryness.[20]

such as inflexibility, relatively long residence times, the space requirements at mill sites, short-circuiting, and the possible occurrence of anaerobic conditions.

Continuous Biodrying Process

VCU (Vertical Composting Unit), a New Zealand-based company, has developed a continuous composting reactor that works based on a "plug flow" principle, as shown in Fig. 11. Shredded mixed municipal sludge flows from the top to the bottom of the reactor. The compost is removed daily from the bottom. The biological heat generated can raise reactor temperatures up to 40–70°C, which destroys pathogens present in municipal sludge waste. It is claimed that this system is energy efficient and does not require agitation, bio-filtration, external heating, or air injection. With minimal moving components, maintenance, and operating costs, the continuous vertical reactor appears to function well according to both economic and operational aspects.[40] However, the physical characteristics of mixed sludges from the pulp and paper industry differ from municipal sludge.

In addition to the fibrous components (cellulose, hemicelluloses, lignin, and other types of carbohydrates), there are also mineral materials either from papermaking process

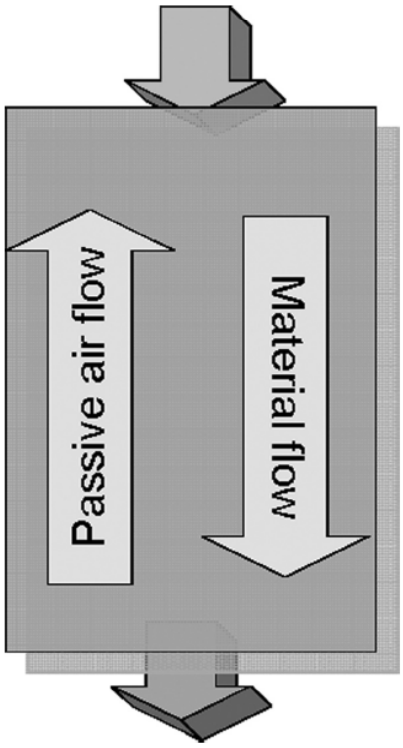

FIG. 11. VCU composting reactor.

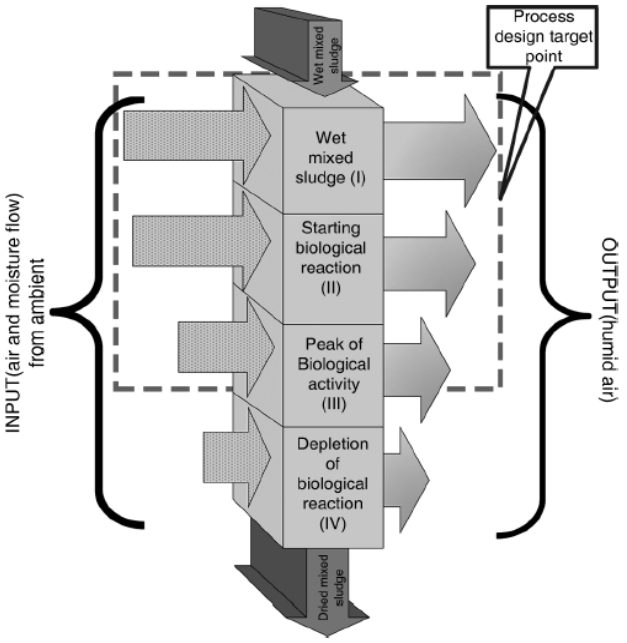

FIG. 12. Proposed schematic of continuous biodrying reactor.

(clay, fillers) or wastewater treatment system (mainly phosphorous, limestone, and nitrogen), microorganisms (tiny biological flocs), and heterogeneous bark or wood waste residues as bulking agent. Therefore, the description of the manner of biological reaction in the biodrying process is highly complex; however, the batch experiments demonstrate that the mixture will dry well through biological heat generation under forced aeration.

The schematic of the proposed continuous biodrying reactor is illustrated in Fig. 12. Airflow is blown through the porous matrix, in order to remove the moisture and water within the reactor. One of the most critical process requirements is good pneumatic conditions along the reactor such that pressure drops across the porous matrix are acceptable and maximum microbial activity can be guaranteed for enhanced drying purposes. In addition to the appropriate pneumatic requirement in each compartment, the air flow rate down the length of the reactor will also be governed by outlet air relative humidity.

The reactor is divided into four nominal compartments. The wet mixed sludge is fed to the reactor top (compartment I) and flows downward by means of gravity. In the first compartment, the high forced aeration removes the free and interstitial water, leaving the surface and bound water, making the porous matrix more susceptible to biological reaction (biodrying). Maximum air flow rates will likely be required in the first compartment, which is expected to result a similar trend of drying rate and

temperature rise shown in Fig. 7 (P1). The drying of surface water takes place at the exposed surface of the particles by convection in compartments I and II. It has been reported that migration of bound water through the solid matrix occurs by molecular diffusion having a flux proportional to the gradient of the chemical potential of the bound (water) molecules.[41]

Once the moisture content is decreased to a thin film of surface water, oxygen from the air must penetrate the thin biofilm to reach the microorganisms. This is most likely to happen in the second and third compartments, where the moisture content favors biological reaction, which helps to evaporate surface and bound water. Consequently, the maximum biological activity will increase the drying rate as well as porous matrix temperature, similar to phase 2 (P2) in Fig. 7. Cooling down the system, however, would limit the metabolic activity. Therefore, the air flow rate is gradually decreased to the control strategy proposed level. A similar process for forced aeration composting has been described elsewhere.[42,43] Diaz et al.[42] reported that excessive aeration cools the porous matrix and leads to large nitrogen (N) losses, while inadequate aeration prevents the proper development of stabilizing temperatures. In compartment IV, the temperature decreases and the second falling rate period will occur, during which it is believed that the biological activity will dramatically decrease due to a lack of sufficient moisture, nutrients, and oxygen, as the last compartment at the bottom of reactor is supplied with minimum aeration. In operational point of view, the behavior of process in compartment IV is more likely to follow phase 3 (P3) in Fig. 7.

Expected Profiles of Moisture Content, Air Temperature, and Air Superficial Velocity

Figure 13 shows the expected profiles of average dryness, matrix temperature (or air temperature in the case of local thermal equilibrium), and air superficial velocity. At the beginning of the process, it is expected that free and interstitial water will be removed rapidly due to a high aeration rate. This drying trend continues until the end of compartment II, where there is no more free and interstitial water left, but only a thin layer of surface water. The porous matrix temperature is expected to follow more or less the same trend as dryness, except that in the first two compartments, the temperature of the matrix increases very slowly due to the high moisture content and aeration (which cools down the matrix), compared to compartments III and IV, where there is a decline in the aeration rate and high exothermic metabolic reaction.

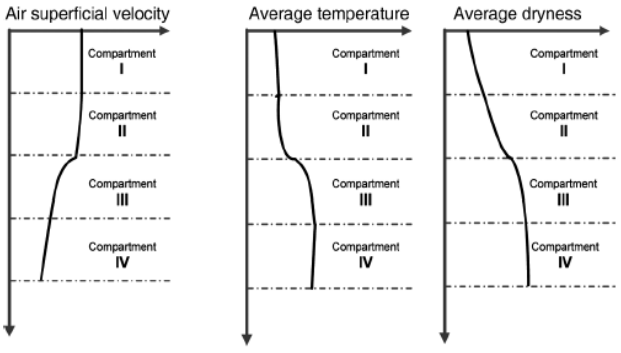

FIG. 13. Expected variation of average dryness, air temperature, and air velocity along the reactor.

Air superficial velocity, which is directly related to the porosity and permeability of the porous matrix, is expected to be almost the same in compartments I and II. The main reason for this expectation is that the inlet air flow rate will not change significantly in the first and second compartments because it is required to remove free, interstitial, and some portion of surface water. Since oxygen must penetrate through the biofilm to reach the microorganisms, the aeration rate must satisfy the efficient metabolic activity. As permeability is expected to increase when drying progresses, more void spaces will be available, and therefore the superficial velocity will decrease.

It should be emphasized that these trend descriptions were hypothesized to be reasonable but experimental verification will reveal the actual process parameter variations.

Modeling as a Design, Optimization, and Scale-Up Tool

Extensive characterization of biodrying behavior using a strictly experimental approach constitutes a formidable challenge due to the excessively large number of variables such as air velocity, inlet air temperature, inlet air humidity, feed dryness, particle size and distribution, ratio of bulking agent, and residence time. Modeling can provide a deterministic approach for controlling the rate of drying and different types of drying kinetics during mixed sludge biodrying. Such a capability could help to provide the knowledge to optimize the biodrying process, to minimize the experimental trials, and to establish the scale up criteria in a reasonable way, without having to resort to an extensive plan of experimental tests.

Modeling is a useful tool that can help to enhance the design of the continuous biodrying reactor. It can be used to establish and explore the optimum design criteria. It can predict the biodrying performance and, most importantly, provide dynamic coupling between mass and heat transfer mechanisms, which cannot be clearly identified through extensive experiments.

Considering the operational obstacles and extremely high costs associated with performing extensive experiments at different scales, there is an additional incentive to simulate the biodrying process mathematically. Through modeling, one can seek the compromise between the extent of biological reaction, in order to achieve the target dryness

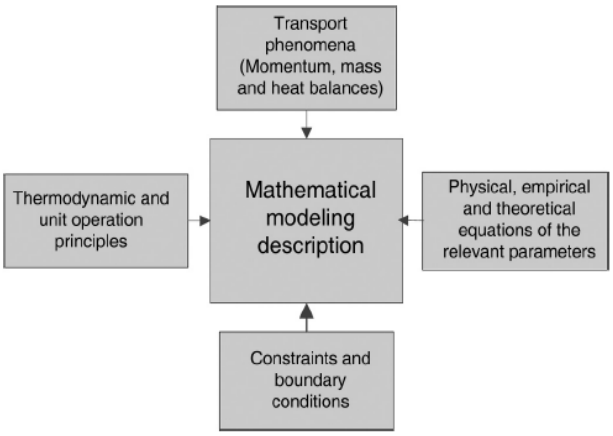

FIG. 14. Components of mathematical modeling and simulation.

level, while at the same time preserving the calorific value of the mixed sludge for maximum energy recovery in the power boiler.

Numerous studies have been conducted at the laboratory, pilot, and full scales in the field of technical modeling and performance of composting.[44–46] However, no work has yet been published on the modeling of the biodrying process. Our modeling strategy will be based on a stepwise approach, starting with simplistic models and adding to the complexity of these models as more insight is gained into the complex transport phenomena involved in this type of process.

Figure 14 describes the different categories and components of the modeling and simulation. In the biodrying process for a continuous reactor, the most important issue is to provide simultaneous coupling between three major phenomena; i.e., momentum, mass transfer, and heat transfer (category one). The basic description of these phenomena in a biodrying reactor is highly complicated for several reasons associated with the complex nature of the feed material, porous matrix, and the biological heat source. Different phases are present and different forces are dominant within the various reactor levels.

In order to facilitate the modeling task, a thermodynamic analysis of the process can be performed, which represents the second category. This will provide an overall picture of the biodrying process without requiring any details inside the reactor. From previous batch biodrying experimental work[24] it was determined that an accurate insight into dynamic biological heat generation can be obtained when thermodynamic analysis is employed. Therefore, thermodynamic analysis will be used to describe the biological heat term in the energy conservation equation. Furthermore, online monitoring and analysis of CO_2 from the outlet gas of each compartment will provide valuable information about the microbial reactions and quantity of generated heat.

The third category in the modeling involves empirical models of the process parameters related to mass and heat or momentum transfers. For instance, the ideal gas law can be employed for air and water vapor, specific heat capacities can be assumed to have a linear relationship with moisture content, and porosity or permeability can be correlated to the moisture content from the experimental data, and so on.

By repeatedly working on these three categories that describe the modeling task, models will be constructed and solved numerically in order to find the distribution of temperature, moisture content, and drying rate. One last step is required before simulations can be performed, which appears explicitly in Fig. 14. It involves accurately determining the constraints and boundary conditions for the specific configuration of the biodrying system. In the case of the continuous biodrying reactor, one of the immediate process constraints is fully saturated air at the outlet of gas flow, which will allow all the process variables to be set accordingly.

Physical Modeling of the Continuous Reactor

As mentioned above, models for composting sludges with forced aeration have been described extensively in the literature. Heat balance analyses were presented by Bach et al.,[47] Harper et al.,[36] Koenig and Tao,[48] and Bari et al.[49] and mass balance evaluations were provided by Robinzon et al.,[50] Batista et al.,[51] and Straatsma et al.[52]

To illustrate, the following mass balance equations for moisture content and oxygen have been reported with the goal of providing simultaneous coupling between mass and energy balances[53]:

$$\frac{dM_b}{dt} = \frac{G_a[H_s(T_a) - H_s(T)] - y_{H_2O/BVS}\frac{d(BVS)}{dt}}{\rho_{db}V_r} \quad (1)$$

where M_b is the material moisture content (kg H_2O/kg-DS), t is the time in (s), G_a is the mass flow rate of inlet dry air (kg/s), H_s is the saturated humidity of outlet air (kg H_2O/kg-dry air), T is the temperature of the matrix (°C), T_a is the ambient temperature (°C), y is the metabolic yield of water (kg H_2O/kg-BVS removed), and ρ_{db} is the bulk density of the porous matrix (kg/m^3).

The metabolic reaction of oxygen is written as follows:

$$\frac{dM_{O_2}}{dt} = \frac{G_a(X_{O_2,a} - X_{O_2,exit}) - y_{H_2O/BVS}\frac{d(BVS)}{dt}}{\varepsilon V_r \rho_a(T)} \quad (2)$$

where BVS is the mass of biodegradable volatile solids (kg), V_r is the working volume of the reactor (m^3), X_{O_2} is the concentration of oxygen (kg-O_2/kg-dry air), ε is the porosity of the porous matrix, and ρ_a is the density of dry air (kg/m^3).

Concerning the energy balance, the following model can be cited[45]:

$$\frac{d(mcT)}{dt} = GH_i - GH_\circ - UA(T - T_a) + \frac{d(\mathrm{BVS})}{dt}H_c \quad (3)$$

where m is the mass of the porous matrix (kg), c is the specific heat capacity of the matrix (KJ/kg °C), G is the mass flow rate of air (kg/s), H_i and H_o are the inlet and exit gas enthalpies (KJ/kg), H_c is the combustion heat of the substrate (KJ/kg), U is the overall heat transfer coefficient (heat loss) (kW/m^2 °C), and A is the surface area of the reactor (m^2).

There have been several models reported for the rate of biological reaction, including first-order reactions,[52,54–56] Monod-type reactions[57–59] and empirical models.[47,60–63] Although these models adequately fit with most biological reaction applications, there are some limitations associated with employing them. For instance, some models require temperature corrections and heat conversion factors. A broad review of these correction factors can be found elsewhere.[45] Recently, Roy et al.[64] employed a thermodynamic approach to estimate biological heat generation in a biodrying system and found results that were in a good agreement with the literature.[38,39] Biological heat can also be automatically monitored.[37,53,54,56,65–66]

These models could be used in a lumped manner for each compartment. It might be possible to employ these models with some correction factors or dimensionless numbers, which could subsequently represent forced convection and highlight the differences between composting and biodrying. However, it should be noted that the aeration rate in the biodrying process is 10–30 times higher than that of the composting process.[37] As a result, if lumped models will probably be first considered in our work, we believe that an adequate and space-dependent description of the transport phenomena governing the continuous biodrying process will ultimately require the development of distributed models based on partial differential equations.

Expected Dominant Transport Phenomena

At the top of the reactor, there are three phases; free and interstitial water, the solid matrix, and gas flow (air and water vapor). Free and interstitial water are separated from the particles and begin to move downwards due to gravity, but the high air flow rate evaporates them quickly. As the free and interstitial water are removed, microorganisms actively start their growth, reproduction, and metabolic reactions. At the end of the second compartment or in the beginning of the third compartment, the air flowrate is decreased to facilitate the biological activity. In terms of energy transfer in compartment I, it is reasonable to neglect the term related to the biological heat production. This will simplify the mathematical analysis of the modeling in this compartment. Convection in the pore space and conduction in the solid phase are the dominant factors in the energy balance in compartment I. Darcy's law for porous media may be used for describing the flow of the gas and liquid phases.

In the middle of the reactor (compartments II and III), moderate aeration influences the convective and diffusion terms of the gas phase, and microbial activity causes the heat source term to be dominant. Therefore, all these terms will be present in the heat transfer equations. Further considerations must be made to simplify the equation. Nevertheless, as the porous matrix is being dried, surface and unbound water move toward the surface of the particles by capillary forces. The porous matrix of mixed sludge contains interconnecting and varying pores and varying particle sizes. Capillary forces that occur due to the meniscus of thin layers of surface water across each pore between the solid particles, provide the driving force for water to move through pores to the surface of the solid particles.

At the bottom of the reactor, only minimum aeration is supplied. The mixed sludge has already been dried and microbial activity faces a number of challenges. The first is a low moisture content that makes it difficult for microorganisms to continue reproduction, growth, and degradation. The second is a low aeration rate, which cannot supply sufficient oxygen for microorganisms. The third problem involves the development of undesirable anaerobic conditions in the porous matrix that can cause variations in the mixed sludge dryness at the bottom of the reactor. In addition to these three deficiencies, insufficient permeability or porosity might be a real challenge due to the load of wet sludge and compaction. All these considerations must be taken into account in order to establish mass and energy balances. Other phenomena like short circuiting, bridging, and/or channeling might also occur. However, none of these obstacles can be confirmed yet as there is no experimental data available or similar work described in the literature.

Comparison of Continuous Biodrying Reactor with Batch Reactor

According to the results described previously, the batch biodrying process has significant potential as a suitable solution for drying pulp and paper mill sludges with minimum energy requirements and side impacts. Nevertheless, the continuous biodrying reactor offers several advantageous performance features over the batch system:

- The movement of mixed sludge is assisted by gravity.
- Different aeration rates along the vertical reactor provide better controllability and performance, and may achieve higher dryness levels within a short residence time.

- Uniform sludge treatment and drying can be achieved via the continuous vertical reactor configuration which is more difficult to achieve with the batch system.
- The lack of space on-site is a major problem for most pulp and paper mills, yet the vertical configuration has a reduced footprint and favors retrofit installation at crowded mill sites.
- The continuous reactor requires fewer shutdowns, cleanings, and startups.
- The continuous reactor is more flexible and can accommodate different operating variables as well as sludges with different characteristics.
- It is possible to design for different capacities and performance by installing continuous vertical reactors in series or in parallel.
- Utilizing bark as a bulking agent can be minimized in continuous biodrying due to the fact that part of the treated sludge can be recycled and mixed with the wet sludge, providing higher initial dryness, uniform porosity, faster start up of biological reaction, and a decrease in the residence time.

CONCLUDING REMARKS

The challenges of mixed sludge disposal in the pulp and paper industry, including current disposal and drying techniques, have been reviewed in this article. Various problems and restrictions associated with landfilling have triggered the search for new energy efficient technologies for the drying of mixed sludge to be burned in power boilers.

The biodrying technology presented here was shown to be an attractive technique for sludge drying. In summary, the main advantage of the biodrying technology compared to conventional drying technologies is that heat is generated within the porous matrix as a consequence of microbial activity, which enhances moisture removal when coupled with forced aeration. Another advantage of the biodrying technology is that the mixed sludge can be dried while largely preserving its calorific value.

Based on preliminary batch biodrying process, the techno-economic feasibility of batch biodrying technology has been proven, and a vertical continuous biodrying reactor configuration proposed. The continuous reactor has potential to provide a more cost-effective solution with minimum external thermal energy requirements for sludge management at pulp and paper mills. The design configuration of the continuous biodrying reactor was described, including virtual reactor compartments with adjustable air flow rates to achieve a target mixed sludge dryness. The fundamentals of mathematical modeling of the continuous reactor were briefly discussed and a critical review of the mass and energy balances in aerated composting processes presented. Such a mathematical simulation coupled with experimental verification would yield significant scientific benefits, unique reactor configurations for a given mixed sludge characteristic, and contribute to the goal of advancing the efficient drying of mixed sludge. The dominant transport phenomena in different zones of the biodrying reactor were described and the expected velocity, temperature, and mixed sludge dryness profiles along the length of the reactor were presented.

NOMENCLATURE

A	Surface area of the reactor (m^2)
BVS	Mass of biodegradable volatile solids (kg)
c	Specific heat capacity of the matrix (KJ/kg °C)
G	Mass flowrate of air (kg/s)
G_a	Mass flowrate of inlet air (kg/s)
H_c	Combustion heat of the substrate (KJ/kg)
H_i	Inlet gas enthalpy (KJ/kg)
H_o	Outlet gas enthalpy (KJ/kg)
H_s	Saturated moisture of outlet air (kg H_2O/kg-dry air)
M_b	Moisture content (kg H_2O/kg-dry solid)
m	Mass of porous matrix (kg)
T	Temperature of matrix (°C)
T_a	Ambient temperature (°C)
t	Time (s)
U	Overall heat transfer coefficient (kW/m^2 °C)
V_r	Working volume of the reactor (m^3)
X_{O_2}	Concentration of oxygen (kg O_2/kg-dry air)
y	Metabolic yield of water (kg H_2O/kg-BVS removed)

Greek Letters

ε	Porosity of the matrix (dimensionless)
ρ_a	Density of dry air (kg/m^3)
ρ_{db}	Bulk density of porous matrix (kg/m^3)

Acronyms

AST	Activated sludge treatment
BC	Base case
CUF	Colony forming units
DM	Dry matter
DS	Dry solid
GHG	Greenhouse gas
PVC	Polyvinyl chloride
VCU	Vertical composting unit

ACKNOWLEDGEMENTS

This work was completed with the financial assistance of the Natural Sciences and Engineering Research Council (NSERC) of Canada.

REFERENCES

1. Elliott, A.; Mahood, T. Survey benchmarks generation: Management of solid residues. Pulp and Paper **2005**, *79* (12), 49–55.
2. Hynninen, P.; Laine, P. *Environmental Control, Papermaking Science and Technology*, Vol. 19; Fapet Oy: Jyväskylä, Finland, 1998; 234.
3. Chen, G.; Yue, P.L.; Mujumdar, A.S. Sludge dewatering and drying. Drying Technology **2002**, *20* (4–5), 883–916.
4. Hippinen, I.; Ahtila, P. Drying of activated sludge under partial vacuum conditions—An experimental study. Drying Technology **2004**, *22* (9), 2119–2134.
5. Kudra, T.; Gawrzynski, Z.; Glaser, R.; Stanislawski, J.; Poirier, M. Drying of pulp and paper sludge in a pulsed fluid bed dryer. Drying Technology **2002**, *20* (4–5), 917–933.
6. Kraft, D.L.; Orender, H.C. Considerations for using sludge as a fuel. Tappi Journal **1993**, *76* (3), 175–183.
7. Tsang, K.R.; Vesilind, P.A. Moisture distribution in sludges. Water Science and Technology **1990**, *22* (12), 135–142.
8. Vanhatalo, A.; Ahtila, P. *Drying of Forest Industry Sludge for Energy Production with Partial Vacuum Technology*; Proceedings of the 2001 ACEEE Summer Study on Energy Efficiency in Industry; American Council for an Energy-Efficient Economy: Washington, D.C.; 2001; 435–443.
9. Tarnawski, W. Emission factors for combustion of biomass fuels in the pulp and paper mills. Fibres & Textiles in Eastern Europe **2004**, *12*, 3(47), 91–95.
10. Bradley, A.J.; Patrick, W.K. Sludge dewatering and incineration at Westvaco. North Charleston, S.C. Tappi Journal **1991**, *74* (5), 131–137.
11. CANMET Energy Technology Centre. *Pulp and Paper Sludge to Energy—Preliminary Assessment of Technologies*; ADI Limited Report, Varennes, QC, Canada, 2005.
12. Hippinen, I.; Ahtila, P. Activated sludge drying in the pulp and paper industry by means of secondary energies. *1st International Conference on Sustainable Energy Technologies*; Porto, Portugal, Paper EES4, 2002.
13. Liang, T.; Khan, M.A.; Meng, Q. Spatial and temporal effects in drying biomass for energy. Biomass and Bioenergy **1996**, *10* (5–6), 353–360.
14. Banerjee, S.; Mahmood, T.; Phelan, P.M.; Fouke, R.W. Impulse drying sludge. Water Research **1998**, *32* (1), 258–260.
15. Beckley, J.; Banerjee, S. Operational issues with impulse drying sludge. Water Science & Technology **1999**, *40* (11–12), 163–168.
16. Vaxelaire, J.; Bongiovanni, J.M.; Mousques, P.; Puiggali, J.R. Thermal drying of residual sludge. Water Research **2000**, *34* (17), 4318–4323.
17. Léonard, A.; Blacher, S.; Marchot, P.; Pirard, J.P.; Crine, M. Convective drying of wastewater sludges: Influence of air temperature, superficial velocity, and humidity on the kinetics. Drying Technology **2005**, *23* (8), 1667–1679.
18. Frei, K.M. *Novel Drying Process Using Forced Aeration Through a Porous Biomass Matrix*; MSc. Thesis. Ecole Polytechnique de Montreal: Montreal, Canada, 2004.
19. Adani, F.; Baido, D.; Calcaterra, E.; Genevini, P. The influence of biomass temperature on biostabilization–biodrying of municipal solid waste. Bioresource Technology **2002**, *83* (3), 173–179.
20. Roy, G. Modélisation technique et économique d'un réacteur de bioséchage discontinue; MSc. Thesis. Ecole Polytechnique de Montréal, Montréal, Canada, 2005 (in French).
21. Madigam, M.T.; Martinko, J.M.; Parker, J. *Brock Biology of Microorganisms*, English Ed.; Prentice Hall: Upper Saddle River, NJ, 1997.
22. Prescott, L.M.; Harley, J.P.; Klein, D.A. *Microbiology*, 2nd Ed; W.C. Communications Inc.: Dubuque, IA, 1993.
23. Nakasaki, K.; Aoki, N.; Kubota, H. Accelerated composting of grass clippings by controlling moisture level. Waste Management & Research **1994**, *12* (1), 13–20.
24. Liang, C.; Das, K.C.; McClendon, R.W. The influence of temperature and moisture contents regimes on the aerobic microbial activity of a biosolids composting blend. Bioresource Technology **2003**, *86* (2), 131–137.
25. Klaus, H. *Control and Measurement Method for the Biological Drying of Sewage Sludge*. European Patent, EP0508383, 1992.
26. Klaus, H. *Process for the Biological Drying of Sewage Sludge*. European Patent, EP0508382, 1992.
27. Nellist, M.E.; Lamond, W.J.; Pringle, R.T.; Burfort, D. *Storage and Drying of Comminuted Forest Residues*, Vol. I; AFRC Silsoe Research Institute: Bedford, UK, 1993; 1–82.
28. Nellist, M.E. Storage and drying of arable coppice. Aspects of Applied Biology—Biomass and Energy Crops **1997**, *49*, 349–359.
29. Choi, H.L.; Richard, T.L.; Ahn, H.K. Composting high moisture materials: Biodrying poultry manure in a sequentially fed reactor. Compost Science & Utilization **2001**, *9* (4), 303.
30. Hansjoerg, H.; Hans-Joachim, B.; Gurudas, S.; Kurt, S.; Barbara, R.; Juergen, R. *Process and Apparatus for Biological Drying of Residual Waste, Sewage Sludge and/or Biomass*. European Patent EP1408021, 2004.
31. Sugni, M.; Calcaterra, E.; Adani, F. Biostabilization—Biodrying of municipal solid waste by inverting air-flow. Bioresource Technology **2005**, *96* (12), 1331–1337.
32. Lhadi, E.K.; Tazi, H.; Aylaj, M.; Genevini, P.L.; Adani, F. Organic matter evolution during co-composting of the organic fraction of municipal waste and poultry manure. Bioresource Technology **2005**, Article in press.
33. Laflamme-Mayer, M.; Bellec, S.; Gaudreault, C.; Thibodeau, J.-B.; Stuart, P.R. Techno-economic evaluation of some emerging sludge management options for mills with activated sludge treatment. Pulp & Paper Canada **2004**, *105* (6), 33–37.
34. Frei, K.M.; cameron, D.; Stuart, P.R. Novel drying process using forced aeration through a porous biomass matrix. Drying Technology **2004**, *22*, 1191–1215.
35. Mote, C.R.; Griffis, C.L. Heat production by composting organic matter. Agricultural Wastes **1982**, *4*, 65–73.
36. Harper, E.; Miller, F.C.; Macauley, B.J. Physical management and interpretation of an environmentally controlled composting ecosystem. Australian Journal of Experimental Agriculture **1992**, *32* (5), 657–667.
37. Haug, R.T. *The Practical Handbook of Compost Engineering*; Lewis Publishers: Boca Raton, FL, 1993.
38. Frei, K.M.; Cameron, D.; Jasmin, S.; Stuart, P.R. Novel sludge drying process for cost-effective on-site sludge management. Pulp and Paper Canada **2006**, *107* (4).
39. Roy, G.; Jasmin, S.; Stuart, P.R. Economical modeling of a batch biodrying reactor for treating pulp and paper mill sludge. Tappi Journal **2006**, submitted.
40. VCU Technology LTD, Vertical Composting Units, VCU, Auckland, New Zealand. http://www.vcutechnology.com (accessed November 2005).
41. Stanish, M.A.; Schajer, G.S.; Kayihan, F.A. Mathematical model of drying for hygroscopic porous media. AIChE Journal **1986**, *32* (8), 1301–1311.
42. Diaz, L.F.; Savage, G.M.; Eggerth, L.L.; Golueke, C.G. *Composting and Recycling*; Lewis Publishers: Boca Raton, FL, 1993.
43. Barrington, S.; Choinière, D.; Trigui, M.; Knight, W. Compost convective airflow under passive aeration. Bioresource Technology **2003**, *86* (3), 259–266.
44. Mason, I.G.; Milke, M.W. Physical modelling of the composting environment: A review. Part 1: Reactor systems. Waste Management **2005**, *25* (5), 481–500.
45. Mason, I.G. Mathematical modelling of the composting process: A review. Waste Management **2006**, *26*, 3–21.
46. Mason, I.G.; Milke, M.W. Physical modelling of the composting environment: A review. Part 2: Simulation performance. Waste Management **2005**, *25* (5), 501–509.

47. Bach, P.D.; Nakasaki, K.; Shoda, M.; Kubota, H. Thermal balance in composting operations. Journal of Fermentation Technology **1987**, *65* (2), 199–209.
48. Koenig, A.; Tao, G.H. Accelerated forced aeration composting of solid waste. In *Proceedings of the Asia-Pacific Conference on Sustainable Energy and Environmental Technology*; Greenfield, P.F.; Liu, C.Y.; Tay, J.H.; Lu, G.Q.; Lua, A.C.; Toh, K.C., Eds.; World Scientific: Singapore, 1996; 450–457.
49. Bari, Q.H.; Koenig, A.; Guihe, T. Kinetic analysis of forced aeration composting. I. Reaction rates and temperature. Waste Management & Research **2000**, *18* (4), 303–312.
50. Robinzon, R.; Kimmel, E.; Avnimelech, Y. Energy and mass balances of windrow composting system. Transactions of ASAE **2000**, *43* (5), 1253–1259.
51. Batista, J.G.F.; van Lier, J.J.C.; Gerrits, J.P.G.; Straatsma, G.; Griensven, L.J.L.D. Spreadsheet calculations of physical parameters of phase II composting in a tunnel. Mushroom Science **1995**, *14*, 189–194.
52. Straatsma, G.; Gerrits, J.P.G.; Thissen, J.T.N.M.; Amsing, J.G.M.; Loffen, H.; van Griensven, L.J.L.D. Adjustment of the composting process for mushroom cultivation based on initial substrate composition. Bioresource Technology **2000**, *72* (1), 67–74.
53. Higgins, C.; Walker, L. Validation of a new model for aerobic organic solids decomposition: Simulations with substrate specific kinetics. Process Biochemistry **2001**, *36* (8–9), 875–884.
54. Finger, S.M., Hatch, R.T.; Regan, T.M. Aerobic microbial growth in semi-solid matrices: Heat and mass transfer limitations. Biotechnology and Bioengineering **1976**, *18*, 1193–1218.
55. Smith, R.; Eilers, R.G. *Numerical Simulation of Activated Sludge Composting*, EPA-600/2-8C-191; USEPA: Cincinnati, OH, 1980.
56. Scholwin, F.; Bidlingmaier, W. Fuzzifying the composting process: A new model based control strategy as a device for achieving a high grade and consistent product quality. In *Proceedings of the Fourth International Conference of ORBIT Association on Biological Processing of Organics: Advances for a Sustainable Society*; ORBIT Association: Weimar, Germany, 2003; 739–751.
57. Kaiser, J. Modelling composting as a microbial ecosystem: A simulation approach. Ecological Modelling **1996**, *91* (1–3), 25–37.
58. Stombaugh, D.P.; Nokes, S.E. Development of a biologically based aerobic composting simulation model. Transactions of ASAE **1996**, *39* (1), 239–250.
59. Seki, H. Stochastic modeling of composting processes with batch operation by the Fokker–Planck equation. Transactions of ASAE **2000**, *43* (11), 169–179.
60. Kishimoto, M.; Preechaphan, C.; Yoshida, T.; Taguchi, H. Simulation of an aerobic composting of activated sludge using a statistical procedure. MIRCEN Journal **1987**, *3*, 113–124.
61. Nakasaki, K.; Kato, J.; Akiyama, T.; Kubota, H. A new composting model and assessment of optimum operation for effective drying of composting material. Journal of Fermentation Technology **1987**, *65* (4), 441–447.
62. Van Lier, J.J.C.; van Ginkel, J.T.; Straatsma, G.; Gerrits, J.P.G.; van Griensven, L.J.L.D. Composting of mushroom substrate in a fermentation tunnel—Compost parameters and a mathematical model. Netherlands Journal of Agricultural Science **1994**, *42* (4), 271–292.
63. VanderGheynst, J.; Walker, L.; Parlange, J. Energy transport in a high-solids aerobic degradation process: Mathematical modeling and analysis. Biotechnology Progress **1997**, *13* (3), 238–248.
64. Roy, G.; Jasmin, S.; Stuart, P.R. Technical modeling of a batch biodrying reactor for pulp and paper mill sludge. (accepted for 9th Conference on Process Integration, Modelling and Optimisation for Energy Saving and Pollution Reduction, 27–31 August 2006 (Prague - Czech Republic))
65. Anderson, R.K.I.; Jayaraman, K.; Voisard, D.; Marison, I.W.; von Stockar, U. Heat flux as an on-line indicator of metabolic activity in pilot scale bioreactor during the production of *Bacillus thuringiensis* var. *galleriae*–based biopesticides. Thermochimica Acta **2002**, *386* (2), 127–138.
66. von Stockar, U.; Duboc, P.; Menoud, L.; Marison, I.W. On-line calorimetry as a technique for process monitoring and control in biotechnology. Thermochimica Acta **1997**, *300* (1–2), 225–236.
67. Turner, R.H.; Kleiser, J.D.; Ross, P.D. Solar sludge drying. In *Solar Engineering 1989—Proceedings of the Eleventh Annual ASME Solar Energy Conference*; ASME: San Diego, CA, 1989; 47–51.
68. Crews, R.S. *Cyclonic Dryer*; US Patent 5791066, 1998.

A2. Development and Experimental Evaluation of a 1-D Distributed Model of Transport Phenomena in a Continuous Biodrying Process for Pulp and Paper Mixed Sludge

Development and Experimental Evaluation of a 1-D Distributed Model of Transport Phenomena in a Continuous Biodrying Process for Pulp and Paper Mixed Sludge[1]

Shahram Navaee-Ardeh, François Bertrand, Paul R. Stuart
Chemical Engineering Department, École Polytechnique de Montréal, Canada

Running head: "Continuous biodrying process for pulp and paper sludge"

Correspondence: François Bertrand, Chemical Engineering Department, École Polytechnique de Montréal, C.P. 6079, succ. Centre-ville Montréal, H3C 3A7, Canada; E-mail: francois.bertrand@polymtl.ca; Tel. +(1) 514-340-4711 ext. 5773; fax: +(1)514-340-4105

Abstract

Effective sludge management is increasingly critical for pulp and paper mills due to high landfill costs and complex regulatory frameworks for disposal options such as sludge landspreading and composting. A novel continuous biodrying process has been developed to dry mixed sludge so that it can be combusted efficiently in a biomass boiler for energy recovery. Modeling this process is important in order to better understand the transport phenomena in the biodrying reactor, and for design and scale-up of the process. A 1-D distributed model for heat transfer coupled with mass and biological transfer phenomena is introduced in this paper, which shows that the temperature of the sludge matrix is a critical parameter. The model assumes lumped parameters in the gas flow direction, and distributed parameters in the (vertical) solids flow direction. Bioheat as a source term and evaporative heat as a sink term are critical issues. In order to evaluate the parameters and assess the model accuracy, a series of experiments was performed. The matrix temperatures predicted by the model were found to be in reasonable agreement with the experimental results, showing that the main transport phenomena were reflected in the model. Some discrepancies between the model-predicted values and the experimental data were indentified at high temperatures, which can be attributed to the complex mechanisms governing the growth cycle of mesophilic and thermophilic bacteria. A dimensionless analysis was performed to identify key dimensionless groups as well as the most dominant transport phenomena in the biodrying process. The results confirmed that convection processes dominated heat transfer at the top of the reactor, and the exothermic aerobic bioenergy dominated at its bottom.

Keywords: Biodrying; Bioheat; Transport phenomena; Pulp and paper; Sludge; Dimensionless analysis

INTRODUCTION

A typical pulp and paper mill wastewater treatment system consists of two systems: primary (mechanical) treatment and secondary (biological) treatment. During primary wastewater treatment, settleable materials are removed by gravity, settling/clarification, and/or flotation.[1] The primary sludge mainly contains fibers (cellulose) and fillers. Primary treatment is followed by biological treatment, often an activated sludge treatment (AST) system, in which wastewater organic matter is broken down by means of aerobic biodegradation.[1] The combined sludge from primary and secondary treatments, the so-called mixed sludge, consists of a muddy mass of microorganisms, fibrous materials, lignin, mineral components (e.g. limestone and phosphorus), clay, inert solids rejected during the recovery process, and water.[2,3] Mixed sludge contains unbound and bound water.[4,5,6,7] Bound water is the most challenging because it is not removed by advanced mechanical techniques and requires thermal drying techniques. Due to the unique characteristic of mixed sludge, including low heating value, applying advanced drying techniques is not economically viable. Combustion can provide a competitive disposal method as long as the dry solids content of the sludge is maintained above approximately 45%, a critical level for good combustion.[8,9] A broad review of emerging drying technologies for pulp and paper mixed sludge revealed that many of these have significant

[1] This paper is accepted at Drying Technology

technical uncertainties and/or questionable economics.[7,10] It is the objective of this work, therefore, to develop an efficient way to increase the dry solids content of mixed sludge from pulp and paper mills to values above critical levels for safe and economic combustion.

Biological drying, or simply biodrying,[7,11] has the potential to consistently raise the dry solids content of mixed sludge, allowing for disposal in boilers with viable steam and/or power generation. In the biodrying process, the drying of sludge is augmented by biological heat in addition to forced aeration. In fact, there are two main mechanisms by which moisture can be removed: convection and diffusion. Convection is mainly related to the air flowrate, temperature, and humidity, whereas diffusion is related to the biological heat and the moisture gradient within the particles. These combined phenomena preserve the caloric value of mixed sludge, leading to higher energy recovery in the boiler.

Our research group previously explored two bench-scale batch reactor configurations for the biodrying of mixed sludge. The initial study determined that a sludge to woodwaste ratio of 2:1 (dry basis) provided acceptable pneumatic conditions in the biodryer.[12] The internal heat generation from aerobic biological activity (bioheat) raised temperatures to peak values of approximately 65°C, and carbon losses due to biological activity ranged from 5% to 18%. The results of this study highlighted a clear correlation between the peak temperature of the matrix and the rate of water removal. The study also included a techno-economic analysis that demonstrated the mill configurations under which the technology was economically viable in the Canadian pulp and paper industry. [13]

In a second study, a series of experiments were performed using a modified batch biodrying reactor configuration with the goal of optimizing the process. [14] The biological heat provided by aerobic microbial activity was recognized to be the major source of energy in the batch biodrying system. The study included a thermodynamic analysis of the process to quantify bioheat, and it was found that the biological energy produced in the batch biodrying system could vary from 3900 to 6500 W/m^3. These values are similar to those reported by Mote and Griffis [15] (3400-4800 W/m^3) and Harper et al. [16] (3400-6500 W/m^3) for aerobic composting processes.

Although both studies confirmed the applicability and economic viability of a biodrying process, several shortcomings were identified. These included process inflexibility, relatively long residence times for achieving target dry solids levels (up to 16 days), scale-up limitations associated with the batch configuration, short-circuiting due to non-uniform aeration at large scale, and the occurrence of anaerobic conditions ("hot spots"). In order to overcome these limitations, a new vertical biodrying reactor was designed to operate in continuous mode. Figures 1 and 2 describe the vertical biodrying reactor designed and operated for this study. The reactor is divided into four compartments, providing flexibility for different operating conditions in different compartments that target preferred water removal conditions. The wet mixed sludge is fed to the reactor top (1^{st} compartment), and flows downward by means of gravity.

In a general context, microbial species responsible for biological activity in biomass can be classified into four groups based on temperature preferences: psychrophiles (active at 0-20^oC), mesophiles (active at 8-48^oC), thermophiles (active at 42-68^oC) and hyperthermophiles (active at 70-110 ^oC).[17] However, as reported by Frei et al. [12] and Roy et al. [14], only mesophilic and thermophilic bacteria are considered in biodrying processes because they are active within the typical operating temperature range of the reactor (25-55^oC).

Characterization of the biodrying process using only an empirical experimental approach is challenging due to the number of variables involved, including air velocity in each reactor compartment, inlet air temperature and relative humidity, inlet feed dry solids content, ratio of bulking agent (in this study, recycle ratio of biodried sludge), and residence time. Modeling can provide insight into critical understanding of the transport processes in the biodrying reactor, and assist in process design and optimization.

Numerous modeling studies have been conducted related to laboratory, pilot, and full scales of composting operations.[18,19,20] Energy balance analyses were presented by Bach et al. [21], Koenig and Tao [22], Bari et al. [23], and Harper et al. [16]. Mass balance evaluations have been made by Robinzon et al. [24], Batista et al. [25], Straatsma et al. [26]. All of these studies were performed on composting processes where, in contrast to the biodrying process, the goal is to fully biodegrade and stabilize the biomass.

Mathematical models incorporating heat and mass transfer have also been developed for solid state fermentation and composting.[27,28,29] In recent modeling work related to heat and mass transfer in a porous matrix containing biological materials, Prud'homme and Jasmin [30] used an inverse solution approach to describe the biochemical heat source. However, this study only investigated a free convection system and the results were not verified experimentally. Our recent modeling work related to continuous biodrying revealed that lumped models were too coarse to capture adequately the transport phenomena dominating in the different compartments of the reactor.[31] The lumped model that was developed predicted higher dry solids contents than those observed

experimentally. Therefore, a more rigorous model is needed to improve the shortcomings of this lumped model, suitable for resolving the transport phenomena prevailing in the biodrying reactor.

The objective of this work, and hence its contribution, is to develop a 1-D model for heat and mass transfer in a novel continuous biodrying reactor for the biodrying of mixed sludge coming from the pulp and paper industry which is suitable for biodryer design. First, the model is introduced. Its accuracy is next assessed through a comparison with experimental data obtained from the pilot-scale reactor that was built in our laboratory. Finally, a dimensionless analysis is presented, which highlights the key operating parameters for this biodrying process.

MATERIALS AND METHODS

Experimental Set-Up

Two pilot-scale vertical stainless-steel reactors were designed and built for this work, each 200 cm high (effective height 160 cm), 100 cm deep and 40 cm wide (Figures 1 and 2). One of these is fully instrumented and controlled online, whereas the other is used to generate additional data and to examine experimental repeatability. Only results from the instrumented biodrying reactor are considered in this paper for modeling purposes (Figure 2). The set-up permits the online monitoring of internal temperature and pressure, changes in CO_2 levels, relative humidity and temperature of the inlet and only outlet airstreams in each compartment. Temperature and relative humidity, pressure and CO_2 were measured using six relative humidity probes, 12 pressure probes and a CO_2 analyzer. The process variables, including incoming gas temperature and relative humidity, were logged at 8 min intervals.

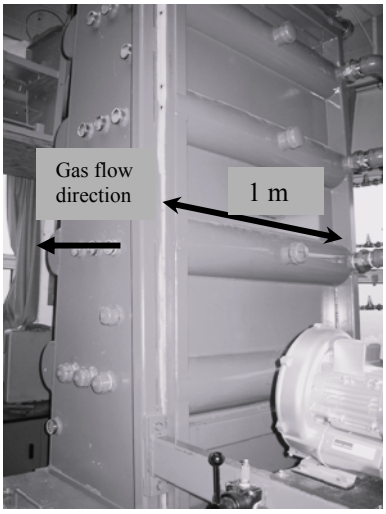

FIG. 1 Pilot-scale continuous biodrying reactor

The continuous reactor is divided into four compartments, each with separate feed and discharge ports. The dried sludge is extracted by two parallel screws installed at the bottom of the reactor, and the fresh sludge (received from the pulp and paper mill) and recycle sludge (obtained from the discharge of the biodryer) are mixed in a 40 liter container and fed to the top of the reactor. Air flow is provided by two blowers, one forcing air into the porous matrix and one extracting air, and is uniformly distributed in each compartment through a plenum with perforated plates. When sludge is extracted from the reactor bottom, the materials flow downward due to gravity.

In order to generate experimental results for model verification, two sets of experiments were conducted. The first series consisted of 8 individual experiments using an experimental design method with the following conditions: total air flowrate of 28-34 m^3/h, recycle ratio of 15-30% (d.b.), and residence times of 4 and 8 days. Note that the recycling of sludge provides pneumatic conditions in the matrix of the biodrying reactor such that no bulking agent (e.g. bark) is required as was the case in the batch reactor configuration. It also contributes to a shorter microbial lag phase since the discharge sludge has acclimated thermophilic bacteria (measured as CFU/g) than that of fresh sludge.[32] The chosen range of residence times was recommended by Roy et al. [14] for an economically feasible batch biodrying process. The second set of experiments was performed for a 6-day residence time, a 30% recycle ratio, under a controlled outlet relative humidity profile with a 40-75 m^3/h total air flowrate. Table 1 summarizes the overall experimental program. Only four cases are used in this study for the modeling

assessment. Feed and discharge of sludge was made twice a day, at 12 h intervals and a mass flowrate of 10-22 kg (d.b).

Table 1. Overall experimental program

Run	Case	Residence (days)	Recycle ratio (%)	Air flowrate (m^3/h)	Outlet relative humidity (%)
1	1	6	30	75(26,5,26,18)	85,85,85,85
2		6	30	55	85,85,96,96
3		6	30	64	96,96,85,85
4	2	6	30	46(16.5,8,14,7)	96,96,96,96
5		4	15	34	
6	3	4	15	28(7,7,7,7)	
7		4	30	28	
8		4	30	34	
9		8	15	34	
10	4	8	15	28(7,7,7,7)	
11		8	30	28	
12		8	30	34	

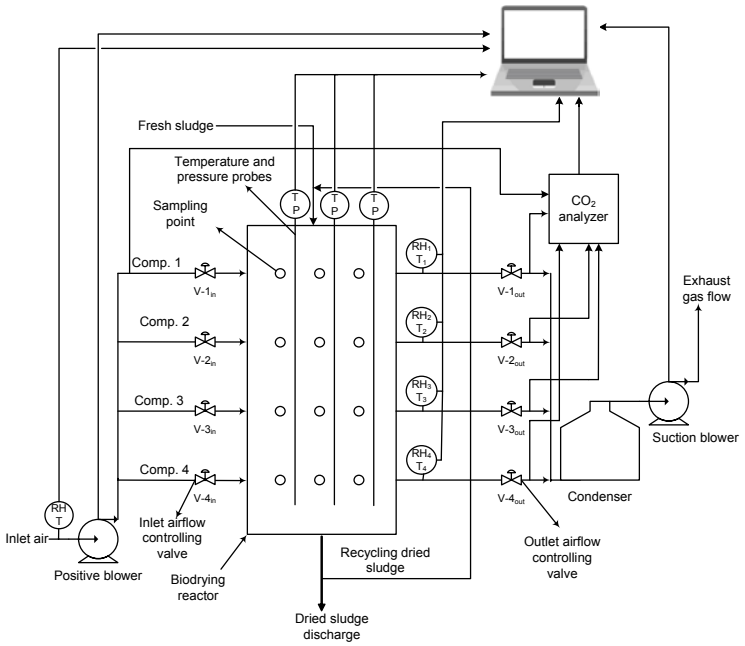

FIG. 2 Schematic of pilot-scale set-up

Mixed Sludge Analyses

The mixed sludge was a mixture of primary sludge (45% dry mass basis) and secondary sludge (55% dry mass basis) collected from an activated sludge wastewater treatment plant at an Eastern Canadian TMP pulp and paper mill, and shipped in 25 gallon barrels to our lab. After arrival at the laboratory, material characterization was conducted daily. Characterization included measurements of the dry solids content, higher heating value, as well as the density and porosity of the mixed sludge. Elemental analyses were also made to measure the quantity of carbon, hydrogen, nitrogen, oxygen and sulphur present in the sludge. To measure the dry solids content, 16 samples of mixed sludge were taken from different sampling points and oven dried at 105^{o}C for 24 h. Elemental analyses were

made to determine the C/N ratio and constant coefficients of Eq. (2). The higher heating values (HHV) were measured using an Oxygen Bomb Calorimeter (Parr Instrument Company, Illinois, USA). The porosity of the mixed sludge in each compartment was measured using an approach adapted from Richard et al. [33] and Ahn et al. [34]. The particle size distribution was obtained for each compartment using a 5-stage sieve.

Biodrying Reactor Performance Demonstration: Overall Water Balance

Water balances are important to track the main components of the biodrying process as well as for scale-up purposes. Saucedo-Castaneda et al. [35] showed that water balance is critical in large-scale solid-state fermentation bioreactors. The overall water balance for the biodrying reactor was completed for both gas and solid phases. Fresh, recycled and discharge sludge as well as inlet and outlet gases were considered for the water mass balance.

$$Water\ in - Water\ out + Water\ generation = Water\ Accumulation \quad (1)$$

The accumulation term in the right-hand side of Eq. (1) vanishes due to steady-state conditions. This approach is similar to the approach used by Ledakowicz et al. [36].

The water generation term is the result of the following exothermic microbial reaction:

$$Substrate + aO_2 \rightarrow bCO_2 + cH_2O + New\ cell,\ \Delta H_r < 0 \quad (2)$$

The values of *a*, *b*, and *c* are obtained using the results of elemental analyses. Table 2 summarizes the results of the elemental analysis for a typical experiment, the operating conditions of which are summarized in Table 3. The results of these elemental analyses are similar to values found in the literature.[37] The C/N values are between 15 and 30, which indicates the potential for active microbial growth.[38]

Table 2. Elemental analysis of the sludge in each compartment of the biodrying reactor

Compartment	% Nitrogen	% Carbon	% Hydrogen	% Oxygen	C/N
Feed Sludge	1.77	51.44	5.34	41.44	29.0
Compartment 1	1.80	51.23	5.79	41.17	28.4
Compartment 2	1.87	51.20	5.80	41.15	27.4
Compartment 3	2.08	51.00	5.86	41.10	24.5
Compartment 4	2.23	50.73	5.95	41.09	22.8

Table 3. Experimental conditions

	Q_g (m^3/h)	RH_{in} (%)	T_{in} (°C)	RH_{out} (%)	T_{out} (°C)
Compartment 1	18.2	14	24	94	18
Compartment 2	8.5	14	24	78	23.6
Compartment 3	16.2	14	24	100	25
Compartment 4	9.2	14	24	80	27.2

Cellular water produced by the microbial aerobic oxidation of the substrate was calculated based on elemental analysis results (Table 2) and Eq. 2. Experimental data in Table 2 were converted to molar basis and the values of *a, b,* and *c* were obtained from molar elementary balances. As can be seen in Table 4, cellular water (called "water generation") is very small compared to the other components of the water mass balance.

The water content in the gas phase was calculated from the relative humidity, temperature and air flowrate according to Eq. (5). The relative humidity and the temperature of the inlet gas were the same for all compartments. The water content was calculated from the total mass flowrate of sludge and its dry solids content. Fresh, feed and discharge sludge dry solids contents were 37, 40, and 51%, respectively. The recycle ratio was 30%.

Table 4 shows the results for the corresponding water balance. A closed water balance is obtained, which confirms the reliability of the experimental data and the techniques applied for the parameter measurements. This procedure was followed for all four cases and acceptable water balance was achieved for all of them (error <2%).

Table 4. Summary of water mass balance

Mass balance components	kg/day
water In by airflow	4

water In by feed	47.4
water generation	0.5
water Out by airflow	24.85
water Out by discharge	28
Total water In	51.8
Total water Out	52.8

Modeling Procedure

A 1-D distributed model of global heat transfer is presented based on the principles of chemical and biochemical reaction engineering in porous media. The model includes biological heat production, an evaporative sink term, and convective and conductive heat transfer. Two types of convective heat transfer are represented: convection due to the solid phase, which brings into play the sensible heat, and convection due to the gas phase. The model elaborates these heat transfer terms in a single equation solved for each compartment separately using the boundary conditions as a link between any two adjacent compartments. The model assumes lumped parameters in the gas flow direction and distributed parameters in the solids flow direction, as shown in Figure 3a.

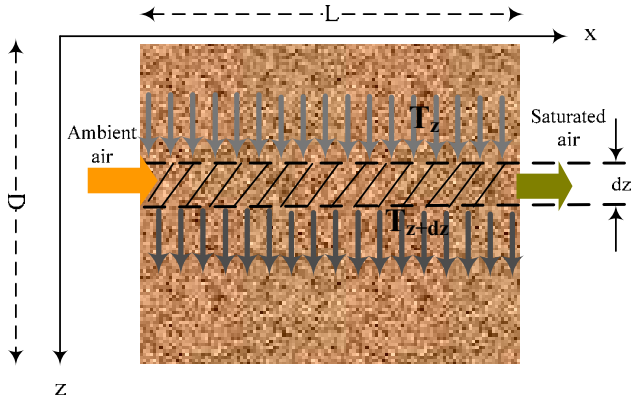

(a)

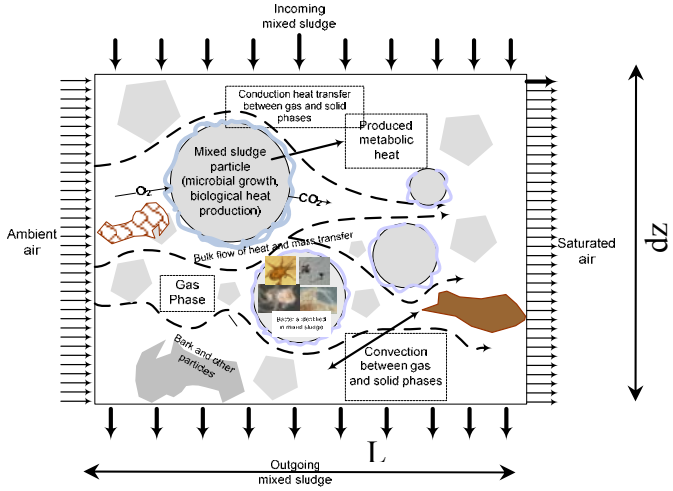

(b)

FIG. 3 Schematic of control volume in each compartment of the biodrying reactor in (a) macroscopic and (b) microscopic scales

For this 1-D model, the following simplifications and/or assumptions have been made:

- Gas phase mass conservation is assumed;
- The solids and gas phases in the matrix are at the same temperature (thermal equilibrium between phases). Du and Wang [39] found that for porous media with forced convection, local thermal equilibrium is a reasonable assumption if Re>10. In this study, as shown in Table 6, Reynolds numbers are much higher than

10. Note that the difference in water concentration between the solids and the gas phases provides an important driving force for the mass transfer of water;

- The process is at steady-state. This assumption is justified by the fact that reasonably stable matrix temperatures and drying rates have been observed experimentally;
- The heat loss through the walls of the reactor is assumed to be negligible. The reactor is insulated with UHMW (ultra high molecular weight) polyurethane on the inside and other insulation materials on the outer surface. This assumption has been shown to be valid for similar systems that have a small surface/volume ratio; [18]
- There is enough oxygen in the porous matrix for microbial biodegradation. This assumption is valid for processes under forced aeration such as solid-state fermentation;[40]
- The specific thermal heat capacity of the solid phase is constant for each compartment;
- For aerobic processes such as biodrying, it is essential to have adequate pneumatic conditions in the reactor to ensure that oxygen in the air reaches the microorganisms and that anaerobic hot spots are minimized. A uniform gas flow distribution is assumed for each compartment, although this is an approximation;
- For aerobic processes, the CO_2 production rate is equal to the O_2 consumption rate.[38] Therefore, the biological heat rate can be directly determined from the CO_2 production rate, or equivalently from the O_2 consumption rate, as follows:

$$\dot{Q}_{bio} = Q_{bio-standard}\ \rho_{O_2}\left(\left(\frac{V_{O_2}}{V_{Air}}\right)_{in} - \left(\frac{V_{O_2}}{V_{Air}}\right)_{out}\right)\frac{Q_g}{WLD} \tag{3}$$

where $Q_{bio\text{-}standard}$, the amount of biological heat generated per gram of oxygen consumed, is equal to 16 kJ/g-O_2 for different microbial species, following Bailey and Ollis [41]. This is close to the rule of thumb value used for aerobic composting designs, namely 14 kJ/g-O_2.[38] It is assumed that the generated biological heat is uniformly released and distributed in each compartment.

Based on these assumptions, and the control volume and the heat transfer mechanisms illustrated in Figure 3, the following heat transfer balance is obtained for each compartment:

$$\begin{aligned}
&-\dot{m}_{total,i}\left(w_{ms,i}Cp_{ms,i} + (1-w_{ms,i})Cp_{H_2O}\right)(T_i - T_r)\Big|_z^{z+dz} \quad \text{Sensible heat transfer due to solid phase}\\
&+k_s(1-\varepsilon_i)LW\frac{dT_i}{dz}\Big|_z^{z+dz} \quad \text{Conductive heat transfer due to solid phase}\\
&+(d\dot{m}_{g,i})Cp_{g,i}(T_{in} - T_r) - (d\dot{m}_{g,i})Cp_{g,i}(T_i - T_r) \quad \text{Convective heat transfer due to gas phase}\\
&+\dot{Q}_{bio,i}(1-\varepsilon_i)LWdz - \Delta H_{eva}a_{w,i}(X_{out,i} - X_{in})d\dot{m}_{g,i} = 0
\end{aligned} \tag{4}$$

Biological heat source term

Evaporative heat sink term

for i=1,2,3,4

The first term represents the sensible heat change due to the solids flow in the reactor. The second and third terms represent the conductive heat transfer due to the solid phase and the convective heat transfer due to the gas phase, respectively. The fourth term represents the bioheat generated through the exothermic metabolic activity of aerobic microorganisms, and the last term is a sink term representing the quantity of energy removed from the matrix through water evaporation.

The values of the physical parameters in Eq. (4) are given in Tables 5 and 6. The following comments apply:

- The uniform gas flow distribution assumption, as discussed earlier, leads to $d\dot{m}_{g,i} = \frac{\dot{m}_{g,i}}{D} dz$;
- $X_{out,i}$–X_{in} represents the net amount of water transferred to the gas phase, that is the difference of absolute humidity between outlet and inlet (kg H_2O/kg air). It is evaluated using the relative humidity and temperature of the inlet and outlet airstreams, and the following equation from Geankoplis [42]:

$$X_i = 0.622 \times \left(\frac{\frac{RH_i}{100} \times 10^{(8.896 - \frac{2233}{T_i + 273})}}{760 - \frac{RH_i}{100} \times 10^{(8.896 - \frac{2233}{T_i + 273})}} \right) \tag{5}$$

- The latent heat of water evaporation, ΔH_{eva}, has a negative correlation with temperature. In order to incorporate this in Eq. (4), a constant value of ΔH_{eva}=2270 kJ/kg H_2O [43] was used along with a correction factor, $a_{w,i}$, so that the last term in Eq. (4) remains constant for each compartment but varies from one compartment to another as the dry solids content varies;
- The correction factor, $a_{w,i}$, used in the last term of Eq. (4), was fit using data obtained from isotherm experiments on mixed sludge with saturated salt solutions, by means of a procedure adapted from Rowley and Mackin [44] and Labuza [45]:

$$a_{w,i} = 4.286 w_{ms,i}^2 - 4.74 w_{ms,i} + 2.009 \tag{6}$$

  A similar model was also reported for solid-state fermentation by Von Meien and Mitchell [27];
- The heat capacity of the gas phase, $Cp_{g,i}$, is determined from the following correlation:[42]
  $Cp_{g,i} = 1005 + 1880 X_{out,i}$
- The reference temperature, T_r, is assumed to be equal to T_{in}, the inlet gas temperature.

Based on these comments, Eq. (4) leads to the following differential equation:

$$k_s(1-\varepsilon_i)LW \frac{d^2T_i}{dz^2} - \alpha_i \frac{dT_i}{dz} - \frac{\dot{m}_{g,i}}{D} Cp_{g,i}(T_i - T_{in}) + \dot{Q}_{bio,i}(1-\varepsilon_i)LW - \Delta H_{eva} a_{w,i}(X_{out,i} - X_{in}) \frac{\dot{m}_{g,i}}{D} = 0 \tag{7}$$

or

$$\frac{d^2T_i}{dz^2} - \frac{\alpha_i}{k_s(1-\varepsilon_i)LW} \frac{dT_i}{dz} - \frac{\dot{m}_{g,i} Cp_{g,i}}{k_s(1-\varepsilon_i)LWD} T_i = - \frac{\dot{m}_{g,i} Cp_{g,i} T_{in} + \dot{Q}_{bio,i}(1-\varepsilon_i)LWD - \Delta H_{eva} a_{w,i}(X_{out,i} - X_{in})\dot{m}_{g,i}}{k_s(1-\varepsilon_i)LWD} \tag{8}$$

where $\alpha_i = \dot{m}_{total}(w_{ms,i} Cp_{ms,i} + (1 - w_{ms,i}) Cp_{H_2O})$

Note that Eq. (8) is a convection-diffusion ordinary differential equation for each compartment (i=1,2,3,4) that, along with boundary conditions, can be solved analytically.

For the boundary conditions, the inlet temperature in compartment 1 is equal to T_{in}, and the inlet temperature in the other compartments is equal to the temperature at the outlet of the previous compartment. Note that one of the exponential terms in the analytical solution vanishes due mainly to highly convective phenomena so that only an upstream boundary condition in each compartment was needed to derive it. This analytical solution is given in Appendix A.

Dimensionless Analysis

Dimensionless analysis can provide insights into the basic mechanisms that govern the transport phenomena taking place in the biodrying reactor. A dimensionless form of Eq. (8) was derived, which is expressed with dimensionless groups:

$$\frac{d^2T_i^*}{dz^{*2}} - A_i\frac{dT_i^*}{dz^*} - Pe_iT_i^* + B_i = 0 \text{ , for } i\text{=1, 2, 3, 4} \tag{9}$$

where $T_i^* = \frac{T_i - T_{in}}{T_{bot} - T_{in}}$ is the dimensionless temperature, T_{bot} is the matrix temperature at the bottom of the biodrying reactor, $z^* = \frac{z}{D}$ is the dimensionless height, and A_i, B_i and Pe_i are given by:

$$A_i = \frac{D\alpha_i}{k_s(1-\varepsilon_i)LW} \tag{10}$$

$$B_i = \frac{\dot{Q}_{bio,i}(1-\varepsilon_i)LWD^2 - \Delta H_{eva}a_{w,i}(X_{out,i} - X_{in})\dot{m}_{g,i}D}{k_s(1-\varepsilon_i)(T_{bot} - T_{in})LW} = E_{1,i}(E_{2,i} - 1) \tag{11}$$

$$E_{1,i} = \frac{\Delta H_{eva}a_{w,i}(X_{out,i} - X_{in})\dot{m}_{g,i}D}{k_s(1-\varepsilon_i)(T_{bot} - T_{in})LW} \tag{12}$$

$$E_{2,i} = \frac{\dot{Q}_{bio,i}(1-\varepsilon_i)LWD^2}{\Delta H_{eva}a_{w,i}(X_{out,i} - X_{in})\dot{m}_{g,i}D} \tag{13}$$

$$Pe_i = \frac{\dot{m}_{g,i}Cp_{g,i}D}{k_s(1-\varepsilon_i)LW} \tag{14}$$

The A_i represents the ratio of the mixed sludge sensible heat to the conductive heat, and Pe_i, the Peclet number, the ratio of the convective heat to the conductive heat. B_i, which brings into play two dimensionless numbers, $E_{1,i}$ and $E_{2,i}$, the ratio of the net heat generated to conductive heat. The net heat generated is the amount of the biological heat minus the heat lost through evaporation. $E_{1,i}$ is the ratio of the evaporative heat to the conductive heat, and $E_{2,i}$ is the ratio of the bioheat to the evaporative heat. $E_{2,i}$ is similar to the Damkohler number (*Da*), the ratio of the metabolic reaction rate to the convective rate. *Da* is used frequently in aerobic composting processes to control the biodegradation rate.[46] All three of these terms (A_i, Pe_i and B_i) are important and their relative values may vary in the 4 compartments of the biodrying reactor. The interpretation of these dimensionless parameters will be discussed in the next section.

RESULTS

This section presents experimental results, and the characteristic curves from four experimental cases, which were described earlier in section Experimental Set-up. The goal is to investigate different scenarios for the biodrying process and identify 1-D model flexibility and limitations using four experimental cases. These four cases where chosen because they represent diverse experimental conditions that were examined in the overall experimental program in Table 1. Cases 1 and 2 are at 6-day residence time, 30% recycle ratio, and under controlled outlet relative humidity profile, whereas cases 3 and 4 are at the total aeration rate 28 m^3/h, 15% recycle ratio, and 4- and 8-day residence times, respectively. The 1-D model is tested against the experimental data, and the results obtained are analyzed and interpreted using the dimensionless numbers reported in Table 6.

Experimental Data

The four cases that were examined for the 1-D model assessment, involve two types of physical parameters, some with fixed values (Table 5), and some having values that vary from one experiment to another (Table 6).

Table 5. Fixed values used for the 1-D model

	Comp. 1	Comp. 2	Comp. 3	Comp. 4	Reference
Cp_{H_2O} (J/(kg ^oC))	4200	4200	4200	4200	Bird et al. [47]
$Cp_{ms,i}$ (J/(kg ^oC))	2360	2000	1800	1700	Perry and Green [43]
D(m)	0.4	0.4	0.4	0.4	Reactor geometry
d_p(mm)	1.5	1.3	1	0.8	Biodrying experiments
k_s (W/(m ^oC))	0.15	0.15	0.15	0.15	Geankoplis [42]
L(m)	0.4	0.4	0.4	0.4	Reactor geometry
W (m)	1	1	1	1	Reactor geometry
ΔH_{eva} (kJ/kg H_2O)	2270	2270	2270	2270	Geankoplis [42]
ρ_g (kg/m^3)	1.16	1.16	1.16	1.16	Geankoplis [42]
ε_i	0.4±0.012	0.45±0.013	0.5±0.015	0.55±0.016	Biodrying experiments
μ(Pa.s)	1.5×10^{-5}	1.5×10^{-5}	1.5×10^{-5}	1.5×10^{-5}	Bird et al. [47]

$Cp_{mix,i}$ and ε_i vary as function of sludge dry solids content.

Table 6. Experimental parameter values used for the 1-D model

	Case 1				Case 2				Case 3				Case 4			
	Comp. 1	Comp. 2	Comp. 3	Comp. 4	Comp. 1	Comp. 2	Comp. 3	Comp. 4	Comp. 1	Comp. 2	Comp. 3	Comp. 4	Comp. 1	Comp. 2	Comp. 3	Comp. 4
$Q_{g,i}$ (m^3/h)	26.40	5.0	26.0	18.0	16.5	8.0	14.0	7.7	7.91	7.41	7.31	7.38	7.04	7.11	7.63	7.65
$\dot{Q}_{bio,i}$ (W/m^3)	0	0	1000	2500	200	400	2200	2400	511	550	1200	2800	0	50	2000	3500
$w_{ms,i}$	0.42	0.43	0.45	0.47	0.42	0.44	0.46	0.50	0.37	0.41	0.42	0.45	0.42	0.44	0.5	0.54
$a_{w,i}$	0.78	0.76	0.75	0.73	0.78	0.75	0.74	0.71	0.84	0.79	0.77	0.76	0.78	0.75	0.71	0.7
$RH_{out,i}$(%)	73	66	88	89	68	72	92	55	80	97	75	80	41	83	92	100
$T_{out,i}$(°C)	18	20	25.6	27.3	23.5	25	28	42.8	29	30	31	33.8	23	24.3	36	40
Pe_i	101	20	117	90	63	33	63	39	30	30	33	37	27	29	34	38
$Re_i = \frac{u_{g,i}\rho_g d_p}{\varepsilon_i \mu}$	468	68	246	124	291	109	133	53	140	101	69	51	125	97	72	53
$E_{2,i}$	0	0	0.54	1	0.2	0.65	1.13	1.5	0.53	0.45	1.17	1.96	0	0.07	1.15	1.32
RT (days)	6				6				4				8			
RR(%)	30				30				15				15			
RH_{in}(%)	13				14				12				10			
T_{in}(°C)	24				25				27				26			
$\dot{m}_{total}$ (kg/s)	0.001128				0.001128				0.001692				0.000846			

Biomass Characteristic Curves: Dry Solids Content, and HHV

Dry solids content (w_{ms}) is important because it is the objective of the innovative biodrying process. It also appears in the sensible heat term of the solid phase as well as in the correction factor (a_w) of the evaporation term (Eqs. 4 and 6). The higher heating value (HHV), or the sludge calorific value, is a critical factor for the economic feasibility of the combustion as it represents the quantity of energy that can be recovered in the boiler. The change in dry solids content is shown for four cases in Figure 4. HHV is available only for case 4 (Figure 5).

Dry Solids Content

Figure 4 shows that the mixed sludge dry solids content increases as the sludge moves downward in the biodrying reactor. The standard error of the mean was estimated to be ±2% using 5 measurements on a typical sludge sample obtained in biodrying reactor. The dry solids content is nearly flat in the 1st and 2nd compartments in all cases, and increases significantly in the 3rd and 4th compartments. This is due mainly to the impact of higher bioheat and higher temperatures in the bottom compartments (Tables 6 and 7), which increase the water holding capacity of the gas phase and the water transfer from the solid phase to this gas phase.

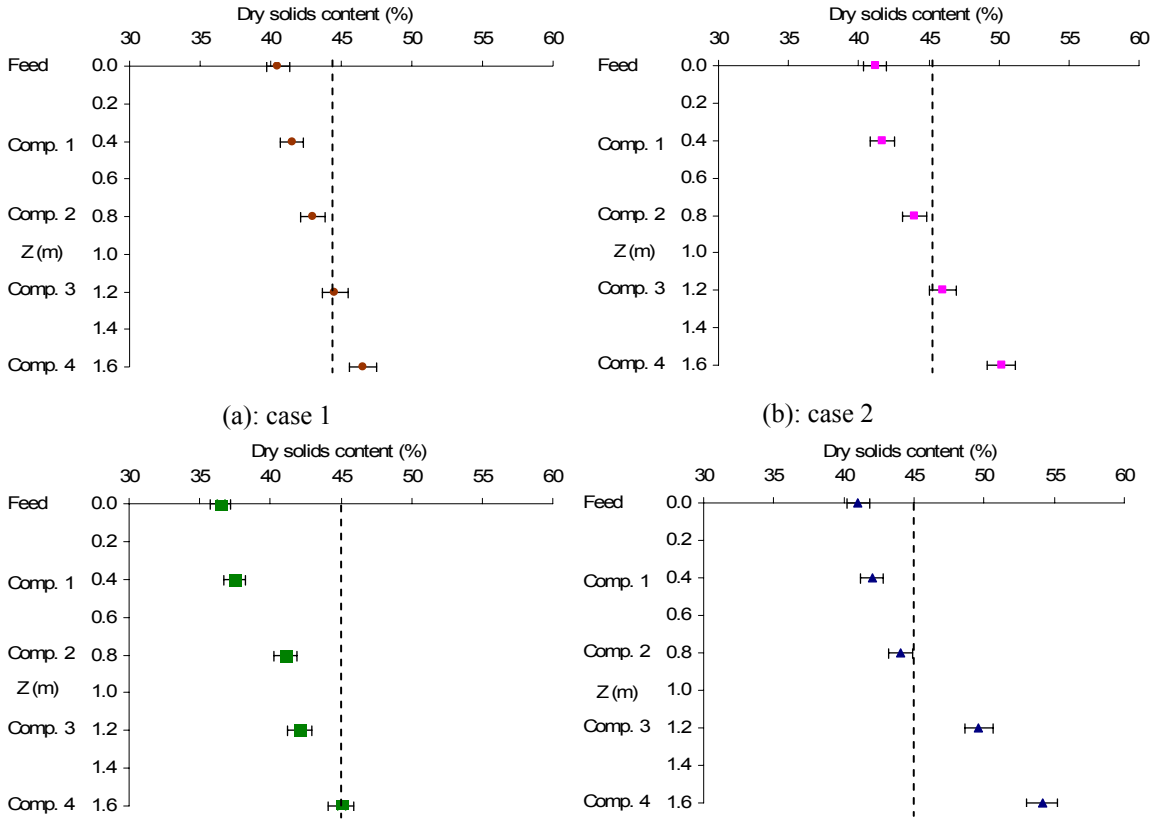

(a): case 1 (b): case 2

(c): case 3 (d): case 4

FIG. 4 Dry solids content change in the continuous biodrying reactor
The error bars represent one standard deviation above and below the mean

Higher Heating Value (HHV)

Figure 5 illustrates the change in HHV in the biodrying reactor for case 4. The standard error of the mean was estimated to be ±1.5% using 5 measurements on a typical sample obtained in the biodrying reactor.

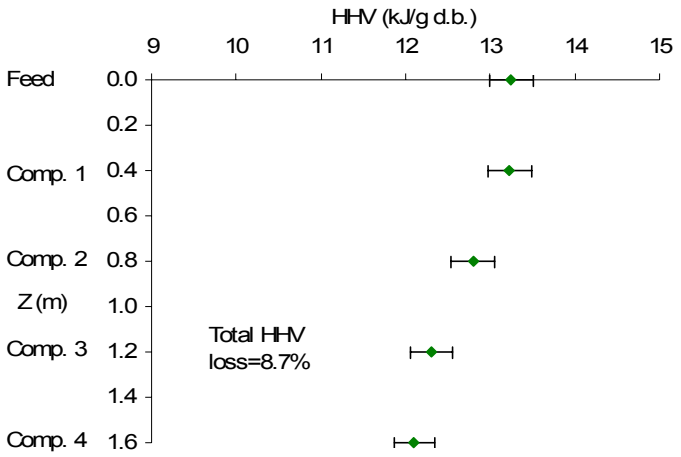

FIG. 5 Sludge higher heating values along the reactor length (Case 4)
The error bars represent one standard deviation above and below the mean

In this work, the highest dry solids content was achieved for an 8-day residence time (case 4), but the total calorific value loss in this case was the greatest. Therefore, a compromise between the extent of the biodegradation (calorific value loss) and the final dry solids level is always required to maximize the energy recovery in the subsequent combustion process.

Assessment of the 1-D Model Accuracy

In this section, the accuracy of the 1-D model is assessed against the experimental temperature data of Table 7. For each compartment, the experimental temperature values in the gas flow direction are averaged and the averaged values (last column in Table 7) are used for the 1-D model accuracy assessment.

Table 7. Experimental temperatures in the continuous biodrying reactor

		T_{in} (°C)	x=7.5 cm	x=17.5 cm	x=27.5 cm	T_{out} (°C)	Averaged Temperature
Case 1	Comp. 1	24	13	13	14	18	13
	Comp. 2	24	13	15	16	20	15
	Comp. 3	24	15	15	20	26	17
	Comp. 4	24	19	20	27	27	22
Case 2	Comp. 1	25	15	16	17	24	16
	Comp. 2	25	17	18	23	25	19
	Comp. 3	25	19	28	38	28	28
	Comp. 4	25	30	38	47	43	38
Case 3	Comp. 1	27	12	20	30	29	21
	Comp. 2	27	14	16	23	30	18
	Comp. 3	27	18	26	30	31	25
	Comp. 4	27	29	44	54	34	42
Case 4	Comp. 1	26	18	20	23	23	20
	Comp. 2	26	13	14	20	24	16
	Comp. 3	26	22	30	42	36	31
	Comp. 4	26	43	50	56	40	49

Eq. (8) was solved analytically (see Appendix A) for temperature in each of the four compartments of the reactor. The temperature results calculated by the 1-D model are compared to experimental data in Figure 6. Although specific operating conditions result in specific temperature profiles across the four compartments, the overall trend is similar for all cases. Overall, the predicted temperatures are in good agreement with the averaged experimental data. One may argue that this is not surprising because the values of some of the data used in the 1-D model were back-calculated from the experimental data. One must however keep in mind that the system is governed by transport phenomena occurring in both the sludge and gas flow directions, and that lumped parameters

were considered in the latter. We believe that one of the reasons for the good agreement down the reactor with this simplified 1-D model is the offset between the exothermic biological heat and the latent heat of water evaporation.

However, larger differences can be noticed in the 4th compartment for cases 3 and 4. These discrepancies are most likely due to the growth behavior of the mesophilic and thermophilic microorganisms, which strongly depends on temperature (see INTRODUCTION for the effect of temperature on microbial activity). In both cases 3 and 4, the higher temperature in the 4th compartment favors the growth rate of thermophilic bacteria, which results in higher bioheat release into the matrix of mixed sludge. This contradicts the assumption of a uniform bioheat release and distribution, which was made for the development of the 1-D model (section Modeling Procedure). Note however that such an assumption was made to simplify the 1-D model and obtain an analytical solution.

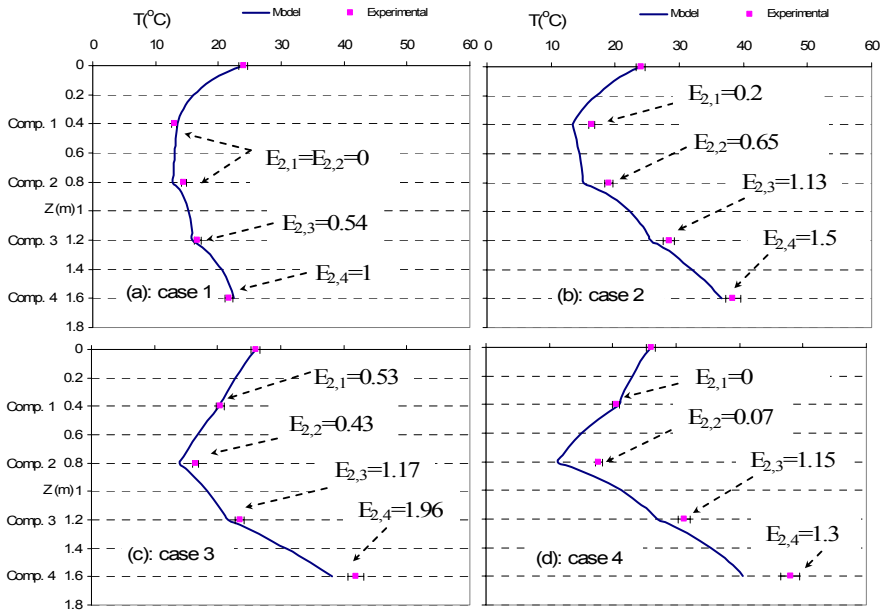

FIG. 6 Comparison of the predicted temperatures to the experimental data
The error bars represent one standard deviation above and below the mean

Analysis of the Temperature Profiles and General Discussion

Figure 7 displays the temperature profiles for all four cases. There are two zones along the reactor height: a convection-dominated zone in the 1st and 2nd compartments and a diffusion-dominated zone in the 3rd and 4th compartments. In the first zone, a drop in the matrix temperature can be observed in all cases. In this zone, as shown in Figure 4, the dry solids content does not significantly increase in the 1st and 2nd compartments. The evaporation of unbound water substantially cools the porous matrix of mixed sludge.

It also follows from the values of the ratio of bioheat to evaporative heat ($E_{2,i}$) in Table 6 that, in the first zone, the biological heat is not large enough to raise the temperature of the matrix. The decline of the matrix temperature is sharper in cases 1 and 2, which can also be inferred from the *Re* and *Pe* values in Table 6. The higher air flowrates, and hence the higher *Re* and *Pe* values, cause convection to dominate over diffusion and, since the evaporation of unbound water takes place at wet-bulb temperature, the matrix temperature declines. Two phenomena occur simultaneously here. One is the low bioheat generation in the 1st and 2nd compartments due mainly to the delay in the microbial start-up caused by the microbial lag phase. The other one is the cooling effect of the evaporation of the unbound water, which occurs at wet-bulb temperature.

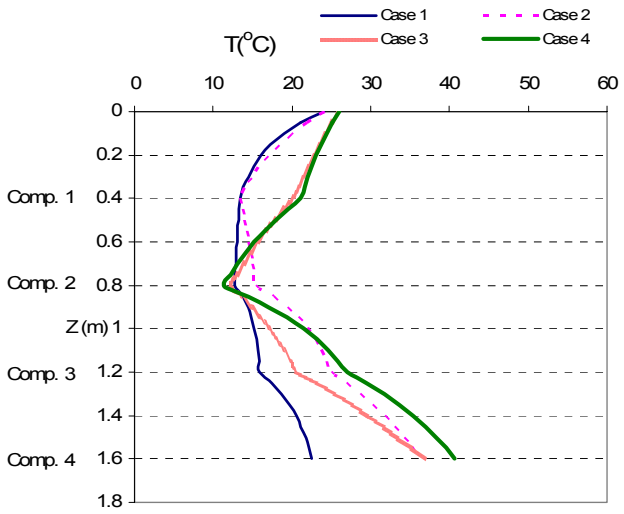

FIG. 7 Predicted temperature profiles for all four experimental cases

Upon feeding the wet sludge into the biodrying reactor, some areas of the particle surface, and thus some portion of unbound water, are exposed to the air stream. Due to convective mass transfer, those areas become dry whereas the rest of the particle, not exposed to the airflow stream retains some quantity of unbound water. The convective evaporation, the amount of which is correlated to the air flowrate, therefore cools down the matrix. The lower matrix temperature is more noticeable in cases 1 and 2 than in cases 3 and 4, which can be attributed to the higher 1st compartment air flowrates (Table 6).

The particle sizes measured in the reactor decreased down its length. This is likely due to drag force and inter-particle friction, coupled with the load pressure due to the sludge weight in the upper compartments. These phenomena break up particle agglomerates, thereby enabling fresh areas to be exposed having unbound water. This phenomenon results in further convective evaporation. Nevertheless, one may observe that, except in case 1 where high air flowrate prevails, the temperature starts increasing at the end of the 2nd compartment and reaches a value at the end of the 4th compartment (T_{bot}) that is higher than that at the entrance of the 1st compartment.

In the second zone, the 3rd and 4th compartments, the temperature gradient quickly becomes positive, which accelerates the evaporation of bound water, and results in an increase of dry solids content. This occurs because the bioheat released to the gas phase increases the gas phase moisture holding capacity (RH_{out} in Table 6), which then results in the transfer of more water to the gas phase (Figure 4). However, the higher bioheat released from aerobic activity in the 3rd and 4th compartments results in higher losses of HHV (Figure 5). As can be seen in Table 6, the ratio of bioheat to evaporative heat ($E_{2,i}$) significantly jumps in the 3rd and 4th compartments, resulting in a rise of the matrix temperature in Figure 6.

The diffusion and capillary forces create a water gradient between the interior and the exterior of the particles.[48] Although it is a diffusion-dominated mechanism in the 3rd and 4th compartments, the higher temperatures related to the bioheat release enhance the drying rates. Under these conditions, the biological heat generated surpasses the cooling effect of water evaporation ($E_{2,i}$ values >1 in Figure 6 and Table 6) .

The *Re* and *Pe* numbers in the 3rd and 4th compartments for cases 3 and 4 are less than those for cases 1 and 2 (Figure 7).

Finally, the highest temperature is found at the end of the 4th compartment for case 4. This is attributed to a higher level of biodegradation ($Q_{bio,4}$=3500W/m^3, Table 6). Due to the low air flowrate in this case, the rate of bioheat released in the matrix of mixed sludge is higher than the rate of heat removed by the air flow. As a result, the accumulated heat leads to higher microbial activity, which further increases the temperature of the matrix.

Table 8 summarizes the characteristics of the transport phenomena prevailing in each compartment.

Table 8. Qualitative description of different cases

	Experimental conditions	Dominating transport phenomena
Case 1	This experiment was controlled by outlet relative humidity for all compartments at lower limit (85%), a 6-day residence time, and 30 % recycle	In this case it is highly a convection dominated mechanism in all compartments of the biodrying reactor ($E_{2,i}\leq1$), and biological

	ratio.	activity does not significantly develop due to very high air flowrate and cold porous media. The 1-D model works well for this case both for matrix temperature (Figure 6) and drying rate (Figure 8). This is because of the small variation of temperature in gas flow direction for this case.
Case 2	This experiment was controlled by outlet relative humidity for all compartments at higher limit (96%), a 6-day residence time, and 30 % recycle ratio.	In this case it is highly a convection dominated ($E_{2,i} \leq 1$) at the top and an exothermic aerobic bioenergy dominated ($E_{2,i} > 1$) at the bottom of the biodrying reactor.
Case 3	This experiment was controlled by air flowrate in all compartments at lower limit ($7m^3/h$), a 4-day residence time, and 15% recycle ratio.	In this case it is a convection dominated ($E_{2,i} \leq 1$) at the top and a highly exothermic aerobic bioenergy dominated ($E_{2,i} > 1$) at the bottom of the biodrying reactor.
Case 4	This experiment was controlled by air flowrate in all compartments at lower limit ($7m^3/h$), an 8-day residence time, and 15% recycle ratio.	In this case it is a convection dominated ($E_{2,i} \leq 1$) at the top and an exothermic aerobic bioenergy dominated ($E_{2,i} > 1$) at the bottom of the biodrying reactor.

Sensitivity Analysis

Sensitivity analyses were performed on the temperature of porous matrix (results not shown due to lengthy mathematical formulations) with respect to the matrix porosity (ε), oxygen consumption ($\Delta O_2\%$), air flowrate (Q_g), mixed sludge dry solids content (w_{ms}), and water removal rate including the combined effect of inlet and outlet air temperatures and relative humidity (X_{out}-X_{in}). It was found that the most influential parameters are the oxygen consumption rate (which is related to the bioheat), and the air flowrate (which is related to the water removal rate) and controlling transport phenomena in the reactor. The bioheat terms is essential for the diffusion of bound water from the sludge particle interior to its surface, whereas the air flowrate is manipulated to obtain a desired outlet relative humidity profile along the reactor height.

Usefulness and Shortcomings of the 1-D Model

Sludge drying rate in the continuous biodrying reactor can be used to estimate the final dry solids level. The dry solids level is critical for an economically feasible combustion operation of a combustion boiler.

The model-predicted temperatures were used to calculate the water removal rate (drying rate) for different cases. These results were compared to experimental data. As shown in Figure 8, the 1-D model is good only if the temperature variation in a given compartment does not vary significantly from the gas inlet to the gas outlet (see Table 7). For instance, the temperature variation in each compartment for case 1, and the 1st and 2nd compartments of all other cases is very small, and hence a good agreement can be observed between the model predicted drying rate and the experimental values. However, the agreement is not as good for the 3rd and 4th compartments in cases 2, 3, and 4, in which the exothermic aerobic bioenergy is the dominating mechanism. The usefulness of the 1-D model is then limited in such cases, because it poorly predicts the 2-D transport phenomena governing the higher aerobic exothermicity in the reactor, a situation which is likely to arise in an industrial biodrying reactor.

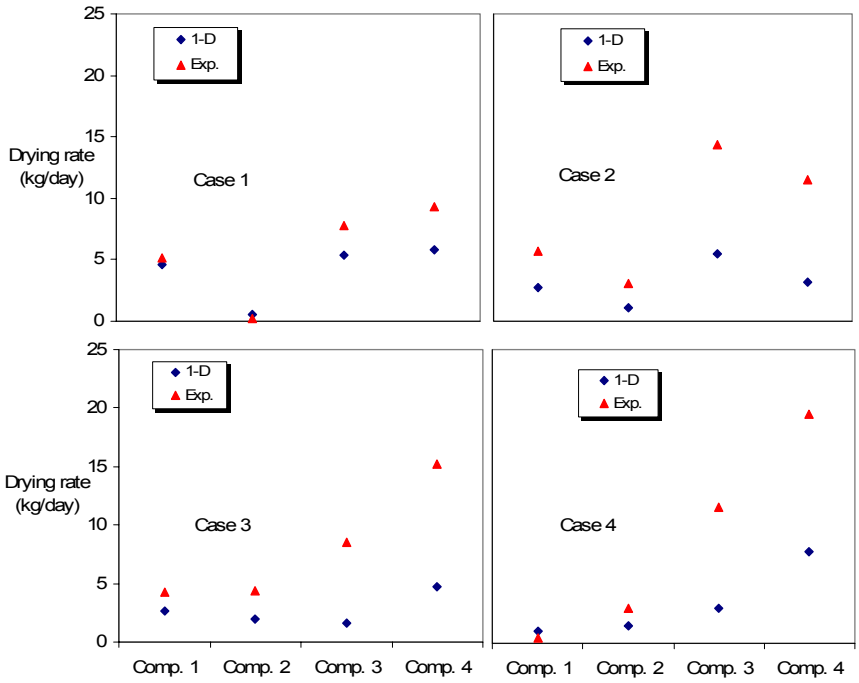

FIG. 8 Comparison of 1-D model versus experimental data for sludge drying rate

CONCLUSIONS

A simple 1-D model based on lumped parameters in the gas flow direction and distributed parameters in the solids flow direction was developed for a continuous biodrying reactor. The model was solved analytically, and tested against experimental data. The model predicts vertical temperature profiles in the porous matrix which are in good agreement with cross-section averaged experimental data, indicating that the heat and mass transfer mechanisms along with the boundary conditions were appropriately incorporated in the energy equation. The 1-D model is an easy tool for preliminary understanding of the transport phenomena prevailing in the biodrying reactor, and provides information for an early assessment of the biodrying reactor.

A dimensionless analysis revealed that in addition to *Re* and *Pe*, the ratio of the bioheat to the evaporative heat ($E_{2,i}$) plays a significant role in the variation of the matrix temperature and the transport phenomena. It was found that the temperature decreases when $E_{2,i}<1$ and increases when $E_{2,i}>1$.

The discrepancies between the predicted and experimental results are attributed to the following:

- The biological heat release was assumed to be uniform in a given compartment. In reality, it may vary due to the effect of temperature in the gas flow direction on microbial activity of mesophilic and thermophilic bacteria;
- The 1-D model assumes a uniform and flat air flow distribution in each compartment, which makes it impossible to take into account the effect of possible two-dimensional hot spots that are likely in full-scales in the matrix of mixed sludge. This may lead to unexpected results such as spontaneous firing or non-uniform final materials;
- Experimental results confirmed large disagreement between the predicted water removal rate and experimental data from the zone with higher aerobic exothermicity (the 3rd and 4th compartments). This is mainly related to the lack of 1-D model that cannot account for the temperature in the gas flow direction;

Therefore, despite the simplicity of the 1-D model, a 2-D distributed model is required to overcome the above-mentioned limitations and to improve the prediction capability of the model not only in the solids flow direction but also in the gas flow direction.

ACKNOWLEDGMENTS

This work was carried out with the financial support of FQRNT and NSERC for the research, and CFI for the cost of reactor. The dedicated assistance of Carl Tchoryk, Kheng Huynh, Omar Ben Ndiaye and Antonin Paquet

for the experimental part are gratefully acknowledged. Fruitful discussions concerning the project were held with Professors Jamal Chaouki and Mario Jolicoeur from the Department of Chemical Engineering at Ecole Polytechnique of Montreal, Professor Tom Richard from the Department of Agricultural and Biological Engineering at Pennsylvania State University, and Professor Stephen Whitaker from the Chemical Engineering Department at California State University.

NOMENCLATURE

a	Constant coefficient of the microbial growth reaction
A_i	Dimensionless number for compartment i
$a_{w,i}$	Correction factor for compartment i
B_i	Dimensionless number for compartment i
b	Constant coefficient of the microbial growth reaction
c	Constant coefficient of the microbial growth reaction
$Comp.\ i$	Compartment i, i=1,2,3,4
$Cp_{g,i}$	Specific thermal heat capacity of the gas phase in compartment i (J/(kg ^oC))
Cp_{H_2O}	Specific thermal heat capacity of water (J/(kg ^oC))
$Cp_{ms,i}$	Specific thermal heat capacity of dried solids in compartment i (J/(kg ^oC))
$d.b.$	Dry basis
d_p	Average particle size (mm)
D	Height of each compartment (0.4 m)
$d\dot{m}_{g,i}$	Mass flowrate of inlet air through control volume in compartment i (kg/s)
$dV = LWdz$	Control volume (m^3)
dz	The height of the element concerned (m)
$E_{1,i}$	Ratio of evaporative heat to conductive heat
$E_{2,i}$	Ratio of bioheat to evaporative heat
k_s	Thermal conductivity of the solid phase (W/(m ^oC))
L	Width of the biodrying reactor (0.4 m)
$\dot{m}_{total}$	Total mass flowrate of the solid phase (kg/s)
$\dot{m}_{g,i} = Q_{g,i}\rho_g$	Mass flowrate of gas phase in compartment i (kg/s)
Pe_i	Peclet number in compartment i
$\dot{Q}_{bio,i}$	Bioheat produced in the matrix of compartment i through metabolic activities (W/m^3)
$Q_{bio\text{-}standard}$	Standard biological heat production in aerobic systems (J/ kg O_2)
$Q_{g,i}$	Gas flowrate in compartment i (m^3/s)
Re_i	Reynolds number in compartment i
$RH_{out,i}$	Relative humidity of the outlet gas in compartment i(%)
RH_{in}	Relative humidity of the inlet gas (%)
RR	Recycle ratio of discharge biodried sludge (%)
RT	Residence time (days)
T_{bot}	Temperature of matrix at the bottom of the biodrying reactor (z=1.6m) (^oC)
T_{in}	Inlet gas temperature or initial temperature of mixed sludge (^oC)
T_i	Temperature of the matrix at z in compartment i (^oC)
$T_i^* = \frac{T_i - T_{in}}{T_{bot} - T_{in}}$	Dimensionless temperature in compartment i
T_i^H	Analytical solution of Eq.(16) in compartment i
T_i^{NH}	Analytical solution of non-homogeneous part of Eq.(8) in compartment i
T_r	Reference temperature (=T_{in}) (^oC)
$T_{out,i}$	Temperature of the outlet gas in compartment i(^oC)
$(V_{O_2}/V_{Air})_{in}$	Volume percentage (absolute value) of oxygen at the inlet gas flow
$(V_{O_2}/V_{Air})_{out}$	Volume percentage (absolute value) of oxygen at the outlet gas flow
W	Depth of the biodrying reactor (1 m)

w.b.	Wet basis
$w_{ms,i}$	Mixed sludge dry solids content in compartment *i*
x	Distance of local experimental point from gas inlet port, cm
X_{in}	Absolute moisture content of inlet gas (kg H_2O/kg Air)
$X_{out,i}$	Absolute moisture content of outlet gas (kg H_2O/kg Air)
$z^* = \frac{z}{D}$	Dimensionless height

Greek letters

α_i	Thermal diffusivity of the solid phase in compartment *i* (J/(s.K))
β_i	Constant coefficient of the temperature equation
γ_i	Constant coefficient of the temperature equation
δ_i	Constant coefficient of the temperature equation
ϕ_i	Constant coefficient of the temperature equation
φ_i	Constant coefficient of the temperature equation
ΔH_r	Exothermic heat of biological reaction (J/kg-biomass)
ΔH_{eva}	Latent heat of water evaporation (kJ/kg-H_2O)
ε_i	Porosity of the matrix in compartment *i*(dimensionless)
μ	Viscosity of the gas phase (Pa.s)
ρ_g	Density of the gas phase (kg/m^3)
$\rho_{ms,i}$	Density of mixed sludge in compartment *i*(kg/m^3)
ρ_{O_2}	Density of oxygen (1.35 kg/m^3)[43]

REFERENCES

1. Hynninen, P.; Laine, P. *Environmental Control, Papermaking Science and Technology* (19). Helsinki, Finland, Fapet Oy, 1998.
2. Chen, G.; Yue, P.L.; Mujumdar, A.S. Sludge dewatering and drying. Drying Technology **2002**, 20(4-5), 883-916.
3. Hippinen, I.; Ahtila, P. Drying of activated sludge under partial vacuum conditions-An experimental study. Drying Technology **2004**, 22(9), 2119-2134.
4. Tsang, K.R.; Vesilind, P.A. Moisture distribution in sludges. Water Science and Technology **1990**, 22(12). 135-142.
5. Lee, D.J. Interpretation of bound water data measured via dilatometric technique. Water Research **1996**, 30(9), 2230-2232.
6. Vaxelaire, J.; Cezac, P. Moisture distribution in activated sludges: a review, Water Research **2004**, 38, 2215–2230.
7. Navaee-Ardeh, S.; Bertrand, F.; Stuart, P.R. Emerging biodrying technology for the drying of pulp and paper mixed sludges. Drying Technology **2006a**, 24(7), 863-878.
8. Kudra, T.; Gawrzynski, Z.; Glaser, R.; Stanislawski, J.; Poirier, M. Drying of pulp and paper sludge in a pulsed fluid bed dryer. Drying Technology **2002**, 20 (4-5), 917-933.
9. Kraft, D.L.; Orender, H.C. Considerations for using sludge as a fuel. Tappi J. **1993**, 76(3), 175-183.
10. CANMET Energy Technology Centre. *Pulp and Paper Sludge to Energy- Preliminary Assessment of Technologies*. ADI Ltd. Report, Canada, 2005.
11. Choi, H.L.; Richard T.L.; Ahn, H.K. Composting High Moisture Materials: Biodrying Poultry Manure in a Sequentially Fed Reactor. Compost Science and Utilization **2001**, 303-311.
12. Frei, K.M.; Cameron, D.; Stuart, P.R. Novel drying process using forced aeration through a porous biomass matrix. Drying Technology **2004**, 22(5), 1191-1215.
13. Frei, K.M.; Cameron, D.; Jasmin, S.; Stuart, P.R. Novel sludge drying process for cost-effective on-site sludge management. Pulp and Paper Canada **2006**, 107(4), 47-53.
14. Roy, G.; Jasmin, S.; Stuart, P.R. Technical modeling of a batch biodrying reactor for pulp and paper mill sludge. *17th CHISA International Congress of Chemical and Process Engineering*, 2006.

15. Mote, C.R.; Griffis, C.L. Heat production by composting organic matter. Agricultural Wastes **1982**, 4, 65-73.
16. Harper, E.; Miller, F.C.; Macauley, B.J. Physical management and interpretation of an environmentally controlled composting ecosystem. Australian Journal of Experimental Agriculture **1992**, 32(5), 657-667.
17. Madigan, M.T.; Martinko, J.M.; Parker, J. *Brock Biology of Microorganisms*. Prentice Hall, 6th edition, USA, 2006.
18. Mason, I.G.; Milke, M.W. Physical modeling of the composting environment: A review. Part 1: Reactor systems. Waste Management **2005a**, 25(5), 481-500.
19. Mason, I.G.; Milke, M.W. Physical modeling of the composting environment: A review. Part 2: Simulation performance. Waste Management **2005b**, 25(5), 501-509.
20. Mason, I.G. Mathematical modeling of the composting process: A review. Waste Management **2006**, 26(1), 3-21.
21. Bach, P.D.; Nakasaki, K.; Shoda, M.; Kubota, H. Thermal balance in composting operations. Journal of Fermentation Technology **1987**, 65(2), 199-209.
22. Koenig, A.; Tao, G. H. Accelerated forced aeration composting of solid waste. *In Proceedings of the Asia-Pacific Conference on Sustainable Energy and Environmental Technology*, 1996, 450-457.
23. Bari, Q.H.; Koenig, A.; Guihe, T. Kinetic analysis of forced aeration composting: I. Reaction rates and temperature. Waste Management & Research **2000**, 18(4), 303-312.
24. Robinzon, R.; Kimmel, E.; Avnimelech, Y. Energy and mass balances of windrow composting system. Transactions of ASAE **2000**, 43(5), 1253-1259.
25. Batista, J.G.F.; van Lier, J.J.C.; Gerrits, J.P.G.; Straatsma, G.; Griensven, L.J.L.D. Spreadsheet calculations of physical parameters of phase II composting in a tunnel. Mushroom Science **1995**, 14, 189-194.
26. Straatsma, G.,; Gerrits, J.P.G.; Thissen, J.T.N.M.; Amsing, J.G.M.; Loffen, H.; van Griensven, L.J.L.D. Adjustment of the composting process for mushroom cultivation based on initial substrate composition. Bioresource Technology **2000**, 72(1), 67-74.
27. Von Meien, O.F.; Mitchell, D.A. A two-phase model for water and heat transfer within an intermittently-mixed solid-state fermentation bioreactor with forced aeration. Biotechnology and Bioengineering **2002**, 79(4), 416-428.
28. Rajagopalan, S.; Modak, J.M. Heat and mass transfer simulating studies for solid-state fermentation processes. Chemical Engineering Science **1994a**, 49, 2187-2193.
29. Rajagopalan, S.; Modak, J.M. Modeling of heat and mass transfer for solid state fermentation process in tray bioreactor. Bioprocess Engineering **1994b**, 13, 161-169.
30. Prud'homme, M.; Jasmin, S. Inverse solution for a biochemical heat source in a porous medium in the presence of natural convection. Chemical Engineering Science **2006**, 61, 1667-1675.
31. Navaee-Ardeh, S.; Bertrand, F.; Stuart, P.R. Lumped modeling of a novel continuous biodrying reactor. *56th Canadian Chemical Engineering Conference*, Sherbrooke, Canada, 2006b.
32. Navaee-Ardeh, S.; Tchoryk, C.; Bertrand, F.; Stuart, P.R.; Tolnai, B. Novel continuous biodrying reactor: principles, screening experiments and results, *58th Canadian Chemical Engineering Conference*, Ottawa, Canada, 2008.
33. Richard, T.L.; Veeken, A.H.M.; de Wilde, V.; Hamelers, H.V.M. Air-filled porosity and permeability relationships during solid-state fermentation. Biotechnology Progress **2004**, 20(5), 1372-1381.
34. Ahn, H. K.; Richard, T. L.; Glanville, T. D. Laboratory determination of compost physical parameters for modeling of airflow characteristics. Waste Management **2008**, 28, 660-670.
35. Saucedo-Castaneda, G.; Lonsane, B.K.; Krishnaiah, M.M.; Navarro, J.M.; Roussos, S.; Raimbault, M. Maintenance of heat and water balances as a scale-up criteria for the production of ethanol by Schwannimyces castelli in a solid state fermentation system. Process Biochemistry **1992**, 27, 97-107.
36. Ledakowicz, S.; Zawadzka, A.; Krzystek, L. Biodrying of organic fraction of municipal solid waste. In *Proceedings of 8th World Congress of Chemical Engineering, Montreal, Canada, August 23-27,* 2009.
37. Larsen, K.L.; McCartney, D.M. Effect of C/N ratio on microbial activity and N retention: bench scale study using pulp and paper biosolids. Compost Science & Utilization **2000**, 8(2), 147-159.

38. Haug, R.T. *The Practical Handbook of Compost Engineering*. Lewis Publishers, Boca Raton, FL, USA, 1993.
39. Du, J.H.; Wang, B.X. Forced convective heat transfer for fluid flowing through a porous medium with internal heat generation. Heat Transfer-Asian Research **2001**, 30(3), 213-221.
40. Gowthman, M.K.; Ghildyal, N.P.; Raghava Rao, K.S.M.S.; Karanth, N.G. Interaction of transport resistances with biochemical reaction in packed-bed solid state fermenters: the effect of gaseous concentration gradients. Journal of Chemical Technology and Biotechnology **1993**, 56, 233-239.
41. Bailey, J.E.; Ollis, D.F. *Biochemical engineering fundamentals*. McGraw Hill International editions Inc., Singapore, 1986.
42. Geankoplis, C. J. *Transport processes and unit operations*. Prentice Hall, NJ, USA, 1993.
43. Perry, R.H.; Green, D.W. *Perry's chemical engineers' handbook*. McGraw-Hill, USA, 1997.
44. Rowley, G.; Mackin, L.A. The effect of moisture sorption on electrostatic charging of selected pharmaceutical excipient powders. Powder Technology **2003**, 135-136, 50-58.
45. Labuza, T.P. Moisture sorption: Practical aspects of isotherm measurement and use. In: American Association of Cereal Chemists, USA, 1984.
46. Nakayama, A.; Nanasaki, K.; Kuwahara, F.; Sano, Y. A lumped parameter heat transfer analysis for composting processes with aeration. Transactions of the ASME **2007**, 129(7), 902-906.
47. Bird, R. B.; Stewart, W. E.; Lightfoot, E.N. *Transport Phenomena*. USA, John Wiley& Sons Inc., 2002.
48. Stanish, M.A.; Schajer, G.S.; Kayihan, F. A mathematical model of drying for hygroscopic porous media. AIChE J. **1986**, 32(8), 1301-1311.

Appendix A: Analytical approach

Eq. (8) is a second-order ordinary differential equation. It is linear since the physical parameters are assumed to be constant in each compartment of the biodrying reactor. Its analytical solution can be written as:

$$T_i(z) = T_i^H(z) + T_i^{NH}(z) \tag{15}$$

where $T_i^H(z)$ is the solution of the corresponding homogeneous equation:

$$\frac{d^2T_i}{dz^2} - \frac{\alpha_i}{k_s(1-\varepsilon_i)LW}\frac{dT_i}{dz} - \frac{\dot{m}_{g,i}Cp_{g,i}}{k_s(1-\varepsilon_i)LWD}T_i = 0 \tag{16}$$

and $T_i^{NH}(z)$ is a particular solution of Eq. (8). The general solution of Eq. (8) that satisfies boundary conditions $T_1(z=0)=T_{in}$ and $T_i(z=0.4)=T_{i+1}(z=0)$
is given by:

$$T_i(z) = T_i^H(z) + T_i^{NH}(z) = \beta_i + \gamma_i e^{\delta_i z} + \phi_i e^{\varphi_i z} \tag{17}$$

where β_i, γ_i, and δ_i are given in Table 9. Note that the second exponential term in Eq. (17) vanishes due to very large value of the power term, and therefore, the overall solution becomes:

$$T_i(z) = \beta_i + \gamma_i e^{\delta_i z} \tag{18}$$

Table 9. Overall solution parameters for the four compartments of the biodrying reactor

Compartment 1	$\beta_1 = T_{in} + \frac{\dot{Q}_{bio,1}(1-\varepsilon_1)LWD - \Delta H_{eva} a_{w,1}(X_{out,1} - X_{in})\dot{m}_{g,1}}{\dot{m}_{g,1} Cp_{g,1}}$ $\gamma_1 = T_{in} - \beta_1$ $\delta_1 = \frac{\alpha_1}{2LW(1-\varepsilon_1)k_s} - \sqrt{\left(\frac{\varepsilon_1}{2LW(1-\varepsilon_1)k_s}\right)^2 + \frac{\dot{m}_{g,1} Cp_{g,1}}{Dk_s(1-\varepsilon_1)LW}}$ $\alpha_1 = \dot{m}_{total}(w_{ms,1} Cp_{ms,1} + (1-w_{ms,1}) Cp_{H_2O})$
Compartment 2	$\beta_2 = T_{in} + \frac{\dot{Q}_{bio,2}(1-\varepsilon_2)LWD - \Delta H_{eva} a_{w,2}(X_{out,2} - X_{in})\dot{m}_{g,2}}{\dot{m}_{g,2} Cp_{g,2}}$ $\gamma_2 = \beta_1 - \beta_2 + \gamma_1 e^{0.4\delta_1}$ $\delta_2 = \frac{\alpha_2}{2LW(1-\varepsilon_2)k_s} - \sqrt{\left(\frac{\varepsilon_2}{2LW(1-\varepsilon_2)k_s}\right)^2 + \frac{\dot{m}_{g,2} Cp_{g,2}}{Dk_s(1-\varepsilon_2)LW}}$ $\alpha_2 = \dot{m}_{total}(w_{ms,2} Cp_{ms,2} + (1-w_{ms,2}) Cp_{H_2O})$
Compartment 3	$\beta_3 = T_{in} + \frac{\dot{Q}_{bio,3}(1-\varepsilon_3)LWD - \Delta H_{eva} a_{w,3}(X_{out,3} - X_{in})\dot{m}_{g,3}}{\dot{m}_{g,3} Cp_{g,3}}$ $\gamma_3 = \beta_2 - \beta_3 + \gamma_2 e^{0.4\delta_2}$ $\delta_3 = \frac{\alpha_3}{2LW(1-\varepsilon_3)k_s} - \sqrt{\left(\frac{\varepsilon_3}{2LW(1-\varepsilon_3)k_s}\right)^2 + \frac{\dot{m}_{g,3} Cp_{g,3}}{Dk_s(1-\varepsilon_3)LW}}$ $\alpha_3 = \dot{m}_{total}(w_{ms,3} Cp_{ms,3} + (1-w_{ms,3}) Cp_{H_2O})$
Compartment 4	$\beta_4 = T_{in} + \frac{\dot{Q}_{bio,4}(1-\varepsilon_4)LWD - \Delta H_{eva} a_{w,4}(X_{out,4} - X_{in})\dot{m}_{g,4}}{\dot{m}_{g,4} Cp_{g,4}}$ $\gamma_4 = \beta_3 - \beta_4 + \gamma_3 e^{0.4\delta_3}$ $\delta_4 = \frac{\alpha_4}{2LW(1-\varepsilon_4)k_s} - \sqrt{\left(\frac{\varepsilon_4}{2LW(1-\varepsilon_4)k_s}\right)^2 + \frac{\dot{m}_{g,4} Cp_{g,4}}{Dk_s(1-\varepsilon_4)LW}}$ $\alpha_4 = \dot{m}_{total}(w_{ms,4} Cp_{ms,4} + (1-w_{ms,4}) Cp_{H_2O})$

A3. Key Variables Analysis of a Novel Continuous Biodrying Process for Drying Mixed Sludge

Key Variables Analysis of a Novel Continuous Biodrying Process for Drying Mixed Sludge[1]

Shahram Navaee-Ardeh, François Bertrand, Paul R. Stuart
École Polytechnique de Montréal, Chemical Engineering Department, P.O. Box 6079,
succ. Centre-ville Montréal, H3C 3A7, Canada

Corresponding author: paul.stuart@polymtl.ca, Tel: +(1)514-340-4711 ext. 4384, Fax: +(1)514-340-5150

Abstract

To increase the effectiveness and combustion efficiency of pulp and paper mixed sludge in biomass boilers, a novel continuous biodrying process has been developed whose goal is to increase the dry solids content of the sludge to economic levels. The drying rates in the process are enhanced by the metabolic heat produced by aerobic microorganisms naturally present in the mixed sludge. The goals of this study were to systematically analyze the continuous biodrying reactor and understand the basic transport phenomena occurring in it. By performing a series of screening experiments and a variable analysis, it was found that the outlet relative humidity profile was the key variable in the biodrying reactor. The influence of different outlet relative humidity profiles was then evaluated using biodrying efficiency index. It was found that the continuous biodrying reactor can dry the mixed sludge to economic dry solids levels (>45% w/w) in a reasonably short period of time (less than 6 days). Such economic dry solids level avoids removal of large amounts of bound moisture. The best outlet air relative humidity profile down the reactor length was determined as a function of the nature of the unbound/bound water being removed at a given height in the reactor, which in turn resulted in wet/dry bulb drying conditions. It was found that by employing an outlet relative humidity of 85%/85%/96%/96% in the four compartments of the reactor, the mixed sludge could be dried in one case from an initial dry solids content of 40% w/w to above 52% w/w in 6 days.

Keywords: Biodrying process, pulp and paper mixed sludge, biodrying efficiency, transport phenomena, relative humidity profile

1. Introduction

An estimated 2.6 million tonnes of mixed sludge is produced from Canada's pulp and paper mills every year (Elliott and Mahmood, 2005), and its disposal can represent a significant cost. Until recent years disposal strategies such as landfilling and landspreading have been widely used, but environmental restrictions have made these practices increasingly difficult. Sludge composting requires a relatively long residence time (30-50 days), and thus becomes less practical for large quantities of sludge. These limitations coupled with increasing energy costs have made combustion an attractive sludge management option for many pulp and paper mills. However, a sludge dry solids content of 45%w/w or more is typically required for efficient combustion in woodwaste and other boilers (Kudra et al., 2002; Kraft and Orender, 1993).

In the primary wastewater treatment system of a pulp and paper mill, effluent solids are removed by settling/clarification and flotation (Hynninen and Laine, 1998). The primary sludge mainly contains wood fibers and fillers. Primary treatment is followed by biological treatment, often an activated sludge treatment (AST) system, in which wastewater organic matter is broken down by means of aerobic biodegradation. The combined sludge from the primary and secondary treatments comprises mixed sludge, consisting of a complex mixture of microorganisms, fibrous materials, lignin, mineral components (limestone and phosphorus), and clay (Chen et al., 2002; Hippinen and Ahtila, 2004).

As described by many researchers (Tsang and Vesilind, 1990; Lee, 1994; Vaxelaire and Cezac, 2004; Navaee-Ardeh et al., 2006), mixed sludge contains unbound and bound water: unbound water is relatively easy to remove using mechanical techniques, whereas bound water is the most challenging to remove, typically requiring extended thermal drying techniques. Due to the distinct characteristics of mixed sludge such as its stickiness and relatively low heating values, the application of many drying technologies can be technically and economically challenging. A review of emerging drying technologies for pulp and paper mixed sludge can be found in the literature (Navaee-Ardeh et al., 2006; CANMET Energy Technology Centre, 2005). These studies reveal that many approaches have significant technical uncertainties and/or questionable economics. In fact, efficient drying technologies that increase dry solids content of pulp and paper mixed sludge to values above critical levels for economic combustion are needed to address this important challenge.

Biological drying (Choi et al., 2001; Navaee-Ardeh et al., 2006), or simply "biodrying" has the potential to raise the dry solids content of mixed sludge to dry solids levels allowing for disposal in boilers with steam and/or power generation. In the

[1] This paper is accepted at Bioresource Technology

biodrying process, the drying rate of sludge is augmented by biological heat in addition to forced aeration. This biological heat provided by the aerobic microorganisms naturally present in biological (secondary) sludge is essential for the biodrying process. The exothermic aerobic reaction can be represented as follows:

$$Substrate + aO_2 \rightarrow bCO_2 + cH_2O + New\ cell, \Delta H_r < 0 \quad (1)$$

The biodrying reactor is self-heating, relying on microbial heat production to obtain the required process temperatures. This is an advantage over conventional drying systems that depend on external heat sources (Mason and Milke, 2005a and 2005b).

Bacteria responsible for biological activity can be classified into four groups based on temperature preferences (Fig. 1): psychrophiles (active at 0-20°C), mesophiles (active at 8-48°C), thermophiles (active at 42-68°C) and hyperthermophiles (medium and extreme) (active at 70-110 °C) (Madigan and Martinko, 2006). However, only mesophilic and thermophilic bacteria are important in the biodrying process because they are active within the typical temperature range of the reactor. Indeed, as reported by Frei et al. (2004) and Roy et al. (2006), the typical temperature range in the biodrying process is 15-55°C, although temperatures of up to 65°C have been observed. These bacteria are sensitive to the temperature of the matrix in which they grow. As shown in Fig. 1, too high temperatures kill mesophilic bacteria while favoring the growth of thermophiles. There are also other factors that affect the biological reaction, namely (a) the moisture content of the substrate, (b) oxygen, and (c) nutrient availability. A portion of the biologically-generated heat in the solid matrix is utilized by the microorganisms to support their preservation, growth, and multiplication, whereas the rest serves to enhance the evaporation of bound water in the porous matrix (Prescott et al., 1993; Bailey and Ollis, 1986). The metabolic reaction can theoretically take place at high moisture levels, but such levels decrease the availability of oxygen needed to sustain aerobic decomposition, due mainly to the slow diffusion of oxygen into the liquid film surrounding the microorganisms. Nakasaki et al. (1994) reported that the optimum moisture content for the microbial activity is 45-65% w/w. This has been confirmed elsewhere (Liang et al., 2003).

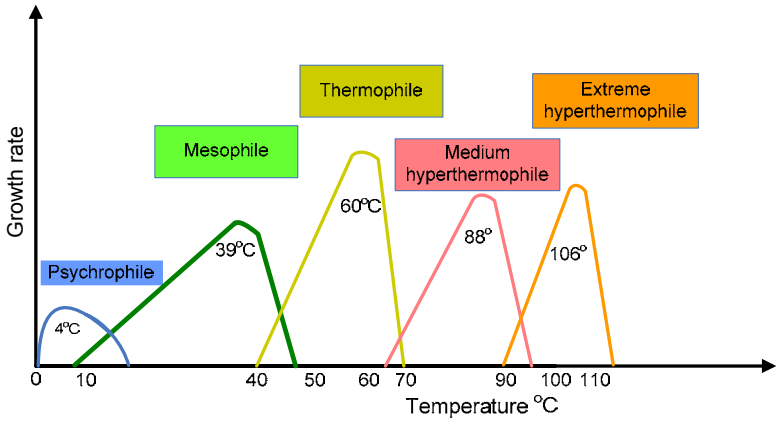

Fig. 1. Effect of temperature on the microbial growth rate of different microbes (adapted from Madigan and Martinko, 2006)

In earlier bench-scale batch biodrying reactors conducted in our laboratories, temperature and pressure were measured within the porous matrix of the mixed sludge, and the relative humidity and air flowrates were measured in the inlet and outlet air flows. During earlier testing it was determined that a sludge to woodwaste ratio of 2:1 (dry mass basis) provided good pneumatic conditions in the porous matrix of the batch biodrying reactor (Frei et al., 2004). The pneumatic performance of the biodrying reactor is critical for good system control and uniform air distribution throughout the matrix. The internal bioheat generation raised porous medium temperatures to peak values of approximately 65°C, and carbon losses from biological activity ranged from under 5% to as high as 18%. The results highlighted a clear correlation between the high matrix temperatures and the rate of water removal. The study also included a techno-economic analysis that demonstrated the economic viability of implementing the technology in the Canadian pulp and paper industry (Frei et al., 2006).

In the second study conducted by Roy et al. (2006), a series of batch biodrying reactor experiments were performed using a modified batch reactor configuration. The influence of several parameters on the drying rate was investigated, which included air flowrate, initial dry solids content (mixed sludge & bark), C/N ratio and initial matrix temperature. It was found that lower air flowrates favor bioactivity, but results in less biodrying. At higher air flowrates, bioactivity is limited due to the cooling effects of moisture evaporation. The bioheat was recognized to be the major source of energy in the batch biodrying system. The study included a thermodynamic analysis, where it was found that the biological energy produced in the batch biodrying system varied from 3900 to 6500 W/m^3-matrix, similar to values reported by Mote and Griffis (1982) (3400-4800 W/m^3) and Harper et al. (1992) (3400-6500 W/m^3) for aerobic composting processes.

In the same study, Roy et al. (2006) performed a techno-economic assessment for a full-scale biodrying system comprising two 625-m^3 reactors of 5m in height, 5m in width and 25m in length. The effect of final material dry solids content was investigated on the capital and operational costs as well as on the system performance. As shown in Fig. 2, an optimum

return on investment (ROI) was obtained in all scenarios for dry solids levels in the range of 43-45% w/w. This techno-economic assessment indicates that it is not required to remove the bound water to a large extent.

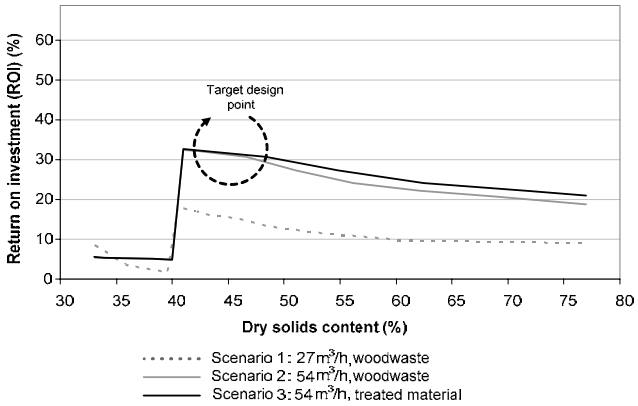

Fig. 2. Effect of dry solids content on ROI (Adapted from Roy et al. (2006))

Although these two studies confirmed the potential for economic viability of the batch biodrying technology, several shortcomings were identified including operational inflexibility, relatively long residence times to reach economic dry solids levels, non-uniform matrix conditions, larger required footprint than desired, and the possible occurrence of anaerobic conditions (hot spots) in the reactor. These limitations resulted in variable dry solids content for the final product.

Therefore, a novel pilot-scale continuous biodrying reactor was designed and built in our laboratory to overcome the limitations of the batch biodrying reactor, and raise the dry solids content of the mixed sludge to the economic level in shorter residence time.

In a previous study, a 1-D computational model was developed whose goal was to investigate the dominating transport phenomena in the continuous biodrying reactor (Navaee-Ardeh et al., 2009). This and several other aspects of such a process have to be studied. Hence, the objectives of this paper are: to demonstrate the performance of a novel continuous biodrying reactor, to identify the key variable(s) for the continuous biodrying reactor through process system analysis, and to assess the impact of key variable(s) on the overall performance and the complexity of the continuous biodrying reactor.

2. Methods

2.1. Biomass characteristics

The biomass fed to the biodrying process was pulp and paper mixed sludge in a ratio of 45/55 (% w/w) primary to secondary sludge, collected from a typical wastewater treatment plant at an Eastern Canadian TMP-newsprint mill. Material characterization was conducted on a daily basis and included determination of dry solids content, elemental analysis (carbon, hydrogen, nitrogen, oxygen and sulphur), and microbial counts. More details are given in Navaee-Ardeh et al. (2009).

2.2. Experimental set-up

Two pilot-scale vertical stainless-steel biodrying reactors were designed and built, each of 40-cm length × 100-cm width × 200-cm height (Fig. 3). One biodrying reactor is fully instrumented and controlled on-line, whereas the second reactor has limited instrumentation and used primarily to generate data for repeatability purposes. The instrumented biodrying reactor is shown schematically in Fig. 4. It is divided into four nominal compartments. Temperatures (T) and relative humidity (RH), pressure (P), and CO_2 were measured using six RH probes (HMW60U/Y, Vaisala, Helsinki, Finland), 12 pressure probes (Dwyer Instrument Inc., USA), and 5 CO_2 sensors connected to an analyzer (MSA Instrument Division, Ultima gas monitor, USA), respectively. The on-line measurement of carbon dioxide was used to estimate the rate of biodegradation and biological heat. Temperature and relative humidity served to determine the drying rate (water removal rate). These measured quantities were also used to assess the complexity of the transport phenomena prevailing in the biodrying reactor. Along with the incoming gas temperature, relative humidity and air flowrates, they were logged at 8 min intervals using the LabView program (LabView 8.0.1, National Instrument Inc., USA).

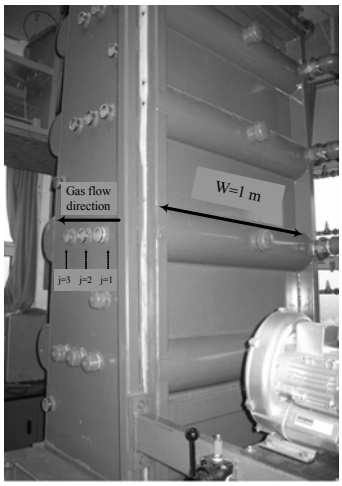

Fig. 3. Pilot-scale biodrying reactor

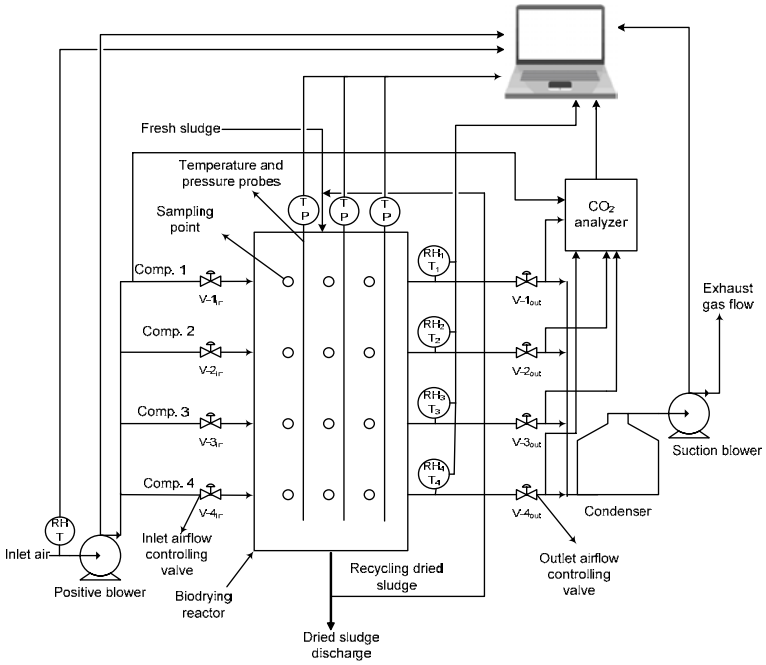

Fig. 4. Schematic diagram of the pilot-scale continuous biodrying reactor set-up

2.3. Experimental procedure

Mixed sludge was fed and biodried sludge discharged twice a day from the biodryer batch wise at about 10-22 kg solids (dry basis) per batch. The sludge was extracted by two parallel screws installed at the bottom of the reactor. Fresh sludge received from the mill was then mixed with the dried sludge prior to being manually charged into the reactor top so that good pneumatic conditions prevailed throughout the experiments. Airflow was supplied by forced air and inductive blowers, driving the air in the reactor cross-flow direction in each of the four compartments. The sludge residence time in the biodryer was 4-8 days, the total air flowrate was 28-75 m^3/h and the dried sludge recycle ratio was 15-30% w/w. This range of residence times, which was recommended by Roy et al. (2006), is expected to provide an economically viable biodrying process. The dried sludge recycle ratio was recommended by Frei et al. (2004). The air flowrates were adjusted to obtain desired outlet relative humidity profile in the reactor.

2.4. Commissioning and troubleshooting

Two experimental issues were identified and addressed during the commissioning experiments: (1) the occurrence of cavities in the sludge matrix due to non-uniform residence times across the reactor, and (2) the re-evaporation of condensed water in the outlet conduits, which made it difficult to control the outlet relative humidity in each compartment.

2.4.1. Non-uniform residence time across the biodrying reactor

In the early commissioning phase it was found that the occurrence of non-uniform residence times of the sludge across the reactor depth led to the formation of cavity near the sludge discharge port and variable dry solids contents in the discharged materials (Fig. 5). The discharge screw geometry was subsequently modified to provide uniform residence times across the reactor depth. To verify the effect of each modification, twelve balls with similar size and density as those the mixed sludge particles were uniformly distributed at the top of the reactor, and the normalized residence time of each ball was measured. The discharge screw was modified until satisfactory results were obtained (see Fig. 5).

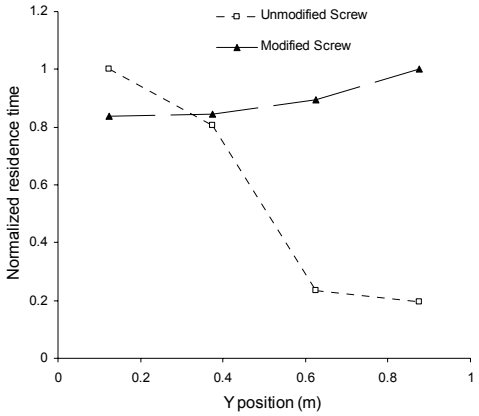

Fig. 5. Residence time distribution of sludge across the biodrying reactor depth for unmodified and modified sludge discharge screws

2.4.2. Effect of re-evaporation of condensed water on relative humidity

The relative humidity of the exit airflow is critical for the control of the reactor biodrying conditions. Due to heat exchange between the outlet airflow in the conduits and the surrounding environment, some of the water vapour was observed to condense, causing high variability in the exit relative humidity profile (Fig. 6a). To prevent such variations, the conduits were heat-traced and subsequently modified. Fig. 6b shows that the modified conduits resulted in a more stable humidity profile.

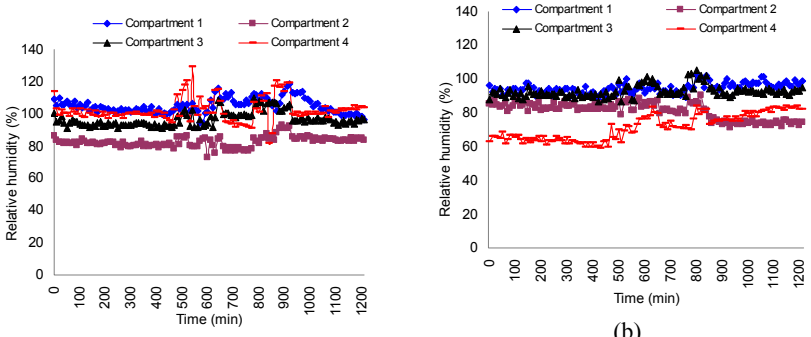

Fig. 6. Outlet relative humidity of (a) unmodified and (b) modified conduits

2.5. Process performance

2.5.1. Base case experimental data

In total, 12 experiments were conducted and 6 cases that represent diverse operating conditions (Table 1) and address the objectives of this paper are presented here. Cases 1 and 2 are at controlled air flowrates ($Q_g \approx 28$ m^3/h), 15% w/w recycle ratio (RR), and 4- and 8-day residence times (RT), respectively. Cases 3, 4, 5, and 6 are at controlled outlet relative humidity (RH_{out}), a 6-day residence time, and 30%w/w recycle ratio. The outlet relative humidity profile for cases 3, 4, 5, and 6 are 85/85/85/85%, 96/96/96/96%, 96/96/85/85%, and 85/85/96/96%, respectively. The temperature (T_{in}) and relative humidity (RH_{in}) of the inlet air were 24-26^{o}C, and 10-14%, respectively.

Table 1 Experimental operating conditions

		Q_g (m^3/h)	RH_{out} (%)	RH_{in}(%)	T_{in} (^oC)	RT (day)	RR(% w/w)
Case 1	Comp. 1	7.04		10	26	8	15
	Comp. 2	7.11					
	Comp. 3	7.63					
	Comp. 4	7.65					
Case 2	Comp. 1	7.91		12	26	4	15
	Comp. 2	7.41					
	Comp. 3	7.31					
	Comp. 4	7.38					
Case 3	Comp. 1	26.4	85	13	24	6	30
	Comp. 2	5.0	85				
	Comp. 3	26.0	85				
	Comp. 4	18.0	85				
Case 4	Comp. 1	16.5	96	14	24	6	30
	Comp. 2	8.0	96				
	Comp. 3	14.0	96				
	Comp. 4	7.7	96				
Case 5	Comp. 1	25.4	96	14	24	6	30
	Comp. 2	4.5	96				
	Comp. 3	25.3	85				
	Comp. 4	6.2	85				
Case 6	Comp. 1	5	85	13	24	6	30
	Comp. 2	11	85				
	Comp. 3	16	96				
	Comp. 4	5	96				

2.5.2. Water balance

Overall water balances were performed, which included fresh, recycled and discharge sludges as well as inlet and outlet gases:

Water in-Water out +Water generation =0 (2)

Steady-state conditions were identified when the matrix temperatures and the dry solids contents became constant over time.

The water content in the gas phase was calculated from the relative humidity, temperature and air flowrate, whereas for the solid phase it was directly obtained from the total mass of sludge and its dry solids content.

Cellular water produced by the microbial aerobic oxidation of substrate (Eq. 1) was estimated from the elemental analysis results (Table 2) and the carbon dioxide generated in each compartment.

Table 2 Elemental analysis results for the mixed sludge in the biodrying reactor

From the top to the bottom of the biodrying reactor	% w/w Nitrogen	%w/w Carbon	% w/w Hydrogen	%w/w Oxygen	C/N
Feed	1.48	45.67	4.72	36.60	30.8
Compartment 1	1.58	44.92	5.08	36.10	28.4
Compartment 2	1.64	44.90	4.95	36.25	27.4
Compartment 3	1.81	44.65	4.79	35.80	24.7
Compartment 4	1.85	44.61	4.79	35.80	24.1

Typical experimental conditions used for the water balance are given in Table 3. This specific case correspondence to a 6-day residence time, 30%w/w recycle ratio, and a total air flowrate of 52m^3/h.

Table 3 Typical experimental data used for the water balances

	Q_g (m^3/h)	RH_{out} (%)	T_{out} (^oC)	RH_{in} (%)	T_{in} (^oC)
Compartment 1	18.2	94	18	20	24
Compartment 2	8.5	78	23.6	20	24
Compartment 3	16.2	100	16.2	20	24
Compartment 4	9.2	80	27.2	20	24

Note that the relative humidity and the temperature of the inlet gas were the same for all compartments, as all lines were connected to the same inlet air stream. Fresh, feed and discharge sludge dry solids contents were 37, 40.3, and 51% w/w, respectively. Fig. 7 shows the results of the water balance, which closes within less than 1%.

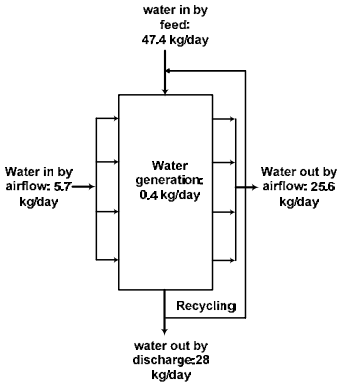

Fig. 7. Water balance in the continuous biodrying reactor

Water balance was performed for all experimental runs (cases 1-6), and satisfactory results were achieved for all of them (error<2%). This confirms the validity of our experimental methodology.

2.5.3. Dry solids content evolution

Fig. 8 shows the evolution of dry solids content in the continuous biodrying reactor for the six cases. The error was estimated to be ±2% from 5 different measurements on a typical sample. These data were obtained in a steady-state regime when the sludge properties in each compartment did not change over time.

As discussed earlier in section 1, the main goal of the biodrying reactor is to achieve an economic dry solids level. This concept is very important in the drying process as it avoids excessive bound water removal. As expected, the mixed sludge dry solids content increases as the sludge moves downward in the biodrying reactor. The largest dry solids content gains occur in the 3rd and 4th compartments. This trend is slightly different from what was expected (Navaee-Ardeh et al., 2006). Indeed, it was first thought that the dry solids content would increase more at the top of the reactor and level off in the 3rd and 4th compartments. However, as shown in Fig. 8, the dry solids content is nearly flat in the 1st and 2nd compartments in all cases, and increases significantly in the 3rd and 4th compartments. This is due mainly to the significant impact of higher bioheat and higher temperatures in the bottom compartments (Navaee-Ardeh et al., 2009), which increase the water holding capacity of the gas phase and the water transfer from the solid phase to the gas phase. As can be seen, the economic dry solids level is achieved in all cases.

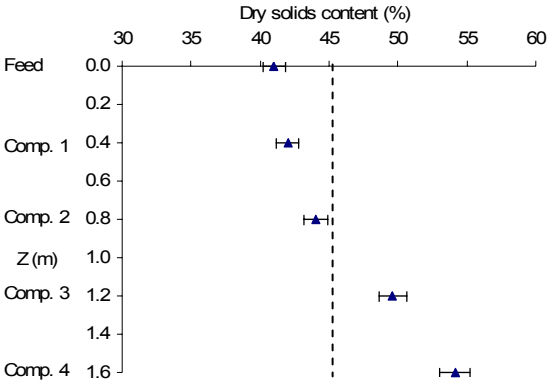

(d): case 1

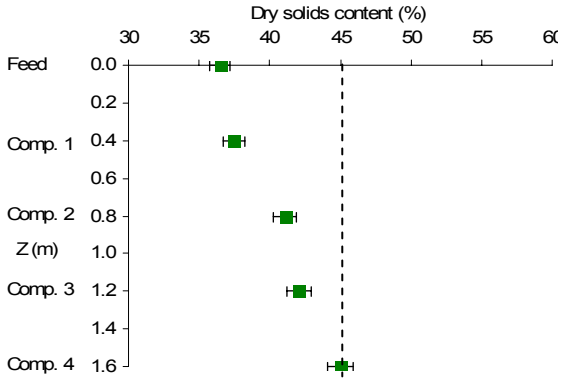

(c): case 2

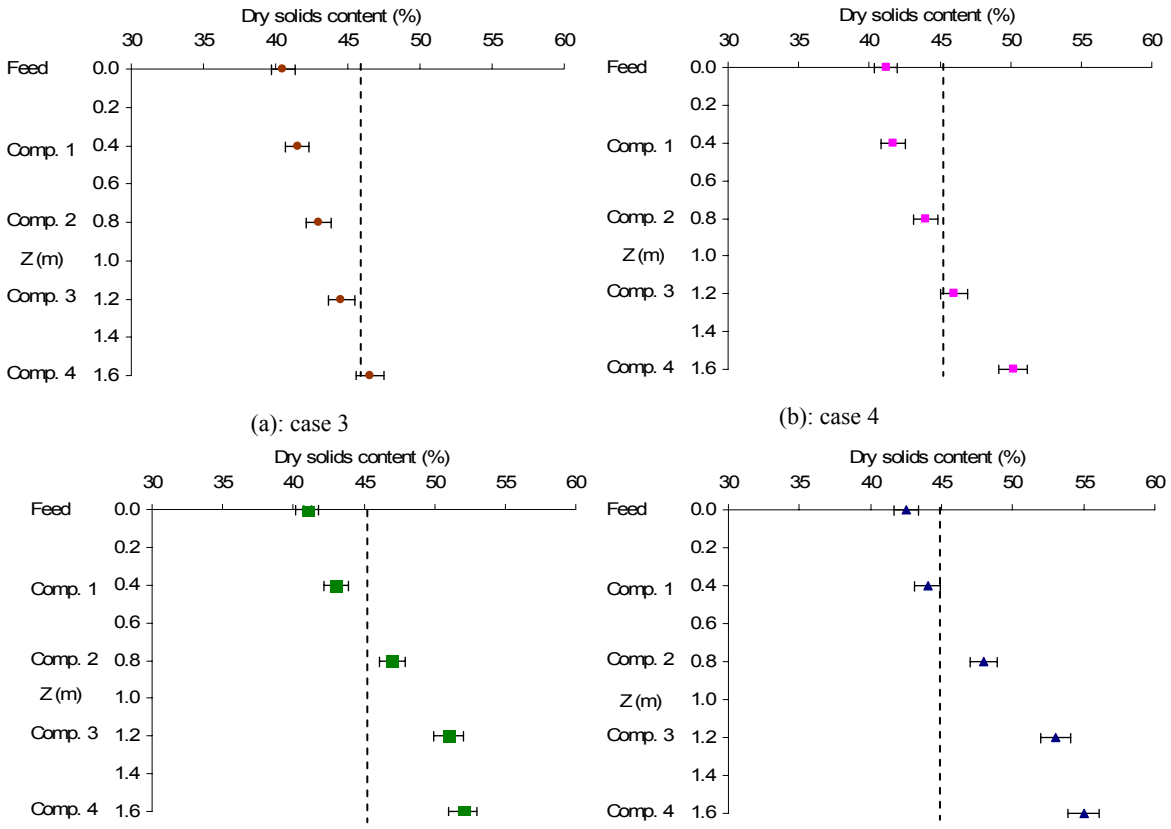

(a): case 3 (b): case 4

(e): case 5 (f): case 6

Fig. 8. Dry solids content change in the continuous biodrying reactor.
The dashed line indicates the economic dry solids content.

3. Results and discussion

In this section, first, a process system analysis is performed to identify key variable(s) in the continuous biodrying reactor, and then the impact of the key variable(s) is discussed on the overall performance of the biodrying reactor and the complexity of the transport phenomena in the continuous biodrying reactor.

3.1. Identification of biodrying key variables

The goal of these experiments was to determine the key variables that affect the operation and the performance of the continuous biodrying reactor. The following variables were investigated: biomass feed, pH of mixed sludge, C/N ratio, residence time, recycle ratio, and outlet relative humidity profile. These are the most relevant variables that are considered in the aerobic composting processes. Table 4 summarizes the biodrying variables and the potential impact of each of these variables on the biodrying operation. Note that the effect of inlet air relative humidity and temperature are not investigated here because of their small variation during the experiments.

Table 4 Two types of variables in the biodrying reactor for the screening experiments

Biodrying variable	Range	Potential impact on biodrying process
Type of biomass feed	Mill specific	Represents nutrient availability for biodrying operation
pH of biomass	6.4-6.8	Very high (>7) or very low (<5) values could be harmful for the microbial activity and biodrying operation
Nutrient level (C/N ratio)	24-29	Out of range values (<15 or >30) are harmful to microbial activity (Haug, 1993) and biodrying operation
Residence time (day)	4,6,8	Recommended by Roy et al. (2006). This affects reactor performance and economic viability of the process

Recycle ratio (%w/w)	0,15,30	Recommended by Frei et al. (2004). This helps microbial acclimation, and increases porosity and permeability for better air flow in the matrix
Outlet relative humidity (%)	85,96	May have significant impact on the transport phenomena in the biodrying reactor as it controls the mechanism of unbound and bound water removal

3.1.1. Biomass feed

The type of biomass feed and its properties could potentially affect the performance of the biodrying process, extent of microbial reaction, and feasibility of the process. Some of the key biomass properties include initial feed dry solids content, biomass feed temperature, initial active microbial population of biomass feed, and nutrient level in the biomass feed. Since the biomass feed was obtained from a given TMP pulp and paper mill, there were not significant changes on these properties from one experiment to another. For instance, the fresh feed dry solids content, the ash content, and microbial counts remained nearly constant. Therefore, the feed biomass was a fixed parameter for this study.

3.1.2. pH of biomass

The pH of the substrates in the matrix of mixed sludge must be near neutral (≈7) because most of the biological systems balance their cationic and anionic ions near the neutrality. In the biodrying experiments for this study, the pH of the mixed sludge was not significantly affected by the process, which could be due to the buffered microbial environment. The mixed sludge pH varied from 6.8 in the fresh feed to about 6.3 in discharge materials. This range is optimum for microbial activity in aerobic composting facilities (Fitzpatrick, 1993).

3.1.3. C/N ratio

Roy et al. (2006) reported the C/N ratio as one of the most influential experimental parameters in the batch biodrying process. Larsen and McCartney (2000) found that bioheat has a negative correlation with C/N ratio. An out of range C/N ratio (<15 or >30) can therefore jeopardize the success of the biodrying process, so a regular elemental analysis of the mixed sludge was conducted for each compartment.

Although C/N ratio was observed to decrease in the biodrying reactor (Table 2), it stayed within the range of active microbial regime (between 15 and 30 (Haug, 1993). The results obtained are similar to values reported in the literature (Larsen and McCartney, 2000). The C/N ratio of mixed sludge is part of the biodrying feed characteristics. As a critical variable, the C/N ratio needs to be measured to ensure good operation of the biodrying reactor. In this work, the mixed sludge came from one single mill and the elemental analyses revealed nearly constant C/N values for all feeds.

3.1.4. Residence time

Residence time affects not only the efficiency of the biodrying process, but also its capital cost. Removing unbound water (in the 1st and 2nd compartments) requires less residence time, whereas bound water removal (in the 3rd and 4th compartments) is based on diffusion mechanism and requires longer residence times. One of the goals of the pilot-scale continuous biodrying reactor was to significantly reduce the residence time required to achieve economic dry solids levels, so as to reduce capital costs. A broad range of residence times were tested: 4, 6 and 8 days, which on average resulted in 6, 10 and 15%w/w dry solids content increases, starting from an initial dry solids content of 38% w/w. First, an 8-day residence time was tested that resulted in 54% w/w dry solids content for discharge sludge. This level of dry solids content is significantly above the economic dry solids content (43-45% w/w in Fig. 2), and therefore is less attractive (Navaee-Ardeh et al., 2008). Then a 4-day residence time was tested. As shown in Fig. 8b, the economic dry solids level was achieved. However, to ensure that the biodrying operation always receives a 4-day treatment and the microbial activity acclimates well, the residence time was fixed at 6 days.

3.1.5. Recycle ratio

The recycling of dried sludge into the feed stream may be required for enhanced sludge acclimation, and as well, to ensure that the necessary pneumatic conditions prevail in the porous medium. The microbial lag phase occurs because microbial acclimation is needed when there is a change in environmental conditions (Madigan and Martinko, 2006). Therefore, 15% w/w of the discharge stream (dry mass basis) was recycled and mixed with 85% w/w of fresh sludge (dry mass basis) and then fed into the bioreactor. This led to an improved matrix temperature in all compartments. Table 5 compares the microbial population counts for both mesophilic and thermophilic bacteria for three recycle ratios: 0% (100% fresh sludge), 15% w/w (85% w/w fresh feed), and 30% w/w (70% w/w fresh sludge). It can be observed that the population of mesophilic and thermophilic bacteria are about 200 times and 20 times greater, respectively, in the case of a 30% w/w recycle ratio.

Table 5 also shows that the microbial population counts are similar for a second feed (30% w/w recycle ratio).

Table 5 Mesophilic and thermophilic microbial population count in fresh feed and mixed feed

Recycle ratio (% w/w)	Mesophilic (CFU/g)	Thermophilic (CFU/g)
0	4.3×10^{5}	2.1×10^{8}
15	6.05×10^{7}	2.03×10^{9}
30 (first feed)	1.02×10^{8}	4.04×10^{9}
30 (second feed)	9.03×10^{7}	4.04×10^{9}

Another improvement due to the recycling of biodried sludge into the feed stream is the increase of the pneumatic conditions, which results from a reduction of the pressure drop across the reactor width in each compartment. This can be observed in Fig. 9, which compares the pressure drops across each compartment between the gas inlet and outlet for 0, 15 and 30% w/w recycle ratios. Increasing recycle ratio reduced pressure drop in all compartments. As anticipated, the pressure drops in the 1st and 2nd compartments are higher than the pressure drops in the 3rd and 4th compartments mainly attributed to the wetness of the sludge. A sharp decrease can also be seen in the pressure drop from the 2nd compartment to the 3rd one. This can be explained by significant increase of the dry solids content across these compartments, as shown in Fig. 8. Indeed, the drier the sludge, the smaller the pressure drop. A dryer sludge has also a better resistance toward the compaction.

Note that if the pressure drop is too high, it may affect the distribution of air in the matrix, cause the development of unpleasant hot spots, reduce the performance of the biodrying reactor, and result in non-uniform biodried sludge.

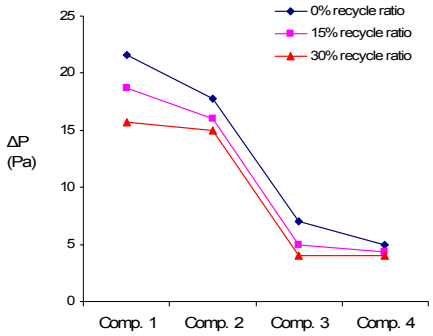

Fig. 9. Effect of recycle ratio on pressure drop in the reactor

For a full-scale reactor, hot dewatered immediately acclimated sludge will be conveyed directly to it which may not require recycling, which reduces the capital costs of the biodryer. However, recycling may be necessary for those mixed sludges that have higher proportion of tiny secondary (activated) sludge. Based on this assessment, the recycle ratio was fixed at 30% w/w in this experimental program.

3.1.6. Outlet relative humidity profile

The outlet relative humidity profile along the biodrying height is a priori a critical process variable since the air provides oxygen for the aerobic biological activity, cools the matrix when air flowrates is high enough, and transports water vapor and some of the bioheat out of the reactor. Blowing large amount of air in the upper part of the reactor helps reduce the residence time by accelerating drying, but it cools the matrix of sludge and prolongs the microbial lag phase period. Adequate combinations of air flowrate and outlet relative humidity profiles may result in optimum conditions for unbound water removal at the top of the reactor, and bound water removal at the bottom. For good biodrying conditions, each sludge type requires a specific combination of outlet relative humidity to prevent excessive biodegradation, and to achieve an adequate water removal rate (drying rate) and an economically feasible residence time. Therefore, various combinations of outlet relative humidity profiles and air flowrates were investigated in this study. Two outlet relative humidity profiles were investigated following the relevant literature (Mujumdar, 2007) and the controllability of the pilot-scale biodrying reactor: a higher outlet relative humidity (96%) and a lower outlet relative humidity profile (85%).

The total air flowrate was varied from 28 to 75 m^3/h, depending on the target outlet relative humidity profile: 85/85/85/85% (case 3), 96/96/96/96% (case 4), 96/96/85/85% (case 5) and 85/85/96/96% (case 6). Lower air flowrates were needed to achieve higher outlet relative humidity (96%), and higher air flowrates were required for lower outlet relative humidity (85%). The lower outlet relative humidity profile controls the biodrying process at wet-bulb temperature (Mujumdar, 2007), and is therefore efficient in the constant drying rate period which corresponds to the removal of unbound water. The higher outlet relative humidity controls the biodrying process at dry-bulb temperature, activates the development of microbial biodegradation (Berg et al., 2002), and is efficient in the falling drying rate period (Nissan et al., 1959), which corresponds to

the bound water removal. The impact of outlet relative humidity profile (cases 3, 4, 5 and 6) on biodrying performance is next discussed.

3.2. Effect of outlet relative humidity profile on biodrying performance

Fugere et al. (2007) stated that the biodrying performance is a critical parameter for the techno-economic assessment of a biodrying process, since the biodryer accounts for about 35% of the total direct capital cost, and the capital cost of the biodryer is strongly related to its efficiency. Navaee-Ardeh et al. (2009) found that there are two main heat transfer mechanisms that play significant role in the biodrying reactor: heat loss due to the latent heat of water evaporation, and exothermic bioheat generated through metabolic activity of aerobic microorganisms. These two components are also critical for the removal of unbound and bound water. The biodrying efficiency index (η) can be defined, which considers the biological heat available to enhance bound water diffusion and provide the latent heat of water evaporation:

$$\eta = \frac{\dot{Q}_{Evaporation}}{\dot{Q}_{Biological}} = \frac{\sum_{1}^{4} \Delta H_{latent} \rho_g Q_{g,i} (X_{out,i} - X_{in})}{\sum_{1}^{4} \dot{Q}_{bio,i}} \quad (3)$$

ρ_g is the density of air (= 1.16 kg/m^3) obtained from Perry and Green (1997). Biological heat ($\dot{Q}_{bio}$) can be directly determined from the CO_2 production rate, or equivalently from the O_2 consumption rate for aerobic processes, as follows (Navaee-Ardeh et al., 2009):

$$\dot{Q}_{bio} = Q_{bio-standard}\ \rho_{O_2} Q_g \left(\left(\frac{V_{O_2}}{V_{Air}} \right)_{in} - \left(\frac{V_{O_2}}{V_{Air}} \right)_{out} \right) \quad (4)$$

where, $Q_{bio\text{-}standard}$, the amount of biological heat generated per gram of oxygen consumed, is equal to 16 kJ/g-O_2 for different microbial species (Bailey and Ollis, 1986), ρ_{O_2} is the density of oxygen (=1.35 kg/m^3) obtained from Perry and Green (1997), and $(V_{O_2}/V_{Air})_{in}$ and $(V_{O_2}/V_{Air})_{out}$ are the volume percentage (absolute value) of oxygen experimentally obtained at the inlet and outlet gas flows, respectively.

$X_{out,i}$–X_{in} represents the net amount of water transferred to the gas phase, that is the difference of absolute humidity between outlet and inlet (kg H_2O/kg air). It is evaluated using the relative humidity and temperature of the inlet and outlet airstreams, and the following modified equation from Geankoplis (1993) and Haug (1993):

$$X_i = 0.622 \times \left(\frac{\frac{RH_i}{100} \times 10^{\left(8.896 - \frac{2233}{T_i + 273}\right)}}{760 - \frac{RH_i}{100} \times 10^{\left(8.896 - \frac{2233}{T_i + 273}\right)}} \right) \quad (5)$$

Note that the numerical values; 8.896 and 2233 are constant coefficients for partial pressure of water vapor in Antoine's equation obtained from Haug (1993).

As shown in Fig. 10, blowing more air at the top of the reactor (lower outlet relative humidity (85%)) and slowing it down at the bottom (higher outlet relative humidity (96%)) seems to result in the best biodrying efficiency index (case 6). In this case, the amount of evaporative heat is 3 times greater than the biological heat generated. This indicates that the biodrying reactor has performed well in this case with higher water evaporation and less biodegradation. As a result, the final dry solids content in case 6 is greater than that of the other cases (see Fig. 8). It is essential to avoids large biodegradation rates in the biodrying reactor in order to preserve calorific values of mixed sludge and obtain higher energy recovery in a combustion boiler.

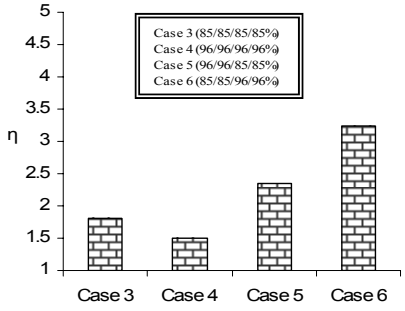

Fig. 10. Biodrying efficiency index evaluated at four outlet relative humidity profiles

3.3. Effect of outlet relative humidity profile on the complexity of transport phenomena in the biodrying reactor

Understanding the nature of transport phenomena in the biodrying reactor is essential for design, scale-up and process control. The temperature of the porous matrix in the biodrying reactor can primarily be used to describe the complexity of the biodrying reactor. It affects several physical properties, microbial activities (see Fig. 1), as well as drying process. Navaee-Ardeh et al. (2009) developed a 1-D model to describe the transport phenomena in the biodrying reactor. However, it was found that the usefulness of the 1-D model was limited to certain conditions that result in less complexity of transport phenomena in the biodrying reactor, because it poorly predicted the 2-D transport phenomena governing the higher aerobic exothermicity in the reactor, a situation which is likely to arise in an industrial biodrying reactor.

Therefore, it is important to explore the impact of the key variable on the complexity of transport phenomena in the biodrying reactor so that an appropriate model (1-D or 2-D) can be developed/applied for each condition.

More precisely, we are interested in assessing the impact of the outlet relative humidity profile on the complexity of temperature profile in the biodrying reactor. To do so, the following complexity index (*CI*) is introduced:

$$CI = \sum_{i=1}^{4} \sum_{j=1}^{3} (T_{i,j} - T_{i,in})^2 \tag{6}$$

where, $T_{i,j}$ and $T_{i,\text{in}}$ are the temperature at local j (j=1,2,3 in Fig. 3) in compartment i (i=1,2,3,4) and the inlet gas temperature in compartment i, respectively. In fact, it quantifies the importance of the variation of the velocity profile along the gas flow direction.

Fig. 11 shows values of the complexity index for cases 3, 4, 5, and 6. In cases 3, 5 and 6, where higher air flowrates were applied (low outlet relative humidity along the reactor height), the temperature variation in the gas flow direction was not significant, indicating a less complex transport phenomena in the biodrying reactor that can be described with a 1-D model. In fact, our 1-D modeling results confirmed acceptable accuracy for theses cases (Navaee-Ardeh et al., 2009). In case 4, however, the complexity index is very large indicating a more complex biodrying reactor that requires a sophisticated model (e.g. a 2-D model) for the description of the transport phenomena. The large complexity in this case is attributed to a lower air flowrate (higher outlet relative humidity profiles (96%)) that favors the development of higher temperatures in the biodrying reactor and results in a higher aerobic exothermicity in the reactor. In fact, it was found that the 1-D model poorly predicted the 2-D transport phenomena governing in the reactor for case 4 (Navaee-Ardeh et al., 2009).

Interestingly, the complexity index (*CI*) in cases 5 (blowing low at the top and high at the bottom) and 6 (blowing high at the top and low at the bottom) are equal, even though the biodrying efficiency index in case 6 is higher than that of case 5. This indicates that *CI* alone is not sufficient to fully grasp the complexity of the heat transfer mechanisms prevailing in the reactor. It appears that combining *CI* and biodrying efficiency index (η) would be more appropriate.

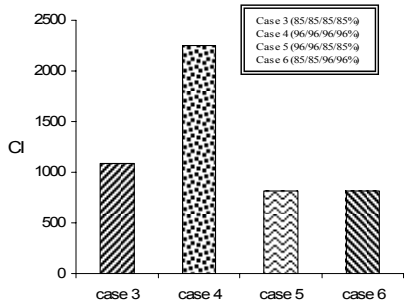

Fig. 11. Complexity index versus outlet relative humidity profiles

It follows from these results that a 2-D model is needed to describe the transport phenomena in the biodrying reactor more accurately and represent adequately the complexity of the reactor under a wide variety of operating conditions.

4. Conclusions

A novel continuous biodrying process was demonstrated to show significant promise for drying pulp and paper mixed sludge. Different operating conditions were applied and, in all cases, economic dry solids levels were achieved.

Through a variable analysis, it was found that the outlet relative humidity profile is the key variable for this continuous biodrying reactor. Four outlet relative humidity profiles were examined by adjusting the air flowrates in each compartment: case 3 (85/85/85/85%), case 4 (96/96/96/96%), case 5 (96/96/85/85%), and case 6 (85/85/96/96%), and it was found that the sixth case resulted in the best biodrying efficiency index.

The impact of outlet relative humidity profile was investigated on the complexity of transport phenomena in the biodrying reactor, and it was found that at higher outlet relative humidity profile (case 4) the biodrying reactor is a more complex problem which requires a 2-D model for the description of the transport processes prevailing in the reactor.

The continuous biodrying reactor is a novel process that combines forced convection (from aeration) and bioheat (from exothermic metabolic activity of bacteria naturally present in the sludge) to dry the mixed sludge to economic dry solids level in short residence times. It has great potential for sludge management in the pulp and paper industry.

Acknowledgments

This work was completed with the financial support of NSERC and FQRNT. The dedicated assistance of Carl Tchoryk, Kheng Huynh, Omar Ben Ndiaye and Antonin Paquet for the experimental work is gratefully acknowledged. We also wish to acknowledge fruitful discussions with Professor Tom Richard from the Department of Agricultural and Biological Engineering at Pennsylvania State University. We also thank Professor Jamal Chaouki for the use of his equipment for some analyses of mixed sludge characteristics.

References

Bailey, J.E., Ollis, D.F., 1986. Biochemical engineering fundamentals. McGraw Hill International editions Inc., Singapore.

Berg C.G., Kemp I.C., Stenstrom S., Wimmerstedt, R., 2002. Transport equations for moist air at elevated wet bulb temperatures. *13th International Drying Symposium*, Beijing, China, Conference Proceedings 135–144.

CANMET Energy Technology Centre, 2005. Pulp and Paper Sludge to Energy- Preliminary Assessment of Technologies. ADI Ltd. Report.

Chen, G., Yue, P.L., Mujumdar, A.S., 2002. Sludge dewatering and drying. *Drying Technology* 20(4-5), 883-916.

Choi, H.L., Richard, T.L., Ahn, H.K., 2001. Composting high moisture materials: biodrying poultry manure in a sequentially fed reactor. *Compost Science and Utilization*, 303-311.

Elliott, A., Mahmood, T., 2005. Survey benchmarks generation: management of solid residues. *Pulp and Paper* 79(12), 49-55.

Fitzpatrick, G.E., 1993. A program for determining co-compost belding ratios. Compost Science and Utilization, summer, 30.

Frei, K.M., Cameron, D., Jasmin, S., Stuart, P.R., 2006. Novel sludge drying process for cost-effective on-site sludge management. *Pulp and Paper Canada* 107(4), 47-53.

Frei, K.M., Cameron, D., Stuart, P.R., 2004. Novel drying process using forced aeration through a porous biomass matrix. *Drying Technology* 22(5), 1191-1215.

Fugere, M., Farand, P., Chabot, R., Stuart, P.R, 2007. Design and techno-economic analysis of a process for transforming pig manure into a value-added product. *The Canadian Journal of Chemical Engineering* 85(6), 360-368.

Geankoplis, C. J., 1993. Transport processes and unit operations. Prentice Hall, .NJ, USA.

Harper, E., Miller, F.C., Macauley, B.J., 1992. Physical management and interpretation of an environmentally controlled composting ecosystem. *Australian Journal of Experimental Agriculture* 32(5), 657-667.

Haug, R.T., 1993. The Practical Handbook of Compost Engineering. Lewis Publishers, Boca Raton, FL, USA.

Hippinen, I., Ahtila, P., 2004. Drying of activated sludge under partial vacuum conditions-An experimental study. *Drying Technology* 22(9), 2119-2134.

Hynninen, P., Laine, P., 1998. Environmental Control, Papermaking Science and Technology (19). Helsinki, Finland, Fapet Oy.

Kraft, D.L., Orender, H.C., 1993. Considerations for using sludge as a fuel. *Tappi J.* 76(3), 175-183.

Kudra, T., Gawrzynski, Z., Glaser, R., Stanislawski, J., Poirier, M., 2002. Drying of pulp and paper sludge in a pulsed fluid bed dryer. *Drying Technology* 20(4-5), 917-933.

Larsen, K.L., McCartney D.M., 2000. Effect of C/N ratio on microbial activity and N retention: bench scale study using pulp and paper biosolids. *Compost Science & Utilization* 8(2), 147-159.

Lee, D.J., 1994. Measurement of bound water in waste activated sludge: use of the centrifugal settling method. *J. Chem Technol Biotechnol* 61, 139–144.

Liang, C., Das, K.C., McClendon, R.W., 2003. The influence of temperature and moisture contents regimes on the aerobic microbial activity of a biosolids composting blend. *Bioresource Technology* 86(2), 131-137.

Madigan, M.T., Martinko, J.M., 2006. Brock Biology of Microorganisms. Upper Saddle River, NJ: Prentice Hall.

Mason, I.G., Milke, M.W., 2005a. Physical modelling of the composting environment: A review. Part 1: Reactor systems. *Waste Management* 25(5), 481-500.

Mason, I.G., Milke, M.W., 2005b. Physical modelling of the composting environment: A review. Part 2: Simulation performance. *Waste Management* 25(5), 501-509.

Mote, C.R., Griffis, C.L., 1982. Heat production by composting organic matter. *Agricultural Wastes* 4, 65-73.

Mujumdar, A.S., 2007. Handbook of Industrial Drying CRC Press. Taylor & Francis Group, Boca Raton, 3rd edition, FL, USA.

Nakasaki, K., Aoki, N., Kubota, H., 1994. Accelerated composting of grass clippings by controlling moisture level. *Waste Management & Research* 12(1), 13-20.

Navaee-Ardeh, S., Bertrand, F., Stuart, P.R., 2006. Emerging biodrying technology for the drying of pulp and paper mixed sludges. *Drying Technology* 24(7), 863-878.

Navaee-Ardeh, S., Tchoryk, C., Bertrand, F., Stuart, P.R., Tolnai, B., 2008. Novel continuous biodrying reactor: principles, screening experiments and results. *58th Canadian Chemical Engineering Conference*, Ottawa. Canada.

Navaee-Ardeh, S., Bertrand, F., Stuart, P.R., 2009. Development and experimental evaluation of a 1-D distributed model of transport phenomena in a continuous biodrying process for biomass dying. Accepted at *Drying Technology*.

Nissan, A.H., Kaye, W.G., Bell, J.R., 1959. Mechanism of drying thick porous bodies during the falling rate period. I. The pseudo-wet-bulb temperature, *AIChemE J.* 5(1), 103–110.

Perry R. H., Green D. W., 1997. Perry's chemical engineers' handbook. McGraw-Hill, USA.

Prescott, L.M., Harley, J.P., Klein, D.A., 1993. Microbiology. W.C. Communications Inc., 2nd Edition, USA.

Roy, G., Jasmin, S., Stuart, P. R., 2006. Technical modeling of a batch biodrying reactor for pulp and paper mill sludge. *17th CHISA International Congress of Chemical and Process Engineering, Prague, Czech Republic.*

Tsang, K.R., Vesilind, P.A. 1990. Moisture distribution in sludges. *Water Science and Technology* 22 (12). 135-142.

Vaxelaire, J., Cezac, P., 2004. Moisture distribution in activated sludges: a review, *Water Research* 38, 2215–2230.

A4. A 2-D Distributed Model of Transport Phenomena in a Porous Media Biodrying Reactor

A 2-D Distributed Model of Transport Phenomena in a Porous Media Biodrying Reactor [1]

Shahram Navaee-Ardeh, François Bertrand, Paul R. Stuart
Chemical Engineering Department, École Polytechnique de Montréal, Canada

Running head: "Continuous biodrying process for pulp and paper sludge"

Correspondences: 1) François Bertrand, Chemical Engineering Department, École Polytechnique de Montréal, C.P. 6079, succ. Centre-ville Montréal, H3C 3A7, Canada; E-mail: francois.bertrand@polymtl.ca; Tel. +(1) 514-340-4711 ext. 5773; fax: +(1)514-340-4105
2) Paul Stuart, Chemical Engineering Department, École Polytechnique de Montréal, C.P. 6079, succ. Centre-ville Montréal, H3C 3A7, Canada, Email: paul.stuart@polymtl.ca, Tel: (+1)514-340-4711 Ext. 4384, Fax: (+1)514-340-5150

Abstract

A novel continuous biodrying reactor has been developed for drying pulp and paper mixed sludge to raise the dry solids levels so that the dried sludge can be combusted economically in a biomass boiler for energy recovery. In our previous modeling study, a 1-D model was developed to better understand the prevailing transport phenomena in the biodrying reactor, based on lumped parameters in the gas flow direction. The model did not predict the two-dimensional nature of the transport phenomena in the continuous biodrying reactor, especially under conditions of high levels of aerobic exothermicity which are likely to arise in this industrial biodrying process. Therefore, the aim of this work was to develop a 2-D model that follows the same approach as the 1-D model but also takes into account coupled mass, heat, and biological transport processes for both gas and solid flow directions. This model was solved numerically using the finite element method. The predicted temperatures reflect the two-dimensionality of the transport phenomena in the biodrying reactor. Despite some discrepancies between the temperature predicted by this model and the experimental data, the estimated water removal rates are in good agreement with measured ones. It was found that only one third of the total water removal takes place in the convection-dominated zone of the reactor, whereas the rest takes place in its bioheat- and mass-diffusion-dominated zone. It was also found that conduction heat transfer plays only a minor impact on the matrix temperature, relative to the bioheat source term and evaporative heat sink term that play important roles.

Keywords: Biomass, pulp and paper mixed sludge, biodrying, porous media, 2-D model, transport phenomena, water removal rate.

INTRODUCTION

Navaee-Ardeh et al. [1, 2, 3] developed a novel continuous biodrying reactor for pulp and paper mixed sludge. The biodrying reactor troubleshooting, the reactor performance assessment, and the key variables analysis have been published earlier.[2,3] These studies revealed that the continuous biodrying reactor is a reliable process for drying pulp and paper mixed sludge to economic dry solids levels, and that the outlet air relative humidity profile was the key variable in the process. The experimental set-up includes two pilot-scale vertical stainless-steel reactors, each of which is 200 cm high (effective height is 160 cm), 100 cm deep and 40 cm wide. One of the

[1] This paper is under review at Drying Technology

reactors is fully instrumented and controlled online, and the other is used to generate additional data for repeatability purposes. The instrumented biodrying reactor permits online monitoring of internal temperature and pressure, changes in CO_2 levels due to exothermic biological reaction, relative humidity, and temperature of the inlet and outlet airstreams (Figure 1). The continuous reactor is divided into four compartments and is provided with feed and discharge ports (Figure 1). The dried sludge is extracted by two parallel screws installed at the bottom of the reactor and the fresh mixed sludge and recycle sludge (obtained from the discharge of the biodryer) are mixed in a 40-liter container prior to manual feeding it into the top of the reactor. Air flow is provided by two blowers, one pushing the air into the porous matrix and one pulling it out. It is uniformly distributed in each compartment through a series of perforated plates. When the screws turn, the materials flow downward due to gravity. More details of the experimental set-up can be found in Navaee-Ardeh et al. [2,3].

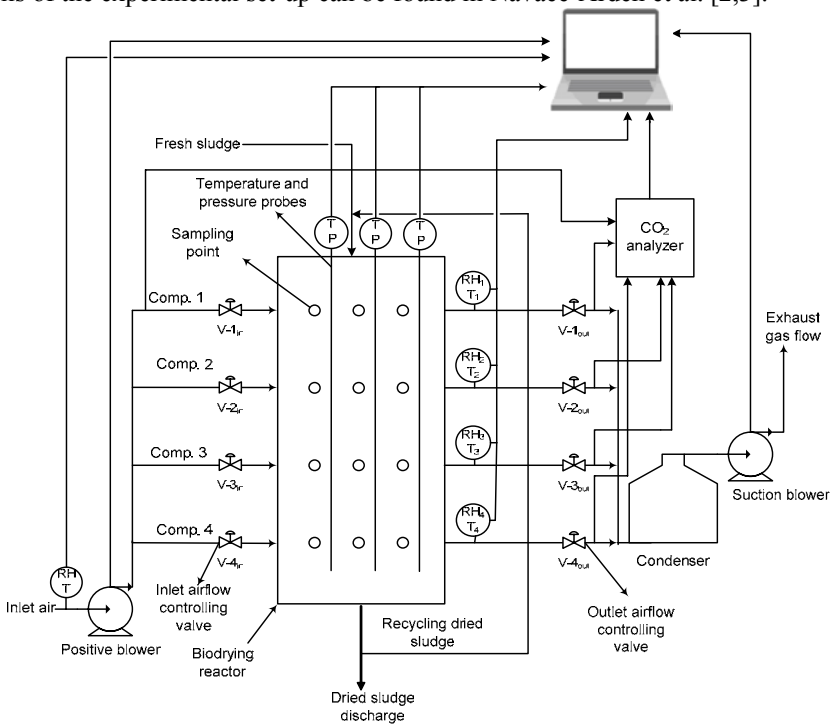

Figure 1 Schematic of pilot-scale set-up

Modeling of the biodrying process is helpful for better understanding of the transport phenomena prevailing in the reactor as well as for scale-up and control. In our previous study,[2] a simple 1-D model was developed to investigate the dominating transport phenomena in the continuous biodrying reactor. The 1-D model was based on lumped parameters in the gas flow direction and distributed parameters in the solid flow direction. This means that an average temperature was solved for in the gas flow direction. Although good agreement was obtained between the predicted temperature and the experimental data, the water removal rate for the higher aerobic exothermic zones of the reactor (the 3rd and 4th compartments) showed significant discrepancies. In fact, the usefulness of the 1-D model was observed to be limited to cases where the temperature variation in the gas flow direction at a given height was very small. In other words, the 1-D model is a useful tool for cases in which the so-called complexity index in the biodrying reactor is low.[3] Our experimental observations thus revealed that the transport phenomena in the continuous biodrying reactor are two-dimensional. The third dimension of the reactor helps increase the capacity of reactor.

The objective of this work is to introduce a 2-D model of the transport phenomena prevailing in the continuous biodrying reactor for drying pulp and paper mixed sludge. First, the model is presented. Its accuracy is next assessed through a comparison with experimental data obtained from the pilot-scale reactor. The 2-D model results are then used to estimate the water removal rate in the biodrying reactor, and the values obtained are compared to those predicted by the 1-D model as well as to the experimental data.

METHODOLOGY

In this section, first the material characterization is briefly introduced following Navaee-Ardeh et al. [2]. The 2-D modeling procedure is discussed, and the steps that were taken differently from the 1-D model are fully described. In particular, temperature data in the gas flow direction are used in their original (not averaged) form for the 2-D model assessment. These data are then used to estimate the water removal rate for the biodrying reactor.

Material characterization

The mixed sludge was a mixture of primary (45% w/w) and secondary (55% w/w) from an Eastern Canadian TMP pulp mill. The material characterization including mixed sludge analysis and other experimental measurements are explained in detail in Navaee-Ardeh et al. [2].

Modeling

A 2-D distributed model of global heat transfer is introduced, which follows along the line of Navaee-Ardeh et al. [2]. Based on concepts of chemical and biochemical reaction engineering in porous media, it includes biological heat, evaporative heat, and convective and conductive heat transfer due to the solid and gas phases. Two types of convective heat transfer are represented: convection due to the solid phase, which brings into play sensible heat, and convection due to the gas phase.

All assumptions made for the 1-D model and described in Navaee-Ardeh et al. [2] are valid except:

- Specific heat capacities of the solid and gas phases are not constant;
- Heat conduction due to gas phase is negligible and only heat conduction in solid phase in both directions is considered;
- Gas flow distribution is not uniform and follows the ideal gas law (see Table 1).

Each compartment is discretized in the *x* and *z* directions as illustrated in Figure 2.

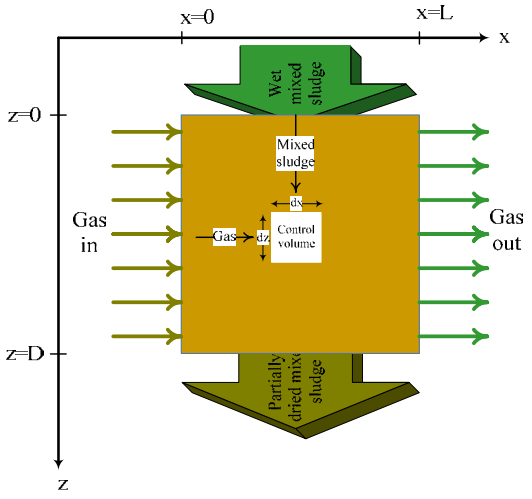

(a)

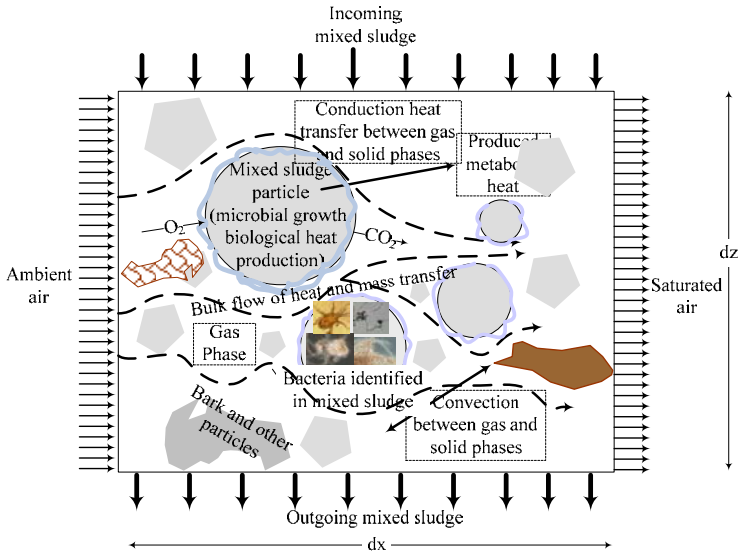

(b)

Figure 2 Schematic of a control volume at (a) macroscopic and (b) microscopic scales

Based on the assumptions and the control volume, and the heat transfer mechanisms illustrated in Figure 2, the following energy balance is obtained for the control volume in each compartment:

Conductive heat transfer due to solid phase in vertical direction

Conductive heat transfer due to solid phase in gas flow direction

$$W\frac{\partial}{\partial z}((1-\varepsilon_i)k_s\frac{\partial T_i}{\partial z})dzdx + W\frac{\partial}{\partial x}((1-\varepsilon_i)k_s\frac{\partial T_i}{\partial x})dzdx$$

$$-\frac{\partial(\Delta H_{eva,i}(T_i)X_i(x)d\dot{m}_{g,i})}{\partial x}dx \quad \text{Evaporative heat sink term}$$

$$-\frac{\partial(Cp_{g,i}d\dot{m}_{g,i}(T_i-T_r))}{\partial x}dx \quad \text{Convective heat transfer due to gas phase}$$

$$-\frac{\partial}{\partial z}\left(d\dot{m}_{s,i}Cp_{mix,i}(T_i-T_r)\right)dz + \dot{Q}_{bio,i}W(1-\varepsilon_i)dxdz = 0 \qquad (1)$$

Sensible heat transfer due to solid phase

Biological heat source term

i=1,2,3,4

The description of these terms can be found in Navaee-Ardeh et al. [2]. Note that the conductive heat transfer due to the solid phase in both directions is included in the 2-D model.
The following comments are in order:

- The mass flowrate of solid phase obtained from $d\dot{m}_{s,i} = \frac{\dot{m}_{total}}{LW}dx$;
- The mass flowrate of gas phase is given by $d\dot{m}_{g,i} = u_{g,i}\varepsilon_i\rho_{g,i}Wdz$;
- The biological heat was determined using the same approach as described in Navaee-Ardeh et al. [2];
- Reference temperature (T_r) is chosen to be that at the inlet (T_{in});
- Cp_{mix} is modeled as function of the reactor height $Cp_{mix} = az^2 + bz + c$, where coefficients *a, b,* and *c* are set from experimental data (see Table 3);

- Due to the difficulty of finding an appropriate global bioheat model for the entire biodrying reactor, experimental bioheat values were used for the 1st and 2nd compartments (see Table 3), and correlation in Table 1 was employed for the other compartments.

Based on these assumptions, Eq. (1) leads to the following differential equation:

$$
\begin{aligned}
&-\frac{\partial}{\partial x}((1-\varepsilon_i)k_s\frac{\partial T_i}{\partial x})-\frac{\partial}{\partial z}((1-\varepsilon_i)k_s\frac{\partial T_i}{\partial z})\\
&=\dot{Q}_{bio,i}(1-\varepsilon_i)-(T_i-T_{in})\frac{\dot{m}_{total}}{LW}\frac{\partial Cp_{mix,i}}{\partial z}\\
&-u_{g,i}\varepsilon_i\rho_{g,i}\left((T_i-T_{in})\frac{\partial Cp_{g,i}}{\partial T_i}+Cp_{g,i}+X_i\frac{\partial \Delta H_{eva,i}}{\partial T_i}+\Delta H_{eva,i}\frac{\partial X_i}{\partial T_i}\right)\frac{\partial T_i}{\partial x}\\
&-Cp_{mix,i}\frac{\dot{m}_{total}}{LW}\frac{\partial T_i}{\partial z}
\end{aligned}
\tag{2}
$$

Note that this equation can be written as:

$$\vec{\nabla}.(-k\vec{\nabla}T)=Q-\rho\mathrm{Cp}\vec{\mathbf{u}}.\vec{\nabla}T \tag{3}$$

where

$$k=\begin{pmatrix}k_s(1-\varepsilon_i) & 0\\ 0 & k_s(1-\varepsilon_i)\end{pmatrix}$$

$$\rho\mathrm{Cp}\vec{\mathbf{u}}=\begin{pmatrix}u_{g,i}\varepsilon_i\rho_{g,i}\left((T_i-T_{in})\frac{\partial Cp_{g,i}}{\partial T_i}+Cp_{g,i}+X_i\frac{\partial \Delta H_{eva,i}}{\partial T_i}+\Delta H_{eva,i}\frac{\partial X_i}{\partial T_i}\right) & 0\\ 0 & Cp_{mix,i}\frac{\dot{m}_{total}}{LW}\end{pmatrix}$$

$$Q=\dot{Q}_{bio,i}(1-\varepsilon_i)-\frac{\dot{m}_{total}}{LW}(T_i-T_{in})\frac{\partial Cp_{mix,i}}{\partial z}$$

Using the boundary conditions, $T(0, z)=T_{in}$ and $T(x,0)=T_{in}$, the set of four partial differential equations given in Eq. (2) were solved numerically using the convection-conduction heat transfer module in COMSOL Multi-physics (Version 3.5). Navaee-Ardeh et al. [2] found that in the continuous biodrying reactor the convection heat transfer is greater than the conduction one. Therefore, a convective flux boundary condition, $\mathbf{n}.(-k\nabla T)=0$, was prescribed along the other two sides of the computational domain.

Preliminary simulations were done with coarse and fine meshes of P_2 Lagrange- quadratic triangular elements, which showed that the use of a 182 finite element mesh was adequate. Consequently, all simulations discussed in the next section were carried out with this mesh.

Table 1 Parameters in 2-D model

Parameter	Correlation, expression or value	Reference
$Cp_{g,i}$	$1005+1880X_i$	[6]
$\Delta H_{eva,i}$ (J/kg H_2O)	$2320226-2427T_i$	[6]
ε_i	$0.125z_i+0.375$	Biodrying experiment
$\rho_{g,i}$ (kg/m^3)	1.16	[6]
$u_{g,i}$(m/s)	$(\frac{T_i+273}{T_{in}+273})\frac{Q_{g,i}(m^3/h)}{16.25}$	Biodrying experiment
RH (%)	$16.06+\frac{84.4(100x)}{1.24+(100x)}$	Biodrying experiment
$\dot{Q}_{bio,i}$ (W/m^3)	$(\frac{T_i+273}{T_{in}+273})\delta_1 e^{\delta_2 z_i}$	Biodrying experiment
X_i (kg H_2O/kg Air)	$0.622\times\left(\frac{\frac{RH_i}{100}\times 10^{(8.896-\frac{2233}{T_i+273})}}{760-\frac{RH_i}{100}\times 10^{(8.896-\frac{2233}{T_i+273})}}\right)$	[7]
D(m)	0.4	Pilot-scale set-up
k_s (W/kg)	0.15	[6]
L(m)	0.4	Pilot-scale set-up
W (m)	1	Pilot-scale set-up

RESULTS

In this section, the accuracy of the 2-D model is assessed by means of data obtained from three experiments that are fully described in a related paper [2] and that are briefly recalled here. Total water removal rates are then estimated using results of the 2-D model, and are compared to experimental values as well as to those predicted by our 1-D model in Navaee-Ardeh et al. [2].

Assessment of 2-D Model Accuracy

Table 2 shows the overall experimental program considered in Navaee-Ardeh et al. [2]. Three experimental runs that represent the diversity of the operating conditions are chosen from this experimental program for the 2-D model assessment. The recycle ratios were chosen following Frei et al. [4] for acceptable pneumatic conditions in the porous matrix of mixed sludge, and the residence times were determined from the work of Roy et al. [5] for an economically feasible batch biodrying process. Feed and discharge were carried out twice a day with a mass flowrate of 10-22 kg (d.b). A more comprehensive description of the overall experimental program can be found in Navaee-Ardeh et al. [2,3].

Table 2 Overall experimental program from Navaee-Ardeh et al. [2]

Run	Case	Residence time (days)	Recycle ratio (%)	Total air flowrate (m^3/h)	Outlet relative humidity (%)
1		4	15	34	
2	1	4	15	28	
3		4	30	28	
4		4	30	34	
5		8	15	34	
6	3	8	15	28	
7		8	30	28	
8		8	30	34	
9		6	30	75	85,85,85,85
10	2	6	30	46	96,96,96,96
11		6	30	55	85,85,96,96
12		6	30	64	96,96,85,85

Fixed and case-dependent parameters required by the model can be found in Table 1, respectively. Note that, in the all cases the results reported correspond to steady-state conditions.

Table 3 Experimental parameters required for the 2-D model

	Case 1				Case 2				Case 3			
	Comp 1	Comp 2	Comp 3	Comp 4	Comp 1	Comp 2	Comp 3	Comp 4	Comp 1	Comp 2	Comp 3	Comp 4
$Q_{g,i}$ (m^3/h)	7.91	7.41	7.31	7.38	16.5	8.0	14.0	7.7	7.04	7.11	7.63	7.65
$\dot{Q}_{bio,i}$ (W/m^3)	511	402	1200	2800	494	511	1770	2000	0	50	2000	3500
E_i	0.53	0.45	1.17	1.96	0.20	0.65	1.13	1.5	0.00	0.07	1.15	1.32
RT (days)	4				6				8			
RR (%)	15				30				15			
T_{in} (^{o}C)	26				24				26			
RH_{in} (%)	12				14				10			
a	156.8				78.1				51.6			
b	102.5				274.7				408			
c	3054				2891				2759			
δ_1(m^{-1})	1.38				1.56				1.68			
δ_2(W/m^3)	322.5				210				336.7			

Table 4 shows the experimental temperature data required for the 2-D model assessment for three cases. Note that, the experimental observations with a perforated (for gas phase) and a stainless steel (for solid phase) thermocouples revealed very small differences (<4%) between the gas and the solid phase temperatures. Therefore, the experimental data in Table 4 are counted for both solid and gas phases (thermal equilibrium).

Table 4 Experimental temperature in the continuous biodrying reactor for cases 1, 2, and 3

		T_{in} (°C)	x=7.5 cm	x=17.5 cm	x=27.5 cm	T_{out} (°C)
Case 1	Comp. 1	27	12	20	27	29
	Comp. 2	27	14	16	23	30
	Comp. 3	27	18	26	30	31
	Comp. 4	27	29	44	54	34
Case 2	Comp. 1	25	15	16	17	24
	Comp. 2	25	17	18	23	25
	Comp. 3	25	19	28	38	28
	Comp. 4	25	30	38	47	43
Case 3	Comp. 1	26	18	20	23	23
	Comp. 2	26	13	14	20	24
	Comp. 3	26	22	30	42	36
	Comp. 4	26	43	50	56	40

Temperature Profile in the Gas Flow Direction

The accuracy of the 2-D model is first assessed by comparing the numerical results to the experimental data in the gas flow direction. Although different operating conditions is expected to result in different temperature profiles in all four compartments, Figure 3 shows that the overall trend is fairly similar for all cases. The experimental error was estimated at ±3% using 5 temperature measurements taken at a typical location in the reactor. Overall, the predicted temperatures are in good agreement with the experimental data. The largest discrepancies were observed in the 4th compartment (about 30%). This is believed to be due to the complexity of the microbial growth behavior of the mesophilic and thermophilic microorganisms, which are not only space- and temperature-dependent but are also influenced by the moisture and nutrient availability in the matrix. In fact, the bioheat model (Table 1) does not take into account the effect of C/N ratio and moisture content. It was reported elsewhere that these two parameters also have a strong impact on the microbial growth in the aerobic composting processes.[7] Several global bioheat models were developed and tested in this study, but were not accurate enough to estimate the bioheat in different compartments.

Note that a thorough investigation of the velocity profile would require adding momentum equation to the current set of equations, which would result in a more complex system to be solved. Therefore, only a flat velocity profile based on ideal gas law was used in all simulations.

The numerical results in the gas flow direction are presented in Figure 3. Due to a rapid exchange between the gas and the solid phases, a sharp decrease can be noticed in every compartment when it enters the reactor (x<7.5 cm). In fact, this type of porous medium is known to be a very efficient heat exchanger.[8,9] However, one may observe that the temperature tends to increase in the second section (x>7.5 cm) of each compartment. The extent of this temperature rise depends on the quantity of bioheat generated in each compartment. More precisely, in the 3rd and 4th compartments, after a slight decrease (up to x=7.5 cm), the temperature increases all the way to the gas outlet in the reactor. This is mainly due to the availability of higher biological heat and exothermic activity of thermophilic bacteria (see Table 3). In the 1st and 2nd compartments, because of an evaporative heat dominating mechanism, the matrix temperature does not recover as much and stays below the inlet gas temperature.

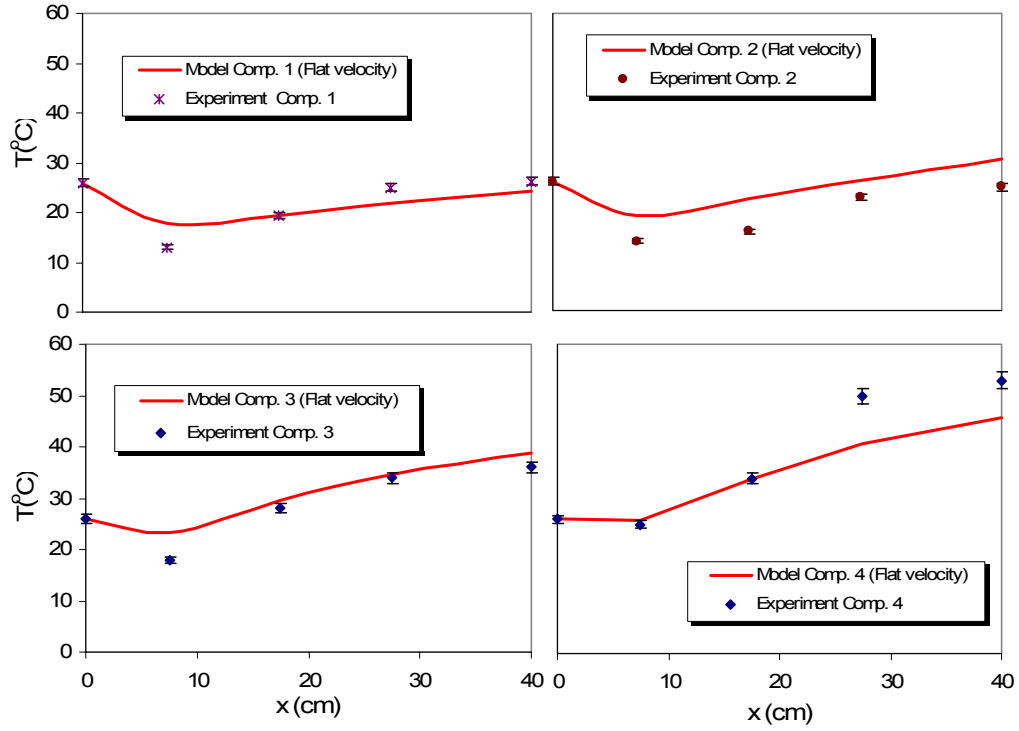
Model Comp. 1 (Flat velocity)
Experiment Comp. 1
Model Comp. 2 (Flat velocity)
Experiment Comp. 2
Model Comp. 3 (Flat velocity)
Experiment Comp. 3
Model Comp. 4 (Flat velocity)
Experiment Comp. 4
T(°C)
x (cm)

Case 1

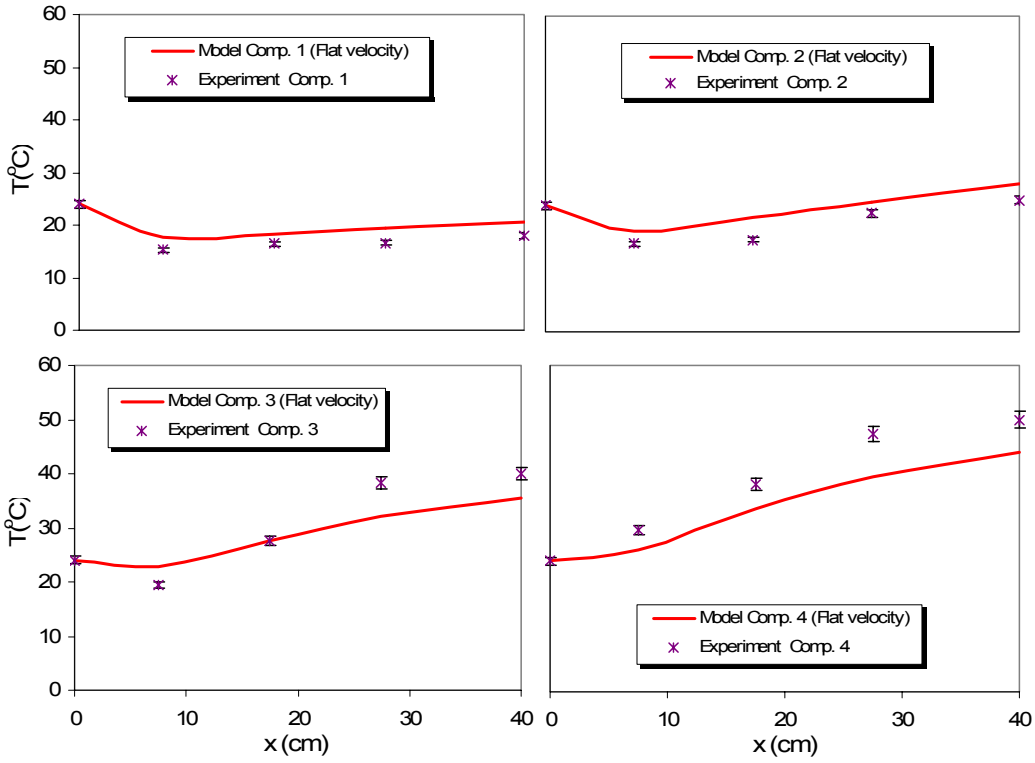
Model Comp. 1 (Flat velocity)
Experiment Comp. 1
Model Comp. 2 (Flat velocity)
Experiment Comp. 2
Model Comp. 3 (Flat velocity)
Experiment Comp. 3
Model Comp. 4 (Flat velocity)
Experiment Comp. 4
T(°C)
x (cm)

Case 2

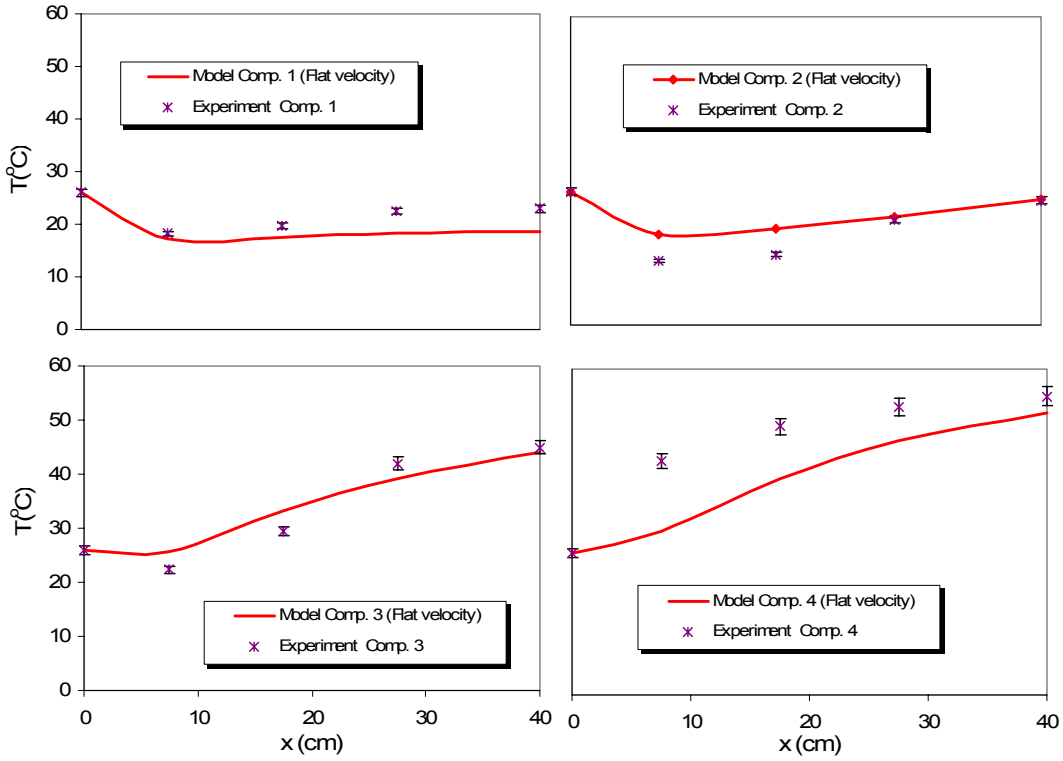

Case 3

Figure 3 Predicted temperatures vs. experimental data in the gas flow direction

Temperature Profile in the Solid Flow Direction

Figure 4 compares the numerical results obtained with the 2-D model to the experimental data. Only case 3 is considered here because similar behavior was observed in the other two cases. As can be seen in Figure 4, there is a good agreement between the experimental data and these numerical results. The upper bound discrepancy observed in the first section (x<7.5 cm) of the 4th compartment is 30%. However, this discrepancy decreases when approaching to the gas outlet. Possible explanations are due to the gas flow pattern at the entrance of each compartment or the dependency of the biological heat on the mixed sludge moisture content and nutrition level (C/N). The higher temperature in the 4th compartment favors the exponential growth rate of thermophilic bacteria, resulting in higher bioheat release into the matrix of mixed sludge and more bound water diffusion toward the surface of the particles.

In all cases, two zones can be recognized for the temperature profile in the biodrying reactor: a convection-dominated zone that is comprised of the 1st and 2nd compartments, and a diffusion- and bioheat-dominated zone that is comprised of the 3rd and 4th compartments. Consistent with the results of the 1-D model in the first zone, a large drop in the matrix temperature can be observed. This can be explained by the values of the bioheat to evaporative heat ratio (E_i) (see Table 3) that are smaller in the first zone, which means that the biological heat is not large enough to raise the temperature of the matrix. The dependence of this ratio on the temperature profile was observed in one of the related papers.[2] It was then established that the temperature decreases when $E_i<1$ and increases when $E_i>1$.

In the second zone (the 3rd and 4th compartments) the higher bioheat results in a significant temperature rise in the matrix of mixed sludge. Navaee-Ardeh et al. [2] stated that the moisture content in these compartments leads to enhanced microbial activity. The diffusion of bound water out of the sludge particles is favored by higher temperature, which also speeds up drying. In the biodrying reactor, water removal mainly takes place in the second zone, because of the higher matrix temperature in this zone. This can be inferred from Figure 5 where it shows that more than 70% of the total water removal takes place in the second zone. Note that, as a rule of thumb, an increase

of 11°C in temperature causes a 50% drop in the air relative humidity,[6] which improves mass transfer from the solid phase to the gas phase.

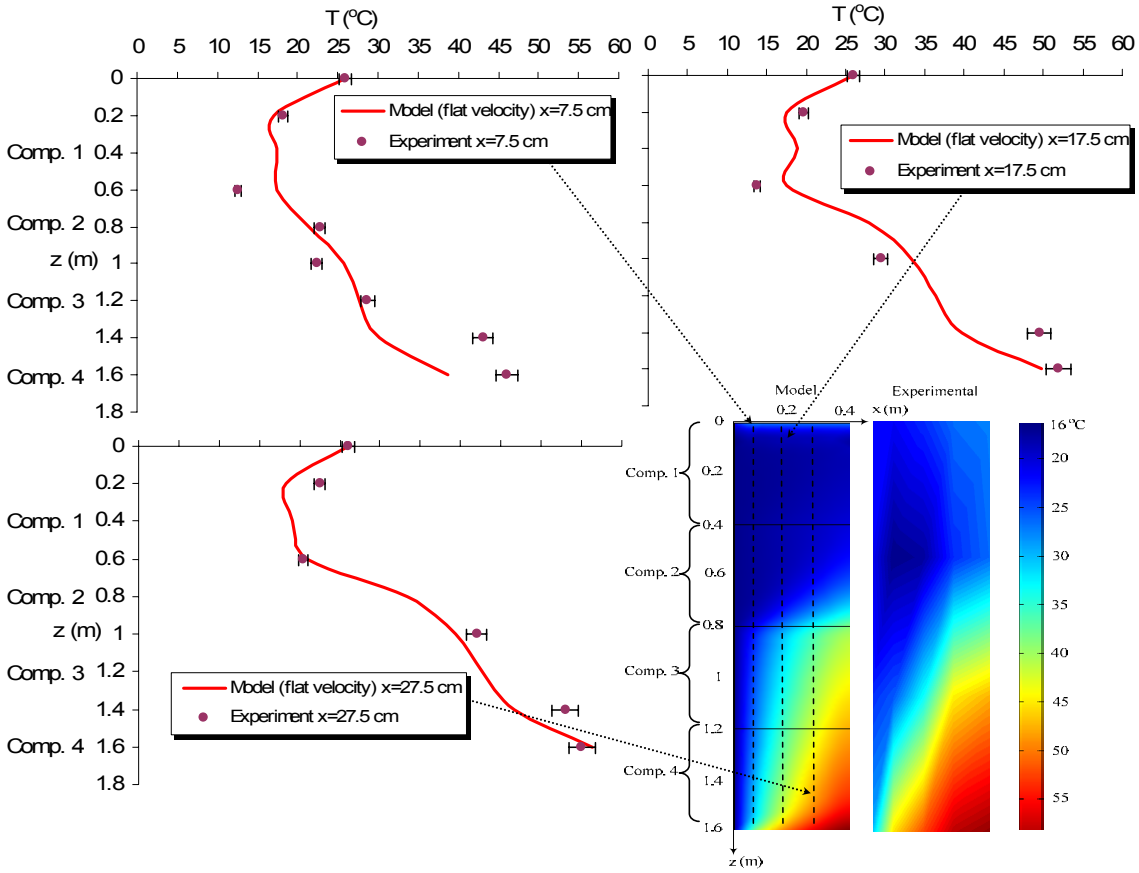

Figure 4 Predicted temperatures vs. experimental data in solid flow direction

The discrepancies between the experimental data and the model predicted values in the gas and solid flow directions are not only due to the experimental error. Other possible causes are: (1) the presence of anaerobic zones due to uneven distribution of gas velocity profile which were not investigated, (2) the complex mechanisms of water diffusion out of the particles in the mixed sludge which was not taken into account, (3) the numerical error inherent to the estimation of bioheat, and (4) the possibility of local thermal non-equilibrium which was not considered.

Water Removal Rate

The final level of dry solids content in the mixed sludge depends on transfer mechanisms that were discussed in the previous section. The amount of water removed from the sludge depends on the temperature in the reactor in the gas flow direction. The water removal rate (*WRR* (kg/day)) can be determined using the following relationship:

$$WRR_i = 24(X_{out,i} - X_{in})Q_{g,i}\rho_g \qquad i=1, 2, 3, 4 \tag{4}$$

In order to determine the absolute moisture content of the gas into (X_{in}) and out of (X_{out}) the reactor, two components must be proven: temperature and relative humidity. The temperature is predicted by the 2-D model, and the relative humidity is determined from experimental data by means of the correlation given in Table 1.

Figure 5 shows that the water removal rates predicted for all three cases are in good agreement with the experimental data, which confirms the usefulness of the 2-D model developed in this work. It also highlights the limitations of the 1-D model,[2] more specifically in the 3rd and 4th compartments in the gas flow direction where more important temperature variations were observed (Figure 3). As stated earlier, more than 70% of the total water removal takes place in the bioheat- and mass-diffusion-dominated zone (the 3rd and 4th compartments). This implies that a better water diffusion and removal rate may be achieved using a smaller particle size.

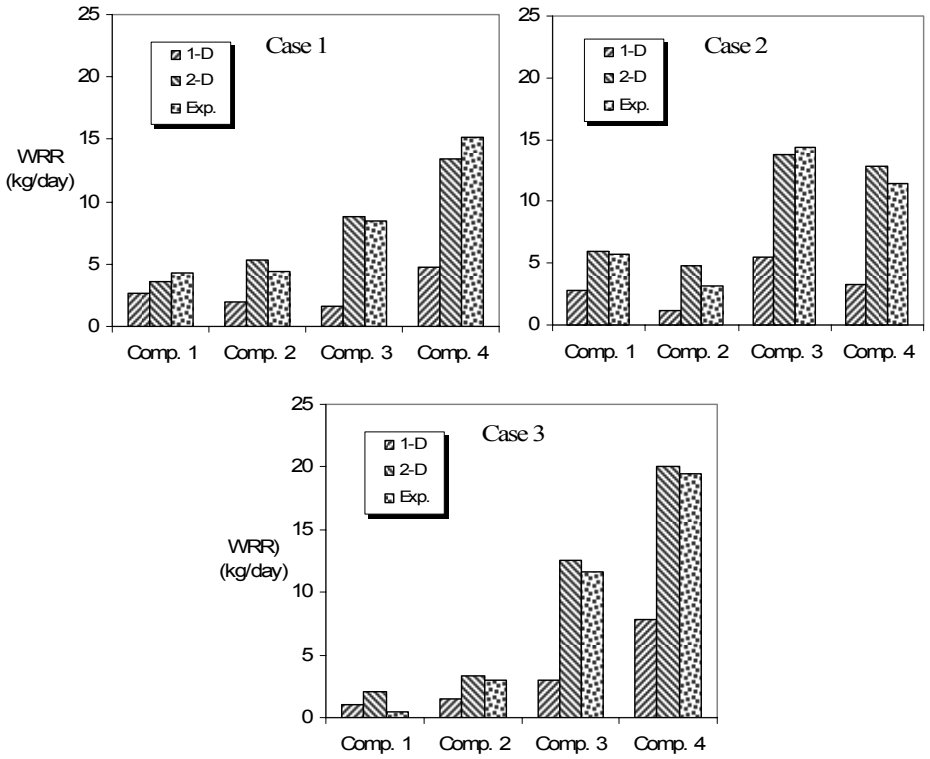

Figure 5 Water removal rate (WRR): numerical results vs. experimental data

Figure 6 shows the water removal rate down the reactor height for case 3. Two steep rises in the water removal rate were observed at the end of the 2nd and 4th compartments. This trend supports the vertical variation of dry solids content in the biodrying reactor.[2] Microbial count measurements showed that these sharp rises are related to the maximum microbial activity of the mesophilic bacteria at the end of the 2nd compartment and the thermophilic bacteria at the end of the 4th compartment, respectively.

These results show the implication of the 2-D model for design of a continuous biodrying reactor.

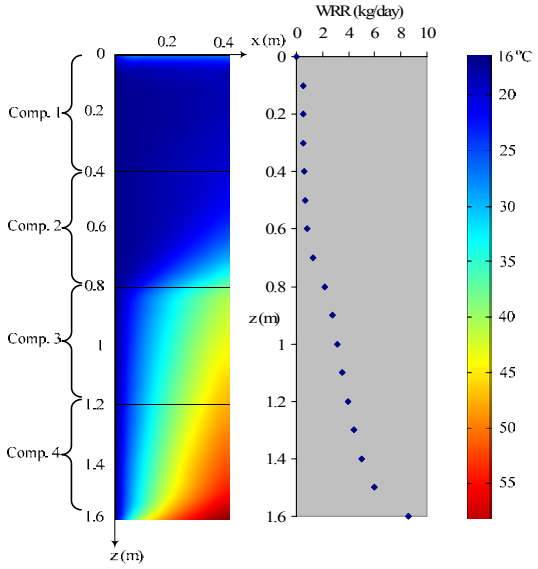

Figure 6 Vertical profile of water removal rate in the continuous biodrying reactor (case 3)

Finally, Table 5 summarizes the advantages and limitations of the 1-D and 2-D models.

Table 5 Comparison between the 1-D and 2-D models

	Advantage	Limitations or drawbacks
1-D model	- Analytical solution - Easy to perform sensitivity analysis - Good agreement with the averaged temperature	- Unable to predict temperature variation in the gas flow direction - Uses constant physical parameters - Cannot handle complex microbial growth mechanisms - Uses constant values of bioheat in each compartment - Inaccurate in the bottom compartments - Poorly predicts the water removal rate - Cannot vary the gas velocity profile
2-D model	- Predicts the temperature in both solid and gas flow directions - Can vary the gas velocity profile - Can handle variable physical parameters - Good agreement with actual experimental data both for the solid and gas flow directions - Can handle complex microbial growth mechanisms - Accurately predicts the water removal rate	- No analytical solution - Bioheat model does not take into account the moisture content and C/N ratio

CONCLUSIONS

A 2-D distributed model was developed and solved numerically using the finite element method. It simulates transport phenomena including particularly heat transfer in a continuous biodrying reactor for the treatment of pulp and paper sludge. The model can predict the temperature profile in the porous matrix of this reactor in both gas and solid flow directions. The 2-D results were shown to be in satisfactory agreement with the experimental data.

The 2-D model was used for the estimation of water removal rates in the biodrying reactor. It was found that the values estimated with this model were in good agreement with the measured values.

The transport phenomena prevailing in each of the four compartments of the reactor were investigated. Consistent with the results of the 1-D model, it was found that the continuous biodrying process is governed by a convection-dominated heat transfer at the top of the reactor where more unbound water exists, whereas the water diffusion and the bioheat play a dominant role at its bottom.

The gas flow temperature plays critical role in the estimation of the water removal rate. Unlike the 1-D model, by accounting for this gas flow temperature in the 2-D model, it was shown that more than 70% of the total water removal takes place in the water diffusion-dominated zone where the biological heat dominates the evaporative heat. This indicates that, since the diffusion is the main driving force in the biodrying process, further reduction in residence time in the diffusion zone of the biodrying may not be an appropriate strategy.

The 2-D model can be a useful tool for scale-up and design of the continuous biodrying reactor by simplifying it into a modified 1-D model based on the dominating transport phenomena at the top and at its bottom. This will be further considered in a forthcoming part of this modeling study, which will show a systematic strategy for a reactor design tool development. By performing dimensionless analysis on the 2-D model, we believe it is possible to develop scale-up criteria and interpret the dominant transport phenomena at the top and the bottom of the biodrying reactor relevant to the unbound and bound water removal.

ACKNOWLEDGMENTS

This work was carried out with the financial support of NSERC and FQRNT. The assistance of Carl Tchoryk, Kheng Huynh, Omar Ben Ndiaye and Antonin Paquet for the experimental part is gratefully acknowledged. Fruitful discussions with Dr. Christophe Devals from the Department of Chemical Engineering at Ecole Polytechnique Montreal, Prof. Tom Richard from the Department of Agricultural and Biological Engineering at Pennsylvania State University and Prof. Stephen Whitaker from the Department of Chemical Engineering at the University of California are also gratefully acknowledged.

NOMENCLATURE

a	Constant coefficient
b	Constant coefficient
c	Constant coefficient
$Comp\ i$	Compartment i, i=1,2,3,4
Cp	Arbitrary specific heat capacity (J/kg ^oC)
$Cp_{g,i}$	Specific heat capacity of gas phase in compartment i (J/kg ^oC)
$Cp_{mix,i}$	Specific heat capacity of solid phase in compartment i (J/kg ^oC)
D	Height of each compartment (m)
$d\dot{m}_{g,i}$	Mass flowrate of gas phase (kg/s)
$d\dot{m}_{s,i}$	Mass flowrate of solid phase (kg/s)
E_i	Ratio of bioheat to evaporative heat[2]
k	Thermal conductivity of matrix (W/(m^{o}C))
k_s	Thermal conductivity of solid phase (W/(m^{o}C))
L	Width of the biodrying reactor (m)
$\dot{m}_{total}$	Total mass flowrate of solid phase (kg/s)
$\dot{Q}_{bio,i}$	Bioheat generated through metabolic activity in compartment i (W/m^3), i=1,2,3,4
$Q_{bio\text{-}standard}$	Standard biological heat production in aerobic systems (J/ kg O_2)
$Q_{g,i}$	Gas flowrate in compartment i (m^3/h), i=1,2,3,4
RH_i	Relative humidity of gas phase in compartment i (%)
RH_{in}	Relative humidity of gas phase at the inlet (x=0) (%)
RR	Recycling ratio of biodried mixed sludge (%)
RT	Residence time (days)
T_i	Temperature of the matrix (^{o}C)
T_{in}	Temperature of gas phase at the inlet (x=0) (^{o}C) and initial temperature of feed mixed sludge (z=0) (^{o}C)
T_r	Reference temperature =T_{in} (^{o}C)
$\vec{u}$	Velocity vector (m/s)
$u_{g,i}$	Gas phase velocity (m/s)
W	Depth of the biodrying reactor (m)
WRR_i	Water removal rate in compartment i(kg/day), i=1,2,3,4
x	The axial distance from gas inlet in each compartment (m)
X_i	Absolute moisture content of gas phase in compartment i (kg H_2O/kg Air)
X_{in}	Absolute moisture content of gas phase at the inlet (x=0) (kg H_2O/kg Air)
$X_{out,i}$	Absolute moisture content of gas phase at the outlet of compartment i (x=0.4 m) (kg H_2O/kg Air)
z_i	Vertical distance from the reactor top (m)
Greek letters	
δ_1	Constant coefficient (W/m^3)
δ_2	Constant coefficient (m^{-1})
$\Delta H_{eva,i}$	Latent heat of water evaporation in compartment i (J/kg-H_2O)

$\vec{\nabla}$	Gradient operator (m^{-1})
ε_i	Porosity of the matrix in compartment *i* (-)
ρ	Arbitrary density (kg/m^3)
ρ_g	Density of the gas phase(kg/m^3)[10]

REFERENCES

1. Navaee-Ardeh, S.; Bertrand, F.; Stuart, P.R. Emerging biodrying technology for the drying of pulp and paper mixed sludges. Drying Technology **2006**, 24(7), 863-878.
2. Navaee-Ardeh, S.; Bertrand, F.; Stuart, P.R. Development and experimental verification of 1-D distributed model of transport phenomena in a continuous biodrying process for pulp and paper mixed sludge. Accepted at *Drying Technology* **2009a**.
3. Navaee-Ardeh, S.; Bertrand, F.; Stuart, P.R. Key variables analysis of a novel continuous biodrying process for drying pulp mixed sludge. Accepted at *Bioresource Technology* **2009b**.
4. Frei, K.M.; Cameron, D.; Stuart, P.R. Novel drying process using forced aeration through a porous biomass matrix. Drying Technology **2004**, 22(5), 1191-1215.
5. Roy, G.; Jasmin, S.; Stuart, P.R. Technical modeling of a batch biodrying reactor for pulp and paper mill sludge. *17th CHISA International Congress of Chemical and Process Engineering*, 2006.
6. Geankoplis, C.J. *Transport processes and unit operations*. Prentice Hall, NJ, USA, 1993.
7. Haug, R.T. *The Practical Handbook of Compost Engineering*. Lewis Publishers, Boca Raton, FL, USA, 1993.
8. Hayes, A.M.; Khan, J.A.; Shaaban, A.H.; Spearing, I. G. The thermal modeling of a matrix heat exchanger using a porous medium and the thermal non-equilibrium model. International Journal of Thermal Science **2008**, 47, 1306-1315.
9. Pavel, B.; Mohamad, I.; Abdulmajeed, A. An experimental and numerical study on heat transfer enhancement for gas heat exchangers fitted with porous media. International Journal of Heat and Mass Transfer **2004**, 47, 4939-4952.
10. Perry, R.H.; Green, D.W. *Perry's chemical engineers' handbook*. McGraw-Hill, USA, 1997.

APPENDIX B: Complementary Papers

B1. Heat and Mass Transfer Modeling of a Novel Biodrying Process: Lumped System Approach and Preliminary Results

Heat and Mass Transfer Modeling of a Novel Biodrying Process: Lumped System Approach and Preliminary Results [1]

Shahram Navaee-Ardeh, François Bertrand, Paul R. Stuart
École Polytechnique de Montréal, Chemical Engineering Department,
Montréal, Québec, CANADA, H3C 3A7

Abstract

Environmental restrictions have led landfilling of the pulp and paper mixed sludges almost impossible. The combustion of the mixed sludges in the boiler is currently a feasible alternative. However, the dryness of mixed sludges must be above critical levels (>42% w/w) in order to achieve stable boiler's operation and ensure the recovery of the sludge's calorific value. A novel batch biodrying process has been developed at Ecole Polytechnique Montreal whose goal was to valorize the mixed sludges by taking the advantage of biological heat naturally produced in the porous matrix as a result of exothermic metabolic activity of microorganisms. The preliminary results have shown the techno-economic viability of this process and led to the development of a continuous system with expected enhanced properties. The continuous biodrying reactor can be divided into four compartments each of which is governed by specific transport phenomena. Mixed sludges from the pulp and paper industry are full of moisture with highly porous and anisotropic macro and micro structures. Mathematical modeling of such porous matrix is a valuable tool for the design of the reactor as well as for the determination of a stable operating window that leads to an efficient techno-economic process. The objective of this paper is to present a comprehensive lumped model that describes heat and mass transfer in each of the four compartments. The underlying differential equations, which are solved in a coupled manner, allow for the effect of biological heat in the reactor. The dimensionless form of these equations reveals the significance of the Peclet number for heat transfer as well as that of a dispersion number for mass transfer. Numerical profiles of the temperature and moisture content in the porous matrix are also presented.

[1] This paper was presented at CSChE conference in 2006, Sherbrooke, Canada

B2: Distributed Model of a Continuous Biodrying Process for Drying Pulp and Paper Mixed Sludge and Comparison with Experimental Results

Distributed Model of a Continuous Biodrying Process for Drying Pulp and Paper Mixed Sludge and Comparison with Experimental Results[2]

Shahram Navaee-Ardeh, François Bertrand, Paul R. Stuart
École Polytechnique de Montréal, Chemical Engineering Department,
Montréal, Québec, CANADA, H3C 3A7

Abstract

A novel biodrying process is under development whereby aerobic activity enhances drying rates in a porous mixture of mixed sludge from a pulp and paper mill, rendering it suitable for combustion. A 1-D distributed mathematical model of transport phenomena inside the biodrying reactor was investigated. The temperature profile obtained from the model is in good agreement with the experimental data. This model shows that the transport phenomena in the biodrying reactor can be investigated numerically, which can lead in the long term to the development of efficient system design, process optimization and control strategies.

Introduction

Environmental restrictions have made landfilling of pulp and paper mixed sludge expensive which, when coupled with increasing energy costs, has made combustion an increasingly attractive sludge management option for many pulp and paper mills. However, for an efficient combustion of the sludge in woodwaste and other boilers, a sludge dryness of 40% w/w or more is required [1]. A novel continuous biodrying reactor is being developed at Ecole Polytechnique which dries mixed sludge based on the principle of different transport phenomena dominating at various levels of a vertical reactor. The sludge drying process relies to a great extent on the microbial heat produced by exothermic biodegradation reactions and forced aeration [2]. To date there is little information available for the modeling of biodrying reactors. By modeling the transport phenomena inside the biodrying reactor, it will be easier to better understand the process, which can lead eventually to more efficient reactor design, optimization and control.

Modeling

The continuous reactor is vertical and wet fresh mixed sludge enters from top and exits from the bottom. Mixed sludge moves down by gravity in a continuous manner and water removal from the porous matrix is enhanced by forced aeration cross each compartment. The reactor is nominally divided into 4 compartments which are geometrically equal (Figure 1). The heat and mass transfer equations have been solved for each compartment and the interconnection between adjacent compartments was used as a boundary condition. Biologically available heat, which is provided by microorganisms naturally available in the porous matrix, and water evaporation appear as source terms in the heat equations. Two terms, corresponding to convection and conduction heat transfer, are present in these equations in addition to the sensible heat entering and exiting each compartment. Uniform distribution of air was assumed in each compartment thus ignoring horizontal temperature variations within each compartment. The dry solids and water in mixed sludge were taken into account through sensible heat source terms.

Results and comparison

Figure 2 shows an example of the temperature variation from the top to the bottom of the biodrying reactor. The modeling results are in good agreement with the experimental data. Due to high moisture content of the fresh mixed sludge at the top of the reactor and high aeration conditions, the evaporative heat term dominates, resulting in a rapid decrease of temperature in the first compartment. However, as the sludge moves down the reactor, the

[2] This paper was presented at Pan-Pacific Conference in Vancouver in 2008

biological heat source term has a significant effect, resulting in the temperature rise in the reactor below 0.4 m. The air leaves the reactor at close to 100% relative humidity carrying higher moisture content and increasing the efficiency of the biodryer. Various operating conditions were investigated and, in most cases, the model was able to predict the behavior of this complex process with reasonable accuracy.

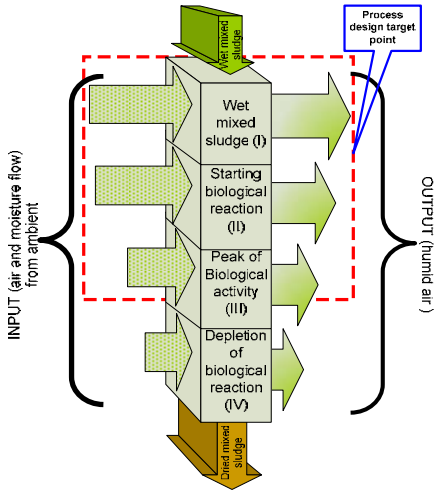

Figure 1. Schematic of continuous biodrying reactor

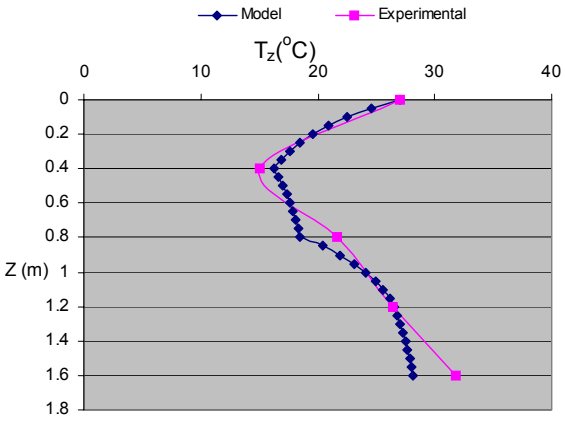

Figure 2. Experimental and predicted temperature profiles

Conclusions

A 1-D model was developed to investigate the transport phenomena occurring inside a continuous biodrying reactor developed at École Polytechnique de Montreal. The modeled values were in good agreement with experimental data for most conditions, showing that this 1-D model is a useful tool that can lead eventually to the development of efficient reactor design, process optimization and control.

References

1- Tsang, K. R.; Vesilind, P.A. Moisture distribution in sludges, Water Science and Technology 1990, 22(12), 135-142.

2- Navaee-Ardeh, S., Bertrand, F., Stuart, P., Emerging Biodrying Technology for the Drying of Pulp and Paper Mixed Sludges, Drying Technology, 2006, 24(7), 863-878.

B3: Novel continuous biodrying reactor: principles, screening experiments and results

Novel Continuous Biodrying Reactor: Principles, Screening Experiments and Results [3]

Shahram Navaee-Ardeh [a], Carl Tchoryk[a], Balázs Tolnai [b], François Bertrand [a], Paul R. Stuart [a]
[a]: Chemical Engineering Department, École Polytechnique Montreal.
[b]: Publication Papers Division, Kruger Inc.

Abstract

A novel continuous biodrying reactor is being developed at École Polytechnique, whose goal is to valorize pulp and paper mixed sludge for economic and efficient combustion in the boiler for steam generation. Drying rates are enhanced by biological heat produced by exothermic microbial reactions under forced aeration through the porous matrix of mixed sludge. Specific transport phenomena dominate in different zones of the reactor, and the variables having the greatest impact on drying rates are relative humidity of exit airflow and incoming sludge characteristics. In this paper, the principles of the continuous biodrying reactor will be presented, followed by a discussion on results obtained from screening experiments. Preliminary experiments have shown that mixed sludge entering at 38% w/w dryness can achieve 47% w/w dryness in approximately 4 days. This results in an economically-viable capital cost and significant reductions in fossil fuel otherwise needed to stabilize boiler operation.

[3] This paper was presented at CSChE conference in Ottawa in 2008

B4: Modeling and Experimental Verification of a Novel Biodrying Process for Drying Pulp and Paper Sludge

Modeling and Experimental Verification of a Novel Biodrying Process for Drying Pulp and Paper Sludge[4]

S. Navaee-Ardeh, F. Bertrand and P.R. Stuart
Chemical Engineering Department, Ecole Polytechnique Montreal

Abstract

A novel biodrying process has been developed whereby thermophilic and mesophilic aerobic activity enhances the drying rate of pulp and paper mixed sludge, to a solids level suitable for combustion. A 1-D distributed mathematical model of transport phenomena is used to investigate the temperature of the porous matrix and identify the parameters that are critical for the process. It is shown that temperature profiles obtained from this model are in good agreement with experimental data. A biodrying efficiency was defined which represents the ratio of biodegradation and evaporation rates. The predicted temperatures yielded biodrying efficiencies ranging from 65% to 90% depending on the operating conditions and the target sludge dryness.

Keywords: Biodrying, 1-D modeling, transport phenomena, pulp and paper mixed sludge

1. Introduction

On a yearly basis, the production of the pulp and paper mixed sludge in Canada is estimated to be about 2.6 million tons (Elliott and Mahmood (2005)). The mixed sludge consists of a complex mixture of microorganisms, fibrous materials, lignin, mineral components (limestone and phosphorus), clay, inert solids rejected during the recovery and water treatment process (Chen et al. (2002), Hippinen and Ahtila (2004)).

Historically, landfilling and landspreading have been commonly used for the management of pulp and paper mixed sludge. Sludge composting requires a relatively long residence time (30-50 days), and thus is is hardly feasible, given the large quantities of sludge produced in pulp and paper mills. Furthermore, environmental restrictions increasingly render landfilling and landspreading of the sludge difficult, which when coupled with increasing energy costs, has made combustion an increasingly attractive sludge management option for many pulp and paper mills. However, for an efficient combustion of the sludge in woodwaste and other boilers, a sludge dryness of 40% w/w or more is typically required (Kudra et al. (2002), Kraft and Orender (1993)). A novel continuous biodrying reactor has been developed by our research group which relies on the energy generated by the metabolic activity of aerobic mesophilic and thermophilic microorganisms naturally present in biological (secondary) sludge (Navaee-Ardeh et al. (2006)). There is little information available for the modeling of this type of process, which would provide insight into the transport phenomena governing sludge drying. The objectives of this paper are then to:

- Develop a 1-D distributed model of the transport phenomena inside the biodrying reactor
- Identify key parameters that are critical for the operation of the biodrying reactor
- Introduce a new definition of biodrying efficiency and use numerical results to estimate its value

2. Modeling

[4] This paper was presented at 4th Inter-American Drying Conference in 8th World Chemical Engineering Conference 2009

The continuous pilot-scale reactor is vertical (dimensions 40cm×100cm×200cm), and wet fresh sludge mixed with 30% (mass basis) of dried sludge is fed from the top and removed from the bottom of the biodrying reactor (Figure 1a and 1b).

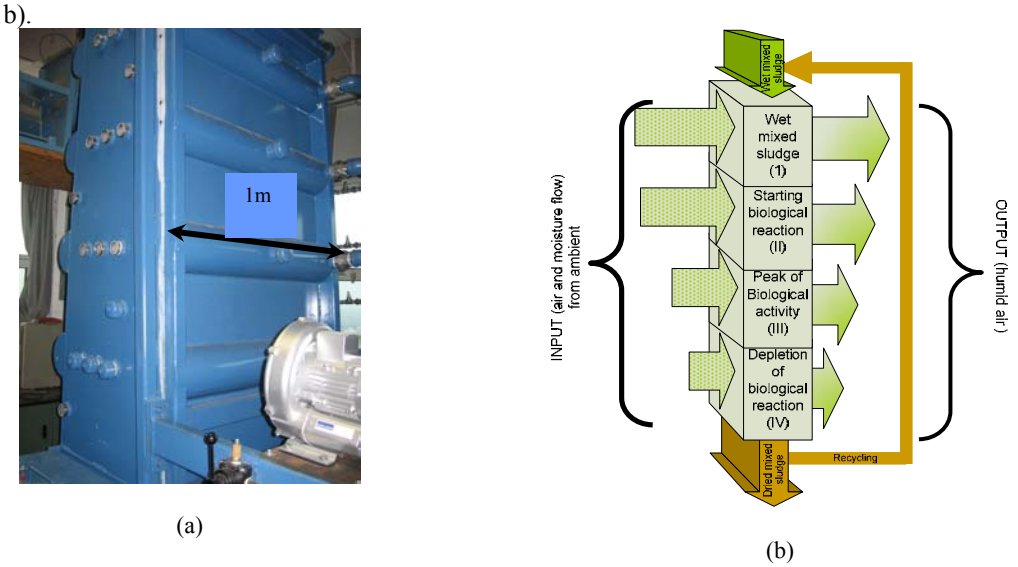

(a) (b)

Figure 1 Pilot scale biodrying reactor

Mixed sludge flows downward in a continuous manner in the reactor. Water removal from the porous matrix is enhanced by forced aeration across the reactor and through the sludge matrix, which can be divided into 4 compartments of equal size and shape (0.4m×1m×0.4m)(Figure 1a and b). Heat and mass transfer has been resolved separately for each compartment, and the interconnection between adjacent compartments taken into account through boundary conditions. Thermal convection and conduction are considered in the energy balance. Bioheat and water evaporation appear in the model as source and sink terms, respectively. Uniform distribution of air is also assumed and horizontal temperature variations in each of compartment are neglected. The dry solids and water in mixed sludge are taken into account through sensible heat source terms. This leads to the following 1-D energy balance:

Sensible heat term by solid and water

$$\dot{m}_{total,i}\left(w_{ms,i}cp_{ms,i}+(1-w_{ms,i})cp_{H_2O}\right)(T_{z,i}-T_r)\Big|_z-\dot{m}_{total,i}\left(w_{ms,i}cp_{ms,i}+(1-w_{ms,i})cp_{H_2O}\right)(T_{z,i}-T_r)\Big|_{z+dz}$$

$$-\underbrace{k_s(1-\varepsilon_i)LW\left.\frac{dT_{z,i}}{dz}\right|_z-\left(-k_s(1-\varepsilon_i)LW\left.\frac{dT_{z,i}}{dz}\right|_{z+dz}\right)}_{\text{Conduction term by solid and water}}+\underbrace{(d\dot{m}_{g,i})cp_g(T_o-T_r)-(d\dot{m}_{g,i})cp_g(T_{z,i}-T_r)}_{\text{Convection term by gas phase}}$$

$$+\underbrace{\dot{Q}_{bio.,i}(1-\varepsilon_i)dV}_{\text{Biological heat source term}}-\underbrace{\Delta H_{eva.}a_{w,i}(X_{outlet,i}-X_{inlet})d\dot{m}_{g,i}}_{\text{Evaporation cooling term}}=0 \qquad i=1,2,3,4 \qquad (1)$$

where $\dot{m}_{total,i}$ is the rate of wet material entering at the top of the reactor (kg/s), $cp_{g,i}$ and $cp_{ms,i}$ are the heat capacity of gas and mixed sludge ($J/kg\ ^oC$), respectively, k_s is the thermal conductivity of solid (W/m.^{o}C), dV is the volume of the compartment (m^3), $T_{z,i}$ is the temperature at a given height z, T_r is the reference temperature equal to T_o (^{o}C) (inlet air and sludge temperature), $w_{ms,i}$ is the mass solids fraction of mixed sludge, ε_i is the porosity of the medium, $a_{w,i}$ is the water activity, X_i is the absolute humidity of gas phase, L and W are length and width of each

compartment (0.4 and 1 m), respectively and $Q_{bio,i}$ (W/m^3) and ΔH_{eva} (J/kg H_2O) are the bioheat and evaporation heat, respectively.

The bioheat is directly determined from the O_2 consumption rate as follows:

$$Q_{bio} = Q_{bio-s\tan dard}\ \rho_{O_2}\left(\frac{V_{O_{2in}} - V_{O_{2out}}}{V_{Air}}\right)\frac{Q_g}{LWD} \tag{2}$$

where Qbio-standard is the constant 16 kJ/g-O2, obtained from Bailey and Ollis (1986), t is time period (h), Q_g is the gas flowrate (m^3/h), ρ_{O_2} is the oxygen density (1.35 kg/m^3), $\frac{V_{O_{2in}} - V_{O_{2out}}}{V_{Air}}$ is the oxygen consumption rate (v/v), and L,W, and D are length, depth and height of each compartment.

The evaporation heat of water, $\Delta H_{eva.}$, has a negative correlation with the temperature. In order to incorporate this into Eq. (1), a constant value of ΔH_{eva}=2270000 J/kg H_2O was used along with the correction factor, a_w, so that the last term in Eq. (1) remains constant for each compartment but varies from one compartment to another compartment.

Note that Eq. (1) leads to a convection-diffusion ordinary differential equation for each compartment that, along with boundary conditions $T_{z,1}(0)=T_0$, $T_{z,2}(0)=T_{z,1}(0.4)$, $T_{z,3}(0)=T_{z,2}(0.4)$, $T_{z,4}(0)=T_{z,3}(0.4)$ can be solved analytically.

3. Results and model verification

An example of the results obtained by solving the heat transfer equations is given in Figure 2. There is reasonable agreement between the model results and the experimental data. More precisely, there is a significant drop in temperature in the 1st compartment. The model predicts that this drop continues in the second compartment whereas the temperature values measured in the reactor remain higher. This discrepancy may be due to either the simplifying assumptions inherent in the 1-D model or the use of an average temperature in the gas flow direction. The bioheat dominates the evaporation heat in the 3rd compartment, which results in a positive value of the net heat in the matrix and a rise of the temperature through to the bottom of the reactor (4th compartment). Therefore, the reactor is characterized by the existence of two zones with phenomenologically different behaviors: a first zone, comprised of the 1st and 2nd compartments, within which cooling occurs owing to the water evaporation (free and interstitial moisture) and a second zone, comprised of the 3rd and 4th compartments, where the bioheat is mainly used to remove the bound water.

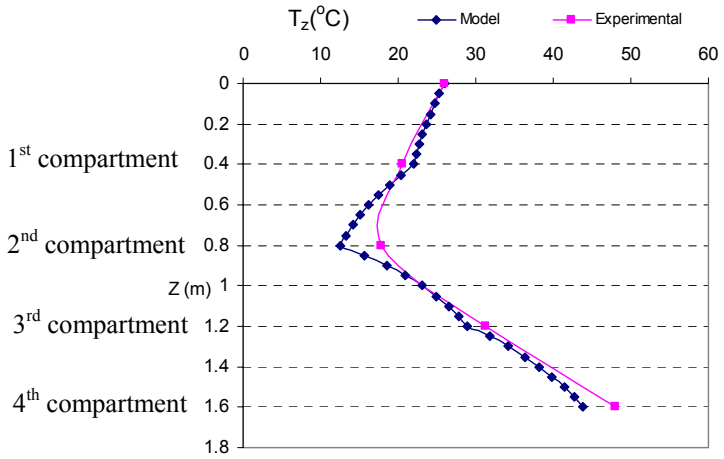

Figure 2: Temperature profile of porous matrix

Sensitivity analyses were used to identify that the oxygen consumption, the air flowrate and the water removal rate are key parameters for this biodrying process. Moreover, the biodrying efficiency, η, is defined as:

$$\eta = 1 - \frac{Total\ Carbon\ Loss}{Total\ Water\ Loss} \quad (3)$$

where the total water loss (TWL) is the evaporation rate and the total carbon loss (TCL) is used to evaluate the biodegradation rate.

Both TCL and TWL are highly dependent on the matrix temperature. For instance, the higher the temperature, the higher the carbon loss and the higher the water holding capacity of the carrying air. It was found that the biodrying efficiency can vary from 65% to 90% depending on the operating conditions and the final sludge dryness.

4. Conclusion

A 1-D model was developed to investigate the transport phenomena occurring inside a continuous biodrying reactor and was tested against experimental data. The model was observed to reasonably predict the experimental data, although discrepancies were noticed in the 2nd compartment. This may be due to the simplifying assumptions such as uniform distribution of the air flow, constant physical parameters and uniform distribution of the bioheat associated with the 1-D model. This has provided the impetus for the development of a 2-D model, currently underway. These models are unique and useful tools for the development and control of a novel biodrying process governed by complex transport phenomena which rarely been systematically studied before.

Acknowledgments

This work was supported financially by FQRNT and NSERC. The assistance of Carl Tchoryk, Kheng Huynh, Omar Ben Ndiaye and Antonin Paquet for the experimental work is gratefully acknowledged. The first author also acknowledges fruitful discussions with Prof. Jamal Chaouki and Prof. Mario Jolicoeur from the Department of Chemical Engineering at Ecole Polytechnique Montreal, and Prof. Tom Richard from the Department of Agricultural and Biological Engineering at Pennsylvania State University.

References

Chen, G., Yue, P.L., and Mujumdar, A.S., (2002). Sludge dewatering and drying. Drying Technology 20(4-5), 883-916.

Elliott, A. and Mahmood, T., (2005). Survey benchmarks generation: management of solid residues. Pulp and Paper 79 (12), 49-55.

Hippinen, I. and Ahtila, P., (2004). Drying of activated sludge under partial vacuum conditions-An experimental study. Drying Technology 22 (9), 2119-2134.

Kraft, D.L. and Orender, H.C., (1993). Considerations for using sludge as a fuel. Tappi J. 76 (3), 175-183.

Kudra, T., Gawrzynski, Z., Glaser, R., Stanislawski, J., and Poirier, M., (2002). Drying of pulp and paper sludge in a pulsed fluid bed dryer. Drying Technology 20 (4-5), 917-933.

Navaee-Ardeh, S., Bertrand, F., Stuart, P.R., (2006). Emerging Biodrying Technology for the Drying of Pulp and Paper Mixed Sludges, Drying Technology 24(7), 863-878.